Genome-wide screening methods in tumors of the central nervous system and cancer predisposition

Dissertation

zur

Erlangung des Doktorgrades (Dr. rer. nat.)

der

Mathematisch-Naturwissenschaftlichen Fakultät

der

Rheinischen Friedrich-Wilhelms-Universität Bonn

vorgelegt von

Vera Riehmer

aus

Bonn

Bonn, im März 2014

Angefertigt mit Genehmigung der Mathematisch-Naturwissenschaftlichen Fakultät der Rheinischen Friedrich-Wilhelms-Universität in Bonn.

1. Gutachterin: Prof. Dr. med. R. G. Weber
2. Gutachter: Prof. Dr. rer. nat. W. Witke
Tag der Promotion: 30. Juni 2014
Erscheinungsjahr: 2014

Table of content

Figures and tables
Abbreviations

1 Introduction 10
1.1 Somatic tumor genetics 10
1.2 Genetics of tumor predisposition 11
1.3 Genome-wide screening methods 12
1.3.1 Array-CGH: BAC versus oligonucleotide arrays 12
1.3.2 Next generation sequencing – exome sequencing 13
1.3.3 Data analysis and filtering strategies in NGS 14
1.4 Classification of glial tumors according to the World Health Organization 15
1.4.1 Gliomas of WHO grade II and WHO grade III 17
1.4.2 Glioblastoma multiforme 18
1.5 Important molecular markers in gliomas 20
1.5.1 *MGMT* (O^6-methylguanine-DNA methyltransferase) gene 20
1.5.2 *IDH1* and *IDH2* (isocitrate dehydrogenase 1 and 2) gene 20
1.5.3 *TP53* (tumor protein 53) gene 21
1.5.4 *EGFR* (epidermal growth factor receptor) gene 21
1.5.5 Combined loss of chromosomal arms 1p and 19q 22
1.6 Pituitary adenomas 22
1.7 Malignant peripheral nerve sheath tumor (MPNST) 23
1.8 German Glioma Network (GGN) 23
1.9 Syndromal phenotypes that include cancer predisposition, e.g. Bloom syndrome 23
1.10 Objectives of the study 25
2 Materials and methods 26
2.1 Materials 26
2.1.1 Chemicals and solutions 26
2.1.2 Equipment 27
2.1.3 Consumables 27
2.1.4 Kits 27
2.1.5 Buffers 28
2.1.6 Primers 29
2.1.7 Software 29
2.1.8 Online resources 30
2.1.9 Patients from the GGN 30
2.1.10 Clinical features of patient 1 30
2.1.11 Clinical features of patient 2 31
2.2 Methods 33
2.2.1 Extraction of genomic DNA from EDTA-blood samples 33
2.2.2 DNA extraction from paraffin sections – phenol-chloroform extraction 33
2.2.3 Determination of DNA concentration 34
2.2.4 Fluorescence *in situ* hybridization (FISH) 34
2.2.4.1 Generating chromosome preparations 35
2.2.4.2 Pretreatment of chromosome preparations 35
2.2.4.3 Labeling of DNA probes – nick translation 35
2.2.4.4 Preparation of hybridization mixture 36
2.2.4.5 Hybridization 36

2.2.4.6 Washing steps and antibody detection ... 37
2.2.5 Array-based comparative genomic hybridization (array-CGH) ... 37
2.2.5.1 DNA labeling for array-CGH ... 38
2.2.5.2 Array-CGH sample preparation for hybridization ... 39
2.2.5.3 Array-CGH hybridization ... 39
2.2.5.4 Preparation of the DNA microarrays for scanning ... 40
2.2.5.5 Scanning of the DNA microarrays ... 40
2.2.5.6 Data processing with the Genepix 6.1 software ... 40
2.2.5.7 Data analysis and interpretation ... 41
2.2.6 Oligonucleotide arrays – NimbleGen ... 41
2.2.7 Sanger sequencing ... 43
2.2.7.1 Primer design ... 44
2.2.7.2 Polymerase chain reaction (PCR) ... 44
2.2.7.3 Enzymatic cleanup of PCR products by ExoSAP-IT ... 45
2.2.7.4 Sequencing reaction using the BigDye Terminator v1.1 Cycle Sequencing Kit ... 46
2.2.7.5 Cleaning up of sequencing reaction and sequencing analysis ... 46
2.2.8 Whole exome sequencing (WES) ... 47
3 Results ... 49
3.1 Project 1: Array-CGH analysis of WHO grade II and WHO grade III gliomas ... 49
3.1.1 Genomic profiles in WHO grade II gliomas ... 49
3.1.2 Frequency of genomic alterations in WHO grade II gliomas ... 51
3.1.3 Genomic profiles in WHO grade III gliomas ... 52
3.1.4 Frequency of genomic alterations in WHO grade III gliomas ... 53
3.2 Project 2: Characterization of long-term survivors of glioblastoma using genome-wide profiling ... 55
3.2.1 Patient characteristics of 94 glioblastoma patients ... 55
3.2.2 Analysis of genomic imbalances in primary glioblastomas by array-CGH ... 59
3.2.3 Combined analyses of genomic and expression data – gene dosage effects ... 65
3.3 Project 3: Genomic patterns of recurrence in *IDH1/2* wild-type glioblastomas, WHO grade IV ... 69
3.3.1 Frequency and pattern of DNA copy number changes in the primary glioblastomas ... 71
3.3.2 Comparison of genomic profiles in primary and recurrent glioblastoma pairs yields three subgroups ... 72
3.3.3 Aberration frequency in the three molecular relapse groups ... 78
3.3.4 Regions of genomic difference between primary and recurrent tumor pairs ... 81
3.4 Project 4: Genomic profiling to assess the clonal relationship between histologically distinct intracranial tumors ... 85
3.5 Project 5: Dissecting the genotype in a patient with cancer predisposition using whole exome sequencing in addition to genome-wide copy number analysis ... 87
3.5.1 Whole exome sequencing on DNA from peripheral blood of patient 2 and her mother ... 92
4 Discussion ... 96
4.1 Project 1: Array-CGH analysis of WHO grade II and WHO grade III gliomas ... 96
4.2 Project 2: Characterization of long-term survivors of glioblastoma using genome-wide profiling ... 97
4.3 Project 3: Genomic patterns of recurrence in *IDH1/2* wild-type glioblastomas, WHO grade IV ... 100
4.4 Project 4: Genomic profiling to assess the clonal relationship between histologically distinct intracranial tumors ... 105

4.5 Project 5: Dissecting the genotype in a patient with cancer predisposition using whole exome sequencing in addition to genome-wide copy number analysis 107
4.5.1 Adjustment of WES filter strategy based on findings in patient 2 – future strategy... 110
5 Summary..... 112
6 Deutsche Zusammenfassung..... 116
7 References..... 120
8 Publications..... 139
9 Acknowledgements..... 140

Figures and tables

Figure 1: Schematic drawing of data analysis strategies in NGS. 15
Figure 2: Malignant progression of glioma. 16
Figure 3: Frequent genetic changes in diffuse astrocytomas in association with the tumor grade..... 18
Figure 4: Array-CGH profiles of WHO grade II diffuse astrocytomas..... 50
Figure 5: Array-CGH profiles of WHO grade II oligoastrocytomas and oligodendrogliomas. 51
Figure 6: Frequency plots of genomic alterations in WHO grade II diffuse astrocytomas stratified according to *IDH1/2* status..... 52
Figure 7: Array-CGH profiles of WHO grade III anaplastic astrocytomas..... 53
Figure 8: Frequency plots of genomic alterations in anaplastic astrocytomas of WHO grade III stratified according to *IDH1/2* status..... 54
Figure 9: Frequency plot of genomic alterations in *IDH1/2* mutant WHO grade III anaplastic oligoastrocytomas 55
Figure 10: Heatmap of genomic imbalances in 89 glioblastomas analyzed by array-CGH. 60
Figure 11: Frequency plots of genomic imbalances according to survival groups and *IDH1/2* status. . 61
Figure 12: Heatmap of supervised clustering of array-CGH data based on molecular subtypes of glioblastomas (classical, mesenchymal, proneural) inferred from gene expression data. 66
Figure 13: Demonstration of the gene dosage effect by combination of array-CGH and mRNA expression data..... 68
Figure 14: Frequency and pattern of DNA copy number changes in primary glioblastomas. 72
Figure 15: Comparison of genomic profiles in paired primary and recurrent glioblastomas: example for an Equal tumor pair. 74
Figure 16: Comparison of genomic profiles in paired primary and recurrent glioblastomas: example for a Sequential tumor pair. 75
Figure 17: Comparison of genomic profiles in paired primary and recurrent glioblastomas: example for a Discrepant tumor pair. 76
Figure 18: Frequency plots of primary and recurrent glioblastomas according to the molecular relapse subtype: Equal, Sequential, and Discrepant. 78
Figure 19: Comparison of array-CGH profiles on chromosomal arm 9p in Equal versus Sequential and Equal versus Discrepant primary tumors. 79
Figure 20: Regions of genomic differences in primary and recurrent glioblastoma pairs. 82
Figure 21: Genome-wide array-CGH profiles of the first and the second intracranial tumor of patient1. 87
Figure 22: Facial features and skin lesions of patient 2. 88
Figure 23: Genome-wide BAC array-CGH profile of DNA from peripheral blood of patient 2..... 89
Figure 24: Enlargement of chromosomal band 22q11.21 from array-CGH profiles of patient 2 and her parents. 90
Figure 25: Enlargement of chromosomal band 6q27 from array-CGH profiles of patient 2 and her parents. 91
Figure 26: Interphase FISH analysis confirmed 22q11.21 microduplication in patient 2 and her mother. 92

Figure 27: Electropherograms showing mutations identified by WES and verified by Sanger sequencing. 94
Figure 28: Pedigree of patient 2 and her family showing the detected genetic alterations..... 95
Figure 29: Scheme of possible genetic and clonal evolution in the defined molecular relapse groups. 102
Figure 30: Scheme of filtering strategy used to reduce the number of variants identified by NGS and to identify the causative variants. 111

Table 1: Growth curve parameters of patient 2 31
Table 2: Pipetting scheme for nick translation 36
Table 3: Protocol of hybridization and stringency washing steps 40
Table 4: Features of the gpr-file 41
Table 5: Pipetting scheme for the hybridization master mix 42
Table 6: Pipetting scheme for standard PCR using *Taq* DNA polymerase from Qiagen 45
Table 7: Temperature profile of a standard PCR 45
Table 8: Thermocycling protocol for enzymatic cleanup 45
Table 9: Pipetting scheme for a sequencing reaction 46
Table 10: Temperature profile of a sequencing reaction..... 46
Table 11: Clinical, histological, and molecular patient characteristics according to survival groups 56
Table 12: Clinical, histological, and molecular characteristics of patients with *IDH1/2*^{wt} tumors according to survival groups..... 58
Table 13: Frequency of copy number changes in different chromosomal regions containing glioma-associated tumor suppressor genes or oncogenes 62
Table 14: Clinical, histological, and molecular patient characteristics of study and reference group. . 70
Table 15: Clinical characteristics of study group by molecular relapse pattern..... 77
Table 16: Distribution of losses in glioma-associated genes on 9p in different molecular relapse groups 80
Table 17: Chromosomal regions affected at least twice by copy number difference and candidate genes involved. 83
Table 18: Functions of the 46 identified candidate genes associated with therapy response or tumor recurrence. 84
Table 19: Genes encoding regulators of apoptosis or chromatin remodelers. 85
Table 20: WES data filtering strategy in patient 2 93

Abbreviations

AIP	**A**ryl hydrocarbon receptor-**i**nteracting **p**rotein
APC	**A**denomatous **p**olyposis **c**oli
ARID1B	**A**T-**r**ich **i**nteraction **d**omain-containing protein **1B**
Array-CGH	**A**rray-based **c**omparative **g**enomic **h**ybridization
BAC	**B**acterial **a**rtificial **c**hromosome
BCR	**B**reakpoint **c**luster **r**egion
Bio-dUTP	**Bio**tin-11-**d**eoxy**u**ridine **t**ri**p**hosphate
BL	**B**ody **l**ength
BLM	**Bl**oo**m** **s**yndrome
bp	**B**ase **p**air
BW	**B**ody **w**eight
C	**C**ytosine
CHEK2	**Che**ckpoint **k**inase **2**
Cy3	**Cy**anine **3**
Cy5	**Cy**anine **5**
DAPI	4',6-**d**i**a**midino-2-**p**heny**l**indole
dCTP	Deoxycytidine triphosphate
Dig-dUTP	**Dig**oxigenin-11-**d**eoxy**u**ridine **t**ri**p**hosphate
DKFZ	**D**eutsches **K**rebs**f**orschungs**z**entrum
DNA	**D**eoxyribo**n**ucleic **a**cid
dNTP	**D**eoxyribo**n**ucleoside **t**ri**p**hosphate
ddNTP	**Did**eoxyribo**n**ucleoside **t**ri**p**hosphate
EDTA	**E**thylene**d**iamine**t**etraacetic **a**cid
EGFR	**E**pidermal **g**rowth **f**actor **r**eceptor
EP300	**E**1A-binding **p**rotein, **300**-KD
EXO	**Exo**nuclease I
FAP	**F**amilial **a**denomatous **p**olyposis
FIGO	**I**nternational **F**ederation of **G**ynecology and **O**bstetrics
FISH	**F**luorescence ***in situ*** **h**ybridization
FITC	**F**luorescein **i**so**t**hio**c**yanate
Fwd	**F**or**w**ar**d**
G	Guanine
gff-file	General feature format-file
GGN	**G**erman **G**lioma **N**etwork
gps-file	**G**ene**p**ix **s**ettings-file
gpr-file	**G**ene**p**ix **r**esults-file
Gy	**G**ray (unit)
HC	**H**ead **c**ircumference
HGMD	**H**uman **G**ene **M**utation **D**atabase
HPLC	**H**igh **P**erformance **L**iquid **C**hromatography
IDH1 and 2	**I**socitrate **d**e**h**ydrogenase **1** and **2**
KCl	Potassium chloride
KPS	**K**arnofsky **p**erformance **s**core
LFS	**L**i-**F**raumeni **s**yndrome
Mb	**M**ega**b**ase
MAF	**M**inor **a**llele **f**requency
$MgCl_2$	**M**a**g**nesium **c**hloride

MGMT	O^6-**m**ethyl**g**uanine-DNA **m**ethyl**t**ransferase
MRI	**M**agnetic **r**esonance **i**maging
Mut	**Mut**ant
NaCl	**S**odium **c**hloride
NF1	**N**euro**f**ibromatosis type **1**
NGS	**N**ext **g**eneration **s**equencing
OS	**O**verall **s**urvival
P	**P**ercentile
PAC	**P**1-derived **a**rtificial **c**hromosome
PARP1	**P**oly(**A**DP-**r**ibose) **p**olymerase-**1**
PCR	**P**olymerase **c**hain **r**eaction
PDGFRA	**Pl**atelet-**d**erived **g**rowth **f**actor **r**eceptor**, a**lpha
Rev	**Rev**erse
PFS	**P**rogression **f**ree **s**urvival
PRDM2	**PR d**o**m**ain containing **2**
PTEN	**P**hosphatase and **t**ensin homolog
RELB	v-rel avian reticuloendotheliosis viral oncogene homolog B
RNA	**R**ibo**n**ucleic **a**cid
rpm	**R**evolutions **p**er **m**inute
RT	**R**adio**t**herapy
SAP	**S**hrimp **a**lkaline **p**hosphatase
SDS	**S**odium **d**odecyl**s**ulfate
SNP	**S**ingle **n**ucleotide **p**olymorphism
SSC	**S**aline-**s**odium **c**itrate
Taq	***T**hermus **aq**uaticus*
TCGA	**T**he **C**ancer **G**enome **A**tlas
TE-buffer	**T**ris-**E**DTA-buffer
TMZ	**T**e**m**o**z**olomide
TP53	**T**umor **p**rotein **53**
TRITC	**T**etramethyl **r**hodamine **i**so**t**hio**c**yanate
U	**U**nit
UBE4B	**Ub**iquitination factor **E4B**
WES	**W**hole **e**xome **s**equencing
WHO	**W**orld **H**ealth **O**rganization
WT	**W**ild-**t**ype

1 Introduction

1.1 Somatic tumor genetics

Over the last decades a lot of research has been done to understand and unravel the mechanisms underlying tumor development. It has been found that tumor development is a complex process involving several factors, e.g. accumulation of genetic alterations and evasion of apoptosis. Generally speaking, cancer is essentially a genetic disease. Tumor development is driven by alterations in three types of genes: oncogenes, tumor suppressor genes and stability genes (Vogelstein and Kinzler, 2004). In the case of oncogenes (e.g. *RAS*, *MYC*), the genetic alterations usually activate genes involved in cellular processes such as cell proliferation, cell differentiation and survival (Alberts, 2008). The activating genetic alteration causes abnormal cell proliferation via increased gene expression or uncontrolled activity of the oncogene encoded protein (Alberts, 2008). The underlying aberration can be a chromosomal translocation, gene amplification or an intragenic mutation affecting a major domain of the gene product and therefore its activity (Vogelstein and Kinzler, 2004). In contrast, genetic alterations in tumor suppressor genes (e.g. *TP53*, *PTEN*) reduce the activity of the gene product. Causes of these inactivations are missense mutations in domains essential for the activity of the gene product, mutations causing truncated proteins, and any kind of deletions or insertions disturbing the gene as well as loss of complete chromosomes (Vogelstein and Kinzler, 2004). For tumor suppressor genes a two-hit hypothesis has been postulated, in 1971 by Knudson, stating that a tumor suppressor needs two inactivating mutations in order to turn a normal cell into a tumor precursor and trigger tumorigenesis (Knudsen, 1971; Strachan and Read, 2011). The third class of genes involved in tumorigenesis consists of the so called stability genes. Their function is to monitor basic cellular processes, such as mismatch repair, nucleotide-excision repair and base excision repair, replication of mistakes or DNA damage after exposure to mutagens (Vogelstein and Kinzler, 2004).

A single mutation is not sufficient to cause cancer. In contrast, several alterations in different genes, indicating a multistep process, are needed for a cell to become cancerous (Hanahan and Weinberg, 2000; Vogelstein and Kinzler, 2004). Since a high number of somatic mutations are found in any kind of cancer, which can now be readily identified because of reduced costs in sequencing technologies, a clear differentiation between driver and passenger mutations has to be made. In general, it is difficult to identify which somatic mutations are driver and which are passenger mutations. All mutations that confer a selective growth advantage to a cell are classified as driver mutations. On the other hand, mutations that have no effect on the malignant transformation are called passenger mutations (Vogelstein et al., 2013).

Not only single base-pair substitutions can render a gene into an active oncogene or an inactive tumor suppressor gene. Also larger chromosomal aberrations such as changes in chromosome number (aneuploidy), translocations, deletions or insertions of various sizes play an important role in the malignant transformation of a normal cell into a tumor cell. When larger parts of a chromosome are affected, it is rather challenging to identify the specific target gene (Vogelstein et al., 2013).

By chromosomal translocations, fusion genes can be generated (Vogelstein et al., 2013). One prominent example is the so called Philadelphia chromosome that is often found in patients with chronic myeloid leukemia. Here, the *BCR* (breakpoint cluster region) gene located on chromosome 9 is fused to the *ABL* (Abelson murine leukemia viral oncogene homolog) gene located on chromosome 22 (Rowley, 1973), resulting in a constitutively activated Abl kinase.

1.2 Genetics of tumor predisposition

Tumor predisposition syndromes may account for up to 5% – 10% of adult cancers (Garber and Offit, 2005). A characteristic of hereditary cancer syndromes is the early onset of disease as well as childhood tumors. Moreover, several first-degree or second-degree family members in the same family line are usually affected. The cause of tumor predisposition syndromes is most frequently a germline mutation, which can be found in a variety of genes and can be passed on to the offspring, if not the individual's ability to have offspring is seriously impaired (Strachan and Read, 2011).

One prominent tumor predisposition syndrome is the so called Li-Fraumeni syndrome (LFS) already described in 1969 by Li and Fraumeni (Li and Fraumeni, 1969). It is a clinically and genetically a heterogeneous tumor syndrome with autosomal dominant inheritance. It is characterized by the early onset of tumors, multiple tumors in an individual and several affected family members. The tumors usually involved are soft tissue sarcomas and osteosarcomas, breast cancer, brain tumors, adrenal cortical carcinoma, and leukemias (Li et al., 1988). In 1990 the underlying cause was identified to be a germline mutation in the *TP53* (tumor protein 53) gene, which maps to chromosome 17p13.1 (Malkin et al., 1990). Further studies have shown that mutations in the *TP53* gene are found in 70% of families with the classic LFS (Varley, 2003a). Additionally, mutations in the *CHEK2* (checkpoint kinase 2) gene have been described to be causative for LFS (Bell et al., 1999; Varley 2003b).

Another prominent hereditary cancer syndrome is familial adenomatous polyposis (FAP). It is also inherited in an autosomal dominant manner, and is caused by a germline mutation in the *APC* (adenomatous polyposis coli) gene located on chromosome 5q22.2 (Kinzler et al., 1991). A characteristic of this disorder is the development of hundreds of adenomatous polyps of the colon and rectum in affected patients. If not treated surgically, these polyps can progress to colorectal carcinoma (Rustgi, 2007). Importantly, the penetrance of developing polyps is 100% at the age of 35 years. Furthermore, the risk of developing colon cancer is also approximately 100% with an average age of diagnosis at 39 years (Garber and Offit, 2005).

Strategies in these tumor predisposition syndromes are early genetic testing for all family members, if the causative mutation is known. If tested positive, tight surveillance is advisable. If an *APC* gene mutation and adenomas have been found in a patient suffering from FAP, prophylactic colectomy is performed regularly (Hampel and Peltomaki, 2000).

1.3 Genome-wide screening methods

The development of genome-wide screening methods such as array-based comparative genomic hybridization (array-CGH) or next generation sequencing (NGS) made high throughput studies feasible. Nowadays, genome-wide screening methods are applied not only to screen different cancer entities, but also in clinical genetics to identify the underlying cause, such as copy number changes or disease causing mutations, of various syndromes. With reduced costs for sequencing whole genomes or exomes as well as for microarray analyses, large numbers of samples can be examined in a timely manner (Vogelstein et al., 2013). In the study described here, different genome-wide screening methods were used. Firstly, bacterial artificial chromosome (BAC)-arrays have been used for the analysis of more than 300 glioma DNA samples, as well as oligonucleotide arrays for the analysis of a patient presenting with a highly complex syndromal phenotype including cancer predisposition. Secondly, whole exome sequencing (WES) was used to unravel and explain the complete phenotype of the same patient.

1.3.1 Array-CGH: BAC versus oligonucleotide arrays

In 1997, array-CGH was described for the first time (Solinas-Toldo et al., 1997; Pinkel et al., 1998). It is a molecular cytogenetic method that can be used to reveal copy number gains or losses across the whole genome, while comparing the copy number of a test and a reference DNA. The copy number changes can range from aberrations of whole chromosomes (aneuploidy) e.g. trisomy 21 in Down syndrome, to microdeletions or duplications e.g. in the 22q11.2 region (Miller et al., 2012). A disadvantage of this method is that balanced chromosomal rearrangements including balanced fusion chromosomes are generally not detected. The overall resolution of an array is determined by the number and size of the probes spotted on the microarray (Strachan and Read, 2011).

In this study, two types of arrays were used, a BAC array (10.6k) with an average resolution of better than 0.5 Mb as well as chromosome specific tiling oligonucleotide arrays (385k). Initially in array-CGH, the DNA microarrays used were glass slides spotted with bacterial artificial chromosomes (BAC) or P1 artificial chromosomes (PAC). These BACs and PACs contained large inserts with a size of about 100 – 150 kb (Fiegler et al., 2007). As an improvement in this technology, oligonucleotide arrays were developed (Lucito et al., 2003). Today, different kinds of oligonucleotide arrays are available. Some manufacturers produce arrays containing oligomers with a size of 50 – 70 bp in order to focus on high quality copy number detection. Other arrays with shorter oligomers size of 25 bp can also be used for genome-wide single nucleotide polymorphism (SNP) genotyping (Shen and Wu, 2009).

There are several advantages of oligonucleotide arrays. Therefore, they have mainly replaced BAC arrays. First of all, the reproducibility of oligonucleotide arrays is better. Additionally, the oligonucleotide probe sequences lack repetitive sequences. Oligonucleotide arrays also have a higher resolution, which results from smaller interprobe spacing leading to a much higher probe density.

Therefore, smaller genomic imbalances can be detected and the breakpoint mapping is more precise. Whereas oligonucleotide probes are designed after the reference human genome sequence, BAC clones need to be selected from existing libraries, and their location needs to be mapped and validated (Shen et al., 2007; Shen and Wu, 2009). Oligonucleotide arrays are also easier to customize, so manufacturers can offer a wide range of microarray types, while the update of BAC arrays and their production is more time consuming. Lastly, with increasing probe numbers in oligonucleotide arrays, a multiprobe confirmation is achieved (Ylstra et al., 2006; Shen et al., 2007; Ou et al., 2008).

The principle of array-CGH is similar when using large insert clone or oligonucleotide arrays. Firstly, the test and reference DNA are labeled with different fluorescent dyes, usually Cy3 and Cy5. Secondly, the samples are co-hybridized to the microarray. Thirdly, the array is scanned and the different fluorescent intensities are measured, finally the data is analyzed (Miller et al., 2012). However, when using large insert clone arrays, a suppression of repetitive DNA sequences using human Cot-1-DNA is required.

1.3.2 Next generation sequencing – exome sequencing

In the last few years, next generation sequencing (NGS) became more and more popular, and started to push aside Sanger sequencing, also called the 'first-generation' technology, as a first-line sequencing technique particularly in research. Improvements were needed to cover the demand of a high throughput method to sequence whole human genomes or to identify all variants located in the coding region of genes in an individual human genome, the so called exome (whole exome sequencing, WES) (Metzker, 2010; Bamshad et al., 2011). Identifying all the variants in a human genome might influence the understanding of how genetic differences affect health and disease.

NGS is based on the combination of different strategies for template preparation, massive parallel sequencing, imaging, sequence alignment to a reference genome and assembly of aligned sequences (Metzker, 2010). Currently, different technologies for the enrichment of DNA to be sequenced using NGS are available. They are based on the same principle and differ only slightly in their target choice, bait density and capture molecule. These baits are employed to capture the fragmented genomic DNA by hybridization enabling the generation of libraries. For exome sequencing, for example, biotinylated oligonucleotide baits covering the human exome regions are usually used to capture the human exome prior it exome sequencing. Enrichment of the bound libraries takes place by a pull down with magnetic streptavidin beads, followed by NGS sequencing technologies (Wheeler et al., 2008; Clark et al., 2011). One disadvantage of WES is currently that depending on the used enrichment kit, 5% – 10% of the exome is poorly enriched and therefore poorly covered by sequencing. For this reason, some exons are missed completely, and have to be analyzed by conventional Sanger sequencing. Besides that, the detection of small insertion and deletions, so called INDELs has to be improved (Alkan et al., 2011; Bamshad et al., 2011). The huge advantage of NGS is that large genomes, such as the human genome, can be sequenced easily and cost effectively.

But the handling of the enormous amounts of data generated and the interpretation of the detected variants is very challenging.

Depending on the technologies used for sequence enrichment and analysis of sequencing data approximately 40,000 single nucleotide variants are found in each whole human exome sequencing analysis on DNA from peripheral blood. When performing WES in clinical genetics. The challenge is to find the causative variants among the many variants identified. In rare diseases, the causative variants can be enriched by excluding variants with a high minor allele frequency (MAF). But not all rare variants are disease causing. Therefore, stringent filter strategies are needed to reduce the number of these variants, in order to find the causative variant of the investigated disease.

1.3.3 Data analysis and filtering strategies in NGS

NGS analysis of a human exome or genome results in an enormous number of identified variants. In order to reduce these numbers and the number of individuals which have to be sequenced, different data analysis and filtering strategies have been developed to single out the causative mutation or gene for the investigated disorder. In the following, some of these strategies are described. One analysis approach is that DNA from a few unrelated individuals with the same disorder are sequenced and subsequently compared, in order to find a gene commonly affected by pathogenic variants in several of these individuals (Figure 1A, page 15). In addition, these genomes are also compared to controls, e.g. healthy individuals or data from dbSNP and the 1000 Genomes Project to identify causative mutations. In this case, large sample sizes are of advantage (Bamshad et al., 2011).

A second approach is a family based procedure of trio sequencing in order to identify *de novo* mutations. Here, the unaffected parents as well as the affected offspring are sequenced, and all the variants inherited from the parents are subtracted from the patient's variants (Figure 1B). Among the few remaining *de novo* variants occurring only in the index patient, it is often possible to pick out the variant probably causative for the disease (Figure 1B). This approach has been found to be quite effective and has identified new candidate genes in several genetic disorders (Vissers et al., 2010; O'Roak et al., 2011; de Ligt et al., 2012).

In the case of the candidate gene strategy, only variants in genes already known to be associated with the analyzed disease are retained. Further *in silico* prediction of pathogenicity of the identified variants is important. Usually only the variants predicted to be pathogenic by two or three different prediction programs are retained and considered to be causative (Figure 1C) (Neveling and Hoischen, 2012).

De Ligt *et al.* developed a workflow of filtering variants detected in DNA from peripheral blood by exome sequencing in patients with intellectual disability. This workflow was shown to be quite effective in identifying the causative mutations in patients with severe intellectual disability, in which all conventional genetic tests were negative (de Ligt et al., 2012). Firstly, variants were separated on the basis of being synonymous or non-synonymous coding. In the case of synonymous coding variants, it was checked if a splice site was affected. If this was not the case, the variant was excluded

from further analysis and was considered not causative. In the case of non-synonymous coding variants, *in silico* prediction was performed and if the variants were classified as pathogenic, they were retained. De Ligt *et al.* further considered the found variants to be causative if the same gene was mutated in other patients with overlapping phenotypes. This gene was then considered a novel intellectual disability gene (de Ligt et al., 2012). If no additional patients were found to carry variants in the same gene, this gene was classified as a candidate intellectual disability gene. With this strategy, the authors were able to identify candidate genes as well as novel genes associated with intellectual disability (de Ligt et al., 2012).

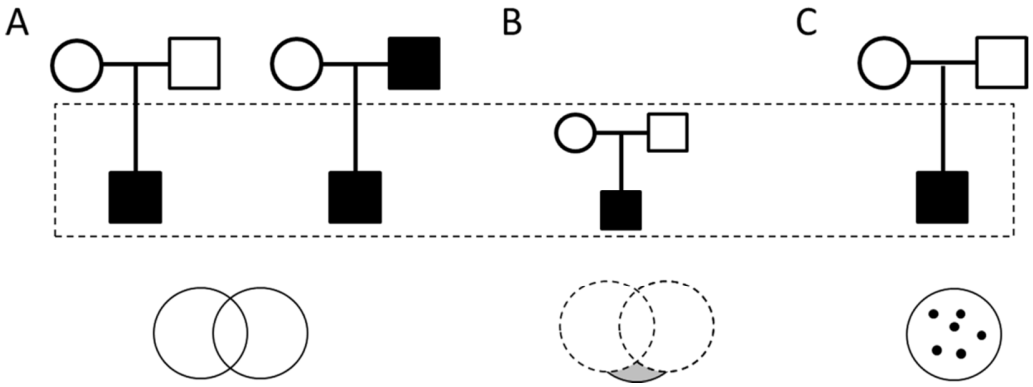

Figure 1: Schematic drawing of data analysis strategies in NGS.
Shown are different pedigrees, persons surrounded by the dotted line are sequenced. The circles beneath the pedigrees represent the identified variants. The circles with solid lines represent variants from affected patients; circles with dotted lines represent variants from unaffected individuals (modified from Neveling and Hoischen, 2012).

1.4 Classification of glial tumors according to the World Health Organization

The World Health Organization (WHO) has graded the tumors of the central nervous system based on their histological features in order to establish a classification and grading system that is accepted worldwide and facilitates e.g. epidemiological studies and clinical trials. The grading system provides information about the malignant potential of the tumor and can give indications about the response to certain therapies. In addition to the histological features, the grading system is increasingly complemented by genetic characterization details of the neoplasms (Louis et al., 2007a). For clinicians, the grading system helps to predict the biological behavior of the tumor and may influence the choice of therapy, e.g. the use of an adjuvant radiation and specific chemotherapy protocol (Louis et al., 2007b).

Gliomas are brain tumors derived from glial cells, which are subdivided into WHO grade I to WHO grade IV tumors. WHO grade I is assigned to tumors displaying low proliferative potential which can be cured by surgical resection. WHO grade II tumors show an infiltrative behavior, although a low proliferative activity is often present. Some tumor types of WHO grade II have been found to progress

to higher grades of malignancy, e.g. low grade diffuse astrocytomas may transform to anaplastic astrocytomas of WHO grade III or even to glioblastomas of WHO grade IV, also known as secondary glioblastomas (Figure 2). In the case of WHO grade III tumors, evidence of malignancy can be found histologically with tumor cells showing nuclear atypia and brisk mitotic activity. WHO grade IV is assigned to the most aggressive tumors, which are typically associated with a rapid pre- and postoperative disease progression and with a fatal outcome. These tumors are cytologically malignant, mitotically active and necrosis prone. Also, widespread infiltration into surrounding tissues is one of the features that makes WHO grade IV glioblastomas so unfavorable (Louis et al., 2007a).

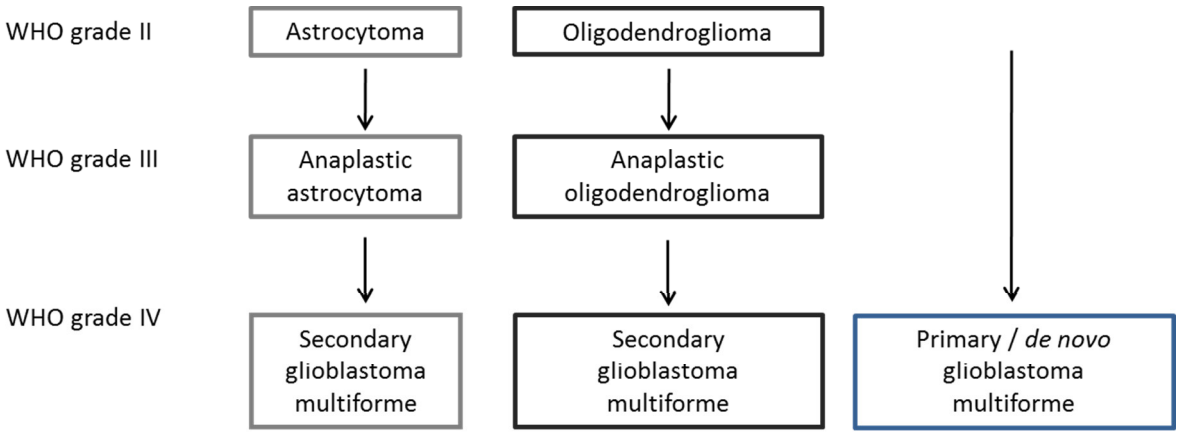

Figure 2: Malignant progression of glioma (modified from Ohgaki and Kleihues, 2005a).

In total, six distinct histological entities of astrocytic neoplasms are recognized by the WHO classification, which can be separated into two major groups. The first group comprises the diffuse infiltrating astrocytic tumors, including diffuse astrocytoma, anaplastic astrocytoma and glioblastoma multiforme. The second group contains the less frequent tumors with a more circumscribed growth behavior such as pilocytic astrocytoma, pleomorphic xanthoastrocytoma, and subependymal giant cell astrocytoma (Riemenschneider and Reifenberger, 2009). In addition, the WHO grading system recognizes two malignancy grades for oligodendroglial tumors, namely the oligodendrogliomas of WHO grade II, which are well differentiated, and the WHO grade III anaplastic oligodendrogliomas. Furthermore, there are oligoastrocytic tumors of WHO grade II and anaplastic oligoastrocytomas of WHO grade III, which are composed of a mixture of two distinct neoplastic cell types. From the morphologic point of view, these tumors display oligodendroglial and astrocytic tumor cells (Reifenberger et al., 2007).

1.4.1 Gliomas of WHO grade II and WHO grade III

Low grade gliomas are subdivided into three types: astrocytomas, oligodendrogliomas, and mixed oligoastrocytomas and are classified as WHO grade II (Louis et al., 2007a). The classification is done according to the morphologies of the tumor cells and their origin. Of all astrocytic brain tumors, 10% – 15% are classified as diffuse astrocytomas (von Deimling et al., 2007). They exhibit a high degree of cellular differentiation and are, therefore, classified as WHO grade II. Even though they have a better disease prognosis than malignant gliomas, they tend to recur and progress to higher grade tumors such as anaplastic astrocytoma of WHO grade III and secondary glioblastomas of WHO grade IV (Figure 2, page 16) (Riemenschneider and Reifenberger, 2009). Diffuse astrocytomas usually develop in the frontal and temporal cerebral lobes, while they are uncommon in the cerebellum. These tumors often occur in younger adults with an age between 30 and 40 years (von Deimling et al., 2007). Mutations in the tumor suppressor gene *TP53* are detected in about 60% of diffuse astrocytomas (Ichimura et al., 2000). It seems that *TP53* mutations are an early event in astrocytoma progression (Figure 3, page 18), because the frequency of *TP53* mutations does not increase in recurrent tumors. Moreover, *MGMT* promoter methylation is also found in up to 50% of astrocytomas (Watanabe et al., 2007). Apart from chromosomal imbalances such as losses on chromosomes 6, 10p, 13q, 19q and 22q, array-CGH analysis showed a frequent gain on chromosomal arm 7q, which has been detected in up to 50% of cases. Combined loss of chromosomal arms 1p and 19q is rarely found in astrocytomas (Reifenberger and Collins, 2004).

In contrast to the above mentioned diffuse astrocytomas, anaplastic astrocytomas of WHO grade III are characterized by a more infiltrative behavior and display nuclear atypia, increased cellularity and significant proliferative activity. They might develop from WHO grade II lesions or *de novo*. The mean age at diagnosis is approximately 45 years (Kleihues et al., 2007). Anaplastic astrocytomas represent an intermediate state of progression between low grade tumors and secondary glioblastomas of WHO grade IV. *TP53* mutations are quite common (in 50% – 60% of tumors), as well as loss of chromosomal arm 10q that can be found in about 35% – 60% (Ichimura et al., 1998; Balesaria et al., 1999; Louis et al., 2007b). About 20% – 30% of anaplastic astrocytomas also exhibit a loss of chromosomal arm 22q (Hartmann et al., 2004).

Anaplastic oligoastrocytomas (WHO grade III) also display increased cellularity and mitotic activity as well as nuclear atypia, and infiltrate surrounding tissues. Patients are diagnosed with a mean age of 44 years (Miller et al., 2006; Reifenberger et al., 2007). Anaplastic oligoastrocytomas often demonstrate genetic alterations characteristic for astrocytomas and oligodendrogliomas, showing *TP53* mutations as well as the combined loss of chromosomal arms 1p and 19q (Mueller et al., 2002; Louis et al., 2007b). Moreover, they often share other genetic alterations commonly found in astrocytomas such as loss of chromosomal arm 9p, including deletions of the *CDKN2A* gene, as well as losses of chromosomes 10 and 11p (Louis et al., 2007b).

Anaplastic oligodendrogliomas are classified as WHO grade III tumors and have by definition focal or diffuse histological features of malignancy and are associated with a less favorable prognosis (Reifenberger et al., 2007). They display a high cellularity, marked cytological atypia, high mitotic

activity, and necrosis. Patients are usually diagnosed between 45 and 50 years of age (Ohgaki and Kleihues, 2005a). Chromosomal and array-CGH analysis showed a combined loss of chromosomal arms 1p and 19q in about two thirds of tumors. But also additional chromosomal aberrations such as gains on chromosomes 7 and 15q as well as losses on chromosomes 4q, 6, 9p, 10q, 11, 13q, 18 and 22 have been found (Jeuken et al., 2004; Reifenberger et al, 2007).

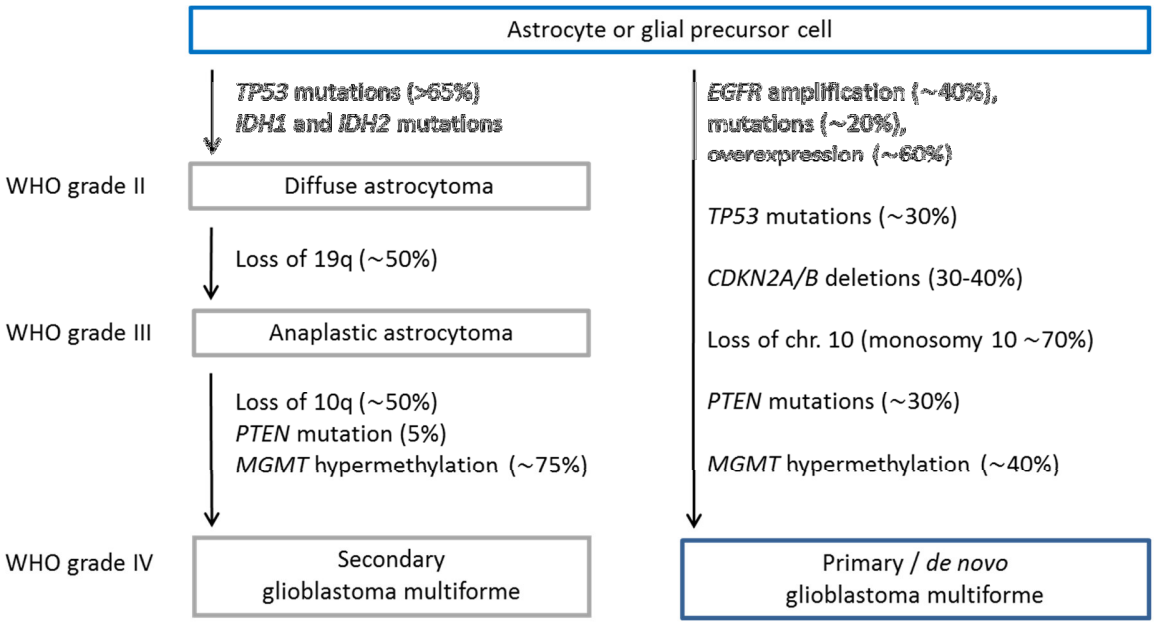

Figure 3: Frequent genetic changes in diffuse astrocytomas in association with the tumor grade.
(modified from Ohgaki and Kleihues, 2005a; Riemenschneider and Reifenberger, 2009)

1.4.2 Glioblastoma multiforme

Glioblastoma multiforme is a distinct glioma entity classified as WHO grade IV. Glioblastomas are the most frequent gliomas and usually develop in a sporadic fashion without any known genetic predisposition. However, a few cases are associated with a hereditary tumor syndrome, e.g. Li-Fraumeni syndrome (Kleihues et al., 1997). So far, no exogenous factors have been identified that are associated with the development of this tumor entity. Glioblastomas mainly develop in the cerebral hemispheres (Kleihues et al., 2007).

On the basis of their clinical presentation, glioblastomas are differentiated into primary and secondary glioblastomas (Figure 2 (page 16) and Figure 3 (page 18)). Primary glioblastomas are characterized by a *de novo* development without any history of a low grade precursor lesion. They often occur in older patients, with a median age of diagnosis of 55 to 60 years. Secondary glioblastomas on the other side may arise from diffuse astrocytoma of WHO grade II and anaplastic astrocytoma of WHO grade III through malignant progression and are usually diagnosed in younger patients with an age at diagnosis of younger than 45 years (Riemenschneider and Reifenberger,

2009). Primary and secondary glioblastoma cannot be separated morphologically (Weller et al., 2012), but on the basis of genetic alterations. With the aid of high throughput methods such as microarray based technologies, vast numbers of tumors could be analyzed. Based on expression analysis, Phillips *et al.* described three distinct molecular subclasses of high-grade astrocytoma, which they proposed to be of prognostic value. They used clustering of 35 signature genes for the identification of the subtypes and named the subclasses after the characteristic dominant features of the genes. The subclasses they identified are named proneural, proliferative and mesenchymal (Phillips et al., 2006). In an independent study from Verhaak *et al.,* similar groups were proposed on the basis of detected genetic aberrations and gene expression analysis. Based on their molecular classification, they described proneural, neural, classical, and mesenchymal subtypes and could show that genetic aberrations and gene expression of *EGFR*, *NF1*, and *PDGFRA/IDH* define the classical, mesenchymal, and proneural subtypes, respectively. Importantly, they could show that the response to aggressive therapy differs between the subtypes (Verhaak et al., 2010).

Glioblastoma patients can also be classified by their clinical characteristics. The age of the patient and the Karnofsky Performance Scale (KPS) score, are important prognostic parameters (Weller et al., 2012). Age is one of the most powerful prognostic factors for glioblastoma patients, since higher age is associated with a poor prognosis (Ohgaki and Kleihues, 2005b). The KPS score has been commonly used since its development in 1948 to assess the general performance of cancer patients. Patients with a KPS from 60 to 100 are considered fit enough to receive standard cancer treatment or participate in clinical trials (Terret et al., 2011). Patients with a value below 60 need more and more assistance, a KPS of 10 describes that the fatal process is progressing rapidly (Terret et al., 2011).

Glioblastoma multiforme is usually associated with poor survival. Despite multimodal aggressive treatment, the median survival time after diagnosis is still in the range of 12 months (Smith and Jenkins, 2000). Nevertheless, 3% – 5% of patients survive longer than 36 months after diagnosis. This group of patients is referred to as long-term survivors. Young age and a good KPS performance score are characteristic in these patients as well as the presence of *MGMT* promoter methylation in the tumors. No environmental or socio-economic factors were associated with the better survival outcome (Krex et al., 2007). The typical genetic aberrations of primary and secondary glioblastoma are described below (1.5, page 20).

The current standard glioblastoma therapy consists of surgical resection followed by local radiotherapy and adjuvant chemotherapy with DNA methylating agents such as temozolomide (TMZ). Importantly, it has been shown that the combined therapy of TMZ administration and radiotherapy results in a significantly increased survival for the glioblastoma patient of 2.5 months versus surgery plus radiotherapy only, without additional toxicity. The two year survival rate of patients treated only with radiotherapy and those treated with radiotherapy and TMZ increased from 10.4% to 26.5% (Stupp et al., 2005). However, the treatment depends strongly on the age and performance score of the patients. Older patients are less often treated by surgical resection, but generally patients operated on showed a better survival (Ohgaki and Kleihues, 2005a). Nevertheless, there is a need for better therapeutic strategies.

1.5 Important molecular markers in gliomas

Various molecular markers e.g. *MGMT*, *IDH1* and *IDH2* (*IDH1/2*), *EGFR* and loss of chromosomal arms 1p and 19q, play also a prognostic or predictive role in gliomas (Figure 3, page 18). Nevertheless, further biological markers are needed as a basis for effective therapies, because most treatment approaches are still based on age and performance status of the patient (Weller et al., 2012). It is important to identify molecular signatures in order to devise personalized treatment strategies. In addition, none of the known molecular markers is completely specific for primary versus secondary glioblastoma, although some alterations such as *EGFR* amplification or *TP53* mutations occur more frequent in either primary or secondary glioblastomas, respectively (Parsons et al., 2008). The most important molecular markers for glioma are described in more detail in the following sections.

1.5.1 *MGMT* (O^6-methylguanine-DNA methyltransferase) gene

MGMT was mapped to chromosomal band 10q26.3 (Nataranjan et al., 1992). The *MGMT* gene encodes a DNA repair protein that removes alkyl groups from DNA, more precisely the O^6 position of guanine, which is an important site of DNA alkylation (Hegi et al., 2005). If the *MGMT* promoter is methylated, the gene is silenced and the cells no longer express *MGMT* (Esteller et al., 2000). Various studies have shown that *MGMT* promoter methylation in glioma is related to responsiveness of a tumor to therapeutic alkylating agents e.g. temozolomide. For this reason, *MGMT* became an important biomarker for glioblastoma. Hegi *et al.* showed that glioblastoma patients with a methylated *MGMT* promoter responded better thus benefited more from temozolomide treatment, while patients displaying no methylated *MGMT* promoter had less benefit. Therefore, they postulated that *MGMT* promoter methylation is an independent predictive factor in glioblastoma patients (Hegi et al., 2005). It has been proposed, that resistance of cancer cells to alkylating agents such as temozolomide can occur due to high levels of *MGMT* activity. Hence, missing *MGMT* promoter methylation might explain treatment failures (Hotta et al., 1994; Silber et al., 1999; Gerson, 2004).

1.5.2 *IDH1* and *IDH2* (isocitrate dehydrogenase 1 and 2) gene

The *IDH1* gene was mapped to chromosomal band 2q33. Somatic mutations in the *IDH1* gene in gliomas were originally described in 2008 (Parsons et al., 2008). Gliomas lacking an *IDH1* mutation can display a mutation in the *IDH2* gene, mapped to chromosomal band 15q26.1. Compared to gliomas, *IDH* mutations in other tumor types are less common (Bleeker et al., 2009). The *IDH1* gene encodes the cytosolic NADP(+)-dependent isocitrate dehydrogenase, an enzyme that is involved in the citric acid cycle. *IDH1* and *IDH2* mutations are early events in the development of gliomas (Figure 3, page 18), meaning that they are frequently found already in WHO grade II and WHO grade III gliomas and also in secondary glioblastomas of WHO grade IV, but only in approximately 10% of primary glioblastomas (Balss et al., 2008; Hartmann et al., 2009; Yan et al., 2009). It has been shown that

gliomas with an *IDH* mutation are clinically and genetically distinct from gliomas displaying no *IDH* mutations (*IDH*^{wt} tumors). It was even proposed that *IDH1* mutations should be used as a marker to distinguish primary from secondary glioblastoma (Nobusawa et al., 2009). All IDH1 mutations are located in the conserved residue R132. This residue is part of the substrate binding site of the IDH protein (Parsons et al., 2008, Riemenschneider et al., 2010). The most common variant results in an amino acid change from arginine to histidine at position 132 (Horbinski, 2013).

IDH mutations are further associated with better survival of patients and can, therefore, be used for prognosis predictions (Parsons et al., 2008; Sanson et al., 2009; Weller et al., 2009). In order to diagnose *IDH* mutations as a diagnostic factor, an antibody was developed detecting the R132H-mutated IDH1 by Western blot analysis and immunohistochemistry of human brain tumor samples (Capper et al., 2010). In cases displaying an *IDH2* mutation, the amino acid R172 of the IDH2 gene is affected (Yan et al., 2009).

1.5.3 *TP53* (tumor protein 53) gene

Molecular aberrations in the *TP53* gene located in chromosomal band 17q13.1 or in *TP53* downstream as well as upstream effector genes are frequently found in many cancers, including gliomas (Parsons et al., 2008; Cancer Genome Atlas Research Network, 2008). It has been found that *TP53* mutations are frequent in WHO grade II and WHO grade III gliomas and secondary glioblastomas with up to 60% of these tumors being mutated (Ichimura et al., 2000). While, in primary glioblastomas, *TP53* mutations are only found in up to 30% of cases (Riemenschneider and Reifenberger, 2009). *TP53* mutations are seen as an early event in glioma development (Figure 3, page 18), due to the fact that their frequency does not increase in tumors with higher WHO grade or in recurrent tumors. Alterations of this tumor suppressor gene were recently shown to be associated with the *IDH* mutation status (Weller et al., 2012).

1.5.4 *EGFR* (epidermal growth factor receptor) gene

EGFR has effects on motility, adhesion, invasion and proliferation of tumor cells, it additionally favors the inhibition of apoptosis and induction of angiogenesis (Nicholson et al., 2001; Marie et al., 2005). Increased EGFR activity is also associated with resistance to irradiation and chemotherapy (Weller et al., 2012). In primary glioblastomas, an amplification of the *EGFR* gene, located in chromosomal band 7p11.2, can be found in about 40% – 50% of cases (Gan et al., 2009; Riemenschneider and Reifenberger 2009). In contrast, in anaplastic astrocytomas (WHO grade III) an *EGFR* amplification is only found in about 10% of tumors (Riemenschneider and Reifenberger, 2009). Increased expression of the *EGFR* gene may result from amplification of the *EGFR* gene or from mutational activation (Weller et al., 2012). Deletions of the *EGFR* exons 2 to 7 result in a mutant receptor termed EGFRvIII. This mutant receptor is constitutively active in the absence of ligand

binding (Gan et al., 2009). Various studies aimed at targeting EGFR in glioblastoma patients, but the tested molecules did not demonstrate significant anti-tumor activity. Nevertheless, the EGFRvIII remains under investigation as a target for immunotherapy (Weller et al., 2012).

1.5.5 Combined loss of chromosomal arms 1p and 19q

Combined loss of chromosomal arms 1p and 19q can be frequently found in gliomas. However, this genetic aberration is more frequent in oligodendrogliomas or tumors with an oligodendroglial component. In primary glioblastomas it is rare and only found in about 10% of cases (Reifenberger et al., 1994; Riemenschneider and Reifenberger, 2009). The combined loss of chromosomal arms 1p and 19q was shown to result from a balanced whole chromosome arm translocation between chromosomes 1 and 19. As a consequence, two derivative chromosomes are formed; a 1q;19p translocation, and a 1p;19q translocation. The subsequent loss of the 1p;19q derivative results in the deletion of 1p and 19q often seen in oligodendroglial tumors (Griffin et al., 2006; Jenkins et al., 2006). Various studies have shown that tumors displaying a combined loss of 1p/19q, are associated with a better prognosis. This might be explained by a less aggressive tumor behavior and a better therapy response as compared to tumors without 1p/19q loss (Felsberg et al., 2004). Therefore, 1p/19q loss presently plays a role in diagnostics and is seen as a prognostic marker (Lass et al., 2013).

1.6 Pituitary adenomas

Pituitary adenomas are non-metastasizing benign tumors developing from different cells of the pituitary gland (Ezzat et al., 2004; Garcia-Arnes et al., 2013). Based on the size of the tumor, they are divided into microadenomas or macroadenomas. Furthermore, they are classified as functional or nonfunctional depending on their overall hormonal activity. Nonfunctional pituitary microadenomas often cause no symptoms. Therefore, they are underdiagnosed and may be found in postmortem examinations. Tumors with hormonal activity (functional tumors) cause clinical symptoms, such as mood disorders, sexual dysfunction, infertility, obesity, hypertension, diabetes mellitus, and accelerated heart disease (Asa and Ezzat, 2002). Tumors rapidly growing even without any hormonal activity can cause compressive mass effects and symptoms such visual (Asa and Ezzat, 2002; Ezzat et al., 2004). Prevalence rates are quite diverse and difficult to assess due to underdiagnoses. One study indicated that the prevalence of pituitary adenoma was 16.7% (Ezzat et al., 2004). Mutations in the *AIP* (aryl hydrocarbon receptor-interacting protein) gene seem to be associated with the development of pituitary adenoma, especially in familial cases (Vierimaa et al., 2006; Garcia-Arnes et al., 2013).

1.7 Malignant peripheral nerve sheath tumor (MPNST)

MPNST are rare tumors which usually develop from a peripheral nerve, but may also originate from ectopic Schwann cells. About 50% of MPNST are associated with neurofibromatosis type 1 (NF1) (Scheithauer et al., 2007). They arise either *de novo* in normal peripheral nerves or develop from neurofibromas (Yamaguchi et al., 2003). MPNST manifest as WHO grade II, III and IV (Scheithauer et al., 2007). Usually adults are affected between 30 and 60 years of age, but if the tumor is associated with NF1 the age of manifestation is younger than that of sporadic cases. Though both genders are affected it was found that sporadic MPNST are more often diagnosed in females, while the NF1-associated tumors occur slightly more often in males. The appearance of MPNST varies greatly, but histological features include hypercellularity, cytological atypia and increased mitotic activity as well as necrosis (Yamaguchi et al., 2003; Scheithauer et al., 2007). Genetic analyses revealed complex karyotypes, with numerical and structural chromosomal aberrations. Overall, MPNST tumors show a poor prognosis with an overall survival rate of 23% after 10 years (Ducatman et al., 1986).

1.8 German Glioma Network (GGN)

The GGN is a prospective, non-interventional cohort study that involves several clinical centers at different university hospitals in Germany (www.gliomnetzwerk.de) and was supported by the German Cancer Aid from 2004 to 2012. The aim of the GGN was to build up a database to connect clinical information, i.e. the therapy applied and the clinical course observed, with the molecular basis underlying glioblastoma development. The centers of the network represent specialists in neurosurgery, neurooncology, neuroradiology, neuropathology, human genetics and biometry. Up to now, the network has collected clinical data from over 4000 patients, and tumor samples for the molecular analyses of genomic alterations and gene expression are available from over 3000 patients. As part of the GGN, this study aimed to generate genomic profiles of the different glioma subtypes, by employing array-based comparative genomic hybridization to allow the identification of chromosomal regions harboring potential oncogenes and tumor suppressor genes. Another aim was to correlate aberrations in the identified glioma relevant genes with tumor type and clinical course of glioma patients to identify new diagnostic and prognostic molecular markers.

1.9 Syndromal phenotypes that include cancer predisposition, e.g. Bloom syndrome

The term syndrome is used when a phenotype is associated with several clinical features. These features include intellectual disability, defined as an IQ of below 70, the malformation of inner organs, facial and growth anomalies and sometimes cancer predisposition. The underlying genetic cause can be microduplications or microdeletions as well as mutations in certain genes. Particularly complex phenotypes might not be explained by a single genetic alteration but by the sum of several different genetic changes. The genetic basis of syndromal phenotypes can be detected by employing

genome-wide screening methods such as array-CGH and, more recently, WES (Classen and Riehmer et al., 2013). A syndromic phenotype associated with cancer predisposition is the so called Bloom syndrome (OMIM BLM# 210900). It was first described by the dermatologist David Bloom in 1954 (Bloom, 1954) and is a rare disease with approximately 220 diagnosed cases between 1975 and 2003 (Hickson, 2003). The Bloom syndrome is an autosomal recessive disorder displaying the following features: pre- and postnatal growth deficiency, sun-sensitivity causing hypo- and hyper-pigmented skin, chromosomal instability and predisposition to malignancy. Other main symptoms have been described to be a narrow face, male infertility, a high pitched voice, immune deficiencies, chronic lung problems, and learning disabilities. The cancer types most frequently associated with Bloom syndrome are non-Hodgkin's lymphoma, leukemia and skin tumors (German, 1993; Knoch et al., 2012). On average, patients with Bloom syndrome develop cancer until an age of about 24 years (German, 1997). Moreover, the patients' death is usually related to cancer and occurs rather early, with the oldest described patient with Bloom syndrome being 49 years old when dying of cancer (German, 1997).

Mutations in the *BLM* gene, mapped to chromosomal band 15q26.1, have been discovered to be the cause of Bloom syndrome. The *BLM* gene is a tumor suppressor and belongs to the family of RecQ helicases, which are involved in the removal of mutations during DNA replication and maintain chromosome stability (Knoch et al., 2012).

1.10 Objectives of the study

The projects described in this work employ two genome-wide screening methods implemented to assess somatic DNA copy number changes in tumors of the central nervous system and in a patient with an unexplained syndromic phenotype including cancer predisposition.

In 1997, array-CGH was described for the first time (Solinas-Toldo et al., 1997) and is nowadays commonly used in research projects as well as in diagnostics. Besides array-CGH analyses, next generation sequencing was used to identify DNA sequence variants throughout the human exome in the germline of a patient with cancer predisposition.

The first project aimed to identify genomic profiles in low grade gliomas including WHO grade II astrocytomas, oligoastrocytomas and oligodendrogliomas as well as in WHO grade III anaplastic astrocytomas and anaplastic oligoastrocytomas. Tumor samples from the different glioma entities were analyzed using array-CGH, in order to detect common genetic imbalances in the different WHO grade II and III glioma entities.

In the second project, in order to identify molecular aberrations associated with long-term survival of patients with WHO grade IV glioblastoma multiforme, primary tumor samples from 94 GGN glioblastoma patients including long- and short-term survivors were analyzed using genome-wide DNA-microarrays. Molecular profiles were generated as well as bioinformatic analyzes were performed to assess the molecular aberrations in the distinct survival groups, taking into account established markers such as the *IDH1* and *IDH2* mutation status as well as *MGMT* promoter methylation.

In the third project, genome-wide DNA-microarrays were used to assess and compare DNA copy number changes in 27 primary and recurrent glioblastoma tumor pairs from patients of the GGN. The 27 tumor pairs were all wild-type *IDH1/2* glioblastomas. The aim was to find regions of genomic difference between primary and recurrent tumor pairs. Additionally, the goal was to identify candidate genes which are associated with therapy response and or tumor recurrence.

The fourth project dealt with the clonal relationship of two intracranial tumors from a 47-year old female patient (patient 1). The two tumors were studied using array-CGH because histological analysis alone could not clarify whether the second tumor was a recurrence of the primary tumor or whether they were distinct unrelated lesions.

In the fifth project, two genome-wide screening methods (array-CGH and whole exome sequencing) were used to identify the genetic basis of the highly complex phenotype of a patient (patient 2) presenting with unexplained syndromic intellectual disability and cancer predisposition.

2 Materials and methods

2.1 Materials

2.1.1 Chemicals and solutions

Product	**Manufacturer**
Standard chemicals (if not mentioned differently)	AppliChem, Darmstadt, Germany Sigma-Aldrich, Taufkirchen, Germany Merck, Darmstadt, Germany ROTH, Karlsruhe, Germany
2.5x Random Primer Solution	Invitrogen, Carlsbad, CA, USA
20x SSC	Invitrogen, Carlsbad, CA, USA
Amphotericin B	MP Biomedicals, Illkirch, France
Anti-avidin D	LINARIS GmbH, Wertheim-Bettingen, Germany
Antifade Vectashield *mounting medium*	Vector Laboratories Inc., Burlingame, CA, USA
Anti-mouse IgG TRITC	Sigma-Aldrich, St. Louis, MO, USA
Betaine	Sigma-Aldrich, St. Louis, MO, USA
β-mercaptoethanol	ROTH, Karlsruhe, Germany
Biotin-16-dUTP	F. Hoffmann-La Roche Ltd., Basel, Switzerland
Blue dextran 2000	GE Healthcare Life Sciences, Uppsala, Sweden
BM condimed	Roche, Mannheim, Germany
Colcemid	Roche, Mannheim, Germany
Cyanine-3-dCTP	Perkin Elmer, Waltham, MA, USA
Cyanine-5-dCTP	Perkin Elmer, Waltham, MA, USA
DAPI	Sigma-Aldrich, Taufkirchen, Germany
Dextran sulfate	GE Healthcare Life Sciences, Uppsala, Sweden
Digoxigenin-11-dUTP	F. Hoffmann-La Roche Ltd., Basel, Switzerland
DNAse I	F. Hoffmann-La Roche Ltd., Basel, Switzerland
DNA polymerase I	F. Hoffmann-La Roche Ltd., Basel, Switzerland
Dye Saver II solution	Genisphere Inc, Hatfield, PA, USA
ExoSAP-IT	Affymetrix, High Wycombe, UK
Fetal calf serum	PAA Laboratories, Pasching, Austria
Fixogum rubber cement	Marabuwerke GmbH&Co., Tamm, Germany
Formaldehyde	Merck, Darmstadt, Germany
HEPES-buffer	Gibco, Invitrogen GmbH, Darmstadt, Germany
Hi-Di™-formamide	Applied Biosystems, Darmstadt, Germany
Human Cot-1 DNA	Invitrogen, Carlsbad, CA, USA
Human genomic DNA: female	Promega Corporation, Madison, WI, USA
Human genomic DNA: male	Promega Corporation, Madison, WI, USA
Klenow fragment 40 U/µl	Invitrogen, Carlsbad, CA, USA
L-glutamine	Sigma-Aldrich, Taufkirchen, Germany
Monoclonal mouse anti-digoxin antibody	Sigma-Aldrich, St-Louis, MO, USA
Penicillin/ streptomycin	MP Biomedicals, Illkirch, France
Pepsin	Sigma-Aldrich, St. Louis, MO, USA
Phenol-chloroform-isoamyl alcohol (25:24:1)	ROTH, Karlsruhe, Germany
Proteinase K	Sigma-Aldrich, Taufkirchen, Germany
REDTaq ReadyMix PCR reaction mix with $MgCl_2$	Sigma-Aldrich, St. Louis, MO, USA
Salmon sperm DNA	Sigma-Aldrich, St. Louis, MO, USA
Sephadex G-50, superfine	Sigma-Aldrich, Taufkirchen, Germany
Sodium acetate	ROTH, Karlsruhe, Germany
Tween® 20	Sigma-Aldrich, Taufkirchen, Germany
UltraHyb Ultrasensitive Hybridization Solution	Invitrogen, Carlsbad, CA, USA

2.1.2 Equipment

Device	Manufacturer
3130XL Genetic Analyzer	Applied Biosystems, Darmstadt, Germany
Centrifuge 5417R (rotor F-45-30-11)	Eppendorf AG, Hamburg, Deutschland
Centrifuge 5810R (rotor A-4-81)	Eppendorf AG, Hamburg, Deutschland
HybArray12TM	Perkin Elmer, Beaconsfield, UK
Fluorescence microscope DCX	Leica, Wetzlar, Germany
Leica DM2500 microscope	Leica, Wetzlar, Germany
Leica DM IL LED	Leica, Wetzlar, Germany
Pipettes	Eppendorf AG, Hamburg, Deutschland
NanoDrop 2000 spectrophotometer	Thermo Scientific, Schwerte, Germany PeqLab, Erlangen, Germany
NimbleGen Hybridization System 4	Roche, Mannheim, Germany
NimbleGen Microarray Dryer	Roche, Mannheim, Germany
NimbleGen MS 200 Microarray Scanner	Roche, Mannheim, Germany
Thermocycler, Professional Trio	Biometra, Göttingen, Germany
Thermocycler PTC 200	MJ Research Inc., Bio-Rad Hercules, CA, USA

2.1.3 Consumables

Product	Manufacturer
10,6k BAC-array	In division of Bernhard Radlwimmer Group, Deutsches Krebsforschungszentrum, Heidelberg, Germany (head: Peter Lichter)
MicroCon YM30 columns	Millipore Corporation, Billerica, MA, USA
Multiscreen 96-well plates, 0.45 µm hydrophilic, low protein binding Durapore membrane	Merck Millipore, Tullagreen, Carrigtwohill, Irland
NimbleGen X1 mixer, includes mixer port seals	Roche, Mannheim, Germany
NimbleGen oligonucleotide array chromosome 6 specific (385k)	Roche, Mannheim, Germany
NimbleGen oligonucleotide array chromosome 22 specific (385k)	Roche, Mannheim, Germany
QualiPCR plate	Kisker Biotech, Steinfurt, Germany

2.1.4 Kits

Product	Manufacturer
BioPrime Array CGH Genomic Labelling System	Invitrogen, Carlsbad, CA, USA
BigDye Terminator v1.1 Cycle Sequencing Kit	Applied Biosystem, Warrington, UK
DyeEx 2.0 Spin Kit	Qiagen, Hilden, Germany
NimbleGen Dual-Color DNA Labeling Kit	Roche, Mannheim, Germany
NimbleGen Hybridization Kit	Roche, Mannheim, Germany
NimbleGen Wash Buffer Kit	Roche, Mannheim, Germany
NimbleGen Array Processing Accessories	Roche, Mannheim, Germany
Taq DNA polymerase including: dNTP's, 5x Q-Solution, *Taq* DNA polymerase, 10x PCR buffer	Qiagen, Hilden, Germany

2.1.5 Buffers

Commonly used buffers		
10x PBS (pH 7.4)	1.4 M 27 mM 15 mM 65 mM	NaCl KCl KH_2PO_4 Na_2HPO_4
20x SSC (pH 7.0)	3 M 0.3 M	NaCl Na-Citrat
Extraction of genomic DNA from EDTA-blood		
Proteinase K [100 mg] dissolved in 10 ml buffer	1% 2 mM	SDS EDTA (pH 8.0)
Lysis buffer (pH 7.4)	155 mM 10 mM 0.1 mM	NH_4Cl $KHCO_3$ EDTA (pH 7.0)
Nucleus lysis buffer (pH 8.0)	75 mM 24 mM	NaCl EDTA (pH 7.0)
TE-buffer	10 mM 1 mM	Tris (pH 8.0) EDTA (pH 8.0)
DNA extraction from paraffin sections – phenol-chloroform extraction		
DNA isolation buffer	75 mM 25 mM 0.5%	NaCl EDTA (pH 8.0) Tween20
Proteinase K	See above	
Phenol/ TE-buffer (pH 7.5)	Phenol is equilibrated with TE-buffer (see above)	
Array-CGH		
dNTP mix	2 mM 2 mM 2 mM 1.1 mM	dATP dGTP dTTP dCTP
Wash buffer A (pH 7.0)	50% 2x 0.1%	Formamide SSC Tween20
Wash buffer B (pH 7.0)	2x 0.05%	SSC Tween20
Wash buffer C (pH 7.0)	1x 0.05%	PBS Tween20
FISH		
Cell culture medium	80% 7% 10% 200 mM 4 mM 0.4% 0.2%	Ham´s F10 medium Fetal calf serum BM condimed L-glutamine HEPES-buffer Penicillin/ streptomycin Amphotericin B
Fixative	3 parts 1 part	Methanol Acetic acid
Pepsin - solution	10 mM 0.07%	HCl Pepsin
10x PBS (pH 7.4)	1.4 M 27 mM 15 mM 65 mM	NaCl KCl KH_2PO_4 Na_2HPO_4 x 2 H_2O

PBS-magnesium chloride	5% 95%	1 M Magnesium chloride 1x PBS
10x NT buffer (storage at -20°C)	0.5 M 50 mM 0.5 mg/ ml	Tris-HCl (pH 7.5) Magnesium chloride BSA
Stopmix (storage at 4°C)	20% (w/v) 1.7 mM 2 mM 2 mM	Blue dextran NaCl EDTA Tris-HCl (pH 7.5)
Mastermix	20% (w/v) ad 20 ml	Dextran sulfate 2x SSC
Denaturation mixture	10% 0.7% 70%	20x SSC HCl Formamide
Blocking solution	0.2% 0.09 g ad 3 ml	Tween20 BSA 4x SSC
Detection solution	1 part 3 parts	Blocking solution 4x SSC/ Tween20
Antibody solution I	10 ng/ µl ad 1 ml	Avidin-FITC Detection solution
Antibody solution II	2.5 ng/ µl 2 µl ad 1 ml	Anti-avidin Anti-dig Detection solution
Antibody solution III	10 ng/ µl 10 µl ad 1 ml	Avidin-FITC Anti-mouse-TRITC Detection solution

2.1.6 Primers

All primers were ordered from MWG Operon, Ebersberg, Germany, used in a working concentration of 10 µM and stored at -20°C.

Gene and exon	**Forward primer 5'→ 3'**	**Reverse primer 5'→ 3'**
BLM exon 6	gct ttt gtg gcc tac cag ag	ggc aat gat gat ttg cta tgg
BLM exon 13	agc aca cat gaa ttc ctt gc	cag ttt gca ttc tac atg tgc
CHEK2 exon 11	ctg gtc ttc tca cag tac tct g	gac aga aca aga acc tgt ctc

2.1.7 Software

Software	**Manufacturer**
BioEdit Sequence Alignment Editor	Ibis Biosciences, Carlsbad, CA, USA
Gene PixPro 6.1	Molecular Devices Corporation, Sunnyvale, CA, USA
Leica CW 4000 FISH	Leica, Wetzlar, Germany
NimbleGen MS200 Data Collections Software Version 1.2	Roche, Mannheim, Germany
NimbleScan Version 2.5	Roche, Mannheim, Germany
SeqPilot	JSI Medical Systems GmbH, Kippenheim, Germany
SignalMap Version 1.9	Roche, Mannheim, Germany

2.1.8 Online resources

Database	URL
Chipyard framework	http://www.dkfz.de/genetics/ChipYard/
Ensembl Genome Browser	http://www.ensembl.org/index.html
Genome Trax™	https://portal.biobase-international.com/cgi-bin/portal/login.cgi
GGN	www.gliomnetzwerk.de
MutationTaster	http://www.mutationtaster.org
PolyPhen-2	http://genetics.bwh.harvard.edu/pph2/
PROTEOME™	http://www.biobase-international.com/product/proteome
SIFT	http://sift.jcvi.org/
TCGA	http://tcga-portal.nci.nih.gov/tcga-portal/AnomalySearch.jsp
UCSC Genome Browser	http://genome.ucsc.edu/

2.1.9 Patients from the GGN

Being part of the GGN, we received DNA from more than 300 glioma samples. The DNA had been extracted from shock-frozen tumor samples by ultracentrifugation over caesium chloride (van den Boom et al., 2003) and was stored at 4°C. Only samples were chosen for molecular analyses with a histologically estimated tumor cell content of 80% or more. All tumors were reviewed at the Brain Tumor Reference Centre of the German Society of Neuropathology and Neuroanatomy. Classification was done according to the World Health Organization (WHO) Classification of Tumors of the Central Nervous System (Louis et al., 2007a). For all samples, molecular analysis to detect the *IDH1* and *IDH2* mutation status had been performed by Sanger sequencing or pyrosequencing. The *MGMT* promoter methylation status had also been determined. All patients included in this study gave their written informed consent for the participation in the GGN and its research projects.

Characteristics of patients in project 2 are listed in the Results section in Table 11 and Table 12 (3.2, page 55). Characteristics of patients in project 3 are listed in Table 14 and Table 15 (3.3, page 69). All patient characteristics data was collected in a database of the GGN and was prepared in cooperation with the Institute for Medical Informatics, Statistics and Epidemiology of the University of Leipzig.

2.1.10 Clinical features of patient 1

Until female patient 1 presented with headache, reduced performance, deterioration of visual acuity and amenorrhoea at an age of 47 years, the medical history had been unremarkable (Hofer et al., 2012). By magnetic resonance imaging (MRI) the patient was diagnosed with an intra-, para- and suprasellar mass. The tumor was removed surgically and three different Neuropathology reference centers made the histological diagnosis: highly fibrotic pituitary adenoma. Three months after the initial surgery, patient 1 presented with increased fatigue and electrolyte disturbances including low potassium and sodium serum levels. A second tumor was diagnosed in the pituitary region with a size of 4.8 x 4.8 cm by computed tomography (CT) and MRI scans with contrast enhancement. After

treatment of the electrolyte disturbances, the second tumor was surgically removed using a transsphenoidal approach. The tumor could only be partially removed, due to the fact that it was tough and vascularized. Therefore, a third resection one week later was necessary, this time via a pterional approach. An early postoperative MRI revealed that residual tumor remained bilaterally within the cavernous sinus. Therefore, irradiation treatment (49.4 Gy) was initiated. Nevertheless, nine months after the third surgery, the patient was in a comatose state and yet another MRI scan revealed pronounced tumor progression. In spite of a fourth emergency surgery, the patient died.

2.1.11 Clinical features of patient 2

Patient 2 is the second daughter of non-consanguineous parents of German descent (Classen and Riehmer et al., 2013). Already early in life, certain stigmata became apparent, including slightly peculiar facial appearance with a depressed nasal root and widely spaced eyes, numerous café-au-lait spots (diameter >2 cm) and two small white spots.

The patient showed an overall psychomotor and mental delay persisting until adult age. At 23 years of age, her movements show a dystonic atactic component including an asymmetric preference of the left side. Speech understanding is present, whereas active speech reached a maximum of two words. The patient requires full-time care and lives in a special institution for fully handicapped persons.

Throughout life, patient 2 showed persistently low body weight and short stature. At birth (38 + 2 weeks), she was found small for gestational age with a body weight (BW) of 2,160 g (300 g <3rd percentile) and a body length (BL) of 46 cm (10th percentile). This tendency was ongoing throughout life (see Table 1).

Table 1: Growth curve parameters of patient 2

Age	Body weight	Body length	Head circumference
At birth	2,160 g (300 g <3rd P)	46 cm (10th P)	NA
11 months	6,410 g (800 g <3rd P)	70 cm (3rd P)	43.3 cm (3rd P)
8 years	19 kg (3rd P)	125 cm (10th P)	49 cm (10th P)
19 years	45.5 kg (2 kg <3rd P)	148 cm (8 cm <3rd P)	50 cm (10th P)

P: percentile

In the family of patient 2, the maternal grandfather was diagnosed with colon cancer and died from it at the age of 64 years. The maternal grandmother was diagnosed with leukemia and died at the age of 59 years. The patient's first malignancy was diagnosed at the age of eight years and was found to be a both-sided mixed malignant germ cell tumor of the ovaries. According to the staging system of the International Federation of Gynecology and Obstetrics (FIGO) it was stage IIIa. On the left side, it was classified as a mixed malignant germ cell tumor with components of a mature teratoma, immature teratoma, embryonal carcinoma, malignant yolk sac tumor, dysgerminoma and

chorion carcinoma with lymphangitic carcinosis. On the right side, it was a mixed malignant germ cell tumor with components of a gonadoblastoma and dysgerminoma with syncytial giant cells. As a first line treatment, a both-sided salpingo-oophorectomy was performed with subsequent treatment with a stage-adapted chemotherapy according to the GPOH MAKEI-96 protocol for malignant germ cell tumors. The chemotherapy was poorly tolerated.

Later at the age of 19 years, the patient was found to have an acute pre-B-lymphoblastic leukemia after she had presented with anemia, thrombocytopenia and leukocytosis. The leukemic cells did not contain a Philadelphia chromosome or MLL rearrangements, which can often be found in secondary leukemias. In the initial treatment, patient 2 responded well to prednisone and received a polychemotherapy according to the ALL-BFM 2000 protocol with the current modifications. As before, the chemotherapy was not well tolerated. Nevertheless, the patient went into remission. Now at the age of 23 years, the patient is in full remission from both malignancies.

Written informed consent was obtained from the parents of patient 2. The patient's history and molecular findings have been published in Classen and Riehmer et al., 2013.

2.2 Methods

2.2.1 Extraction of genomic DNA from EDTA-blood samples

Genomic DNA was extracted from peripheral blood of patient 2 and her parents. Five to 10 ml of EDTA-blood was transferred into a 50 ml Falcon tube, 35 ml lysis buffer was added. The tube was inverted in order to lyse the erythrocytes. The samples were incubated on ice for about 15 minutes until the lysis of the erythrocytes was complete, as indicated by the clear red color of the sample. A centrifugation step followed for 15 minutes at 1500 rpm and 4°C. The supernatant was discarded; the resulting pellet was resuspended in 5 ml nucleus lysis buffer. Then, 320 µl 10% SDS solution and 160 µl proteinase K (10 mg/ml) were added, the tube was vortexed and incubated overnight at 37°C in a water bath. Saturated sodium chloride (NaCl) solution was added, the tube was vortexed and centrifuged at 4000 rpm for 10 minutes at room temperature. The supernatant was transferred to a new Falcon tube (50 ml) and for precipitation of the DNA, 2.5 ml isopropanol was added. The visible DNA was extracted with a yellow pipet tip and washed in 70% ethanol; subsequently, it was dissolved in 200 – 500 µl TE-buffer and stored at 4°C.

2.2.2 DNA extraction from paraffin sections – phenol-chloroform extraction

The phenol-chloroform extraction is a biochemical DNA extraction method, which can be used to separate proteins, DNA and RNA. It is based on the difference of solubility of the three macromolecules. In this case, DNA was extracted from the formalin-fixed paraffin-embedded tumors of patient 1 as previously described (Weber et al., 1996).

In order to dissolve the paraffin, 1 ml of Xylol was added to the formalin-fixed paraffin-embedded tissue and incubated for 15 minutes at 45°C in a water bath, in between the samples were shortly vortexed. Thereafter, the samples were centrifuged for 15 minutes at 13000 rpm. The supernatant was removed, if necessary the treatment with Xylol was repeated. After removing the supernatant, 1 ml 100% ethanol was added, the samples were vortexed and centrifuged again for 10 minutes at 13000 rpm. This washing step was repeated once. The supernatant was removed and the pellets were dried for 1 h with an open lid at 37°C. The pellets were dissolved in 1 ml 1 M sodium thiocyanate, vortexed and incubated over night at 37°C in a water bath. The next day, the samples were centrifuged for 10 minutes at 13000 rpm and the supernatant was removed. After the addition of 1 ml DNA isolation buffer, the samples were vortexed and centrifuged again at 13000 rpm for 10 minutes. The supernatant was carefully removed, 400 µl DNA isolation buffer and 20 µl proteinase K (10 mg/µl) were added to each sample and incubated over night at 55°C. On day three, 400 µl phenol/ TE-buffer was added and the samples were rotated slowly for 10 – 30 minutes. After that, the samples were centrifuged again for 10 minutes at 13000 rpm. The upper aqueous phase, which contains the DNA, was removed and transferred into a new reaction tube. 400 µl of phenol-chloroform-isoamyl alcohol (25:24:1) was added, the tubes were vortexed and centrifuged for 10 minutes at 13000 rpm. This step was repeated once. Then, only 400 µl of chloroform-isoamyl alcohol

(24:1) was added and the tubes were centrifuged as above. The upper aqueous phase was transferred into a new tube and twice the volume (800 µl) of cold 100% ethanol (4°C) was added. For DNA precipitation, the samples were incubated for several hours at -20°C or 30 minutes at -80°C and centrifuged for 30 minutes at 13000 rpm and 4°C. The supernatant was carefully removed, the pellet was washed with 150 µl of 70% ethanol and the tubes were centrifuged for 10 minutes at 13000 rpm. The supernatant was removed again, and the pellet was dried completely. Subsequently, each pallet it was dissolved in 20 – 40 µl of H_2O depending on the pellet size. The DNA samples were then stored at 4°C.

2.2.3 Determination of DNA concentration

The concentration of the DNA/RNA can be determined by a spectrophotometric measurement. Here, the DNA concentration was determined by using a NanoDrop 2000 spectrophotometer. The absorption at 260 nm indicates the concentration of the measured nucleic acid. In order to evaluate the DNA quality, the absorption is measured at 260 nm and 280 nm. A 260/280 ratio between 1.8 and 2.0 indicates a good DNA or RNA quality. Values below 1.8 indicate a contamination with, for example, proteins.

2.2.4 Fluorescence *in situ* hybridization (FISH)

FISH is a molecular cytogenetic method that can be used to detect or verify microdeletions or microduplications. FISH was performed on interphase nuclei from peripheral blood of patient 2 and her mother. The advantage of interphase FISH is that the chromosomes are much less condensed than during metaphase (Strachan and Read, 2011). The first step of FISH is to do a chromosome preparation in which interphase nuclei are also present. In order to make a chromosome preparation, a cell suspension is required.

Cell suspensions from peripheral blood of patient 2 and her mother were prepared by the cytogenetic diagnostics laboratory of the Institute of Human Genetics, University of Bonn. It was done according to the following protocol. Five ml of heparin blood was mixed with 45 ml cell culture medium and incubated at 37°C for 1 – 2 h with an open lid of the cell culture flask. Then the lid was closed. After 72 h of incubation, 500 µl colcemid (1 µg/100 µl) were added. Colcemid inhibits the spindle fiber formation, so cells cannot go into anaphase during mitosis, resulting in an increase of cells in metaphase. After incubation with colcemid for 15 – 30 minutes at 37°C, the cell suspension was transferred and split into two 50 ml Falcon tubes. Then a centrifugation step followed for 10 minutes at 1200 rpm. The supernatant was discarded and the cell pellet was resuspended in 40 ml 0.0375M potassium chloride (KCl). The tubes were then incubated again at 37°C for 20 minutes in a water bath and centrifuged for 10 minutes at 1200 rpm. The cell pellet was resuspended with 20 ml fixative, consisting of methanol and acetic acid in a ratio of 3:1, and centrifuged for 10 minutes at 1200 rpm and 4°C. The fixation was repeated several times, the cell suspension was stored at -20°C.

2.2.4.1 Generating chromosome preparations

Before the chromosome spreads were prepared, the glass slides were degreased using a mixture of ethanol and acetone (1:1 ratio) and dried. The cell suspension was washed once with the fixative (methanol: acetic acid 3:1 ratio), and tubes were centrifuged for 10 minutes at 1200 rpm and 4°C. Before the cell suspension was dropped onto the glass slide, the glass slides were dipped shortly into the fixative; then approximately 20 µl of the cell suspension was dropped onto the slide. After drying, for final fixation the slides were dipped into 70% acetic acid. The chromosome spreads were checked under the light microscope and the hybridization area was marked on the glass slide.

2.2.4.2 Pretreatment of chromosome preparations

In order to increase the hybridization efficiency of the labeled DNA probe to the chromosome preparations, the chromosome preparations were pretreated with the enzyme pepsin to digest the remaining cytoplasm. Subsequently, an additional fixation step was done with formaldehyde to preserve the chromosomal morphology. Then the chromosome preparations were dehydrated using increasing alcohol concentrations. The following protocol was used.

The slides were equilibrated shortly in 2x SSC buffer. The pepsin digestion consists of incubation with pepsin for 10 minutes at 37°C. Afterwards, the slides were washed twice for 5 minutes in 1x PBS and a third time for 5 minutes in 1x PBS supplemented with magnesium chloride (5% of 1 M $MgCl_2$). The post-fixation was done for 10 minutes in a solution containing 2.8% formaldehyde and PBS-magnesium chloride. Before dehydration the chromosome preparations were washed once again for 5 minutes in 1x PBS. Dehydration was done for 3 minutes each in 70%, 90% and 100% ethanol. Then, the glass slides were dried.

2.2.4.3 Labeling of DNA probes – nick translation

Nick translation is a method that can be employed to incorporate labeled nucleotides into DNA probes. Endonucleases such as DNase I can be used to introduce single strand breaks into double stranded DNA templates, so called nicks. These nicks serve as starting points for introduction of labeled nucleotides by the DNA polymerase I (Strachan and Read, 2011). The labelled nucleotides used were biotin-16-dUTP (bio-dUTP) and digoxigenin-11-dUTP (dig-dUTP), which can be detected by avidin or antibodies, respectively. Different DNA probes were labeled; dig-dUTP was used to label the test-probe, located in a chromosomal area that was suspected of harboring a duplication or deletion. Bio-dUTP was used to label the reference-probe.

For labeling of 1 µg DNA the following protocol was used, aqua dest was added to the reaction mixture to a final volume of 50 µl.

Table 2: Pipetting scheme for nick translation

Volume	Reagent
5 µl	10x NT-buffer
5 µl	0.1 M β-mercaptoethanol
5 µl	dNTPs
1 µl	Dig- or- bio-dUTPs (1 mM)
1 µl	DNase I (1 mg/ml)
1 µl	DNA polymerase I (500 U)
X µl	DNA-sample (1 µg)
ad 50 µl	H_2O

The resulting mixture was incubated for 1 h at 37°C and then cooled on ice to temporarily stop the reaction. In order to verify if the DNA probe has the desired length of 100 – 500 bp, agarose gel electrophoresis was performed. When necessary, the incubation of the reaction mixture was resumed at 37°C, until the desired length was achieved, then the same volume of stopmix (50 µl) was added to the mixture. The labeled DNA probe was stored at -20°C if not used immediately.

2.2.4.4 Preparation of hybridization mixture

Equal amounts of biotin and digoxigenin-labeled DNA (15 µl) were mixed with 6 µl human Cot-1-DNA and 1 µl salmon sperm DNA. The unlabeled human Cot-1-DNA was added to the hybridization mix to suppress repetitive DNA sequences. For precipitation, 1/10 of the volume of 3 M sodium acetate (3.7 µl) was added as well as 2.5x the volume of ice cold 100% ethanol (102 µl). The mixture was mixed well and incubated for 30 minutes at -80°C. Afterwards, the tubes were centrifuged for 30 minutes at 13000 rpm and 4°C. The supernatant was discarded, and the pellet was washed 3 times with 500 µl 70% ethanol and dried.

2.2.4.5 Hybridization

Due to the fact that the DNA probes as well as the template/chromosomes are double stranded, they had to be denatured, which was done by heat. The melting temperature, i.e. the temperature at which the double stranded DNA separates, depends on the composition of the DNA. The melting temperature rises, for example, with an increasing length of the DNA probe and its GC content due to the three hydrogen bonds between the complementary nucleotides. Addition of formamide destabilizes the hydrogen bonds and therefore reduces the melting temperature.

The precipitated DNA from the hybridization mix was dissolved in 6 µl formamide for at least 1 h at 37°C under constant shaking. 6 µl of a "mastermix", containing dextran sulfate, which increases the hybridization sensitivity, was added and mixed well. The DNA was denatured for 5 minutes at 75°C. Preannealing took place for 40 minutes at 37°C. During that time the slides with the chromosome preparations were incubated with 100 µl denaturation mixture (formamide, HCl and 20x SSC) for 1.45 minutes at 72°C in a metal box. Subsequently, the slides were dipped into ice cold 2x SSC and

dehydrated for 3 minutes each in ice cold 70%, 90% and 100% ethanol and dried. Then the prepared DNA probes were applied to the chromosome preparations, covered with a cover slip and sealed with fixogum. Hybridization took place at 37°C overnight in a dry chamber.

2.2.4.6 Washing steps and antibody detection

The slides were washed after hybridization to remove unbound DNA probes and minimize background staining. The labeled DNA probes were detected by avidin or antibodies; a counter stain with DAPI was used to visualize the chromosomes.

The slides were taken out of the hybridization chamber and the fixogum seal as well as the cover slip were removed. The slides were washed in 2x SSC at 37°C for 10 minutes under constant shaking. Then, the slides were washed twice in 0.2x SSC at 53°C for 7 minutes, shortly dipped and equilibrated in 4x SSC supplemented with Tween20. Following the washing steps, incubation with 150 µl blocking solution (containing BSA, Tween20 and 4x SSC) for 30 minutes at 37°C was performed in a moist chamber to block unspecific protein binding. Then, the slides were shortly dipped and equilibrated in 4x SSC/Tween20, followed by incubation for 30 minutes with 150 µl antibody solution I (containing avidin-FITC) at 37°C in a moist chamber. The slides were washed for 3x 5 minutes in 4x SSC/Tween20 at 45°C with constant shaking. Then, the slides were incubated with the second antibody solution II (containing anti-avidin and mouse anti-dig) for 45 minutes at 37°C in a moist chamber. A washing step followed as before for 3x 5 minutes in 4x SSC/Tween20 at 45°C with constant shaking. Then, incubation with 150 µl antibody solution III (containing avidin-FITC and anti-mouse-TRITC) followed at 37°C for 30 minutes. The slides were washed again for 3x 5 minutes in 4x SSC/Tween20 at 45°C with constant shaking. Then, the counter stain followed by incubation in a DAPI solution (0.03 mg/ ml) for 5 minutes at room temperature. One drop of antifade was added to the slide, which was then covered with a cover slip. Until analyzed by microscopy, the slides can be stored in the dark at 4°C. Images were acquired using the Leica epi fluorescence microscope DCX and image analysis was performed with the Leica CW 4000 FISH software. Monochromatic fluorescence images using filters for FITC, TRITC and DAPI were acquired of at least 20 interphase nuclei per hybridized slide.

2.2.5 Array-based comparative genomic hybridization (array-CGH)

Array-CGH (Solinas-Toldo et al., 1997; Pinkel et al., 1998) was used for the analysis of DNA samples from (i) more than 300 GGN gliomas, (ii) two tumors from patient 1, and (iii) peripheral blood from patient 2. This method can be used to identify copy number changes, such as losses, gains and amplifications, in a test compared to a control genome. The method is based on the hybridization of equal amounts of test and reference DNA together with human Cot-1-DNA, to a genomic DNA microarray.

In this study, a DNA microarray with 10,600 (10,6k array) large insert clones of known chromosomal locations was used. The microarrays were generated in Peter Lichter's group at the German Cancer Research Centre (Heidelberg, Germany), who described this method for the first time in 1997 (Solinas-Toldo et al., 1997). The composition of the 10,6k array was as follows: 3428 clones were from the 1 Mb clone set of Dr. N. P. Carter, Sanger Institute, Hinxton, Cambridge UK (Fiegler et al., 2003); 3000 RCPI (RZPD, Berlin, Germany) and CalTech (Invitrogen, Karlsruhe, Germany) BAC clones were added to increase the resolution to 0.5 Mb; 2000 clones covering the gene rich regions on chromosomes 1, 19 and 22 were added in order to achieve a tiling-path coverage of these regions; 2200 clones were added covering selected disease/ tumor relevant chromosomal regions at high resolution. The production of the microarrays was based on the Sanger Institute protocol (Fiegler et al., 2003; Fiegler et al., 2007).

2.2.5.1 DNA labeling for array-CGH

Before hybridization of the DNA to the microarrays, equal amounts of test and reference DNA were labeled with Cy3-dCTP or Cy5-dCTP using components of a BioPrime Array CGH Genomic Labeling System (Invitrogen, Carlsbad, CA, USA). The random primer and the Exo-Klenow fragment were used for the incorporation of the labeled nucleotides and amplification of the starting material. The used reference DNA contained pooled genomic DNA isolated from peripheral blood of ten healthy men or women. The hybridization was always sex matched. As a starting material, 1 µg of genomic DNA was used, which was mixed with 36 µl 2.5x random primer and 32 µl 5 M betaine and filled up with ddH_2O to a final reaction volume of 77.4 µl. Denaturation of the reaction mixture was done at 95°C for 10 minutes in a thermocycler. Subsequently, the samples were cooled down on ice and additional components of the labeling mixture were added, such as 9 µl 10x dNTP-mix; 1.8 µl 1 mM Cy3-dCTP's or Cy5-dCTP's and 1.8 µl of Klenow fragment (40 U/µl). Labeling of the DNA took place at 37°C overnight for 14 to 16 hours in a thermocycler.

MicroCon YM30 columns were used to purify the samples by removing unincorporated nucleotides as well as random primers. The MicroCon columns were used according to the manufacturers' instructions. The labeled DNA was eluted in 100 µl 0.1x SSC. The total amount of DNA and the dye incorporation into the labeled DNA were measured with an UV spectrophotometer. The absorption at 260 nm (DNA), 550 nm (Cy3) and 650 nm (Cy5) was determined for each sample.

The amount of DNA was calculated using the following formula:

$$\text{Concentration } \left[\frac{\mu g}{\mu l}\right] = \frac{A^{260} \times \text{dilution factor} \times 50\ \mu g}{1000\ \mu g}$$

The incorporation rate of Cy3-dCTP was calculated using the following formula:

$$\text{Cy3-dCTP-incorporation rate}\left[\frac{\text{dye}}{\text{bp}}\right]=\frac{A^{260}}{A^{550}}\times 23.15$$

The ideal value for the Cy3-dCTP incorporation was approximately one labeled nucleotide every 40 bp. But the experiment also worked if a labeled nucleotide was incorporated every 60 to 80 bp.

The incorporation rate of Cy5-dCTP was calculated using the following formula:

$$\text{Cy5-dCTP-incorporation rate}\left[\frac{\text{dye}}{\text{bp}}\right]=\frac{A^{260}}{A^{650}}\times 38.58$$

The ideal value for the Cy5-dCTP incorporation was approximately one labeled nucleotide every 60 bp. But the experiment also worked if a labeled nucleotide was incorporated every 80 to 100 bp.

2.2.5.2 Array-CGH sample preparation for hybridization

Equal amounts of 10 – 15 µg test and reference DNA were co-precipitated with 120 µg human Cot-1-DNA, 1/10 of the reaction volume of 3 M sodium acetate and 2.5x of the reaction volume of 100% ice cold ethanol. The reaction mixture was incubated for at least 30 minutes at -80°C and subsequently centrifuged for 30 minutes at 13000 rpm and 4°C. The supernatant was discarded and the resulting pellet was dissolved in 125 µl UltraHyb hybridization buffer at 37°C overnight while constantly shaking.

2.2.5.3 Array-CGH hybridization

Before a sample was applied to a microarray, the DNA was denatured at 75°C for 10 minutes and a preannealing step followed for 30 – 60 minutes at 37°C. During the annealing step, the microarrays were positioned in the separate hybridization chambers of the HybArray12 System, which permitted the simultaneous hybridization of up to 12 arrays. The hybridization and the subsequent stringency washing steps are listed in the table below:

Table 3: Protocol of hybridization and stringency washing steps

Step	Temperature	Duration
Denaturation of DNA microarrays	75°C	5 minutes
Addition/ injection of the probe	42°C	
Distribution of the probe	42°C	30 minutes
Hybridization	37°C	66 – 72h
Wash buffer B	37°C	30 sec washing, 5 sec holding
Wash buffer B	44°C	15 sec washing, 5 sec holding
Wash buffer A	44°C	20 sec washing, 3 min holding
Wash buffer B	44°C	20 sec washing, 5 sec holding
Wash buffer C	25°C	2 min washing, 5 sec holding

2.2.5.4 Preparation of the DNA microarrays for scanning

After the stringency washing steps, the microarrays were dipped into wash buffer C for a few seconds. For drying, the microarrays were introduced into a 50 ml Falcon tube and centrifuged for 2 minutes at 1500 rpm. Then, the microarrays were coated with Dye Saver II solution in order to prevent fading of the dyes.

2.2.5.5 Scanning of the DNA microarrays

The microarrays were scanned using the MS200 microarray scanner and the MS200 data collection software from NimbleGen, Roche. At first, a scanning area was defined, which was applied to all microarrays. Then, the arrays were scanned at a wavelength of 532 nm detecting Cy3 and at a wavelength of 635 nm detecting the Cy5. The scanning resolution was set to 5 µm at medium speed to increase the sensitivity of the scan. The scan was then saved as a multi-tiff image file and was further analyzed with the Genepix 6.1 software.

2.2.5.6 Data processing with the Genepix 6.1 software

The Genepix 6.1 software was used for the data processing of the multi-tiff image file. Firstly, a gps-file (genepix settings-file) or so called grid was uploaded, which included all information concerning the array design, such as the number of arrayblocks, the number of spots, the spot diameter, the spot distance and the spot name. The grid was placed over the array by a software tool which recognized each individual spot, but had to be corrected manually in some cases. Spots which could not be recognized by the software were excluded from further analysis. For each array, an individual setting was saved. Secondly, a gpr-file (genepix result-file) was generated using the information from the gps-file. The gpr-file summarized all the information about each spot such as location of the spot, chromosomal location, spot name, spot diameter and measured intensities. The most important features of the gpr-file are summed up in Table 4.

Table 4: Features of the gpr-file

Specifications	532 nm	635 nm
Block	F532 median	F635 median
Column	F532 mean	F635 mean
Row	F532 SD	F532 SD
X/Y localization	F532 CV	F635 CV
Spot name	B532 median	B635 median
Spot diameter	B532 mean	B635 mean
	B532 SD	B635 SD
	B532 CV	B635 CV

SD, standard deviation; CV, coefficient of variation; F, feature intensity; B, background

2.2.5.7 Data analysis and interpretation

Data analysis was performed using the Chipyard framework (http://www.dkfz.de/genetics/ChipYard/). Information about the hybridized test DNA samples as well as patient information were integrated into the database. The microarray data was uploaded to the Chipyard program as a gpr-file. There, the data was further processed, and a quality control of the microarrays took place. Spots with low quality were filtered out and the test to control ratio for each spot was calculated, and data normalization performed. A txt-file was generated, including the information for each clone (spotted in triplicate) on the microarray, such as the chromosomal location with chromosomal starting, mid and end point, a list of genes located in that area, as well as the normalized $\log_2$ ratios of test versus reference DNA for each clone (i.e. the calculated mean of the triplicates). A genomic profile was prepared for each analyzed sample, using the $\log_2$ ratios of test versus reference DNA of each clone. The data information was taken from the txt-file generated in Chipyard. Using the genomic profile, DNA copy number changes such as gains and losses were identified. Some frequency plots as well as the heatmaps from the data using different clustering approaches were prepared in cooperation with the Institute for Medical Informatics, Statistics and Epidemiology of the University of Leipzig.

2.2.6 Oligonucleotide arrays – NimbleGen

The hybridization of test and reference DNA to oligonucleotide arrays, in order to analyze copy number changes, is based on a similar principle as array-CGH (2.2.5, page 37). The difference is that the probes spotted on an oligonucleotide array are much shorter than on a BAC-array and do not contain repetitive sequences. They usually consist of 60 nucleotides, so called 60mers. Advantages of oligonucleotide arrays are that they achieve a much higher resolution and that hybridization does not require suppression of repetitive sequences. During this study, chromosome specific 385k (385000 probes) oligonucleotide tiling arrays from NimbleGen, Roche were used to identify the precise breakpoints of microduplications detected by BAC array-CGH in the germline of patient 2 and her parents. Equal amounts of test and reference DNA (from Promega) were labeled with the NimbleGen

Dual-Color DNA Labeling Kit according to the manufacturer's instructions. Only slight modifications were made, such as the reduction of the reaction mixture volume. It has been found that it was sufficient to label only 500 ng of test as well as reference DNA. The total reaction volume of the DNA labeling mixture was also reduced from 80 µl to 40 µl, including 20 µl of Cy3 or Cy5 random nonamers mixture and 500 ng DNA filled up to a final reaction volume of 40 µl with nuclease-free water. Denaturation of the samples was done at 98°C for 10 minutes in a thermocycler; subsequent cooling was performed in an ice cold water bath. Then, 10 µl of dNTP/ Klenow mastermix was added to each sample, including 5 µl 10 mM dNTP-mix, 4 µl nuclease-free water and 1 µl of Klenow fragment (3'->5' exo) 50 U/ µl. The complete reaction mixture of 50 µl was incubated overnight for approximately 14 h at 37°C in a thermocycler. The reaction was stopped with 10 µl 0.5 M EDTA solution. For precipitation of the labeled DNA samples, 6.5 µl 5 M NaCl were added, the tubes were vortexed and centrifuged. The reaction mixture was then transferred into a microcentrifuge tube containing 60 µl isopropanol. The mixture was vortexed again and incubated for 10 minutes in the dark at room temperature. Subsequently, the tubes were centrifuged for 10 minutes at 12000 rpm and the supernatant was carefully removed. A colored pellet, either pink for Cy3 or blue for the Cy5 labeled samples, was then visible. The pellet was washed once with 500 µl ice cold 80% ethanol. Again, the tubes were centrifuged for 10 minutes and 12000 rpm. After removing the supernatant, the pellet was dried, either at room temperature with an open tube lid or for 5 minutes in a SpeedVac. Then, the samples were either stored at -20°C or rehydrated with 15 µl nuclease free water. For complete dehydration, the samples were incubated for 5 minutes at room temperature in the dark. Then the concentration of the labeled DNA samples was determined with a Nanodrop spectrometer. According to the manufacturer's instructions for 385k arrays, 6 µg of labeled test DNA and 6 µg of labeled reference DNA were needed.

$$\text{needed µl} = \frac{6000\ \text{ng}}{\text{measured concentration}\ \left[\frac{\text{ng}}{\text{µl}}\right]}$$

Three hours prior to hybridization, the hybridization chambers were heated to 42°C. The calculated volumes containing 6 µg of labeled test DNA and 6 µg of labeled reference DNA were combined, filled up to a volume of 5 µl with nuclease-free water, and mixed with 13 µl of the hybridization master mix supplied by the hybridization kit. Hybridization master mix was prepared as follows according to the manufacturer's instructions.

Table 5: Pipetting scheme for the hybridization master mix

Hybridization kit components	**Amount for 385k array**
2x hybridization buffer	11.8 µl
Hybridization component A	4.7 µl
Alignment oligo	0.5 µl
Final volume	**17.0 µl**

After addition of the hybridization master mix, the samples were vortexed, centrifuged and incubated for 5 minutes at 95°C. During this time, the X1 mixers were attached to the arrays according to the manufacturer's instructions. The prepared arrays were incubated for at least 5 minutes at 42°C. Then, the samples were applied to the arrays, the fill ports were sealed, and hybridization took place over night for 16 – 20 hours.

Post hybridization steps were all performed according to the manufacturer's instructions. The NimbleGen wash buffer kit was used together with the NimbleGen array processing accessories. The slides were dried with the NimbleGen microarray dryer.

The microarrays were scanned using the MS200 microarray scanner and the MS200 data collection software from NimbleGen, Roche. Firstly, a scanning area was defined, which was applied to all microarrays. Then, the arrays were scanned at a wavelength of 532 nm detecting Cy3 and at a wavelength of 635 nm detecting the Cy5. The scanning resolution was set to 2 µm at medium speed to increase the sensitivity of the scan. The scan was then saved as a single-tiff image file and was further analyzed with the NimbleScan software version 2.5 for copy number analysis. The NimbleScan software was used to align the design file (.ndf) to the array, a procedure called gridding. The design file was provided for each array by the manufacturer and describes the position of the probes on the array. Then, the segMNT algorithm was used to further process the gridded image files (.tif).

Averaging windows of 2000 bp, 4000 bp and 10000 bp were used, meaning that the software takes the raw signal data of all probes inside the defined window and combines it to one single data point.

In the end, gff-files were generated, including the $\log_2$ ratio data for 532 nm and 635 nm. For evaluation and detection of copy number changes, the gff-files were viewed by the SignalMap software. As an additional feature, the software can be used to visualize the positions of genes, known segmental duplications of the human genome and ideograms for each chromosome. This information was also supplied by the manufacturer (Roche).

2.2.7 Sanger sequencing

Sanger sequencing is a method of DNA sequencing, which is also called the chain termination method. This method requires a DNA primer, a DNA polymerase, normal dNTP's as well as dideoxynucleotides (ddNTP's) labeled with a fluorescent dye, which cause termination of the DNA elongation. These ddNTP's lack a 3'-OH group, which is needed for a phosphodiester bond formation between the nucleotides. As soon as a ddNTP is incorporated, the elongation of the DNA stops resulting in synthesized DNA strands of various lengths, that can be separated by size e.g. by capillary electrophoresis. During electrophoresis, the DNA fragments pass a laser, the emitted fluorescence is measured and the sequence of the DNA is detected. The results are then visualized by an electropherogram (Strachan and Read, 2011).

2.2.7.1 Primer design

In order to sequence a certain DNA fragment by the Sanger method it needs to be amplified first. For amplification, for example, of an exon of a gene, polymerase chain reaction (PCR), a primer pair consisting of a forward primer (binding to the sense strand), and a reverse primer (from the anti-sense-strand) in 5'-3'orientation are needed. The primers are designed on the basis of the gene structure, which can be retrieved from databases such as the UCSC Genome Browser or ENSEMBL Genome Browser. The goal is to amplify one specific DNA sequence. So when designing primers, it is important that they are highly specific and are not able to bind to other DNA sequences, than the desired ones.

The following criteria were considered when designing primers:

- The lengths of the primers were kept between 18 – 24 bp, with an approximately equal distribution of all four bases.
- The primer sequence should not include a repeat of the same nucleotide that is longer than three nucleotides.
- The 3'-end of the primer should be a G or a C.

In order to amplify an exon from of genomic DNA, the primers should be located at least 60 bp before or after the exon/ splice site, otherwise sequencing of the complete exon might be difficult. In this study, primers were ordered from Eurofines/ MWG Operon, Ebersberg, Germany.

2.2.7.2 Polymerase chain reaction (PCR)

PCR is an *in vitro* technique to amplify even minute amounts of DNA and has found numerous applications in research and diagnostics. Essential for PCR are primers, which are synthesized oligonucleotides with a size of 18 – 25 base pairs. These primers are needed to target defined sequences, which have to be known. The DNA is amplified by thermocycling, consisting of three steps. The first step is denaturation, i.e. separation of the double stranded DNA template. Secondly, an annealing step follows, meaning that the primers are allowed to bind to their complementary sequence on the single stranded DNA target. Third and last step is the elongation step, in which the DNA polymerase initiates the synthesis of a new DNA fragment (Strachan and Read, 2011). These thermocycling steps are repeated up to 40 times until the desired PCR product is present in a sufficient amount.

In order to amplify the DNA fragment from genomic DNA prior to sequencing, PCR was performed in a volume of 25 µl including *Taq*-DNA polymerase, forward and reverse primer, 100 ng genomic DNA and H_2O. In this study, the RED*Taq* ReadyMix PCR reaction mix with $MgCl_2$ from Sigma or the *Taq* DNA polymerase from Qiagen were used. The ReadyMix already includes all components needed for

the PCR. When using the *Taq* DNA polymerase, 10x buffer, dNTP's and Q-solution had to be added separately.

Table 6: Pipetting scheme for standard PCR using *Taq* DNA polymerase from Qiagen

Reagent	Volume
Q-solution	5 µl
Buffer (10x)	2.5 µl
dNTP's	2.5 µl
Taq DNA polymerase	0.15 µl
Fwd-primer [10 pmol/µl]	1 µl
Rev-primer [10 pmol/µl]	1 µl
DNA [20 ng/µl]	5 µl
H_2O	7.85 µl
Final volume	**25 µl**

Table 7: Temperature profile of a standard PCR

Step	Temperature	Duration	Number of cycles
Pre-annealing	95°C	5 minutes	1
Denaturation Annealing Extension	95°C 60°C 72°C	30 seconds 30 seconds 2 minutes	17
Denaturation Annealing Extension	95°C 58°C 72°C	30 seconds 30 seconds 2 minutes	20
Final extension	72°C	10 minutes	1
Cooling	4°C	Forever	

For all primer pairs, this temperature profile for the PCR was used.

2.2.7.3 Enzymatic cleanup of PCR products by ExoSAP-IT

After PCR, the products were visualized after separation in a 2% agarose gel, in order to see if the PCR yielded a specific PCR product of the desired length. If this was the case, an enzymatic cleanup to remove unbound/ unconsumed nucleotides and the primers was performed in the PCR products. For this cleanup step two enzymes are used. Exonuclease I removes single-stranded DNA such as primers and other single-stranded DNA products generated during PCR. The Shrimp Alkaline Phosphatase (SAP) removes the unbound dNTP's. For cleanup of the PCR products, 2 µl of the ExoSAP-IT solution from the kit were mixed with 5 µl of PCR product. The reaction mixture was incubated in a thermocycler following the protocol detailed in Table 8.

Table 8: Thermocycling protocol for enzymatic cleanup

Step	Temperature	Duration
Enzymatic reaction	37°C	25 minutes
Inactivation of enzymes	80°C	30 minutes
Cooling	12°C	Forever

2.2.7.4 Sequencing reaction using the BigDye Terminator v1.1 Cycle Sequencing Kit

In this step, ddNTP's labeled with a fluorescent dye were incorporated, resulting in DNA fragments of various sizes. For the sequencing reactions, the BigDye Terminator v1.1 cycle sequencing kit from Applied Biosystems was used according to the manufacturer's instructions. The same primers were used as for the amplification of the specific DNA fragment by PCR (2.2.7.2, page 44), this time diluted to a final concentration of 1 pmol/µl. However for sequencing, either the forward or the reverse primer was selected. Sometimes sequencing was repeated with the other primer not used in the first reaction. The pipetting scheme and thermocycling protocol are shown in Table 9.

Table 9: Pipetting scheme for a sequencing reaction

Reagent	**Amount**
BigDye Terminator v1.1	1 µl
5x sequencing buffer	2 µl
Fwd or rev primer [1 pmol/µl]	1 µl
PCR product (ExoSAP-treated)	2 µl
H_2O	4 µl
Final volume	**10 µl**

Table 10: Temperature profile of a sequencing reaction

Step	**Temperature**	**Duration**	**Number of cycles**
Denaturation	95°C	3 minutes	1
Denaturation Annealing Extension	95°C 50°C 60°C	20 seconds 30 seconds 4 minutes	26
Cooling	12°C	Forever	

After the sequencing reaction each sample was diluted 1:1 with 10 µl HPLC-H_2O for another cleanup step.

2.2.7.5 Cleaning up of sequencing reaction and sequencing analysis

Before the samples were analyzed by the sequencer, the sequencing reaction products were cleaned up, in order to remove surplus unbound ddNTP's from the reaction mixture. During this study, two different methods were used, depending on the number of samples analyzed. Sephadex G-50 96-well plates were used when the number of samples was high. After soaking Sephadex G-50 in water, a gel matrix develops, which is used to retain small molecules. For single samples or small sample sizes, the DyeEx 2.0 Spin Kit from Qiagen was used according to the manufacturer's instructions.

In order to prepare the Sephadex plates, the MultiScreen column loader was used, which distributes Sephadex G-50 evenly in each well. A 96-well MultiScreen plate from Millipore was placed on top of it, with the upside facing the MultiScreen column loader plate. Then, both plates were

inverted and the Sephadex G-50 was transferred to the 96-MultiScreen plate. 300 µl HPLC-H_2O was added to each well and incubated for 3 hours at room temperature or overnight at 4°C, to let the Sephadex G-50 swell and form a gel matrix. The MultiScreen plate was centrifuged at 2000 rpm for 5 minutes, the collecting plate was emptied. The MultiScreen plate was washed once with 150 µl HPLC-H_2O and centrifuged again as before. During the centrifugation steps, a QualiPCR plate was prepared, adding 15 µl Hi-Di™-formamide to each well. The MultiScreen plate was then placed on top of the QualiPCR plate, and 20 µl of the diluted sequencing reaction was applied onto the gel matrix. The plates were centrifuged once again as described above. During this step, the sequencing reaction passes the gel matrix, where the unbound ddNTP's remained, and the DNA fragments passed through and were directly added to the Hi-Di™-formamide. The plates were covered and stored at 4°C until they were sequenced on a 3130XL Genetic Analyzer (Applied Biosystems, Darmstadt, Germany).

Alternatively, the DyeEx 2.0 Spin Kit was used for cleaning up the sequencing reactions, according to the manufacturer's instructions. The spin columns were shortly vortexed to resuspend the resin. Then, each the spin column was placed in a 2 ml collecting tube and centrifuged for 3 minutes at 3000 rpm to remove the buffer and to generate a gel matrix. Each column was transferred to a microcentrifuge tube and the diluted sequencing reaction (generated in 2.2.7.4, page 46) was applied onto the gel matrix without touching it. After the sample was loaded to the column, the spin column was centrifuged again for 3 minutes at 3000 rpm. The flow-through was then added to 15 µl Hi-Di™-formamide and stored at 4°C until the probes were sequenced on a 3130XL Genetic Analyzer (Applied Biosystems, Darmstadt, Germany). Electropherograms were analyzed using the BioEdit Sequence Alignment Editor software or the SeqPilot software.

2.2.8 Whole exome sequencing (WES)

WES on genomic DNA isolated from peripheral blood (2.2.1, page 33) of patient 2 and her parents was performed by CeGaT GmbH, Tübingen, Germany. DNA hybridization capture was performed using the Agilent SureSelect whole exome enrichment (v4) kit and samples were sequenced one exome per lane with 75 bp reads on a SOLiD 5500x1 system according to the manufacturer's protocols. All samples were sequenced to a mean target coverage of >50x. Data were analyzed using the CeGaT exome analysis pipeline (Classen and Riehmer et al., 2013).

Filtering of WES data was based on different steps. Firstly, all variants were removed exhibiting a coverage of lower than 20 or a bad quality. Known variants from the CeGaT in-house exomes were also removed. Secondly, only serious variants defined as frameshift mutations, stop gained or lost, non-synonymous coding or essential splice site mutations were retained. Thirdly, predictions of variant deleteriousness were performed using online prediction tools such as SIFT, PolyPhen-2 and MutationTaster. Then, in order to find pathogenic or functionally relevant variants, the serious and deleterious variants were processed by the mining tool Genome Trax™ (Biobase GmbH, Wolfenbuettel, Germany). Genome Trax™ uses peer-reviewed literature to identify variants and provides information about conservation, allele frequency, effect on protein sequence, and

deleterious predictions in order to assess the variants. Data filtering using Genome Trax™ was particularly based on annotations on inherited disease genes from Human Gene Mutation Database (HGMD®), on disease associated mutations from HGMD, and on functional disease-related SNPs (Classen and Riehmer et al., 2013).

3 Results

3.1 Project 1: Array-CGH analysis of WHO grade II and WHO grade III gliomas

The first project of this study aimed at characterizing the genomic imbalances in low-grade gliomas including WHO grade II astrocytomas, oligoastrocytomas and oligodendrogliomas as well as WHO grade III anaplastic astrocytomas and anaplastic oligoastrocytomas. DNA from tumor samples of the different glioma entities was analyzed using array-CGH, with the purpose to detect DNA copy number changes in gliomas of WHO grade II and III.

3.1.1 Genomic profiles in WHO grade II gliomas

In order to characterize DNA of copy number changes on a genome-wide scale in low-grade gliomas, DNA of tumor samples collected within the GGN were analyzed by array-CGH (diffuse astrocytomas: n=53; oligoastrocytomas: n=17; oligodendrogliomas: n=3). Some selected array-CGH profiles of diffuse astrocytomas of WHO grade II are depicted in Figure 4 sorted according to their *IDH* status. Figure 4A – D shows profiles of astrocytomas, which have been found to be *IDH1/2* wild-type, whereas Figure 4E – H depicts genomic profiles of astrocytomas harboring a mutation within the *IDH1* or *IDH2* gene. Interestingly, in the *IDH1/2* wild-type astrocytomas copy number changes were detected which are typically found in *IDH1/2* wild-type glioblastomas. These genetic alterations include copy number gain on chromosome 7 (Figure 4A – D), including a clear amplification of the *EGFR* gene located in 7p11.2 in one case (Figure 4D: 5 clones with a $\log_2$ ratio above 1). Further, gains of chromosomes 19 and 20 were apparent (Figure 4B and 4D). Another genetic imbalance typical for *IDH1/2* wild-type glioblastomas is a loss on chromosome 10, which was also seen in the analyzed diffuse astrocytomas (Figure 4B, C and D). Other genetic alterations could be detected both in *IDH1/2* wild-type and mutant astrocytomas, such as deletions on chromosome 4 (Figure 4A, C, G, H). Further copy number gains could be found in single tumors on chromosome 8 (Figure 4F), chromosome 11 (Figure 4E), and on chromosome 18 (Figure 4E and G). Deletions of chromosomal arm 13q were found in three astrocytomas independent of the *IDH1/2* status (Figure 4D, F and H). The genomic profiles in Figure 4 suggest that DNA copy number changes are more heterogeneous in *IDH1/2* mutant astrocytomas than in *IDH1/2* wild-type astrocytomas.

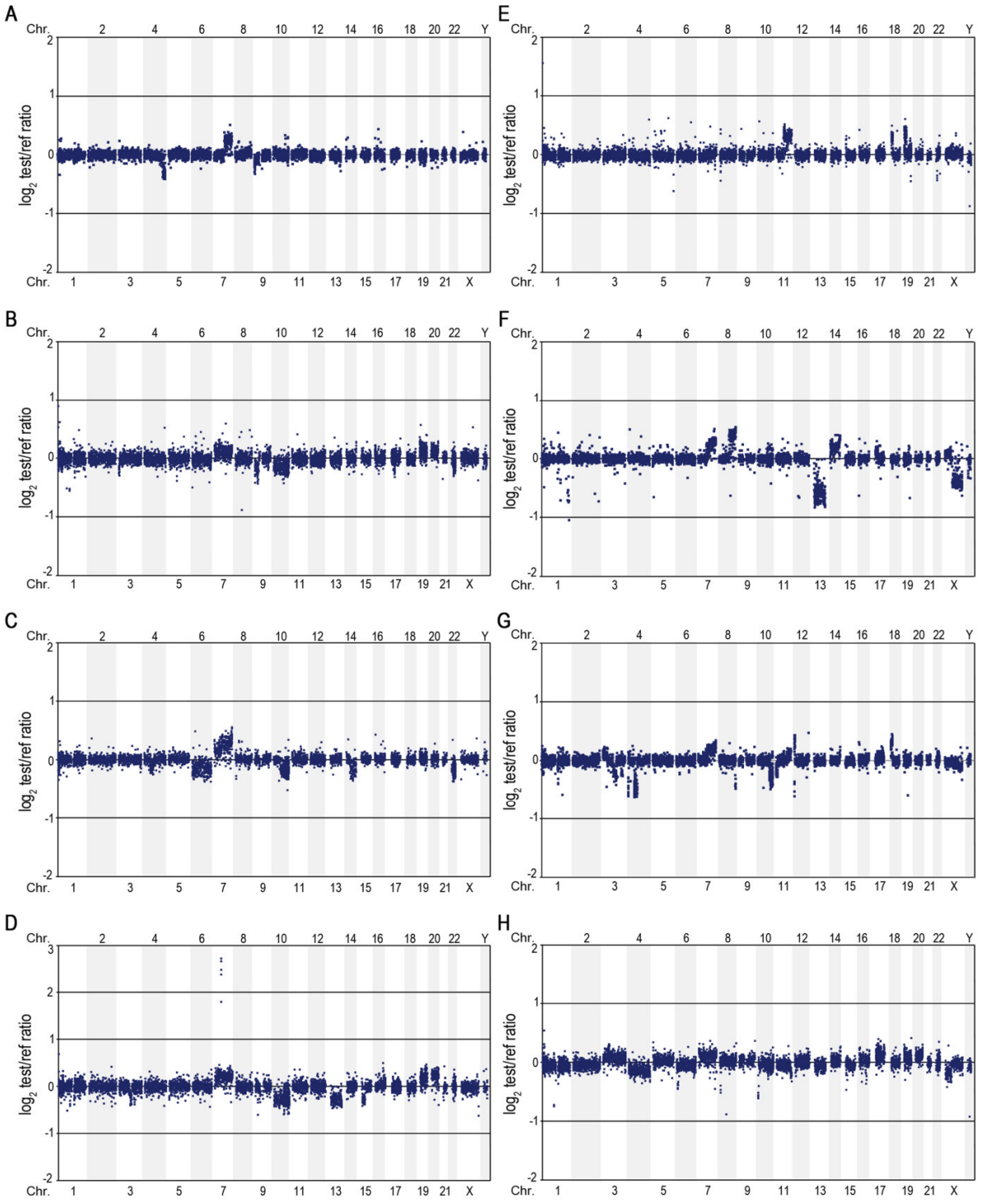

Figure 4: Array-CGH profiles of WHO grade II diffuse astrocytomas.
A-D: Selected array-CGH profiles from astrocytomas with an *IDH1/2* wild-type status show a varying degree of chromosomal alterations. **E-H:** selected array-CGH profiles from astrocytomas with an *IDH1/2* mutant status. The midpoints of all BAC clones are plotted in genomic order from 1p to Yq on the x-axis against their normalized $\log_2$ test to reference ratio on the y-axis.

Figure 5 shows array-CGH profiles of oligoastrocytomas (WHO grade II) (Figure 5A, B) and oligodendrogliomas (WHO grade II) (Figure 5C, D). In all four profiles, a combined loss of chromosomal arms 1p and 19q could be detected, which are known copy number changes in tumors with an oligodendroglial component. Additional changes in the copy number on chromosomes 4, 8, 13, and 15 could only be detected in the mixed tumors containing an astroglial component in addition to oligodendroglial cells (Figure 5A, B).

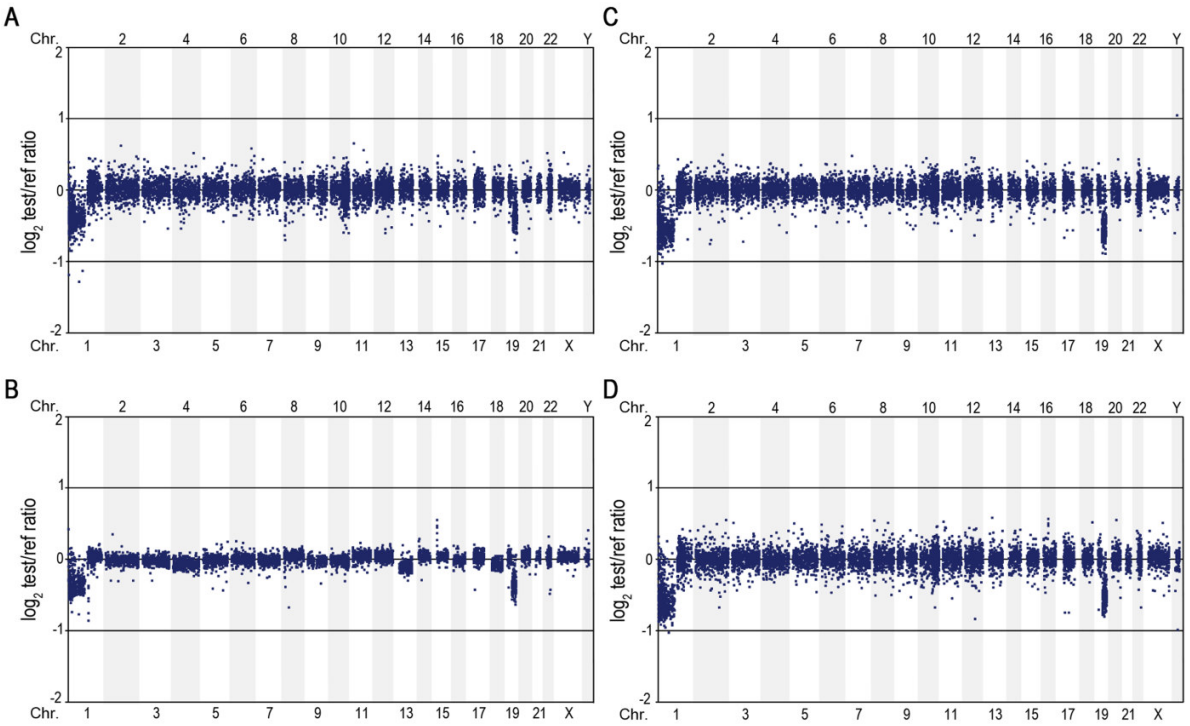

Figure 5: Array-CGH profiles of WHO grade II oligoastrocytomas and oligodendrogliomas.
A and B: selected array-CGH profiles of WHO grade II oligoastrocytomas. **C and D:** selected array-CGH profiles of WHO grade II oligodendrogliomas. In all four tumors, a signature typical for oligodendroglial tumors with a combined loss of 1p and 19q can be seen. The midpoints of all BAC clones are plotted in genomic order from 1p to Yq on the x-axis against their normalized $\log_2$ test to reference ratio on the y-axis.

3.1.2 Frequency of genomic alterations in WHO grade II gliomas

In order to identify and compare common genomic alterations in different WHO grade II glioma entities, frequency plots were prepared that were stratified according to the *IDH1/2* status. Frequency plots aid in analyzing larger numbers of samples due to the fact that they indicate how often a certain chromosomal region is affected by gains or losses in a certain tumor entity. Unfortunately, not all samples analyzed by array-CGH could be included when preparing these frequency plots. Therefore, the number of samples, which were entered in this analysis, is lower than the total number of analyzed samples.

No clear difference in the frequency of genomic imbalances between *IDH1/2* wild-type (n=13) and mutant (n=19) astrocytomas was detected (Figure 6). This may be due to the fact that the numbers of tumor samples, the frequency plots are based on are quite low. The most frequent gain in *IDH1/2* wild-type and mutant astrocytomas, was of chromosomal arm 7q found in 40% – 50% of cases. Loss of chromosome 10 was detected in 20% of *IDH1/2* wild-type and mutant tumors. However, in *IHD1/2* mutant tumors it only affected the long arm of chromosome 10. The most frequent loss in *IDH1/2* wild-type and mutant astrocytomas was in the long arm of chromosome 19.

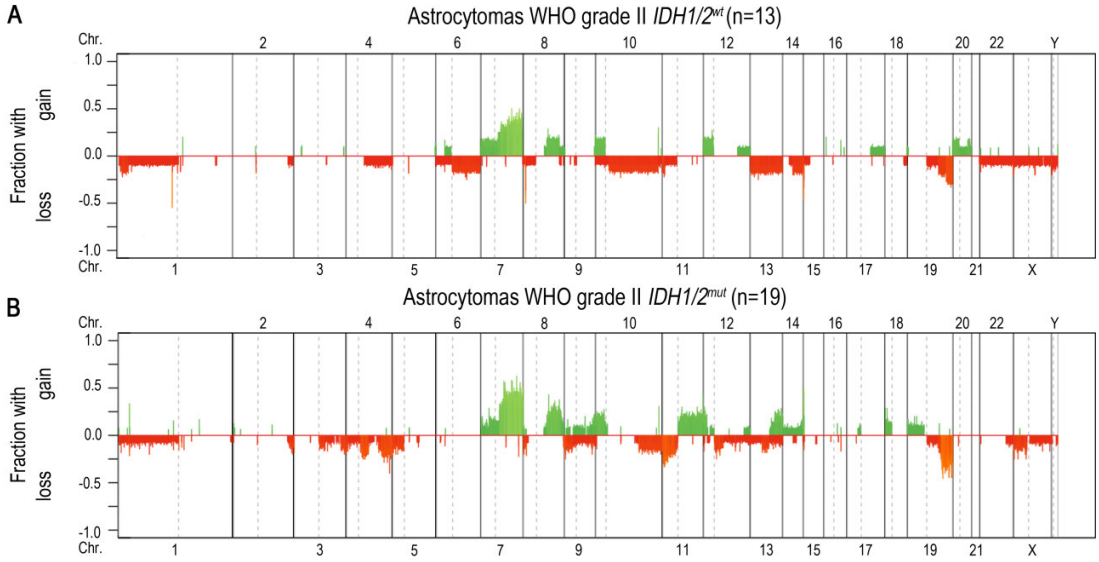

Figure 6: Frequency plots of genomic alterations in WHO grade II diffuse astrocytomas stratified according to *IDH1/2* status.
A: Frequency of genomic imbalances in of 13 *IDH1/2* wild-type astrocytomas of WHO grade II. **B:** Frequency of genomic imbalances in 19 astrocytomas of WHO grade II harboring an *IDH1/2* mutation. Gains are indicated by green bars, losses are indicated by red bars. Gains and losses are plotted in genomic order from 1p to Yq on the x-axis. The y-axis indicates the fraction of cases with copy number changes.

3.1.3 Genomic profiles in WHO grade III gliomas

WHO grade III gliomas are characterized by a more aggressive behavior than diffuse astrocytomas of WHO grade II, and are associated with nuclear atypia, an increased cellularity and significant proliferative activity, suggesting that an increased number of copy number alterations may underlie these histological changes. Therefore, also WHO grade III gliomas such as anaplastic astrocytomas (n=49) and anaplastic oligoastrocytomas (n=36) were analyzed using array-CGH in order to characterize their genomic profile. When, comparing the array-CGH profiles of the anaplastic astrocytomas WHO grade III (Figure 7, page 53) with those of WHO grade II astrocytomas (Figure 4, page 50), it can be seen that the WHO grade III tumors displayed more genetic imbalances and that the number of affected chromosomes (e.g. chromosomes 3, 4, 6, and 14) is more numerous as

compared to the WHO grade II tumors. The genomic profiles depicted in Figure 7A and B are from anaplastic astrocytomas with an *IDH1/2* wild-type status, as opposed to tumors harboring an *IDH1/2* mutation shown in Figure 7C and D. In the *IDH1/2* wild-type tumors, a gain of chromosome 7 and/ or a loss of the entire chromosome 10 could be detected, while the chromosome 10 loss only affects part of the long arm in one *IDH1/2* mutant case (Figure 7C) and chromosome 7 gains are not found.

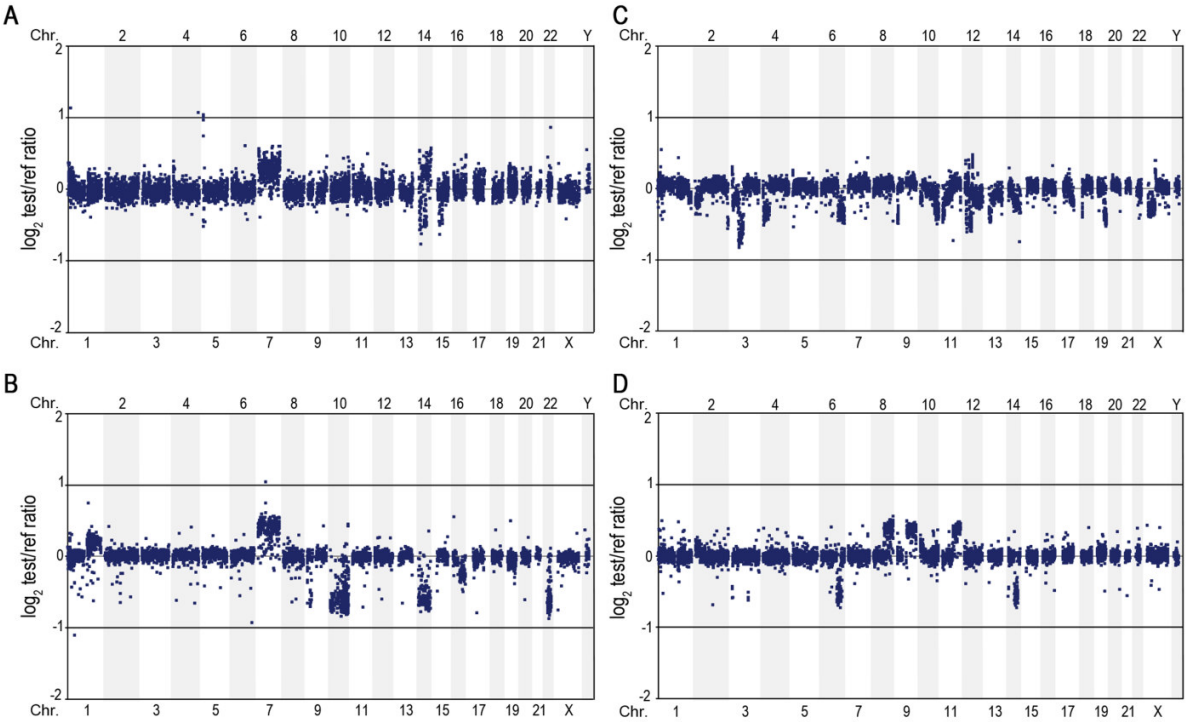

Figure 7: Array-CGH profiles of WHO grade III anaplastic astrocytomas.
A and B: Array-CGH profiles from anaplastic astrocytomas with an *IDH1/2* wild-type status. **C and D:** Array-CGH profiles from anaplastic astrocytomas with an *IDH1/2* mutant status. The midpoints of all BAC clones are plotted in genomic order from 1p to Yq on the x-axis against their normalized $\log_2$ test to reference ratio on the y-axis.

3.1.4 Frequency of genomic alterations in WHO grade III gliomas

In order to identifiy and compare common genomic imbalances in anaplastic astrocytomas of WHO grade III, with wild-type or mutant *IDH1/2*, frequency plots were prepared stratified according to the *IDH1/2* status. Here, differences in the two frequency profiles comparing IDH^{wt} and IDH^{mut} could be seen (Figure 8, page 54). Figure 8A displays the sum of genetic imbalances in eight anaplastic astrocytomas with wild-type *IDH1/2*, demonstrating a clear gain of chromosome 7 in about 80% of the cases as well as a loss of chromosomal arm 9p and losses of chromosomes 10 and on chromosomal arm 14q in about 75% of the cases. Other less frequent genomic alterations were gains on chromosomes 9, 18 and 19 in about 25% – 50% of the cases as well as the loss on chromosomal arm 22q in about 50%. Figure 8B shows the genetic imbalances in 19 anaplastic astrocytomas

harboring *IDH1/2* mutations. In these tumors, the gain on chromosome 7 was less frequent (50%) and affected the long arm only in most cases. The loss of chromosome 10 could ony be detected in 25% of the cases and also affected only the long arm. In contrast to the *IDH1/2* wild-type tumors, the loss of chromosomal arm 19q was more frequent (50%) in the *IDH1/2* mutated tumors. Further differences between the two frequency plots in Figure 8 are the gains on chromosomes 18 and 19, which were not or only rarely present in *IDH1/2* mutant tumors.

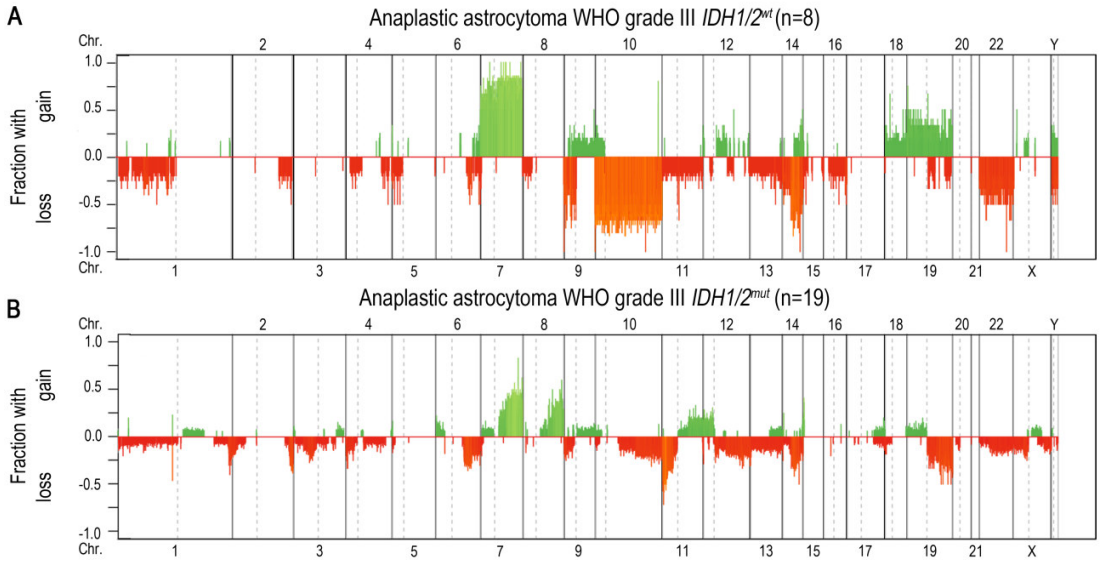

Figure 8: Frequency plots of genomic alterations in anaplastic astrocytomas of WHO grade III stratified according to *IDH1/2* status.
A: Frequency of genomic imbalances in eight *IDH1/2* wild-type anaplastic astrocytomas of WHO grade III. **B:** Frequency of genomic imbalances in 19 anaplastic astrocytomas of WHO grade III harboring an *IDH1/2* mutation. Gains are indicated by green bars, losses are indicated by red bars. All alterations are plotted in genomic order from 1p to Yq on the x-axis. The y-axis indicates the fraction of cases with copy number changes.

Anaplastic oligoastrocytomas are WHO grade III tumors containing an oligodendroglial in addition to the astrocytic component. In this study, 28 *IDH1/2* mutant anaplastic oligoastrocytomas were analyzed. A frequency plot for *IDH1/2* wild-type tumors was not prepared, due to the fact that only one tumor in this cohort was found to be *IDH1/2* wild-type. Analyzing the *IDH1/2* mutant tumors using array-CGH revealed various chromosomal imbalances, the sums of which are displayed in the frequency plot in Figure 9. A combined loss of chromosomal arms 1p and 19q was found in about 75% of the cases. Other chromosomal aberrations were much less common and involved losses on chromosome 4, 13q, 14q and 15q in about 25% – 30% of the cases, as well as a gain on chromosome 7 in about 25%.

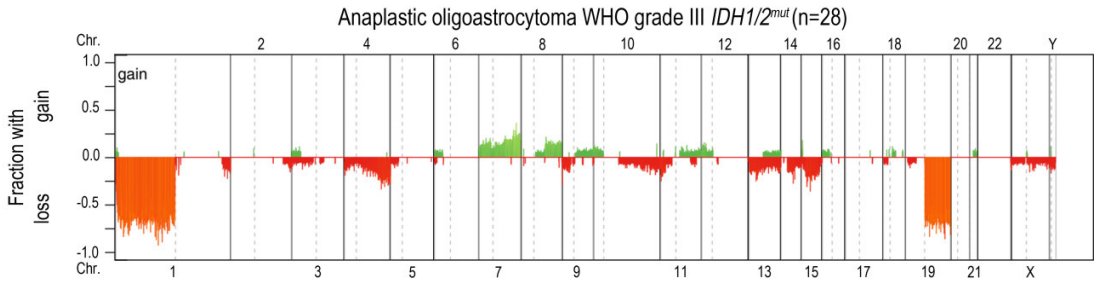

Figure 9: Frequency plot of genomic alterations in *IDH1/2* mutant WHO grade III anaplastic oligoastrocytomas
Gains are indicated by green bars, losses are indicated by red bars. Alterations are plotted in genomic order from 1p to Yq on the x-axis. The y-axis indicates the fraction of cases with copy number changes.

In summary, it could be shown that WHO grade II gliomas including diffuse astrocytomas, oligoastrocytomas and oligodendrogliomas display less frequently copy number changes than gliomas of WHO grade III. Furthermore, a small group of *IDH1/2* wild-type astrocytomas of WHO grade II were detected to display glioblastoma-like imbalances, i.e. gains on chromosome 7, 19 and 20 as well as losses of chromosomes 9 and 10. In contrast, deletions of chromosomal arms 1p and 19q were frequently found in oligodendroglial tumors or in mixed astrocytic tumors displaying an oligodendroglial component. Combined loss of 1p and 19q was significantly less frequent in astrocytic tumors.

3.2 Project 2: Characterization of long-term survivors of glioblastoma using genome-wide profiling

The prognosis of glioblastoma, WHO grade IV, the most malignant glioma type, is poor with only a minority of patients showing long-term survival of more than three years after diagnosis. Survival in primary glioblastoma patients is usually shorter than in patients with secondary glioblastomas (Ohgaki and Kleihues, 2005b). This may be due to the fact that *IDH1/2* mutations are commonly found in secondary glioblastomas which are associated with longer survival. There are a few cases of primary glioblastoma patients that have *IDH1/2* mutant tumors, while 80% – 90% of primary glioblastomas are *IDH1/2* wild-type. It was the aim of project 2 to elucidate the genomic imbalances in primary glioblastomas of long-term survivors and to compare them with those of intermediate-term and short-term survivors. Project 2 has been published in Reifenberger and Weber *et al.*, 2014.

3.2.1 Patient characteristics of 94 glioblastoma patients

In total, 94 patients were included in project 2, all presenting with a histopathological reference diagnosis of glioblastoma. Clinical, histological, and molecular data were collected for each case and are summed up in Table 11. This table includes the more basic data, like age at diagnosis, gender, KPS (Karnofsky performance scale), extent of surgery as well as the reference diagnosis. Additionally,

molecular markers such as the *MGMT* promoter methylation status and the *IDH1* and *IDH2* mutation status were also included. The patients were divided into three groups according to their survival times (group A, B and C). Group A (n=28) comprises long-term survivors that show an overall survival (OS) of more than 36 months. Group B (n=20) represents short-term survivors, showing a progression-free survival (PFS) of less than 6 months and an OS of less than 12 months. Group C (n=46) was defined as patients with an intermediate survival. Death in all patients was tumor-related.

Comparing the three survival groups, the long-term survivors (group A) with a median age of 52 years at diagnosis were younger than the short-term survivor group B (median age 63 years) and the intermediate survival group C (median age 59 years) (p=0.02). No differences between the survival groups were found when gender, KPS and the extent of resection at initial surgery were compared. *MGMT* promoter methylated tumors (p<0.001) and *IDH1/2* mutant tumors (p<0.001) were more frequently found within group A. Being the most frequent first-line therapy, radiotherapy (RT) plus TMZ (temozolomide), was received by all patients in group B and most of group A (24/28) and group C (40/46). The remaining 10 out of the 94 patients received either, no additional therapy except for surgical resection, only radiotherapy or only TMZ. PFS was, as expected, significantly longer in group A patients, with a mean of 26.2 months, than in the other groups (3.5 months for group B and 6.1 months for group C (p<0.001)). Patients from group A and group C more often received a salvage therapy than patients from group B.

Table 11: Clinical, histological, and molecular patient characteristics according to survival groups (Reifenberger and Weber et al., 2014).

	Total n=94	**Group A** n=28	**Group B** n=20	**Group C** n=46
Age at diagnosis (years)				
Median (range)	58 (25-80)	52 (25-74)	63 (37-80)	59 (28-74)
Age classes				
<51	29 (30.9%)	14 (50.0%)	3 (15.0%)	12 (26.1%)
51-60	23 (24.5%)	6 (21.4%)	5 (25.0%)	12 (26.1%)
61-70	36 (38.3%)	6 (21.4%)	9 (45.0%)	21 (45.7%)
>70	6 (6.4%)	2 (7.1%)	3 (15.0%)	1 (2.2%)
Gender				
Female	34 (36.2%)	14 (50.0%)	8 (40.0%)	12 (26.1%)
Male	60 (63.8%)	14 (50.0%)	12 (60.0%)	34 (73.9%)
KPS				
<70	5 (5.3%)	1 (3.6%)	2 (10.0%)	2 (4.3%)
70-80	45 (47.9%)	17 (60.7%)	9 (45.0%)	19 (41.3%)
90-100	44 (46.8%)	10 (35.7%)	9 (45.0%)	25 (54.3%)
Surgery				
Total	47 (50.0%)	12 (42.9%)	8 (40.0%)	27 (58.7%)
Subtotal	27 (28.7%)	8 (28.6%)	8 (40.0%)	11 (23.9%)
Partial	12 (12.8%)	3 (10.7%)	4 (20.0%)	5 (10.9%)
Biopsy	2 (2.1%)	1 (3.6%)	-	1 (2.2%)
Unknown	6 (6.4%)	4 (14.3%)	-	2 (4.3%)

Review diagnosis				
Glioblastoma	84 (89.4%)	22 (78.6%)	19 (95.0%)	43 (93.5%)
Giant cell glioblastoma	1 (1.1%)	-	-	1 (2.2%)
Gliosarcoma	3 (3.2%)	1 (3.6%)	1 (5.0%)	1 (2.2%)
Glioblastoma with oligodendroglial component	6 (6.4%)	5 (17.9%)	-	1 (2.2%)
***MGMT* promoter methylation status**				
Methylated	41 (43.6%)	21 (75.0%)	5 (25.0%)	15 (32.6%)
Weakly methylated	9 (9.6%)	4 (14.3%)	2 (10.0%)	3 (6.5%)
Unmethylated	44 (46.8%)	3 (10.7%)	13 (65.0%)	28 (60.9%)
***IDH1/2* mutation status**				
IDH1 mutant	14 (14.9%)	10 (35.7%)	1 (5.0%)	3 (6.5%)
IDH2 mutant	1 (1.1%)	1 (3.6%)	-	-
IDH1/2 wildtype	79 (84.9%)	17 (60.7%)	19 (95.0%)	43 (93.5%)
First-line therapy				
No therapy	1 (1.1%)	1 (3.6%)	-	-
RT	8 (8.5%)	3 (10.7%)	-	5 (10.9%)
RT plus TMZ	84 (89.4%)	24 (85.7%)	20 (100%)	40 (87.0%)
TMZ	1 (1.1%)	-	-	1 (2.2%)
Median PFS (95%-CI) in months (events)	6.4 (2.7-10.1) (89/94)	26.2 (24.4-28.0) (23/28)	3.5 (2.8-4.3) (20/20)	6.1 (5.4-6.8) (46/46)
First salvage therapy				
Surgery alone	15 (16.0%)	3 (10.7%)	1 (5.0%)	11 (23.9%)
Surgery plus CT	32 (34.0%)	8 (28.6%)	3 (15.0%)	21 (45.7%)
RT plus CT	5 (5.3%)	3 (10.7%)	-	2 (4.3%)
CT alone	13 (13.8%)	5 (17.9%)	1 (5.0%)	7 (15.2%)
OP plus other	1 (1.1%)	-	-	1 (2.2%)
No therapy	28 (29.8%)	9 (32.1%)	15 (75.0%)	4 (8.7%)
Lines of salvage therapy				
1	12 (12.8%)	5 (17.9%)	1 (5.0%)	6 (13.0%)
2	4 (4.3%)	2 (7.1%)	-	2 (4.3%)
>2	3 (3.2%)	2 (7.1%)	-	1 (2.2%)
Median OS (95%-CI) in months (events)	18.7 (16.6-22.7) (85/97)	50.4 (42.0-58.8) (19/28)	4.6 (4.1-5.1) (20/20)	16.7 (14.6-18.8) (46/46)

All the above mentioned criteria were also analyzed for *IDH1/2* wild-type glioblastoma patients only (Table 12), because *IDH1/2* wild-type glioblastomas show a distinct chromosomal profile and behavior. The *IDH1/2* wild-type cohort included 79 patients and was also subdivided into the three survival groups (group A^{wt}, group B^{wt}, group C^{wt}). After the stratification for *IDH1/2* wild-type tumors, a difference in median age at diagnosis could no longer be seen. Still, the *MGMT* promoter methylated tumors were more frequent in group A^{wt} (p=0.002).

Table 12: Clinical, histological, and molecular characteristics of patients with *IDH1/2*^{wt} tumors according to survival groups (Reifenberger and Weber et al., 2014).

	Total^{wt} n=79	**Group A**^{wt} n=17	**Group B**^{wt} n=19	**Group C**^{wt} n=43
Age at diagnosis (years)				
Median (range)	61 (25-80)	59 (25-74)	64 (37-80)	61 (38-74)
Age classes				
<51	16 (20.3%)	4 (23.5%)	2 (10.5%)	10 (23.3%)
51-60	22 (27.8%)	6 (35.3%)	5 (26.3%)	11 (25.6%)
61-70	35 (44.3%)	5 (29.4%)	9 (47.4%)	21 (48.8%)
>70	6 (7.6%)	2 (11.8%)	3 (15.8%)	1 (2.3%)
Gender				
Female	30 (38.0%)	10 (58.8%)	8 (42.1%)	12 (27.9%)
Male	49 (62.0%)	7 (41.2%)	11 (57.9%)	31 (72.1%)
KPS				
<70	4 (5.1%)	-	2 (10.5%)	2 (4.7%)
70-80	38 (48.1%)	12 (70.6%)	8 (42.1%)	18 (41.9%)
90-100	37 (46.8%)	5 (29.4%)	9 (47.4%)	23 (53.5%)
Surgery				
Total	41 (51.9%)	8 (47.1%)	7 (36.8%)	26 (60.5%)
Subtotal	25 (31.6%)	6 (35.3%)	8 (42.1%)	11 (25.6%)
Partial	8 (10.1%)	1 (5.9%)	4 (21.1%)	3 (7.0%)
Biopsy	2 (2.5%)	1 (5.9%)	-	1 (2.3%)
Unknown	3 (3.8%)	1 (5.9%)	-	2 (4.7%)
Review diagnosis				
Glioblastoma	74 (93.7%)	15 (88.2%)	18 (94.7%)	41 (95.3%)
Giant cell glioblastoma	1 (1.3%)	-	-	1 (2.3%)
Gliosarcoma	3 (3.8%)	1 (5.9%)	1 (5.3%)	1 (2.3%)
Glioblastoma with oligodendroglial component	1 (1.3%)	1 (5.9%)	-	-
***MGMT* promoter methylation status**				
Methylated	31 (39.2%)	12 (70.6%)	5 (26.3%)	14 (32.6%)
Weakly methylated	5 (6.3%)	2 (11.8%)	1 (5.3%)	2 (4.7%)
Unmethylated	43 (54.4%)	3 (17.6%)	13 (68.4%)	27 (62.8%)
First-line therapy				
No therapy	-	-	-	-
RT	4 (5.1%)	-	-	4 (9.3%)
RT plus CT	75 (94.9%)	17 (100%)	19 (100%)	39 (90.7%)
CT	-	-	-	-
Median PFS (95%-CI) in months (events)	5.8 (4.7-6.9) (78/79)	24.0 (20.4-27.7) (16/17)	3.8 (3.1-4.4) (19/19)	6.1 (5.3-6.9) (43/43)
First salvage therapy				
Surgery alone	12 (15.2%)	-	1 (5.3%)	11 (25.6%)
Surgery plus CT	29 (36.7%)	6 (35.3%)	3 (15.8%)	20 (46.5%)
RT plus CT	4 (5.1%)	3 (17.6%)	-	1 (2.3%)
CT alone	11 (13.9%)	4 (23.5%)	1 (5.3%)	6 (14.0%)
OP plus other	1 (1.3%)	-	-	1 (2.3%)
No therapy	22 (27.8%)	4 (23.5%)	14 (73.7%)	4 (9.3%)

Lines of salvage therapy				
1	10 (12.7%)	4 (23.5%)	1 (5.3%)	5 (11.6%)
2	3 (3.8%)	1 (5.9%)	-	2 (4.7%)
>2	2 (2.5%)	1 (5.9%)	-	1 (2.3%)
Median OS (95%-CI) in months (events)	17.0 (13.6-20.3) (74/79)	45.0 (37.3-52.6) (19/19)	4.7 (4.3-5.1) (12/17)	17.9 (14.5-21.3) (43/43)

3.2.2 Analysis of genomic imbalances in primary glioblastomas by array-CGH

From 89 of the 94 patients described in Table 11 and Table 12 (3.2.1, page 55), glioblastoma samples were analyzed by array-CGH. For 70 of the 94 gene expression was determined by hybridization to Affymetrix Gene Chip® Human Genome U133 Plus 2.0 arrays in cooperation with the GGN and the Institute of Neuropathology, University of Düsseldorf (data not shown; Reifenberger and Weber et al., 2014). Unsupervised analysis of the array-CGH data showed several distinct tumor clusters (Figure 10A). In Figure 10, four tumor characteristics are given in addition to the genomic imbalance data. First of all, the molecular subtype was determined for each tumor sample according to Verhaak *et al.*, 2010 and is depicted in row 1. Most tumors are found to display either, a mesenchymal, a classical or a proneural molecular signature. As the second and third category, the *MGMT* promoter methylation and *IDH1/2* status were determined and are given in row 2 and 3, respectively. In row 4, the survival group is given as long-term (group A), short-term (group B) and intermediate (group C). No clustering according to the molecular subtype, the *MGMT* promoter methylation status, and the survival groups was apparent (Figure 10). But as apparent in row 3, most *IDH1/2* mutant tumors form subclusters in the right side of the heatmap. Most of the *IDH1/2* wild-type glioblastomas demonstrated gains on chromosome 7, losses of chromosomal arm 9p and of chromosome 10. Additionally, in about half of the cases gains of chromosomes 19 and 20 and/ or losses on chromosomal arms 13q and 22q were detected (Figure 10A). In contrast, *IDH1/2* mutant tumors demonstrated more heterogeneous imbalance patterns with frequent losses of chromosomal arm 1p and 19q. Even though there is no clear clustering based on survival groups or *MGMT* promoter methylation status, two subclusters at the right of the heatmap uniformly show *MGMT* promoter methylated tumors from group A (long-term survivors) (Figure 10A). However, almost all of these tumors also carry an *IDH1/2* mutation, so that the three parameters are not independent from each other.

Supervised clustering of genomic imbalances was performed based on the three survival groups. This approach revealed the frequent glioblastoma associated imbalances, gains on chromosomes 7, 19 and 20 as well as losses on chromosomes 10, 13q and 22q, in most of group B and group C tumors but only a subset of group A tumors (Figure 10B). However, group A tumors without the frequent glioblastoma associated imbalances, most of which carried losses of chromosomal arms 1p and/ or 19q, had an *IDH1/2* mutation. So the different genomic imbalances in these tumors from long-term survivors most likely related to the *IDH1/2* status and are no independent prognostic parameters.

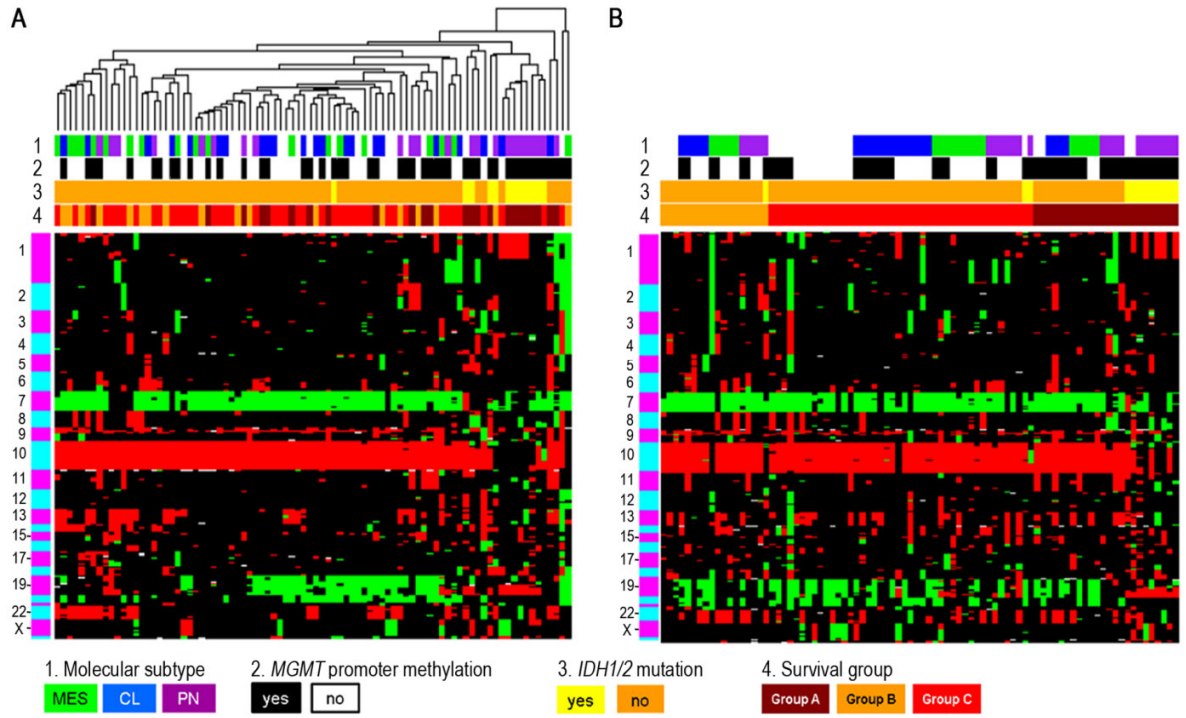

Figure 10: Heatmap of genomic imbalances in 89 glioblastomas analyzed by array-CGH.
A: The result of an unsupervised clustering of the array-CGH data is shown. Depicted on top of the heatmap are the molecular subtype (1: classical (CL), mesenchymal (MES), and proneural (PN)), the *MGMT* promoter methylation status (2), the *IDH1/2* mutation status (3) and survival groups (4: group A, B and C). Certain subclusters were apparent; most *IDH1/2*^{mut} tumors were clustering together apart from the *IDH1/2*^{wt} tumors. Characteristic for the group of *IDH1/2*^{wt} tumors were gains on chromosome 7 and losses of chromosome 10 and chromosomal arm 9p. In larger subgroups of tumors, gains on chromosomes 19 and 20 and losses on chromosomal arm 13q and 22q were detected. *IDH1/2*^{mut} tumors demonstrated more heterogeneous aberration patterns. Group A was distributed more or less evenly over all clusters, showing a shift towards *IDH1/2*^{mut} and *MGMT* promoter methylated tumors to the right of the heatmap. **B:** Heatmap of supervised clustering of array-CGH data based on survival groups, revealing the typical glioblastoma imbalances in a subset of group A, in the majority of group B and group C tumors (Reifenberger and Weber et al., 2014).

Frequency plots of the genomic imbalances in the 89 glioblastoma samples were prepared based on survival groups for tumors with an *IDH1/2*^{wt} status. A separate frequency plot for the *IDH1/2*^{mut} tumors was also prepared (Figure 11). Frequency plots indicate how often a certain chromosomal region is gained or lost in a given set of samples. The frequency plots for group A^{wt}, B^{wt} and C^{wt} were very similar and showed frequent gains on chromosome 7 (approximately 90%), as well as on chromosomes 19 and 20 (40% – 50% of cases). Chromosome 10 was lost in most cases (90%). In contrast, the frequency plot of *IDH1/2*^{mut} showed a different pattern, exhibiting chromosomal imbalances more widely distributed over various chromosomes. Here, the gain and loss on chromosomes 7 (50%) and 10 (40%) were less frequent and more commonly affected the long arm: gain on 7q and loss on 10q were both found in around 50% of tumors. Moreover, losses of chromosomal arms 1p and 19q were more frequent in *IDH1/2*^{mut} tumors when compared to the wild-type tumor groups (1p: 40% – 50%; 19: 80%). It can also be noted, that in the wild-type tumors

chromosome 19 was frequently gained (40% – 50% of cases), whereas the long arm of chromosome 19 was lost in the *IDH1/2*^{mut} tumors.

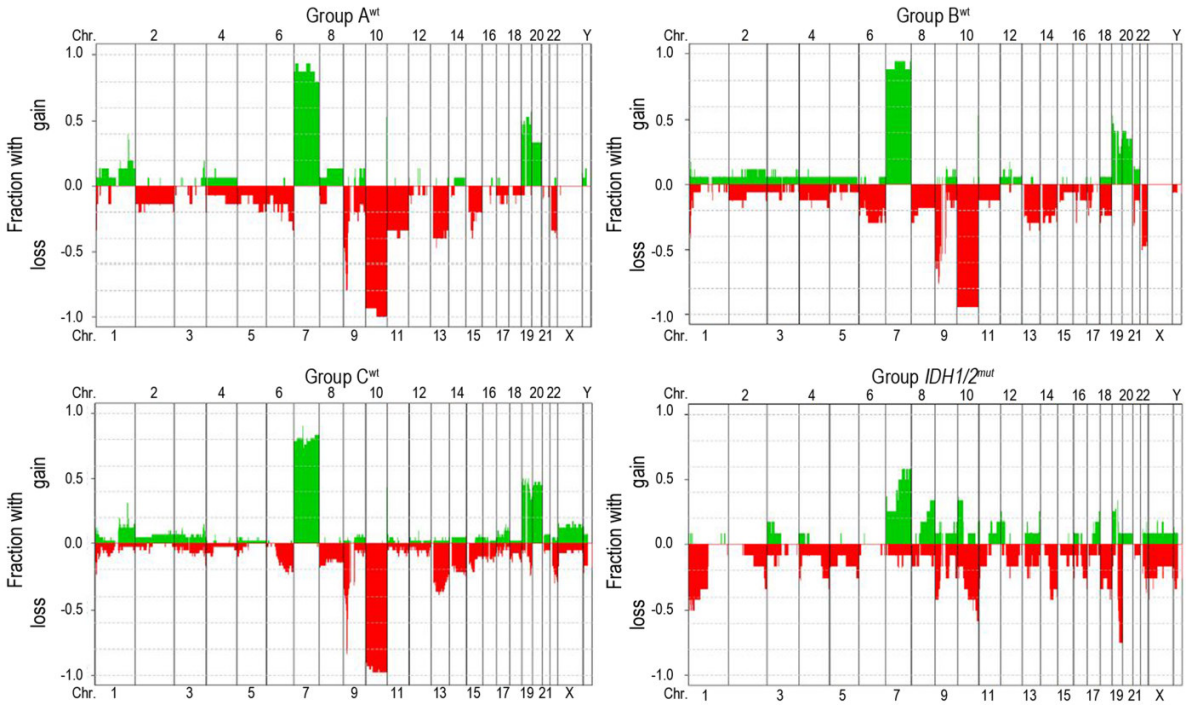

Figure 11: Frequency plots of genomic imbalances according to survival groups and *IDH1/2* status.
Shown are the patterns of genomic imbalances in glioblastomas in the three distinct survival groups (group A^{wt} (n=17), group B^{wt} (n=19) and group C^{wt} (n=43)) and in *IDH1/2*^{mut} (n=15) tumors. The three *IDH1/2*^{wt} groups have a similar pattern of genomic imbalances with frequent gains on chromosome 7, 19, and 20 as well as a frequent loss of chromosome 10. In the *IDH1/2*^{mut} tumors, a different pattern of genomic imbalances was apparent, the gain and loss on chromosomes 7 and 10, respectively, were less frequent. Losses on chromosomal arms 1p and 19q were more frequent in *IDH1/2*^{mut} tumor samples. Gains are indicated by green bars, while losses are indicated by red bars. Gains and losses are plotted in genomic order from 1p to Yq on the x-axis. The y-axis indicates the fraction of cases with copy number changes (Reifenberger and Weber et al., 2014).

Interestingly, four tumors showed combined losses on 1p and 19q (Figure 10), which is a typical change for low-grade tumors or secondary glioblastomas, especially those with an oligodendroglial component. But clinical and histological review confirmed that these tumors were primary glioblastomas without a history of preexisting low-grade lesions. However, three of them also displayed an oligodendroglial tumor component.

The results displayed in Figure 10 and Figure 11 indicate that the genomic imbalances identified are linked to the *IDH1/2* mutation status, rather than long-term versus short-term survival. *IDH1/2* wild-type tumors show a different pattern of DNA copy number changes then *IDH1/2* mutant tumors.

It is of interest to compare frequencies of copy number changes of selected genes in different tumor groups. Table 13 summarizes the frequency of gene copy number changes in selected

chromosomal regions, harboring glioma-related tumor suppressor genes or oncogenes. The table gives frequencies of copy number changes in *IDH1/2* wild-type glioblastomas from the distinct survival groups as well as in *IDH1/2* mutant tumors. After adjusting for multiple testing, there was no significant difference in the frequency of any copy number change in the long-term survival group (group A) as compared to the groups with shorter survival times (see column "p-value *IDH1/2*^{wt}"). Taking the *IDH1/2* status into account, several significant differences were detected in the *IDH1/2*^{wt} versus *IDH1/2*^{mut} tumors (see column "p-value *IDH1/2*^{mut}"). Frequencies of low and high level amplifications were different for *PMS2*, *EGFR*, *HGF*, *CDK6*, *XRCC1,* whereas frequencies of low or high level losses were different for *CDKN2C*, *CDKN2A/B*, *PTEN*, *XRCC1* and *XRCC3*. The association between gene copy number changes in candidate genes and survival groups with respect to *IDH1/2* mutation were analyzed by Fisher's Exact Test using IBM SPSS Statistics Version 20.

Table 13: Frequency of copy number changes in different chromosomal regions containing glioma-associated tumor suppressor genes or oncogenes (modified from Reifenberger and Weber et al., 2014).

Chromosomal region (hg19)	**Candidate genes**	**Group A^{wt} n=17**	**Group B^{wt} n=19**	**Group C^{wt} n=43**	**p-value *IDH1/2*^{wt}**	**Group *IDH1/2*^{mut} n=15**	**p-value *IDH1/2*^{mut}**
Low- and high-level amplifications							
1q32.1	*MDM4* (RP11-563I16) *PIK3C2B* (RP11-739N20)	6/15 (40%)	3/17 (18%)	16/38 (42%)	0.199	1/12 (8%)	0.092
1q44	*AKT3* (RP11-269F20, RP11-370K11)	3/15 (20%)	3/16 (19%)	6/41 (15%)	0.756	1/12 (8%)	0.681
4q12	*PDGFRA* (RP11-231C18)	5/15 (33%)	1/16 (6%)	10/40 (25%)	0.146	2/12 (17%)	1.0
6p21.1	*CCND3* (RP5-973N23, RP11-533O20)	2/15 (13%)	2/17 (12%)	2/41 (5%)	0.453	1/12 (8%)	1.0
7p22.1	***PMS2*** (RP11-90J23)	11/13 (85%)	13/15 (87%)	28/35 (80%)	0.906	4/11 (36%)	**0.003**
7p11.2	***EGFR*** (RP5-1091E12, RP11-339F13)	14/15 (93%)	14/15 (93%)	31/33 (94%)	1.0	4/11 (36%)	**<0.001**
7q21.11	***HGF*** (RP5-1098B1)	9/12 (75%)	12/13 (92%)	34/37 (92%)	0.239	5/9 (56%)	**0.027**
7q21.2	***CDK6*** (RP5-850G1)	13/14 (93%)	10/11 (91%)	34/39 (87%)	1.0	7/11 (64%)	**0.050**
7q31.2	*MET* (CTB-13N12)	11/11 (100)	13/14 (93%)	28/35 (80%)	0.252	6/10 (60%)	0.061
13q34	*SOX1* (RP11-310D8)	0/15	0/16	5/41 (12%)	0.217	3/12 (25%)	0.083
14q32.33	*AKT1* (RP11-982M15)	3/12 (25%)	2/14 (14%)	11/29 (38%)	0.257	0/9	0.097
19p13.3	*STK11* (RP11-50C6)	4/12 (33%)	8/15 (53%)	17/28 (61%)	0.290	4/11 (36%)	0.511

19q13.31	***XRCC1*** (CTB-61I7, RP11-46C6, RP11-122E7)	6/15 (40%)	5/17 (29%)	16/39 (41%)	0.758	1/12 (8%)	**0.052**
19q13.32	*ERCC2* (RP11-43E18)	3/10 (30%)	3/13 (23%)	19/37 (51%)	0.178	2/12 (17%)	0.190
20q12	*TOP1* (RP3-511B24)	2/10 (20%)	6/15 (40%)	22/36 (61%)	**0.050**	3/10 (30%)	0.320
High level amplifications							
1q32.1	*MDM4* (RP11-563I16), *PIK3C2B* (RP11-739N20)	1/15 (7%)	0/17	5/38 (13%)	0.333	0/12	0.585
1q44	*AKT3* (RP11-269F20, RP11-370K11)	0/15	0/16	1/41 (2%)	1.0	0/12	1.0
4q12	*PDGFRA* (RP11-231C18)	2/15 (13%)	0/16	2/40 (5%)	0.302	0/12	1.0
6p21.1	*CCND3* (RP5-973N23, RP11-533O20)	0/15	0/17	0/41	-	0/12	-
7p22.1	*PMS2* (RP11-90J23)	0/13	0/15	0/35	-	0/11	-
7p11.2	***EGFR*** (RP5-1091E12, RP11-339F13)	10/15 (67%)	4/15 (27%)	21/33 (64%)	**0.043**	0/11	**0.001**
7q21.11	*HGF* (RP5-1098B1)	0/12	0/13	0/37	-	0/9	-
7q21.2	*CDK6* (RP5-850G1)	0/14	0/11	0/39	-	0/11	-
7q31.2	*MET* (CTB-13N12)	0/11	0/14	0/35 (0%)	-	0/10	-
13q34	*SOX1* (RP11-310D8)	0/15	0/16	1/41 (2%)	1.0	0/12	1.0
14q32.33	*AKT1* (RP11-982M15)	0/12	0/14	0/29	-	0/9	-
19p13.3	*STK11* (RP11-50C6)	0/12	1/15 (7%)	1/28 (4%)	1.0	0/11	1.0
19q13.31	*XRCC1* (CTB-61I7, RP11-46C6, RP11-122E7)	0/15	0/17	0/39	-	0/12	-
19q13.32	*ERCC2* (RP11-43E18)	0/10	0/13	0/37	-	0/12	-
20q12	*TOP1* (RP3-511B24)	0/10	0/15	0/36	-	0/10	-
Low- and high-level losses							
1p36.32	*AJAP1* (RP11-319A11)	1/7 (14%)	6/12 (50%)	7/28 (25%)	0.258	3/8 (38%)	0.692
1p36.23	*CAMTA1* (RP11-92O17, RP11-338N10)	4/15 (27%)	8/17 (47%)	11/38 (29%)	0.364	4/11 (36%)	1.0

1p32.3	***CDKN2C*** (RP11-116M11)	1/12 (8.3%)	4/16 (25%)	9/36 (25%)	0.553	6/11 (55%)	**0.058**
1q42.12	*PARP1* (RP11-15H13)	0/12	0/12	4/33 (12%)	0.476	0/10	1.0
6q26	*PARK2* (RP11-30F7, RP11-1069J22)	3/13 (23%)	3/17 (18%)	8/36 (22%)	1.0	3/12 (25%)	0.718
9p23-p24.1	*PTPRD* (RP11-175E13, RP11-12I16)	7/14 (50%)	11/16 (69%)	14/41 (34%)	**0.056**	6/12 (50%)	0.765
9p21.3	***CDKN2A/B*** (RP11-149I2)	13/15 (87%)	13/16 (81%)	35/41 (85%)	0.906	6/12 (50%)	**0.013**
10q23.31	***PTEN*** (RP11-380G5)	15/15 (100%)	16/16 (100%)	39/40 (98%)	1.0	5/12 (42%)	**<0.001**
13q14.2	*RB1* (RP11-305D15, RP11-174I10)	5/14 (36%)	6/16 (38%)	17/41 (42%)	0.946	3/12 (25%)	0.521
14q32.33	***XRCC3*** (RP11-73M18)	1/11 (9%)	2/14 (14%)	11/38 (29%)	0.362	6/10 (60%)	**0.021**
17p13.1	*TP53* (P5-1030O14, RP11-199F11)	3/14 (18%)	6/16 (27%)	8/40 (17%)	0.379	5/12 (29%)	0.289
17q11.2	*NF1* (RP11-1107G21, CTD-2370N5)	0/15 (0%)	5/17 (29%)	8/41 (20%)	0.078	1/12 (8%)	0.681
19q13.31	***XRCC1*** (CTB-61I7, RP11-46C6, RP11-122E7)	1/15 (7%)	2/17 (12%)	7/39 (18%)	0.661	9/12 (75%)	**<0.001**
19q13.32	*TIMP3* (RP11-419C14, XXbac-677f7, RP11-616G18)	5/15 (33%)	9/17 (53%)	15/41 (37%)	0.472	4/12 (33%)	0.759
High-level losses							
1p36.32	*AJAP1* (RP11-319A11)	0/7	0/12	0/28	-	0/8	-
1p36.23	*CAMTA1* (RP11-92O17, RP11-338N10)	1/15 (7%)	0/17	1/38 (3%)	0.441	2/11 (18%)	0.087
1p32.3	*CDKN2C* (RP11-116M11)	0/12	0/16	0/36	-	0/11	-
1q42.12	*PARP1* (RP11-15H13)	0/12	0/12	0/33	-	0/10	-
6q26	*PARK2* (RP11-30F7, RP11-1069J22)	0/13	0/17	0/36	-	0/12	-
9p23-p24.1	*PTPRD* (RP11-175E13, RP11-12I16)	0/14	0/16	0/41	-	0/12	-
9p21.3	*CDKN2A/B* (RP11-149I2)	5/15 (33%)	9/16 (56%)	22/41 (54%)	0.382	3/12 (25%)	0.129
10q23.31	*PTEN* (RP11-380G5)	1/15 (7%)	1/16 (6%)	0/40	0.187	0/12	-

13q14.2	*RB1* (RP11-305D15, RP11-174I10)	0/14	0/16	0/41	-	0/12	-
14q32.33	*XRCC3* (RP11-73M18)	0/11	0/14	0/38	-	0/10	-
17p13.1	*TP53* (P5-1030O14, RP11-199F11)	0/14	0/16	0/40	-	0/12	-
17q11.2	*NF1* (RP11-1107G21, CTD-2370N5)	0/15	0/17	0/41	-	0/10	-
19q13.31	*XRCC1* (CTB-61I7, RP11-46C6, RP11-122E7)	0/15	0/17	0/39	-	0/12	-
19q13.32	*ERCC2* (RP11-43E18)	0/10	0/13	0/37	-	1/12 (8%)	0.167
22q12.3	*TIMP3* (RP11-419C14, XXbac-677f7, RP11-616G18)	0/15	0/17	0/12	-	0/12	-

3.2.3 Combined analyses of genomic and expression data – gene dosage effects

For 70 of the glioblastoma samples, mRNA expression data was also available, prepared in cooperation with the GGN and the Institute of Neuropathology, University of Düsseldorf. In order to see if there was a gene dosage effect on mRNA expression a combined analysis of these two data sets was performed. Figure 12 and Figure 13 show the results of a combined analysis of array-CGH and expression data in 70 glioblastomas.

The gene expression data obtained was related to the previously delineated neural, proneural, classical and mesenchymal glioblastoma subtypes (Verhaak et al., 2010). While none of the tumors displayed a neural expression profile, proneural, classical and mesenchymal signatures were identified. A supervised clustering of the chromosomal imbalances according to the molecular subtypes defined by the expression data is depicted in Figure 12. The heatmap indicates that all classical and mesenchymal tumors are *IDH1/2* wild-type and frequently harbor gains on chromosomes 7, 19, and 20 as well as losses on chromosomes 10 and 22q. The proneural cases showed a more heterogeneous array-CGH pattern, composed of more losses than gains. In a subset of proneural tumors with mutant *IDH1/2,* deletions of chromosomal arms 1p and/ or 19q were detected.

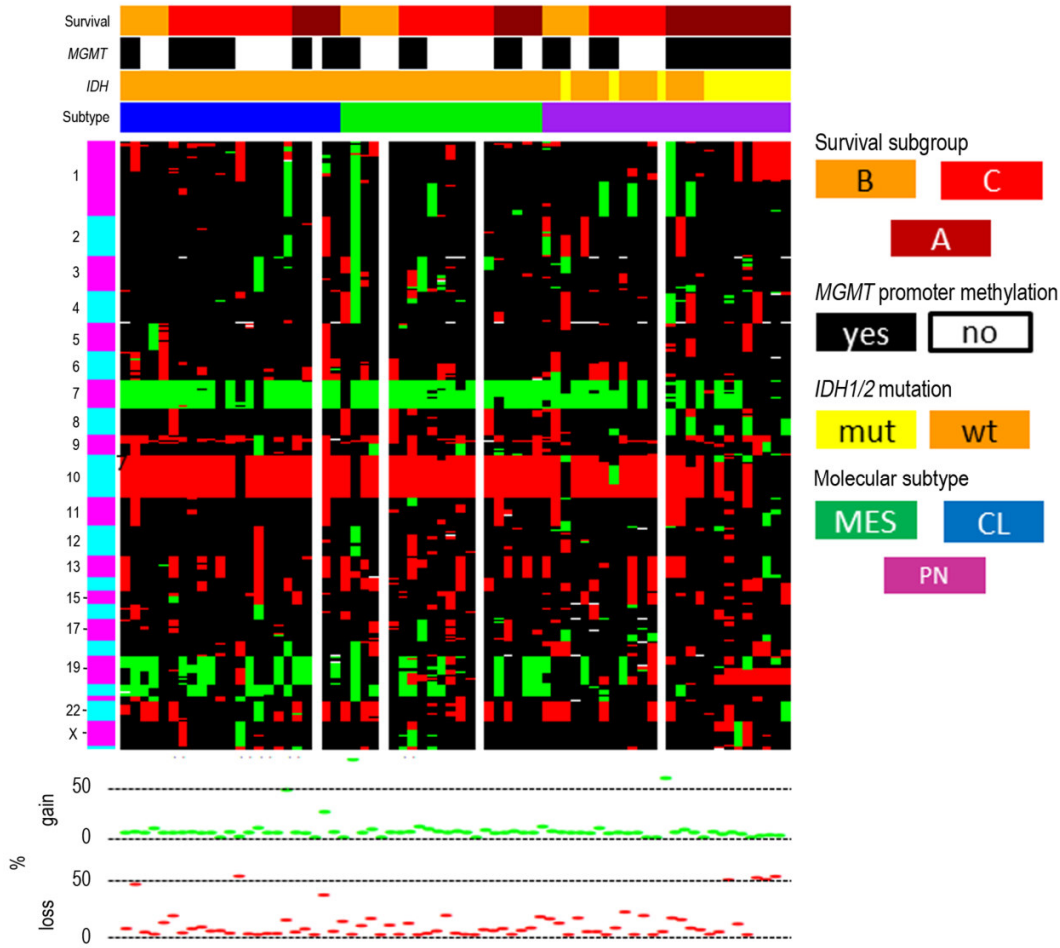

Figure 12: Heatmap of supervised clustering of array-CGH data based on molecular subtypes of glioblastomas (classical, mesenchymal, proneural) inferred from gene expression data.
Depicted on top of the heatmap are the survival groups (A: long-term survivor, B: short-term survivor, C: intermediate survivor), the *MGMT* promoter methylation status, the *IDH1/2* mutation status, and the molecular subtypes (blue: classical (CL), green: mesenchymal (MES), and purple: proneural (PN)). All mesenchymal and classical tumors are *IDH1/2*^{wt} and show typical genomic imbalances including gain on chromosome 7 and loss of chromosome 10. *IDH1/2*^{mut} tumors are all in the proneural group and frequently show 1p and 19q losses. The graph below the heatmap indicates the total fraction of chromosomal segments demonstrating copy number gains or losses in each tumor sample (Reifenberger and Weber et al., 2014).

Genomic alterations such as copy number variants might influence the expression of genes located in the affected chromosomal regions. Therefore, each chromosome was analyzed separately and the influence of the detected gain or loss on the gene expression was assessed by box plots. The box blots in Figure 13 demonstrate that there are a number of cis-regulatory gene dosage effects on gene expression, which are similar in the *IDH1/2* wild-type survival groups but different in the *IDH1/2* mutant group. Percentages of cases with gains or losses involving each chromosome and the relative expression values for all genes located on a particular chromosome are shown for the distinct survival

groups. Although, losses on chromosome 14 were significantly less frequent in the long-term survival group A^{wt}, than in the short or intermediate survival group (B^{wt} or C^{wt}), this difference had only slight effects on the differential gene expression. For the *IDH1/2* mutant tumors, a frequent chromosome 1 loss was detected which also resulted in a significant reduction of gene expression. A similar effect is also seen for the *IDH1/2* wild-type groups and chromosome 10. Here, a frequent monosomy in *IDH1/2* wild-type tumors results in a reduced expression of the genes on this chromosome. In contrast, *IDH1/2* mutant tumors display a higher expression of these genes and a less frequent loss of chromosome 10. Further, the frequent gain of chromosome 7 was also associated with a higher gene expression in *IDH1/2* wild-type tumors. In addition, significant changes between the *IDH1/2* wild-type groups and the *IDH1/2* mutant tumors could be detected for chromosomes 19 and 20. Here, the gain of the chromosome yielded an increased gene expression in the *IHD1/2* wild-type groups.

Analyzing the short and the long arms of each chromosome separately for gene dosage effects, revealed similar results in most cases as when the entire chromosomes were analyzed. This also included the chromosomes 7 and 10 (data not shown). In the case of chromosome 1 and 19, the gene dosage effects were restricted to genes located on the chromosomal arms 1p and 19q (data not shown).

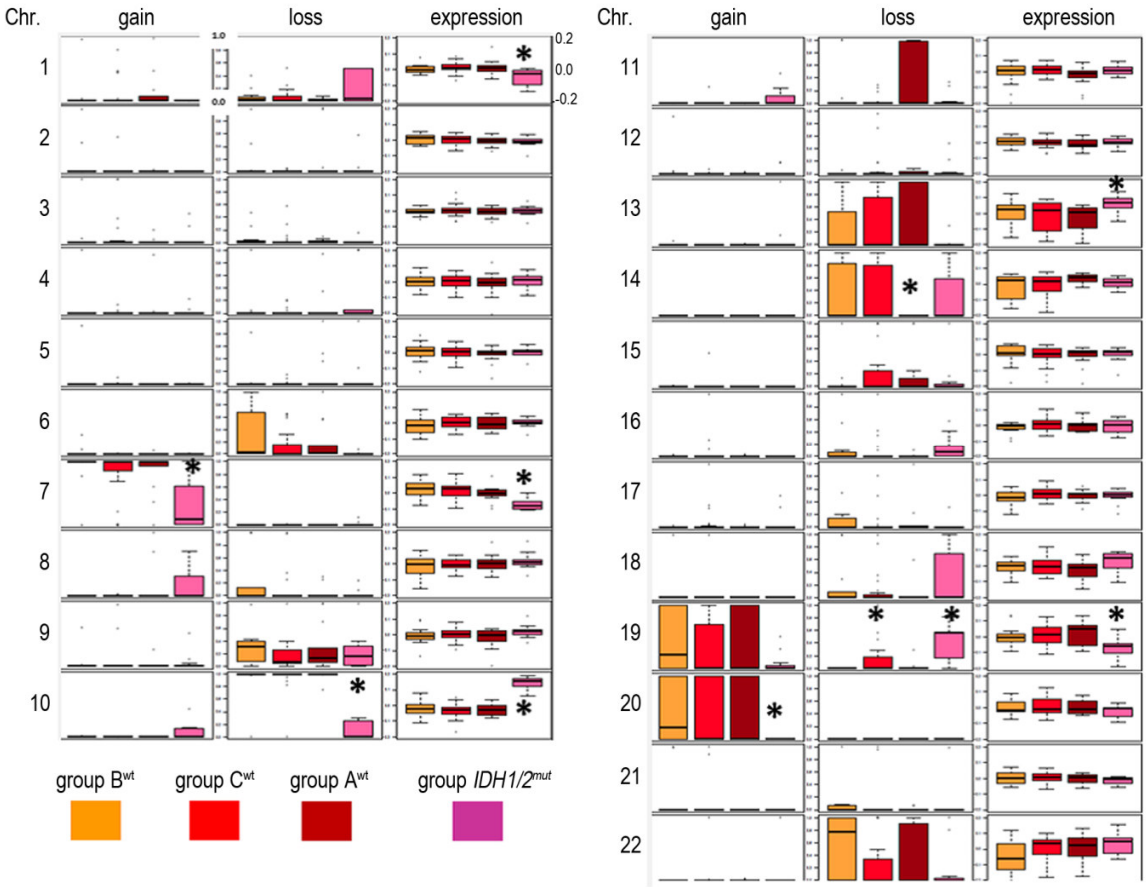

Figure 13: Demonstration of the gene dosage effect by combination of array-CGH and mRNA expression data. In the box plots, the percentage of gains or losses for each chromosome and the relative expression values of all genes located on the respective chromosomes in the different patient groups are shown. Stars demonstrate significant differences. Gene dosage effects were detectable for several copy number changes, for example gains of chromosome 7 and losses of chromosomes 10 and 19. Differences were mostly seen between the *IDH1/2*^{wt} and *IDH1/2*^{mut} tumors. Among the *IDH1/2*^{wt} tumors, significant changes were seen for the loss of chromosome 14, which was less frequent in group A^{wt}, or the loss of chromosome 19 which was more frequent in group C^{wt} tumors. But both changes did not have a significant gene dosage effect. Please note the scales: For chromosome 7 the box plots indicate gains close to 100% and likewise for chromosome 10 almost losses in 100% groups A^{wt}, B^{wt}, C^{wt} (ceiling effect) (Reifenberger and Weber et al., 2014).

In summary, the characterization of long-term survivors in 98 primary glioblastoma patients using genome-wide profiling revealed that the survival is more closely related to the *IDH1/2* mutation status than to any other genetic alteration. *IDH1/2* wild-type glioblastomas displayed a genomic profile distinct from that of *IDH1/2* mutant tumors. Patients with glioblastomas harboring *IDH1/2* mutations had a better prognosis and a higher probability for long-term survival. In addition, *MGMT* promoter methylation was more often found in the group of long-term survivors.

3.3 Project 3: Genomic patterns of recurrence in *IDH1/2* wild-type glioblastomas, WHO grade IV

Glioblastoma show a tendency to recur in spite of combined surgical resection, radiotherapy and TMZ chemotherapy. After recurrence tumor grade is unchanged, i.e. it is still WHO grade IV, and the histopathology is similar. The question arises whether there are differences in the primary and the recurrent tumor on a molecular level. Genome-wide DNA microarrays were used to assess and compare the chromosomal imbalances of 27 primary and recurrent glioblastoma tumor pairs. All 27 tumors pairs were classified as *IDH1/2* wild-type tumors. This is important, because *IDH1/2* wild-type tumors genetically differ from the ones containing an *IDH1/2* mutation and, therefore display a distinct genomic profile (3.2.2, Figure 11, page 61). The aim of this project was to identify possible DNA copy number differences between primary and recurrent tumor from the same patient, and if so, to determine candidate genes that are located within the chromosomal regions with a copy number difference that are associated with therapy response and or tumor recurrence. Project 3 has been published in Riehmer et al., 2014 (in press).

The clinical, histological, and molecular patient characteristics in the study group are listed in Table 14. The study group included 27 patients, 17 male and 10 female, with a median age of 63 years. All patients underwent a tumor resection as first line therapy, additionally the majority were treated with radiotherapy (RT) and TMZ chemotherapy (22/27, 81.5%). The remaining 5 patients (18.5%) were treated with RT alone. Considering the *MGMT* promoter methylation status, 59% of tumors were unmethylated, as compared to 41% of tumors being methylated. The median time between primary and secondary surgery was 9.1 months. While the overall survival was on average 16 months (Table 15, page 77), all patients have died eventually.

In order to determine whether the selected 27 patients in this study were representative of glioblastoma patients with similar initial disease characteristics, a reference group was selected, consisting of 52 patients from the initial GGN cohort (Weller et al., 2009). Patients in this reference group were also treated with surgery and RT plus TMZ, or surgery and RT alone, had at least one surgical reintervention due to disease progression. All tumors were *IDH1/2* wild-type. In comparison, the 27 patients in the study group did not differ significantly from the patients of the reference group. One exception was the patients' age at diagnosis, which was slightly but not significantly younger for the reference group with a median age of 57 years (p=0.083) (Table 14).

Table 14: Clinical, histological, and molecular patient characteristics of study and reference group (Riehmer et al., 2014, in press).

	All patients (n=27)	**Reference group** (n=52)
Age at diagnosis (years)		
Median	63	57
Range	38-70	29-74
Age classes		
<50 years	5 (18.5%)	16 (30.8%)
51-60 years	8 (29.6%)	21 (40.4%)
61-70 years	14 (51.9%)	12 (23.1%)
> 70 years	-	3 (5.8%)
Gender		
Male	17 (63.0%)	39 (75.0%)
Female	10 (37.0%)	13 (25.0%)
KPS		
90-100	15 (55.6%)	30 (60.0%)
70-80	10 (37.0%)	18 (36.0%)
<70	2 (7.4%)	2 (4.0%)
No data	-	2
Primary surgery		
Gross total resection	14 (53.8%)	32 (62.7%)
Subtotal resection (50-99%)	9 (34.6%)	16 (31.4%)
Partial resection (<50%)	3 (11.5%)	3 (5.9%)
No data	1	1
Location (primary tumor)		
Frontal	6 (23.1%)	13 (25.0%)
Temporal	5 (19.2%)	16 (30.8%)
Parietal	6 (23.1%)	7 (13.5%)
Occipital	-	5 (9.6%)
Other	-	1 (1.9%)
Not localized to one site	9 (34.6%)	9 (17.3%)
Multifocal	-	1 (1.9%)
No data	1	-
Review diagnosis		
Glioblastoma	25 (92.6%)	49 (94.2%)
Gliosarcoma	1 (3.7%)	1 (1.9%)
Giant cell glioblastoma	1 (3.7%)	2 (3.8%)
First-line therapy		
RT only	5 (18.5%)	6 (11.5%)
RT plus TMZ	22 (81.5%)	46 (88.5%)
Second-line therapy		
Surgery alone	10 (37.0%)	13 (25.0%)
Surgery plus RT	-	1 (1.9%)
Surgery plus RT plus TMZ/other CT	3 (11.1%)	5 (9.6%)
Surgery plus RT plus other CT	-	5 (9.6%)
Surgery plus TMZ/other CT	3 (11.1%)	9 (17.3%)
Surgery plus other CT	11 (40.7%)	19 (36.5%)
***MGMT* promoter methylation (primary tumor)**		
Strong methylation	9 (33.3%)	20 (38.5%)
Weak methylation	2 (7.4%)	6 (11.5%)
No methylation	16 (59.3%)	26 (50.0%)

Second surgery		
Gross total resection	8 (30.8%)	25 (51.0%)
Subtotal resection (50-99%)	14 (53.8%)	19 (38.8%)
Partial resection (<50%)	4 (15.4%)	5 (10.2%)
No data	1	3
Location (recurrent tumor)		
Frontal	6 (22.2%)	12 (24.0%)
Temporal	6 (22.2%)	11 (22.0%)
Parietal	1 (3.7%)	6 (12.0%)
Occipital	3 (11.1%)	4 (8.0%)
Other	1 (3.7%)	2 (4.0%)
Not localized to one site	9 (33.3%)	14 (28.0%)
Multifocal	1 (3.7%)	1 (2.0%)
No data	-	2

3.3.1 Frequency and pattern of DNA copy number changes in the primary glioblastomas

Array-CGH of 27 primary and recurrent tumor pairs was performed. In Figure 14 the frequency of DNA detected copy number changes (A) and the pattern of copy number changes (B) in the primary tumors are shown. The frequency plot of the 27 primary glioblastomas shows a typical profile for *IDH1/2* wild-type glioblastomas. These typical changes include a gain on chromosome 7 (90%) as well as losses on chromosomal arm 9p (80%) and chromosome 10 (95%). In about half of the tumors, gains on chromosomes 19 and 20 were also detected. In one third of the tumors, a loss on the chromosomal arm 13q was also detected (Figure 14A). Unsupervised clustering of the array-CGH data revealed two major clusters, separated mainly on the basis of the presence or absence of gains on chromosomes 19 and 20 (Figure 14B).

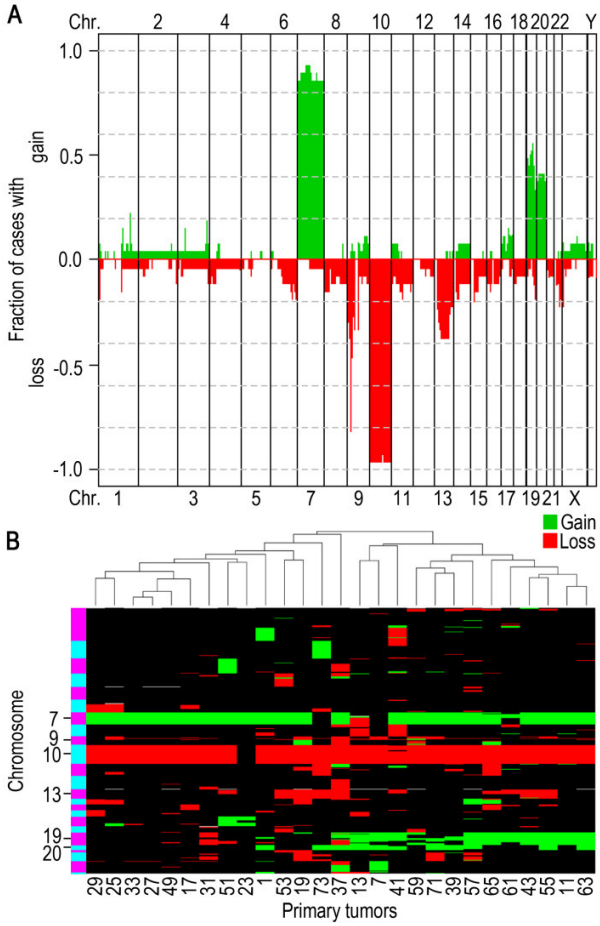

Figure 14: Frequency and pattern of DNA copy number changes in primary glioblastomas (n=27).
A: The frequency plot of 27 primary glioblastomas shows a gain on chromosome 7 and losses on chromosomal arm 9p and chromosome 10 for almost all cases. For about half of the cases, gains of chromosomes 19 and 20 were also detected. The frequency pattern shown here is typical for glioblastomas with *IDH1* and *IDH2* wild-type status. Gains are highlighted in green and losses in red. The copy number changes are plotted in genomic order from 1p to Yq on the x-axis. The y-axis indicates the fraction of cases with copy number change. **B:** The heatmap shows the results of unsupervised clustering of array-CGH data from the primary glioblastomas (n=27). Two subclusters are apparent, reflecting the presence or absence of gains on chromosomes 19 and 20. Green indicates a gain of chromosomal material and red a loss (Riehmer et al., 2014, in press).

3.3.2 Comparison of genomic profiles in primary and recurrent glioblastoma pairs yields three subgroups

An overall aim was to identify possible chromosomal copy number differences between primary and recurrent tumors. Therefore, the genomic profiles of primary and recurrent glioblastomas were compared. In order to correct for the different tumor cell content in the analyzed tumor samples, robust linear regression was used for pairwise value adjustment. Difference profiles of primary and recurrent tumor pairs were generated for all tumors, enabling to detect qualitative differences in the array-CGH profiles of primary and recurrent tumor pairs.

These difference profiles showed three distinctive patterns (relapse signatures) named Equal, Sequential, and Discrepant. Based on the difference profiles, the glioblastoma pairs were classified into one of these relapse groups. Equal pairs had a balanced difference profile, meaning that no qualitative difference between the genomic profile of the primary and respective recurrent tumor could be detected. Seven of the 27 tumor pairs (26%) were classified as Equal, an example is shown in Figure 15 (page 74). Sequential pairs had difference profiles showing additional copy number changes in the recurrent tumors. An example of a tumor pair belonging to the Sequential group, which encompassed nine of 27 samples (33%), is depicted in Figure 16 (page 75). The third group was termed Discrepant, demonstrating the most pronounced differences between primary and recurrent tumor. The term Discrepant was chosen, because the difference profile did not only show additional copy number changes, but, in addition, some chromosomal imbalances were no longer present in the recurrent tumor. Eleven of the 27 tumor pairs (41%) were classified as Discrepant, an example is shown in Figure 17 (page 76).

Clinical characteristics of patients in each molecular relapse group are listed in Table 15 (page 77). For most parameters studied, no noticeable differences were detected, in the three patient groups. The age distribution for the Equal and Sequential groups was similar. In the Discrepant group, the age was higher, with a higher fraction of patients between 60 and 70 years of age. Nevertheless, the median age at diagnosis was similar in all groups. Considering the gender distribution, the Equal group consisted almost only of males, while in the Sequential and Discrepant groups, the gender distribution was almost identical. The median KPS was 90 in all three groups. The extent of resection was also similar in all groups, although the fraction of patients with gross total resection was lower in the Equal group. In the Sequential group, no patient had a frontal localization of the tumor, instead more patients were found to have multiple locations compared to the Equal and Discrepant groups. In addition, there was a higher fraction of cases treated with radiotherapy only in the Sequential group. No differences regarding the overall survival ($p=0.375$) or time between primary and secondary surgery ($p=0.334$) were found when comparing the three relapse groups.

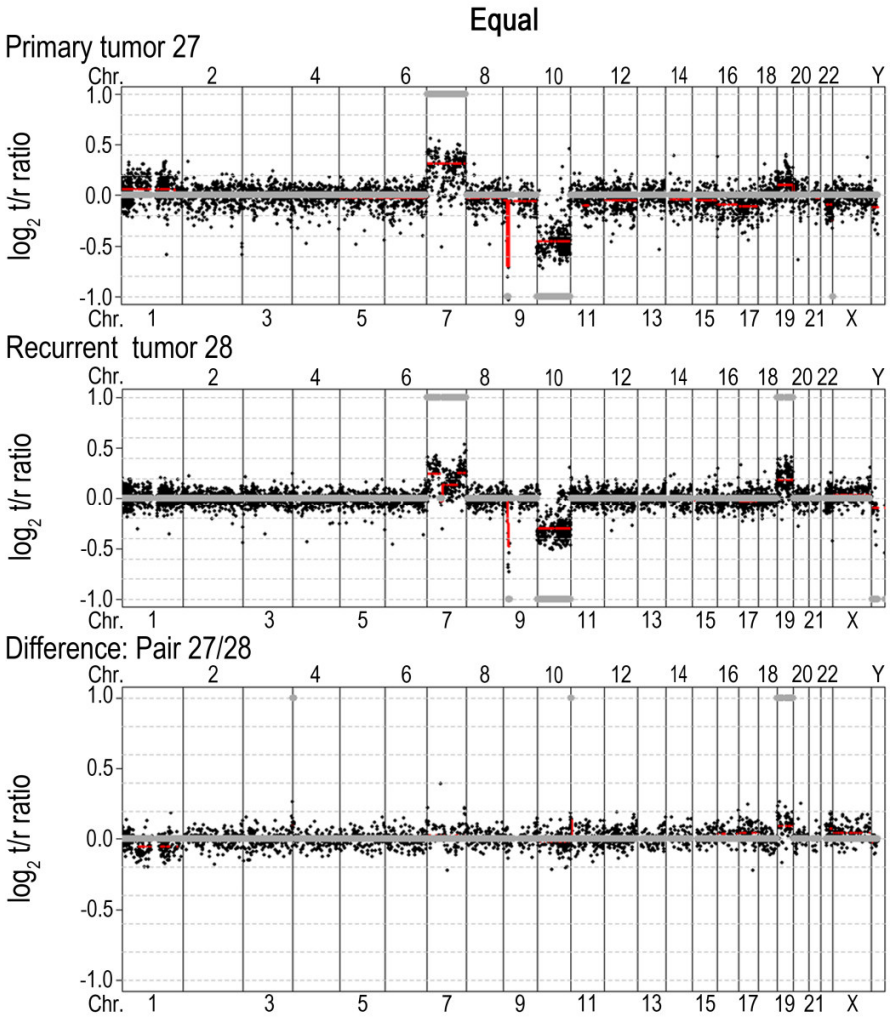

Figure 15: Comparison of genomic profiles in paired primary and recurrent glioblastomas: example for an Equal tumor pair.

Genomic profiles of glioblastoma pair 27/28 are shown, together with the completely balanced difference profile (bottom), demonstrating that the primary (case 27: top profile) and recurrent (case 28: middle profile) tumor share all copy number changes. In all genomic profiles, the midpoints of all BAC clones are plotted in genomic order from 1p to Yq on the x-axis against their normalized $\log_2$ test to reference ratio on the y-axis (Riehmer et al., 2014, in press).

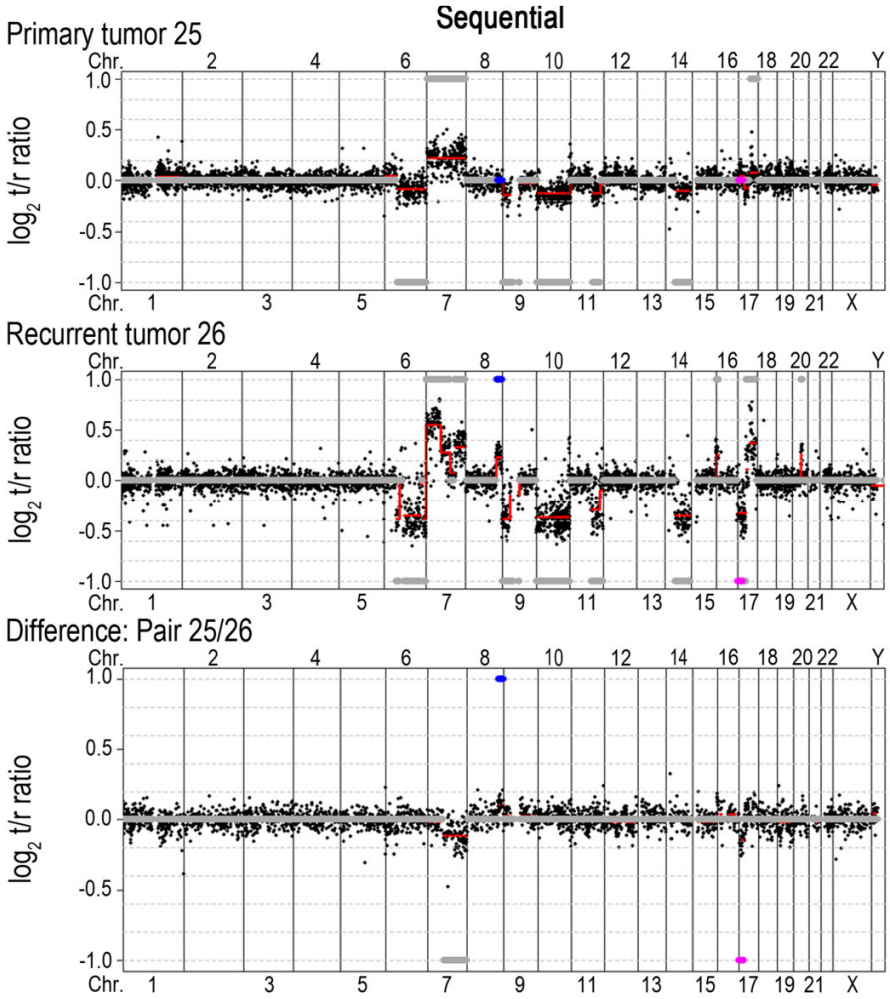

Figure 16: Comparison of genomic profiles in paired primary and recurrent glioblastomas: example for a Sequential tumor pair.

Genomic profiles of tumor pair (25/26) are shown, including the difference profile (bottom). Though primary (case 25: top profile) and recurrent tumor (case 26: middle profile) share copy number changes, additional copy number changes can be detected in the recurrent tumor (horizontal blue line, additional gain: here on 8q (copy number up regulation in recurrent tumor); horizontal pink line, additional loss: here on 17p (copy number down regulation in recurrent tumor)). Horizontal gray lines in the array-CGH profiles of the primary and the recurrent tumor indicate a copy number change present in both primary and recurrent tumor. In all genomic profiles, the midpoints of all BAC clones are plotted in genomic order from 1p to Yq on the x-axis against their normalized $\log_2$ test to reference ratio on the y-axis (Riehmer et al., 2014, in press).

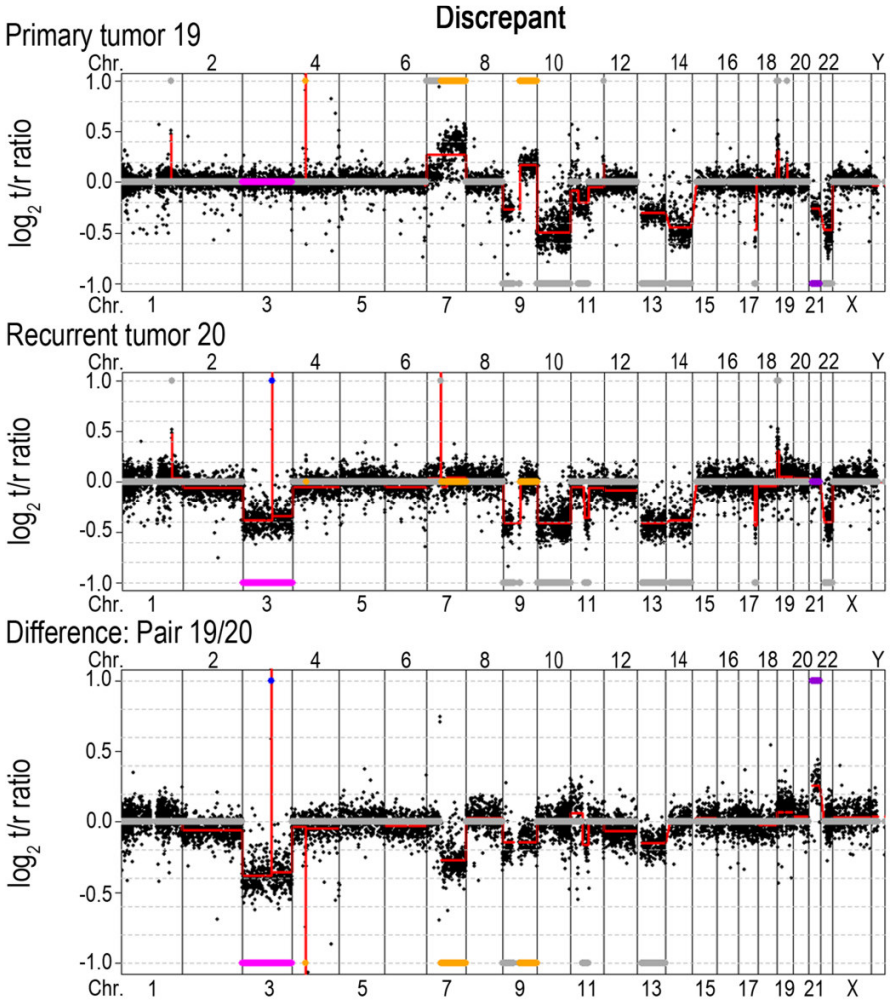

Figure 17: Comparison of genomic profiles in paired primary and recurrent glioblastomas: example for a Discrepant tumor pair.

Genomic profiles of tumor pair (19/20), including the difference profile (bottom), demonstrating that the primary (case 19: top profile) and the recurrent (case 20: middle profile) share copy number changes. Additional copy number changes are apparent (horizontal blue line, additional amplification: here on 3q (copy number up regulation in recurrent tumor); horizontal pink line, additional loss: here of chromosome 3 (copy number down regulation in recurrent tumor)). Changes no longer present are also depicted (horizontal yellow line, gain in the primary tumor no longer present in the recurrent tumor: here on 7q and 9q (copy number down regulation in the recurrent tumor); horizontal purple line, a loss in the primary tumor no longer present in the recurrent tumor: here of chromosome 21 (copy number up regulation in recurrent tumor)). Horizontal gray lines in the array-CGH profiles of the primary and the recurrent tumor indicate a copy number change present in both primary and recurrent tumor. In all genomic profiles, the midpoints of all BAC clones are plotted in genomic order from 1p to Yq on the x-axis against their normalized $\log_2$ test to reference ratio on the y-axis (Riehmer et al., 2014, in press).

Table 15: Clinical characteristics of study group by molecular relapse pattern
(Riehmer et al., 2014, in press).

	Equal (n=7)	Sequential (n=9)	Discrepant (n=11)	Total (n=27)
Age at diagnosis (years)				
Median	58	58	64	63
Range	44-70	38-66	49-68	38-70
Age classes (years)				
<50	2	2	1	5
51-60	2	3	3	8
61-70	3	4	7	14
Gender				
Male	6	5	6	17
Female	1	4	5	10
KPS				
90-100	4	5	6	15
70-80	3	2	5	10
<70	-	2	-	2
***MGMT* promoter methylation (primary tumor)**				
No methylation	5	4	7	16
Weak methylation	-	2	-	2
Strong methylation	2	3	4	9
***MGMT* promoter methylation (recurrent tumor)**				
No methylation	5	5	8	18
Weak methylation	-	2	-	2
Strong methylation	2	1	3	6
No data	0	1	-	1
Primary surgery				
Gross total resection	2	5	7	14
Subtotal resection (50-99%)	4	2	3	9
Partial resection (<50%)	1	2	0	3
No data	0	0	1	1
Location region (primary tumor)				
Frontal	1	-	5	6
Temporal	2	2	1	5
Parietal	1	1	4	6
Not localized to one side	3	5	1	9
No data	0	1	-	1
Location side (primary tumor)				
Left	5	2	6	13
Right	2	7	5	14
First-line therapy				
RT only	1	3	1	5
RT plus TMZ	6	6	10	22
TMZ cycles				
0-2	1	3	3	7
3-5	2	0	4	6
6-7	3	1	3	7
11	0	2	0	2
No data	1	3	1	5

Time between primary and secondary surgery				
Months Median (95% CI)	7.4 (6.7-8.2)	10.9 (6.9-14.8)	9.1 (5.5-12.8)	9.1 (5.9-12.4)
Overall survival				
Months Median (95% CI)	15.9 (15.4-16.4)	17.9 (12.3-23.6)	14.9 (8.2-21.6)	16.0 (14.2-17.7)

3.3.3 Aberration frequency in the three molecular relapse groups

In order to compare the copy number changes in the molecular relapse groups (Equal, Sequential and Discrepant), frequency plots were prepared for primary and recurrent tumors. Figure 18 demonstrates the frequency and extent of genomic imbalances in primary and recurrent tumors with Equal, Sequential and Discrepant signatures. The frequencies of the most common copy number changes were similar in the primary tumors of the three groups. Frequent chromosomal imbalances were gains on chromosomes 7, 19, and 20 as well as losses on chromosomes 10, chromosomal arms 13q and 22q.

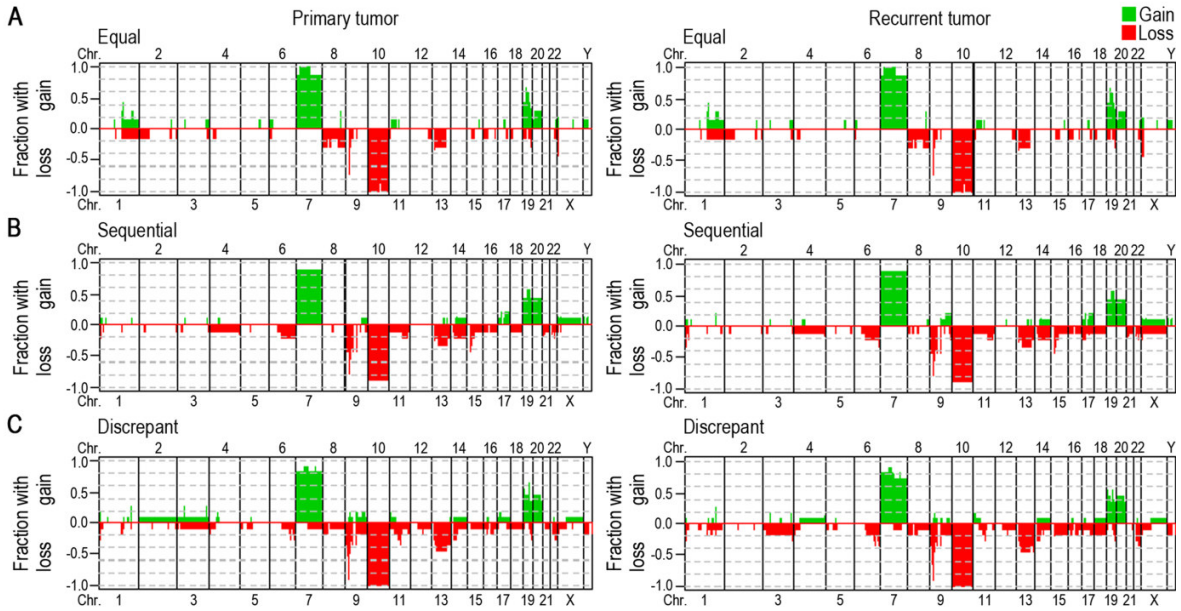

Figure 18: Frequency plots of primary and recurrent glioblastomas according to the molecular relapse subtype: Equal (A), Sequential (B), and Discrepant (C).
Primary glioblastomas from the three relapse groups depicted on the left side show chromosomal imbalances at similar frequencies. Gains on chromosomes 7, 19 and 20 as well as losses on chromosome 10 and chromosomal arm 13q, are found at similar frequencies in all groups. Losses on chromosome 9 are less frequent in the Equal group when compared to the Sequential and Discrepant tumors. Frequency plots for the recurrent tumors are shown on the right side. **A:** The frequency plots for the Equal tumor pairs (n=7) are identical. **B:** For the Sequential group (n=9) few additional changes are seen in the recurrent tumors. **C:** In the Discrepant group (n=11), some differences in primary and recurrent tumors can be seen. Gains are indicated in green, losses are indicated in red. Gains and losses are plotted in genomic order from 1p to Yq on the x-axis. The y-axis indicates the fraction of cases with copy number changes (Riehmer et al., 2014, in press).

Even though a circumscribed loss on chromosome arm 9p was found in tumors of all groups, the region of loss was larger in the Sequential and Discrepant group, i.e. in these cases the loss more frequently encompassed the entire short arm and sometimes even the long arm of chromosome 9 (Figure 18 and Figure 19). Additionally, losses in chromosomal sub-band 9p21.3 were more pronounced in primary tumors with Sequential and Discrepant signatures. While the primary tumors of the Equal group only showed losses of chromosomal sub-band 9p21.3, Sequential and Discrepant tumors also exhibited pronounced losses, of this chromosomal region (Figure 19 and Table 16). Losses with a $\log_2$ test to reference ratio in the range of 0.3 to -1 may correspond to heterozygous deletions, whereas pronounced losses with a ratio lower than -1 more likely correspond to homozygous deletions. The $\log_2$ ratio of the lowest blue or orange clones in Figure 19 containing the genes *CDKN2A/B* or *ELAVL2* in Sequential or Discrepant tumors even reached a value of -2.

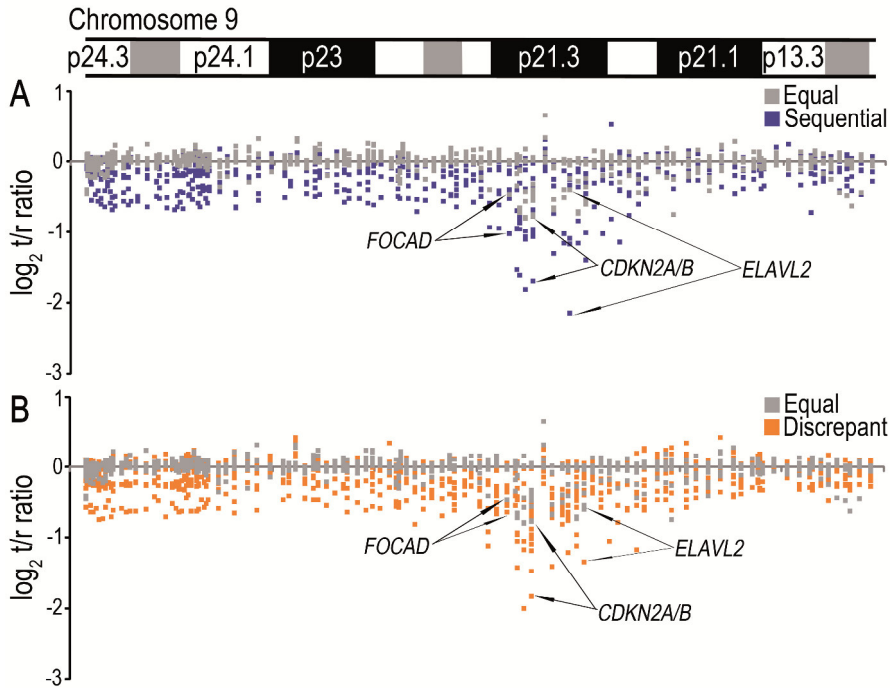

Figure 19: Comparison of array-CGH profiles on chromosomal arm 9p in Equal versus Sequential (A) and Equal versus Discrepant (B) primary tumors.

Midpoints of BAC clones from all tumors (Equal (n=7): grey clones; Sequential (n=9): blue clones; Discrepant (n=11): orange clones) were plotted in genomic order from 9p24.3 to 9p11.2 on the x-axis against their normalized $\log_2$ test to reference ratio on the y-axis. While equal tumors (grey clones) show a circumscribed loss in 9p21.3 harboring genes like *FOCAD*, *CDKN2A/CDKN2B* and *ELAVL2*, they are balanced in other parts of 9p. Sequential (blue) and Discrepant (orange) tumors show losses throughout 9p. Additionally, losses in 9p21.3 are more pronounced in Sequential and Discrepant than in Equal tumors (see arrows pointing to clones containing *FOCAD*, *CDKN2A/CDKN2B*, and *ELAVL2*: upper arrow for each gene, pointing to the grey clone with the most pronounced loss; lower arrow for each gene, pointing to the blue **(A)** or orange **(B)** clone with the most pronounced loss) (Riehmer et al., 2014, in press).

Since the short arm of chromosome 9 displayed the biggest difference in the frequency plots (Figure 18, page 78), a literature search was done in order to identify genes located on chromosomal arm 9p that are reported to be associated with glioma tumorigenesis. The identified genes were *LRRN6C/LINGO2* (9p21.1-p21.2); *ELAVL2, CDKN2A/CDKN2B*, *FOCAD* (9p21.3); *NFIB* (9p22.3-p23); and *PTPRD* (9p23-p24.1).

Table 16 summarizes the number of cases with a loss (log_2 ratio -0.3 to -1) and a pronounced loss (log_2 ratio <-1) on 9p in primary glioblastomas from the three molecular relapse groups. There was no pronounced loss of the 9p clones selected here in Equal tumors. The most frequently lost gene loci were *ELAVL2*, *CDKN2A*/*CDKN2B*, and *FOCAD*. Losses of these three genes were more often detected in the Sequential and Discrepant group when compared to Equal tumors. In order to compare copy number changes in Equal and non-Equal tumors, the Sequential and Discrepant groups were combined. This comparison showed that significantly more non-Equal tumors had losses or pronounced losses of *ELAVL2* than Equal tumors (p=0.025), while the differences were not quite significant for *CDKN2A/CDKN2B* and *FOCAD* (p=0.055 and p=0.067).

Table 16: Distribution of losses in glioma-associated genes on 9p in different molecular relapse groups
(p-values relate to all cases with loss comparing Equal and non-Equal tumors) (Riehmer et al., 2014, in press).

Clone (chromosomal localization)	**Gene**	**Number of primary tumors with loss (log_2 test/reference ratio: -0.3 to -1)/ pronounced loss (log_2 test/reference ratio: <-1)**			
		Equal (n=7)	**Sequential (n=9)**	**Discrepant (n=11)**	**Non-Equal (Sequential plus Discrepant, n=20)**
RP11-32I2 (9p21.1-p21.2)	*LRRN6C/ LINGO2*	0/ 0	0/ 0	3/ 0	3/ 0
RP11-31K16 (9p21.3)	*ELAVL2*	1 / 0	1 / 3	8 / 1	9 / 4 (p=0.025)
RP11-149I2 (9p21.3)	*CDKN2A/ CDKN2B*	4 / 0	3 / 3	5 / 5	8 / 8 (p=0.055)
RP11-512L9 (9p21.3)	*FOCAD*	1 / 0	4 / 1	6 / 0	10 / 1 (p=0.067)
RP11-280O24 (9p22.3-p23)	*NFIB*	0 / 0	1 / 0	2 / 0	3 / 0
RP11-175E13 (9p23-p24.1)	*PTPRD*	0 / 0	2 / 0	2 / 0	4 / 0

3.3.4 Regions of genomic difference between primary and recurrent tumor pairs

The next aim was to identify regions with a different copy number in primary as compared to recurrent tumors and to identify candidate genes residing in these regions associated with therapy response and tumor recurrence. For that reason and in order to visualize the different types of genomic differences in the tumor pairs, a heatmap was generated in cooperation with the Institute for Medical Informatics, Statistics and Epidemiology of the University of Leipzig. This heatmap, depicted in Figure 20, was sorted by the three molecular relapse groups (Equal, Sequential and Discrepant). Each possible chromosomal difference in the primary versus the recurrent tumor was assigned a certain color. Dark blue indicated a novel gain in the recurrent tumor; a novel loss in the recurrent tumor was indicated by a pink color code; a gain no longer present in the recurrent tumor was indicated as orange, a loss no longer present in the recurrent tumor was indicated by a purple color code. The color yellow was assigned to a gain in the primary tumor recurring as a loss in the recurrent tumor. All chromosomal regions, which exhibit a copy number that differs in primary versus recurrent tumor pairs, are given with the color code in Figure 20.

By definition, there is no genomic difference between Equal tumor pairs, as shown in Figure 15 (page 74). So the heatmap for the Equal group is entirely gray. Sequential tumors had only novel gains or losses (dark blue or pink). In contrast, all types of differences were found in the Discrepant tumors (Figure 20A). In order to identify recurrent chromosomal differences, a second heatmap was prepared showing only the regions that were involved in the same type of change in at least two tumor cases (Figure 20B). Strikingly, in 14 of 20 non-Equal tumor pairs, at least one recurrent copy number change difference was found. No consistent difference in therapy, survival or *MGMT* promoter methylation status was detected in the distinct molecular relapse groups.

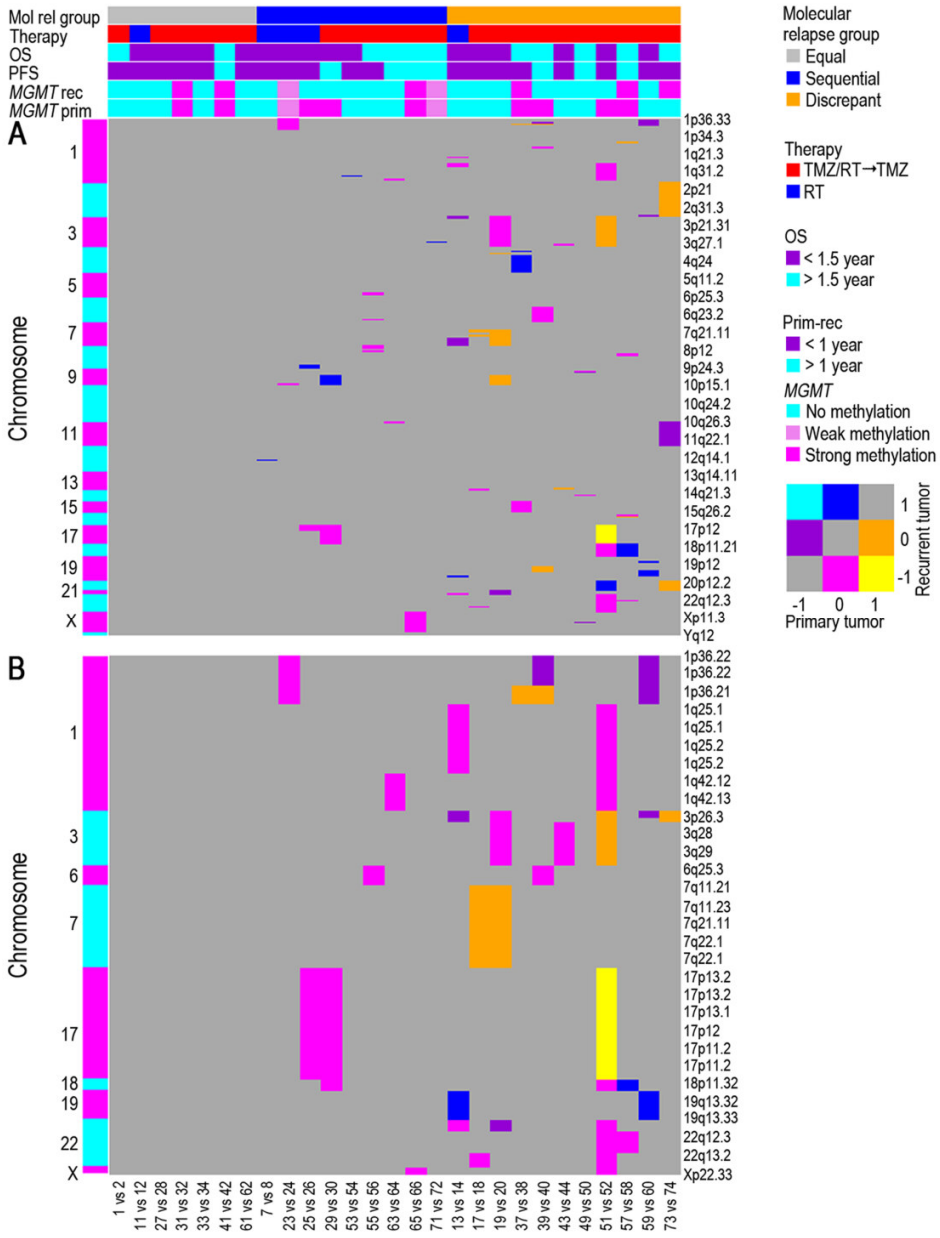

Figure 20: Regions of genomic differences in primary and recurrent glioblastoma pairs.
The heatmaps sorted by molecular relapse groups demonstrate all differing genomic regions **(A)** and regions of genomic difference observed at least twice **(B)**. In the Equal tumor group, no differences in copy number changes were observed. In the Sequential group, only additional aberrations in the recurrent tumors were detected (pink: additional loss; dark blue: additional gain). In the Discrepant group, all kinds of copy number differences were detected (orange: gain no longer present in the recurrent tumor; yellow: gain in the primary tumor that is a loss in the recurrent tumor; purple: loss that is no longer detected in the recurrent tumor; pink: additional loss; dark blue: additional gain). No consistent difference in therapy, survival or *MGMT* status was detected in the distinct molecular relapse groups. Molecular relapse group: grey, Equal; blue, Sequential; orange, Discrepant. Therapy: red, temozolomide + radiation; blue, radiation only. OS: purple, <1.5 years; light blue, >1.5 years. Prim-rec, time between surgery for primary and recurrent tumor: purple, <1 year; light blue, >1 year. *MGMT* rec, *MGMT* promoter methylation in recurrent tumor: light blue: no methylation; light pink: weak methylation; dark pink: strong methylation. *MGMT* prim, *MGMT* promoter methylation in primary tumor: light blue, no methylation; light pink, weak methylation; dark pink: strong methylation (Riehmer et al., 2014, in press).

In order to identify candidate genes playing a role in tumor recurrence, the gene content of chromosomal regions affected at least twice by a copy number change in primary versus recurrent tumors was assessed using the ENSEMBL or UCSC Genome Browser. For all genes the literature was interrogated for an association with tumor recurrence or cancer therapy response. Using this strategy, 46 genes were identified to have a potential association with tumor recurrence or therapy response. Twenty-four of these genes were glioma-related. The results of this survey are listed in Table 17, which also indicates whether the copy number of a candidate gene increased or decreased in the recurrent tumors.

Table 17: Chromosomal regions affected at least twice by copy number difference and candidate genes involved.

Listed are chromosomal regions with copy number increase or decrease in in recurrent versus primary glioblastomas, candidate genes associated with tumor recurrence or therapy response according to the literature, and type of copy number change in the recurrent tumors (Riehmer et al., 2014, in press).

Chr. band	Candidate genes (references)	Copy number change in recurrent versus primary tumor
1p36.23-p22	***CAMTA1**** (Schraivogel et al., 2011), ***PARK7**** (Vasseur et al., 2009; Hinkle et al., 2011), ***UBE4B*** (Zage et al., 2013), ***PLOD1*** (Cleator et al., 2006; Gilkes et al., 2013)	Increase
1p36.21	***PDPN**** (Ernst et al., 2009; Peterziel et al., 2012), ***PRDM2**** (Roversi et al., 2006)	Decrease
1q41-q42.12	***CAPN2**** (Ma et al., 2012), ***PARP1**** (Csete et al., 2009; van Vuurden et al., 2011; Huang et al., 2014)	Decrease
3q27.3-q28	***HRG**** (Kärrlander et al., 2009), ***RFC4*** (Arai et al., 2009), ***BCL6*** (Horn et al., 2013), ***SST**** (Massa et al., 2004), ***TP63**** (Su et al., 2013; Yamaki et al., 2013)	Decrease
6q25.1	*ARID1B** (Sausen et al., 2013)	Decrease
7q11.2	***LIMK1**** (Prudent et al., 2012), ***LAT2**** (Kühne et al., 2009; Svojgr et al., 2012)	Decrease
7q21.11-q22.1	***HGF**** (Guo et al., 2012), ***AZGP1*** (Yip et al., 2011; Huang et al., 2012), ***SERPINE1**** (Colin et al., 2009), ***CUX1*** (Li et al., 2013), ***RELN*** (Okamura et al., 2011)	Decrease
17p13-p11.2	***TNFSF13**** (Roth et al., 2001; Petty et al., 2009), ***ZBTB4*** (Chadalapaka et al., 2012), ***DVL2**** (Pulvirenti et al., 2011), ***CLDN7*** (Lourenço et al., 2010), ***TP53**** (Zheng et al., 2012), ***EFNB3**** (Li et al., 2012), ***AURKB**** (Hodgson et al., 2009; Raverot et al., 2010), ***NTN1*** (Link et al., 2007), ***RCVRN*** (Maeda et al., 2002), ***MAP2K4*** (Ohtsuka and Zhou, 2002; Tesser-Gamba et al., 2012), ***ELAC2*** (Tavtigian et al., 2001), ***PMP22*** (Simpson et al., 2010), ***TRIM16*** (Raif et al., 2009), ***MPRIP**** (Coupienne et al., 2011), ***FLCN*** (Cash et al., 2011), ***SREBF1**** (Guo et al., 2009; Guan et al., 2011), ***LLGL1*** (Lassmann et al., 2007), ***ALDH3A2*** (Ohhira et al., 1996), ***ALDH3A1*** (Hu et al., 2009)	Decrease
19q13.32-q13.33	***CLPTM1*** (Folgueira et al., 2005), ***RELB**** (Josson et al., 2006; Lee et al., 2013), ***FGF21*** (Osawa et al., 2009)	Increase
22q13.2	***EP300**** (Zhao et al., 2011; Sen et al., 2011), ***XRCC6**** (Bau et al., 2011), ***TSPO**** (Bertomeu et al., 2010; Chelli et al., 2008)	Decrease

Bolded entries indicate genes associated with tumor recurrence or therapy response according to the literature.
*Genes associated with glioma according to the literature

The 46 identified candidate genes associated with therapy response and tumor recurrence, were further analyzed regarding their function. To this end, an ontology search and network analysis using the PROTEOME™ software (Biobase, GmbH, Wolfenbuettel, Germany) was performed. Hereby, the candidate genes were found to encode proteins involved in several cellular processes such as cell proliferation, cell cycle, apoptosis, cell adhesion, cellular response to stress or hypoxia, intracellular signal transduction, surface receptor signaling, transcription factor activation and chromatin remodeling. The results of this analysis are listed in Table 18.

Table 18: Functions of the 46 identified candidate genes associated with therapy response or tumor recurrence. Candidate genes are located in the chromosomal regions affected by recurrent copy number difference in recurrent versus primary glioblastomas (Riehmer et al., 2014, in press).

Function*	**Candidate genes**
Cell proliferation	*ALDH3A1, ALDH3A2, AURKB, AZGP1, BCL6, ELAC2, EP300, HGF, LLGL1, MAP2K4, PMP22, RCVRN, SST, TNFSF13, TP53, TRIM16, TSPO*
Cell cycle/DNA replication	*ALDH3A1, CAMTA1, EP300, HGF, PRDM2, RFC4, TP53, TP63, ZBTB4*
Cell death	*AURKB, HGF, MAP2K4, PARK7, PARP1, PRDM2, RELB, SST, TNFSF13, TP53, TP63, UBE4B, XRCC6*
Extracellular matrix component/organization	*PLOD1, RELN*
Cell adhesion/migration	*CLDN7, EP300, FLCN, HGF, LLGL1, NTN1, PDPN, RELB, RELN, SERPINE1, TP63*
Surface receptor signaling	*AZGP1, BCL6, DVL2, ELAC2, EP300, EFNB3, FGF21, FLCN, HRG, LIMK1, MAP2K4, NTN1, PARP1, RCVRN, RELN, SREBF1, SST, TNFSF13, TP53, XRCC6*
Intracellular signal transduction	*AZGP1, CAPN2, DVL2, EP300, FGF21, HGF, LAT2, MAP2K4, MPRIP, PARK7, RELB, SERPINE1, SREBF1, SST, TNFSF13, TP53*
Cellular response to stress	*DVL2, EP300, MAP2K4, MPRIP, PARK7, PARP1, TP53, XRCC6*
Cellular response to hypoxia	*PARP1, TP63, XRCC6*
Transcription factor activity	*ARID1B, BCL6, CUX1, EP300, PARP1, PRDM2, RELB, SREBF1, TP53, TP63, ZBTB4*
Chromatin remodeling/ modification	*ARID1B , AURKB, PARP1, FGF21, EP300, XRCC6*

*according to PROTEOME™ ontology and own literature search

Regulators of apoptosis, in particular members of the p53 family and pathway, showed a changed copy number in 13 of 14 non-Equal (Sequential and Discrepant) tumor pairs displaying a recurrent copy number difference. The copy numbers of *TP53*, *TP63* and *EP300* were downregulated directly or indirectly in nine recurrent tumors. Direct down regulation was detected in seven cases. Indirect down regulation via *UBE4B* copy number increase was found in two cases. In two additional recurrent tumors, copy numbers of positive regulators of apoptosis (*PRDM2* and *PARP1*), were decreased. In another recurrent tumor, an increased copy number of a negative regulator of apoptosis (*RELB*) was detected. In one of the 14 recurrent non-Equal tumors, the copy number of the apoptosis regulators

mentioned before was not changed. But in this case, the copy number of the chromatin remodeler *ARID1B* was decreased (Table 19).

Table 19: Genes encoding regulators of apoptosis or chromatin remodelers.
The copy number of which is changed in at least two recurrent tumors from non-Equal pairs. A copy number increase or decrease of these genes is found in all 14 recurrent non-Equal tumors that carry a copy number difference observed more than once (Riehmer et al., 2014, in press).

Functional group	**Gene (copy number change in recurrent versus primary tumor)**		**Tumor pairs**
TP53 family or pathway	*TP53* (decrease)	Direct	25 vs. 26; 29 vs. 30; **51 vs. 52***
		Indirect via *UBE4B* copy number increase	**39 vs. 40***; **59 vs. 60***
	TP63 (decrease)		**19 vs. 20**; **43 vs. 44**; **51 vs. 52***
	EP300 (decrease)		**17 vs. 18**; **57 vs. 58**
Positive regulators of apoptosis	*PARP1* (decrease)		**51 vs. 52***; 63 vs. 64*
	PRDM2 (decrease)		**37 vs. 38**; **39 vs. 40***
Negative regulators of apoptosis	*RELB* (increase)		**13 vs. 14**; **59 vs. 60***
Chromatin remodelers	*ARID1B* (decrease)		**39 vs. 40***; 55 vs. 56
	PARP1 (decrease)		**51 vs. 52***; 63 vs. 64*

*affected by copy number change of more than one gene listed here encoding an apoptosis regulator or chromatin remodeler
Non-bold, Sequential pairs; bold, Discrepant pairs.

In summary, primary and recurrent glioblastomas from the same patient were analyzed in 27 cases in order to determine genetic patterns of glioblastoma progression. Array-CGH profiles were compared and yielded three molecular relapse groups named Equal, Sequential and Discrepant. Regions of genomic difference between primary and recurrent tumors were identified and found to harbor 46 candidate genes associated with tumor recurrence or therapy response. In particular, copy numbers of genes encoding apoptosis regulators were frequently changed at progression explaining why the tumor cells evaded apoptosis. Losses of chromosomal band 9p21.3 harboring genes such as, *ELAVL2, CDKN2A/CDKN2B*, and *FOCAD* were significantly more common in primary tumors from non-Equal pairs possibly causing an alteration of the clonal composition in the recurrent tumors.

3.4 Project 4: Genomic profiling to assess the clonal relationship between histologically distinct intracranial tumors

Array-CGH was used to retrospectively analyze the clonal relationship of two tumor samples from a 47-year old female patient (patient 1: more detailed patient description can be found in 2.1.10 and in Hofer et al., 2012). The primary tumor was initially classified as an unusual pituitary adenoma by three independent reference pathologists. Pituitary adenoma are considered benign, nevertheless, in

this case the tumor recurred shortly (3 months) after the initial surgery. Histologically, the second tumor differed from the primary tumor (2.1.10, page 30). Nine months later the patient died, suggesting that the patient had been affected by a malignant tumor.

Though the two tumor samples were different in their histopathology, the question arose if the first and the second tumor contained the same copy number changes and thus most likely had the same cellular origin. In order to address this question, array-CGH was performed on DNA isolated from the fibrotic appearing areas of the first tumor. This array-CGH analysis revealed a complex pattern of chromosomal imbalances, affecting all chromosomes but one (chromosome 16). If not the entire chromosome, then at least a chromosomal arm was affected by losses (x1 in karyotype) or gains (x3 in karyotype). From the profile shown in Figure 21A the following karyotype could be deducted:
[arr(3,6,9,10,11,13q,14q,18p,X)x1,(1q,2,4,5,7,8,12,15q,17p,17q21.33q25.3,18q,19,20,21q,22q)x3].

The second profile shown in Figure 21B was obtained from DNA extracted from the second tumor (third surgery). This profile showed a similarly complex karyotype containing the following additional copy number changes: (partial) loss of 1p, 4, 16, 17, 19, 21q [karyotype: arr(1p,3,4p16.1q35.2,6,9,10,11,13q,14q,16,17q11.2q21.2,18p,19q13.2q13.43,21q,X)x1,(1q,2,4p16.1p16.3,5,7,8,12,15,17p,17q21.33q25.3,18q,19p13.3q13.13,20,22q)x3]. About 80% of the 29 detected copy number changes in the second tumor were already present in the first tumor sample, providing strong evidence for a clonal relationship and suggesting that the second lesion indeed represented a recurrent tumor of the first lesion.

Additionally, histological and immunohistochemical analysis revealed that the second tumor showed characteristics of a malignant peripheral nerve sheath tumor (MPNST), WHO grade IV (data not shown). For this reason, the array-CGH data shown here were compared with the profiles of 122 cases of listed in the Progenetix database (http://www.progenetix.org/progenetix/I95403/ideogram.svg). The most frequent copy number changes found in the database for MPNST (losses on 1p, 9, 10, 11, 13q, 17p; gains on 1q, 2, 5, 6, 7, 8, 12, 15q, 17q, 18, 20, and 21q) were almost all detected in the second analyzed tumor, with only few exceptions such as 17p loss and gains on 6 and 21q. Thus, there is a concordance of 83% between the imbalances in the second tumor analyzed here and the MPNST cases reported in the literature. Moreover, these results suggest that array-CGH can be successfully used to identify the clonal relationship between two histologically distinct tumors. This analysis has been published in Hofer et al., 2012.

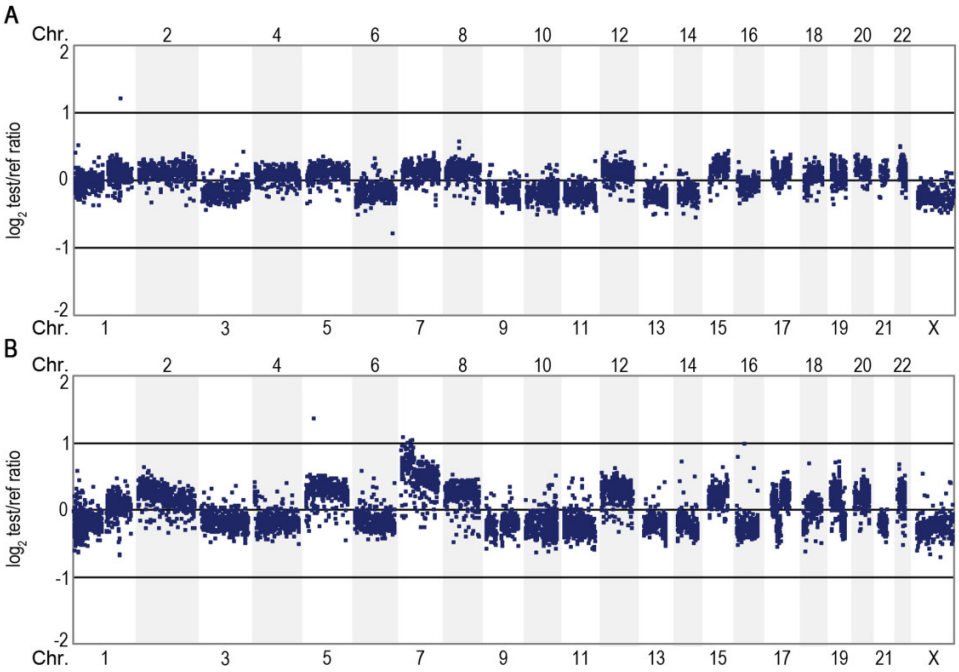

Figure 21: Genome-wide array-CGH profiles of the first (A) and the second (B) intracranial tumor of patient 1. Both profiles show a highly similar pattern of DNA copy number changes. The midpoints of all BAC clones are plotted in genomic order from 1p to Yq on the x-axis against their normalized $\log_2$ test to reference ratio on the y-axis (modified from Hofer et al., 2012).

3.5 Project 5: Dissecting the genotype in a patient with cancer predisposition using whole exome sequencing in addition to genome-wide copy number analysis

In the previous projects of this study DNA from tumor samples was analyzed by array-CGH in order to detect somatic chromosomal imbalances on a genome-wide scale in large cohorts of tumors of the central nervous system. Genome-wide screening methods such as array-CGH or whole exome sequencing (WES) can also be used to analyze the germline of a patient with the aim to identify the genetic basis of a phenotype such as cancer predisposition.

Here, patient 2 presenting with cancer predisposition combined with syndromic intellectual disability was analyzed with two genome-wide genetic screening methods in order to explain this highly complex phenotype. This complex phenotype consisted of facial anomalies (depressed nasal root and widely spaced eyes), skin lesions (numerous café-au-lait and hypopigmented spots), and two neoplastic diseases (a both-sided mixed malignant germ cell tumor of the ovaries and an acute pre-B-lymphoblastic leukemia) in the first two decades of life. The patient also presented with psychomotor and mental delay persisting until adult age as well as low body weight and short stature (more detailed patient description can be found in section 2.1.11, page 31).

Figure 22 shows the facial features of patient 2 at the ages of 11 months (A and B) and 23 years (C and D), whereas Figure 22E depicts areas of skin displaying hypo- and hyperpigmentation on the patient's back at 23 years of age.

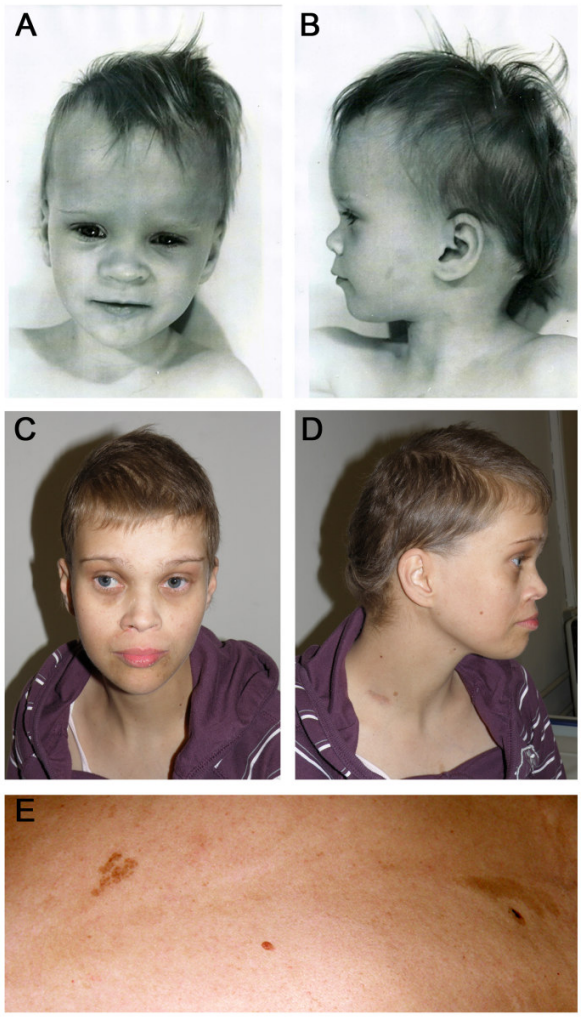

Figure 22: Facial features and skin lesions of patient 2.
A and **B:** Patient 2 at 11 months of age. **C** and **D:** Patient 2 at 23 years of age. The facial features are in line with the diagnosis of Bloom syndrome. **E:** Areas of skin displaying hypo- and hyperpigmentation on patient's back at the age of 23 years (Classen and Riehmer et al., 2013).

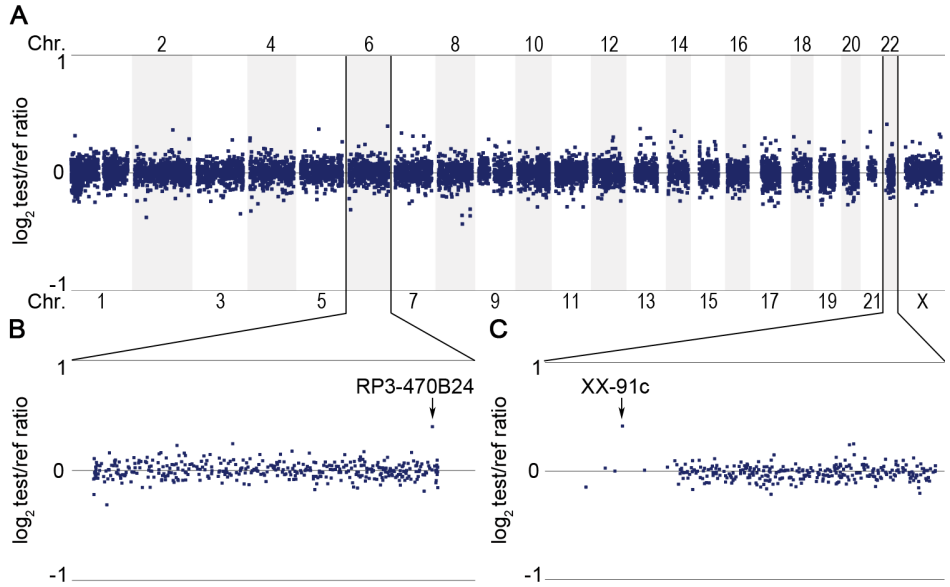

Figure 23: Genome-wide BAC array-CGH profile of DNA from peripheral blood of patient 2 (A).
B: Enlargement of chromosome 6 displaying the duplicated BAC clone RP3-470B24. **C:** Enlargement of chromosome 22 displaying the duplicated BAC clone XX-91c. The midpoints of all BAC clones are plotted in genomic order from 1p to Yq on the x-axis against their normalized $\log_2$ test to reference ratio on the y-axis.

Since the patient presented with a complex phenotype including intellectual disability, which is often caused by chromosomal imbalances such as microduplications or microdeletions, the initial approach was to analyze DNA from peripheral blood of patient 2 using a 10.6k BAC array (Figure 23). Threshold were set and every clone displaying a $\log_2$ test to reference ratio of greater than 0.3 or smaller than -0.3 indicating a microduplication or microdeletion was looked at in more detail. Using the database of genomic variants of the ENSEMBLE Genome Browser or the UCSC Genome Browser, it was checked whether aberrant clones overlapped with known non-pathogenic copy number changes. Clones located on chromosomes 2 and 5 fulfilled the set criteria for the normalized $\log_2$ ratio and did not overlap with known genomic variants. Therefore, a chromosome 2 and a chromosome 5 specific oligonucleotide array were performed. However, the microduplications and microdeletion were not verified and thus considered false-positive (data not shown). With the BAC array also a gain in the chromosomal band 22q11.21 of one clone (XX-91c) was detected (Figure 23C). Additionally, another gain was found involving one clone (RP3-470B24) in chromosomal band 6q27 (Figure 23B). In order to verify the two copy number changes on chromosomes 22q and 6q, the patient's DNA as well as DNA from both parents were hybridized to chromosome 22 and chromosome 6 specific oligonucleotide arrays. This approach aimed at fine mapping the microduplications and determining their exact breakpoints. The parents were analyzed in order to identify whether the microduplications occurred *de novo* or were inherited. Figure 24 displays an enlargement of the duplicated region on chromosome 22 verified by oligonucleotide array-CGH. The microduplication was shown to have a size of 2.518 Mb in the chromosomal band 22q11.21 (hg18:chr22: 17,276,999-19,794,999)

encompassing around 50 genes (top of Figure 24). Furthermore, the mother of patient 2 carried the same microduplication on chromosome 22, whereas the father did not.

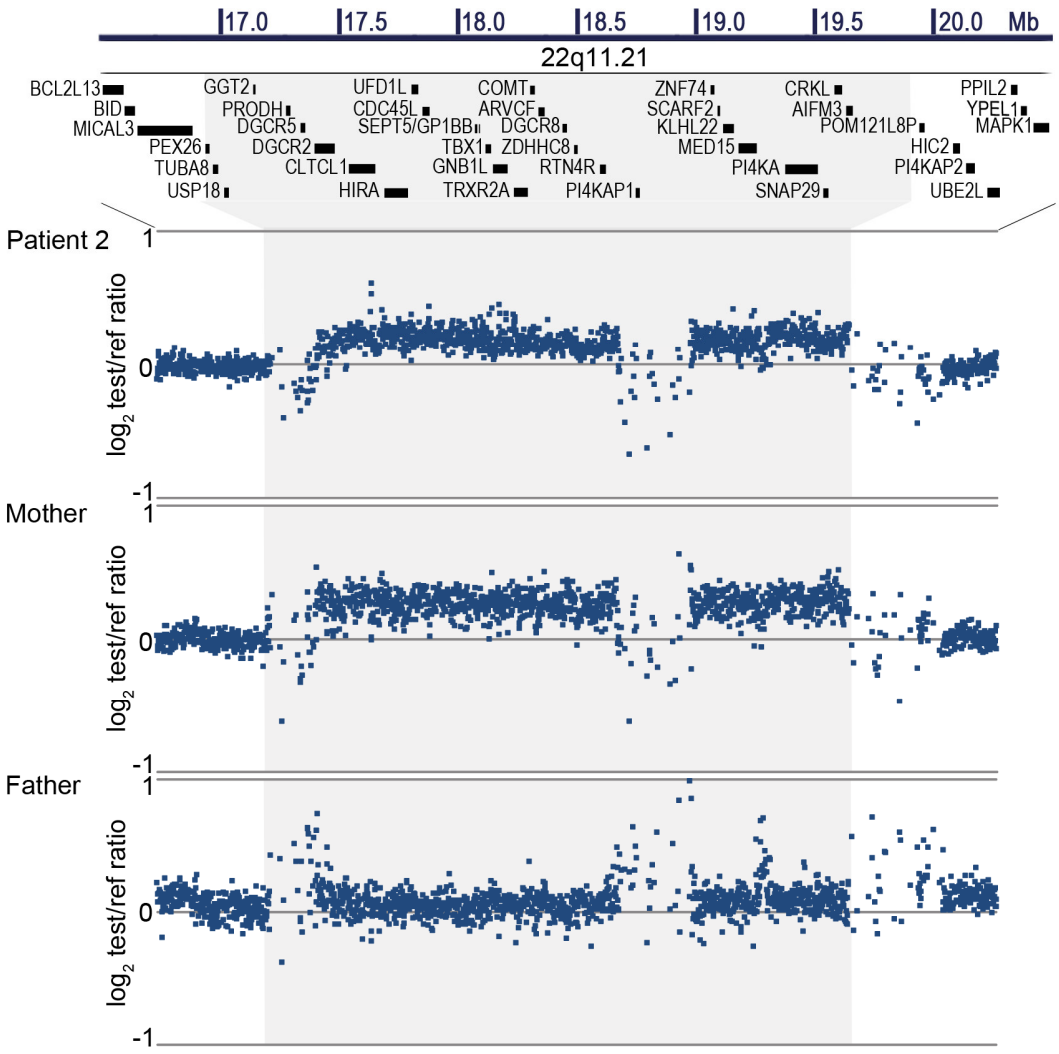

Figure 24: Enlargement of chromosomal band 22q11.21 from array-CGH profiles of patient 2 and her parents. Array-CGH was performed on a chromosome 22 specific tiling oligonucleotide array, demonstrating a microduplication of 2.518 Mb in the chromosomal band 22q11.21 (hg18:chr22: 17,276,999-19,794,999), indicated by the shaded area. The duplication was found in patient 2 and her mother, but not in her father. The microduplication encompassed around 50 genes including *DGCR2*, *CLTCL1*, *CDC45L*, *SEPT5* and *GP1BB*, displayed at the top of the array-CGH profiles (Classen and Riehmer et al., 2013).

In order to verify the gain in chromosomal band 6q27 involving the BAC clone RP3-470B24 and to investigate its inheritance, DNA from patient 2 as well as both parents was hybridized on a chromosome 6 specific oligonucleotide array. The fine mapping revealed a microduplication of 0.261 Mb in size in 6q27 (hg18: chr6:168,076,999-168,337,999) in patient 2 and her mother. This

duplication involved three genes, depicted at the top of Figure 25, and partially disrupting the *MLLT4* gene.

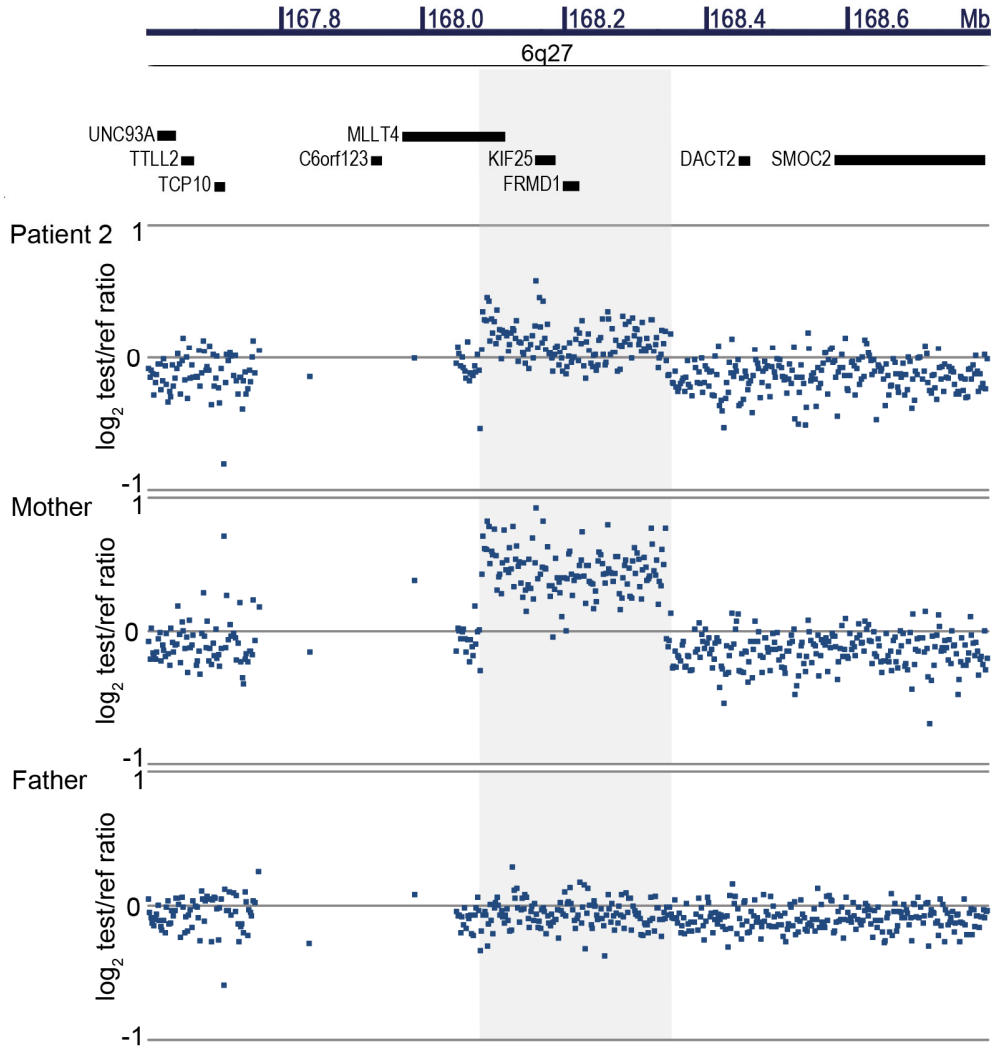

Figure 25: Enlargement of chromosomal band 6q27 from array-CGH profiles of patient 2 and her parents. Array-CGH was performed on a chromosome 6 specific tiling oligonucleotide array, showing a microduplication of 0.261 Mb in chromosomal band 6q27 (hg18: chr6:168,076,999-168,337,999) in patient 2 and her mother but not the father. The microduplication partially encompassed and possibly disrupted the *MLLT4* gene (Classen and Riehmer et al., 2013).

The microduplication on chromosome 22 was further verified by interphase FISH on lymphocytes of patient 2 as well as her mother. The results are demonstrated in Figure 26. A BAC clone that was located in the duplicated area (RP11-1151A3; hg18: chr22:17,445,949-17,587,300) was used for FISH (red signals). As a control, a BAC clone located more distally on chromosome 22 outside of the

duplicated region was used and (green signals: RP11-307O16; hg18: chr22:20,764,128-20,965,434). FISH analysis confirmed the 22q11.21 microduplication in patient 2 and her mother.

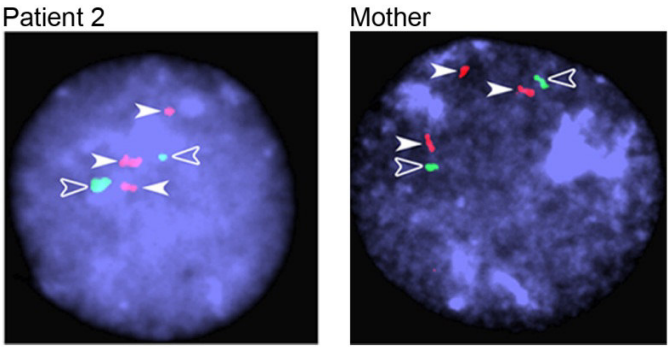

Figure 26: Interphase FISH analysis confirmed 22q11.21 microduplication in patient 2 and her mother.
Interphase FISH analysis using BAC clone RP11-1151A3 (three red signals, indicated by white arrow) from chromosomal band 22q11.21 in patient 2 and her mother confirmed the microduplication. Hybridization of BAC clone RP11-307O16 from chromosomal band 22q11.22 was used as a control (two green signals, open arrows) (Classen and Riehmer et al., 2013).

In summary, the genome-wide screen for genomic imbalances using array-CGH identified two microduplications on chromosomes 6q and 22q. Both microduplications were confirmed by at least one independent method, also indicating that both chromosomal alterations were inherited from the healthy mother. Both microduplications encompass a number of genes, which might be associated with the leukemia patient 2 had developed (*DGCR2*, *CLTCL1*, *CDC45L*, *SEPT5* and *GP1BB* (chromosome 22) and *MLLT4* (chromosome 6)). The microduplication on 22q11.21 might also partly explain the intellectual disability in patient 2.

3.5.1 Whole exome sequencing on DNA from peripheral blood of patient 2 and her mother

The highly complex phenotype of patient 2, including the intellectual disability and leukemia, could be in part explained by the detected microduplications in 22q and 6q (Figure 24 and Figure 25). The fact that the healthy mother displayed the same genetic alterations suggested that there was an additional genetic cause for the patient's phenotype. Furthermore, the cause underlying the bilateral ovarian germ cell tumor as well as the skin lesions remained unsolved. Therefore, as a second genome-wide screening method WES was performed on DNA from peripheral blood of the three family members (patient 2, mother and father) by CeGaT GmbH, Tübingen, Germany to detect DNA sequence variants. The initial approach was a trio-based *de novo* analysis (as described in 1.3.3, page 14) aiming to find *de novo* variants possibly responsible for the unexplained phenotypic features. The maternally as well as the paternally inherited variants are subtracted and only the *de novo* variants in the patient are retained. This approach detected a variant in the *CHEK2* gene

(*CHEK2*,c.1427C>T;p.Thr476Met) (Figure 27). Due to the fact that the results obtained still did not completely explain the complex phenotype of patient 2, a different filtering strategy of the WES data was applied in which the parents variants were not taken into account. Therefore, the total number of variants (26,974) identified by WES in patient 2 were filtered as follows. In order to reduce the number of detected variants to a manageable number, the filter strategies listed in Table 20 were applied. First of all, the number of variants could be remarkably reduced to 1,795 variants by removing bad quality and known variants from in-house exomes. In a second step, the data mining tool Genome Trax™ was used to extract HGMD mutations and COSMIC somatic disease mutations and 30 variants remained. Genome Trax™ primarily utilizes curation of peer-reviewed literature and provides information about conservation, allele frequency, effect on protein sequence, and deleterious predictions, as context to support assessment of the variants (2.2.8). Afterwards, non-coding or synonymous variants were removed, as well as variants predicted to be benign by three prediction programs (Mutation Taster, PolyPhen-2 and SIFT). The four filter steps resulted in 12 variants which were further analyzed for their association with cancer. The remaining 3 variants in 2 genes were finally verified by Sanger sequencing (Figure 27).

Table 20: WES data filtering strategy in patient 2 (modified from Classen and Riehmer et al., 2013).

Filtering steps	**Number of variants in patient 2**
Total number of variants in exome from peripheral blood	26,974
After removing bad quality and known variants from in house exomes (CeGaT)	1,795
After extracting ''HGMD mutations'' and ''COSMIC somatic disease mutations'' using Genome Trax™	30
After removing non-coding or synonymous variants	20
After removing variants predicted to be benign by MutationTaster, PolyPhen-2 and SIFT	12
Variants related to "cancer"	3

Two of the cancer related variants were located in the *BLM* gene. Both were identified to be stop mutations. The first *BLM* variant in exon 6 (*BLM*,c.1642C>T;p.Gln548X) was inherited from the healthy mother, since it was detected both in patient 2 and her mother. In contrast, the other variant found in the *BLM* gene in exon 13 (*BLM*,c.2695C>T;p.Arg899X) was found to be inherited from the healthy father. Patient 2 was, therefore, compound heterozygous for two stop mutations in the *BLM* gene. Importantly, mutations in the *BLM* gene are known to cause Bloom Syndrome associated with cancer predisposition (German et al., 2007). The diagnosis Bloom syndrome not only explains the cancer predisposition in patient 2, but also the other unclear phenotypic features, such as the skin lesions. This filtering strategy had also identified a heterozygous *de novo* rare missense variant in the *CHEK2* gene (rs142763740, genotype frequency C/T: 0.001). This identified variant was classified as disease causing by MutationTaster and SIFT and known validated as a HGMD disease mutation.

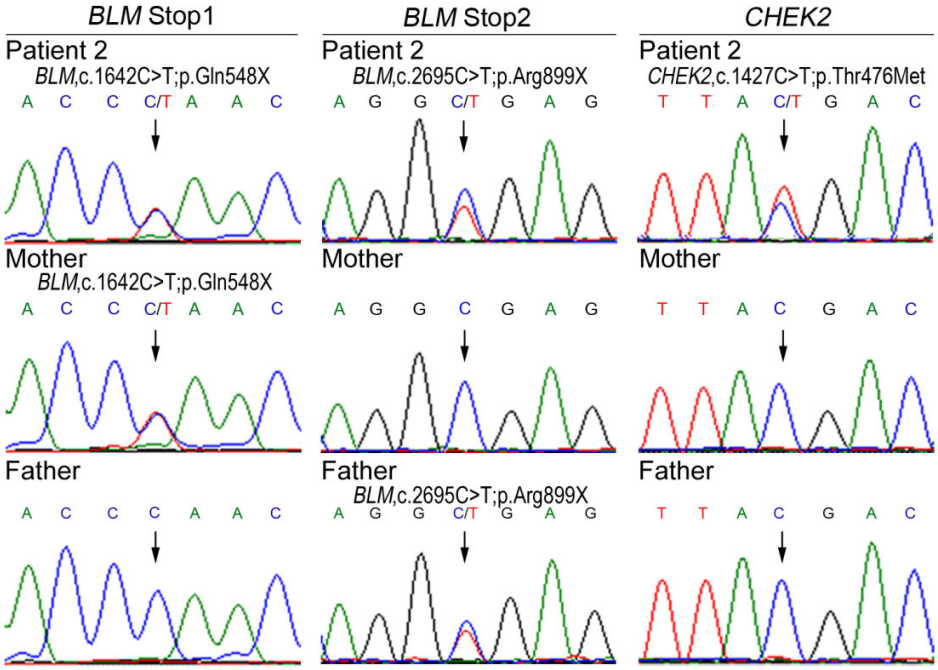

Figure 27: Electropherograms showing mutations identified by WES and verified by Sanger sequencing.
Using WES and a filtering tool identified compound heterozygous *BLM* stop mutations and a *de novo CHEK2* mutation, which were verified by Sanger sequencing. The *de novo CHEK2* mutation (*CHEK2*,c.1427C>T;p.Thr476Met) is a validated "HGMD disease mutation". The first *BLM* stop (*BLM*,c.1642C>T;p.Gln548X; exon 6) mutation was found in patient 2 and her mother, the second *BLM* stop mutation (*BLM*,c.2695C>T;p.Arg899X; exon 13) was identified in patient 2 and her father. The affected nucleotide positions are marked by arrows (Classen and Riehmer et al., 2013).

Figure 28 summarizes the genetic findings in patient 2 found by employing two genome-wide screening methods. The described genetic findings together explain the highly complex phenotype of patient 2. Firstly, using array-CGH microduplications in 6q27 and 22q11.21 were identified, both inherited from the healthy mother (microduplication 6q: gray; microduplication 22q: black). The microduplication in 22q11.21 partially explains the intellectual disability. The severe intelectual disability might be caused by an additive effect of the microduplication 22q11.21 and the Bloom syndrome, both are associated with mild developmental delay. Additionally, both duplicated chromosomal regions harbor genes, which are related to leukemia. In order to explain the malignant germ cell tumor of the ovaries, the skin lesions, and the short stature, which could not be explained by the detected microduplications. WES was performed, revealing 3 mutations in 2 genes, which are associated with cancer. Both parents carry heterozygous stop mutations in the *BLM* gene (light gray), which are located in different exons (horizontal and vertical stripes), leading to compound heterozygous *BLM* mutations in patient 2 causing Bloom syndrome. The genetic findings described here, explain most features adding up to the complex phenotype in patient 2, e.g. short stature, mild craniofacial dysmorphia, hypo- and hyperpigmented skin lesions and cancer predisposition (Classen and Riehmer et al., 2013).

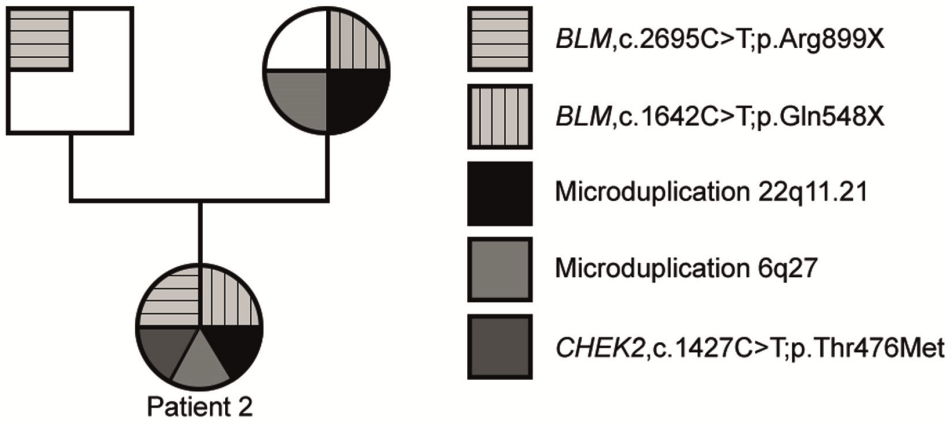

Figure 28: Pedigree of patient 2 and her family showing the detected genetic alterations.
The square represents the father; the circles represent the female members of the family (mother and daughter). Both parents carry heterozygous stop mutations in the *BLM* gene (light gray) but in different exons (horizontal and vertical stripes). In the mother, microduplications in 22q11.21 (black) and 6q27 (gray) were also identified. Patient 2 inherited both *BLM* mutations and microduplications from the parents, and additionally carried a heterozygous *de novo CHEK2* (dark gray) mutation. Patient 2 is affected by combinations of Bloom syndrome, 22q11.21 microduplication syndrome and multi cancer susceptibility syndrome (modified from Classen and Riehmer et al., 2013).

4 Discussion

Since the development of genome-wide screening methods, it has become easier to analyze copy number or single nucleotide variants throughout the exome or genome in large cohorts. This made it possible to compare e.g. the genomic profiles of tumors on a genome-wide scale in order to detect frequency and patterns of genetic alterations in distinct tumor entities. Nowadays, methods such as array-CGH and NGS are also applied in a diagnostic setting. For example, in patients with developmental disabilities or congenital anomalies, array-based analysis is a first-tier diagnostic test (Miller et al., 2010), in order to detect possible causative copy number changes.

In this study two genome-wide screening methods have been applied in order to analyze somatic genomic imbalances in diverse tumors of the central nervous system as well as germline copy number and single nucleotide variants in a patient displaying a complex phenotype including cancer predisposition. Approximately 300 glioma samples were analyzed by array-CGH which had been collected by the German Glioma Network and characterized with respect to their *IDH1/2* mutation status and *MGMT* promoter methylation status. Additionally, information on clinical course of patients was thoroughly collected.

4.1 Project 1: Array-CGH analysis of WHO grade II and WHO grade III gliomas

Approximately 140 diffuse gliomas of WHO grade II and anaplastic gliomas of WHO grade III were analyzed by array-CGH in order to identify molecular subtyped distinguishing WHO grade II and III glioma entities (astrocytomas, oligoastrocytomas and oligodendrogliomas) possibly irrespective of the tumor grade. An exemplary array-CGH profile for each different histological entity and each tumor grade was shown (3.1, page 49), as well as frequency plots in order to visualize frequent genetic imbalances found in the different tumor entities (3.1.2, page 51; 3.1.4, page 53). Due to the results in project 2 (3.2, page 55) which corroborated previous studies (e.g. Toedt et al., 2011), indicating that *IDH1/2* wild-type glioblastomas display a distinct genomic profile from *IDH1/2* mutant glioblastomas, *IDH1/2* status was also taken into consideration when analyzing WHO grade II and grade III gliomas. Some *IDH1/2* wild-type gliomas of WHO grade II and III indeed demonstrated a genomic profile, which showed genetic imbalances often found in primary glioblastomas such as gain on chromosome 7 and loss on chromosome 10. Here, this was found for both diffuse astrocytomas of WHO grade II and anaplastic astrocytomas of WHO grade III. This finding is in agreement with previous studies that described gains of chromosome 7 in about 50% of diffuse astrocytomas and at a similar frequency in anaplastic astrocytomas (Schröck et al., 1996; Wessels et al., 2002; Reifenberger and Collins, 2004). The loss of chromosomal arm 10q was found in anaplastic astrocytomas (Balesaria et al., 1999; Ichimura et al., 1998). In anaplastic astrocytomas this study additionally found a frequent deletion of chromosomal arm 22q, which was also described previously (Hartmann et al., 2004). This genetic aberration was frequently detected in the anaplastic astrocytomas with an *IDH1/2* wild-type status. In contrast, the combined loss of 1p and 19q was reported to be rare in astrocytomas but frequent in

oligoastrocytomas (Mueller et al., 2002; Riemenschneider and Reifenberger, 2009). These findings are in concordance with the results presented here.

Since some WHO grade II and III gliomas display genomic imbalance patterns typical for glioblastomas, these tumors should again be checked histopathological diagnosis, to rule out that they are not underdiagnosed glioblastomas. Additional analyses taking the patient information into account might be helpful. In addition, the array-CGH data should be evaluated together with the gene expression data for these tumors to identify gene dosage effects.

4.2 Project 2: Characterization of long-term survivors of glioblastoma using genome-wide profiling

Glioblastoma multiforme is an aggressive disease associated with short survival times (Smith and Jenkins, 2000), with survival in primary glioblastoma patients being significantly shorter than in patients with secondary glioblastoma (Ohgaki and Kleihues, 2005a). Long-term survival, defined as an overall survival of more than 36 months, is rare and this phenomenon is still poorly understood. It appears as though socioeconomic, environmental and occupational factors do not play major roles (Krex et al., 2007). Molecular markers such as *MGMT* promoter methylation and *IDH1/2* mutation seem to be important and are more frequently found in tumors from long-term survivors than in tumors from unselected glioblastoma patients (Krex et al., 2007; Hartmann et al., 2013). Apart from the *MGMT* promoter methylation and *IDH1/2* status, primary glioblastomas of long-term survivors are poorly characterized on the molecular level.

However, a few studies demonstrated that glioblastomas from long-term survivors showed a distinct gene expression profile or characteristic changes in DNA methylation (Barbus et al., 2011; Donson et al., 2012; Shinawi et al., 2013). Collectively, these data suggest marked differences in tumor biology as a major factor underlying glioblastoma long-term survival. This study aimed to further investigate this hypothesis. Therefore, a clinically well-characterized cohort of 94 primary glioblastoma patients was surveyed. Patients displayed long-term, short-term or intermediate overall survival and all patients had been treated according to the current standards (Stupp et al., 2005). The aim was to assess the molecular aberrations in the distinct survival groups taking into account established molecular markers such as *IDH1* and *IDH2* mutation as well as *MGMT* promoter methylation. Of most of the 94 primary glioblastoma samples, transcriptome-wide profiling data was also available (data not shown; Reifenberger and Weber et al., 2014). Stratification for *IDH1/2* mutation status has been shown to be important, because *IDH1/2* wild-type tumors display a distinct molecular profile (Toedt et al., 2011). Furthermore, *IDH1/2* mutations are more frequent in secondary glioblastomas and can, therefore, be used as a diagnostic tool for the differentiation between primary and secondary glioblastoma (Balss et al., 2008; Hartmann et al., 2009). For the *MGMT* promoter methylation status in this cohort, it was shown that *MGMT* promoter methylation was more frequent in patients with long-term OS (Table 12, page 58). This can be seen in concordance with the fact that

patients with a methylated *MGMT* promoter showed a better response to treatment strategies involving TMZ (Hegi et al., 2005).

Taking the genome and transcriptome data into account, this study confirmed that there is an overrepresentation of tumors with *MGMT* promoter methylation and *IDH1/2* mutations among glioblastomas from long-term survivors (Reifenberger and Weber et al., 2014). The frequency plots generated from the array-CGH data confirmed that there is a distinct genomic profile for *IDH1/2* wild-type tumors in comparison to *IDH1/2* mutant tumors (Figure 11, page 61) supporting previous studies (Toedt et al., 2011; Sturm et al., 2012). Gain on chromosome 7 as well as loss on chromosome 10 were more frequent in *IDH1/2* wild-type tumors and usually involved the entire chromosome. In addition, in about half of the cases gains of chromosomes 19 and 20 were found as well as a loss of chromosomal arm 9p. In contrast, tumors harboring *IDH1/2* mutations displayed a less distinctive genomic profile with imbalances in many different chromosomes. Despite this heterogeneous pattern of copy number changes in most *IDH1/2* mutant glioblastomas, four of 15 cases (26%) showed a more specific change, i.e. a combined loss of chromosomes 1p and 19q. The combined loss of 1p and 19q is typical for low-grade tumors and secondary glioblastomas possessing an oligodendroglial component (Reifenberger et al., 1994). Histological reevaluation confirmed that the 1p/19q deleted tumors indeed were glioblastomas that, however, contained an oligodendroglial tumor component (Reifenberger and Weber et al., 2014).

Considering the frequency of gene copy number changes of glioma-associated tumor suppressor genes or oncogenes, no significant differences were observed between the three *IDH1/2* wild-type survival groups after adjusting for multiple testing. When comparing *IDH1/2* wild-type and mutant tumors, significant differences were detected in the following genes: *PTEN*, *XRCC3* and *XRCC1* located in chromosomal regions showing a loss, as well as *EGFR*, *PMS2* and *HGF* located in regions displaying a chromosomal gain. All six genes have already been described to be glioma-associated or have been investigated in more detail in glioma subgroups (Birchmeier et al., 2003; Kiuru et al., 2008; Verhaak et al., 2010; Felsberg et al., 2011). For example, mutations in the *PTEN* (phosphatase and tensin homolog) gene have been described to be a marker of the mesenchymal glioma subgroup defined by Philipps *et al.* and Verhaak *et al.* (Philipps et al., 2006; Verhaak et al., 2010). *XRCC1* (X-ray repair cross-complementing protein 1) and *XRCC3* (X-ray repair cross-complementing protein 3) are both DNA repair genes, and SNPs in these genes were investigated in respect to an increased risk of developing a brain neoplasm in a large cohort including 320 glioblastoma patients compared to a control cohort (Kiuru et al., 2008). The study did not demonstrate a significant association of the analyzed polymorphisms of either gene with brain tumorigenesis, but suggested that a combination of SNPs in both genes might play a role. *EGFR* (epidermal growth factor receptor) amplification, which is frequently found in glioblastoma, is also a marker for the different subgroups defined by Verhaak *et al.* and Philipps *et al.* (Philipps et al., 2006; Verhaak et al., 2010). Chromosomal alterations of the *EGFR* locus were frequently found in primary but not in secondary glioblastomas (Gan et al., 2009; Riemenschneider and Reifenberger, 2009). *PMS2* (postmeiotic segregation increased 2) is a DNA mismatch repair gene that has also been analyzed in the context of with glioblastoma, especially in

correlation with *MGMT* promoter methylation (Felsberg et al., 2011). *HGF* (hepatocyte growth factor) is known to play a role in tumor progression in various malignancies e.g. of the lung and liver (Birchmeier et al., 2003). Recently, *HGF* was shown to be associated with poor prognosis of patients with glioma and to influence the chemosensitivity of glioma cell lines to cisplatin *in vitro* (Guo et al., 2012).

It is likely that the distinct gene expression profiles in *IDH1/2* wild-type versus mutant tumors found in this study are caused by the *IDH1/2* mutation-associated global changes in DNA methylation, also known as glioma CpG island methylator phenotype (G-CIMP) (Noushmehr et al., 2010; Sturm et al., 2012). Clustering analysis of the molecular evaluation in this study revealed that long-term survival of *IDH1/2* wild-type glioblastoma patients is not linked to distinct DNA copy number changes or expression profiles (Reifenberger and Weber et al., 2014), suggesting that host-related factors seem to be more important in the group of long-term survivors.

By bioinformatics analysis of this study data, it could be shown that various previously reported gene signatures associated with long-term glioblastoma survival are preferentially related to *IDH1/2* status but do not predict survival independent from *IDH1/2* mutations. For example, Donson *et al*. reported an increased expression of immune function-related genes in gliomas of long-term survivors, including a notable T-cell signature that was present within this prognostic immune gene set (Donson et al., 2012). Application of this signature to the data set of this cohort, however, demonstrated an association with *IDH1/2* mutation but not with *IDH1/2* independent long-term survival (Reifenberger and Weber et al., 2014). Likewise, the prognostic gene signature reported by Nutt *et al.* using expression profiling of anaplastic oligodendrogliomas versus primary glioblastomas (Nutt et al., 2003) was also linked to *IDH1/2* mutation but not to survival in *IDH1/2* wild-type patients. Analysis of prognostic methylation signatures reported as being linked to *IDH1/2* mutation (Noushmehr et al., 2010) or to long-term survival of glioblastoma patients (Shinawi et al., 2013), revealed no association with long-term survival in patients with *IDH1/2* wild-type glioblastomas. Additionally, no distinctive gene expression profile in *IDH1/2* wild-type glioblastomas from long-term survivors was identified in an independent cohort of TCGA (The Cancer Genome Atlas) patients.

Taken together, analyzing the DNA copy number changes, *IDH1/2* mutation, and *MGMT* promoter methylation status of 89 primary glioblastoma samples revealed that *IDH1/2* mutations are associated with distinct genomic changes defining a characteristic molecular subtype. This subtype is characterized by better prognosis and a higher probability for long-term survival. Additionally, *MGMT* promoter methylation is also more frequently found in long-term survivors treated according to the current standards including *IDH1/2* mutant and wild-type tumors. Considering the pattern of genomic aberrations and mRNA expression profiles, no distinct changes were found for long-term survivors with *IDH1/2* wild-type glioblastomas.

Since only *IDH1/2* mutations and *MGMT* promoter methylation were found to play an important role for the prognosis of primary glioblastomas so far, future studies should focus on the analysis of more subtle genetic and epigenetic alterations implementing techniques such as whole genome or

epigenome sequencing. Furthermore, proteomic or post-transcriptional alterations should be considered as they might be associated with long-term survival independently of the *IDH1/2* status.

In addition, also host-related factors need to be considered as well, these have been poorly understood up to now. Here, the anti-tumor immune response seems to be an attractive future research area.

4.3 Project 3: Genomic patterns of recurrence in *IDH1/2* wild-type glioblastomas, WHO grade IV

Glioblastoma have a tendency to recur despite the combined treatment of surgical resection, radiotherapy and temozolomide treatment. The recurrent glioblastoma displays the same tumor grade as the primary glioblastoma, i.e. WHO grade IV. To date, the treatment strategy for the recurrent tumor is, therefore, similar to that for the primary tumor and consists of the combination of surgery, temozolomide treatment and other chemotherapy. It is unclear if the recurrent tumor exhibits the same genomic changes as the primary tumor. Therefore, 27 primary and recurrent tumor pairs were analyzed on the molecular level, raising the question if the recurrent tumor displays different copy number changes than the primary tumor. If so, the patient might benefit from a different salvage therapy.

So far, the molecular characterization of primary and recurrent tumors from the same patient has been limited to small numbers of cases or has not been very extensive (Ito et al., 2007; Spiegl-Kreinecker et al., 2007; Martinez et al., 2010; Felsberg et al., 2011; Nickel et al., 2012). For example, Ito *et al.* described a case, in which primary and recurrent glioblastoma were compared (Ito et al., 2007). They reported that the recurrent tumor exhibited less chromosomal imbalances than the primary tumor. The primary tumor displayed a loss of heterozygosity of 1p, 10q and 19q, whereas the recurrent tumor only exhibited allelic loss of 10q. It was stated that this might be due to the fact that the primary tumor encompassed different tumor subclones, and that only the subclone exhibiting a 1p/19q loss was eliminated by the treatment. The recurrent tumor might have developed from the therapy resistant tumor subclone harboring the chromosomal changes that might be responsible for therapy resistance (Ito et al., 2007).

Genomic patterns of progression from primary to recurrent glioblastoma have not been established. This requires genome-wide analysis of tumor pairs from an extensive number of cases, which was done in this study of 27 primary and recurrent glioblastoma pairs. Stratification according to the *IDH1/2* mutation status was done, because *IDH1/2* wild-type tumors display a distinct genomic profile, as it was shown in this study (3.2, page 55) and previously described (Toedt et al., 2011). Furthermore, it is important for the analysis of DNA copy number differences that an adjustment of differences of the tumor cell content of primary and recurrent tumors is performed, in order to achieve a correct comparison between the tumor pairs.

Array-CGH was used to determine DNA copy number changes in 27 primary and recurrent glioblastoma pairs, all tumors displaying a wild-type *IDH1/2* status. The aim was to identify candidate genes that are associated with therapy response and tumor recurrence.

The selected 27 glioblastoma patients had representative clinical characteristics and had had surgical resection of the primary and recurrent tumor. The clinical course of these patients was followed up by the German Glioma Network. Single genomic profiles were processed and qualitative differences determined by pairwise comparison of profiles from primary and corresponding recurrent tumor (Riehmer et al., 2014, in press). A pattern of DNA copy number changes typical for *IDH1/2* wild-type glioblastomas was detected, including gain on chromosome 7 and losses on chromosomal arm 9p and chromosome 10 in almost all cases, as well as gains on chromosomes 19 and 20 and losses on chromosomal arm 13q in about half of the tumors, as described earlier (Beroukhim et al., 2007). Comparing the genomic profiles of primary and recurrent tumor pairs, difference profiles were generated, and three distinct molecular relapse groups were identified and defined for the first time (Riehmer et al., 2014, in press). Seven Equal, nine Sequential and eleven Discrepant tumor pairs were identified (3.3.2, page 72). Equal tumor pairs had balanced difference profiles, Sequential tumor pairs showed additional DNA copy number changes in the recurrent tumor, and Discrepant tumor pairs demonstrated not only additional changes but also chromosomal imbalances that were no longer present in the recurrent tumor. With the achieved resolution, this analysis indicated that about a quarter of the recurrent tumors were genetically identical with the primary tumor (defined as Equal group). In contrast, the Sequential and the Discrepant group displayed genetic differences in the recurrent tumor when compared to its corresponding primary tumor.

Considering the theory that tumors might consist of different subclones, each harboring different chromosomal changes, the tumors defined as Equal might be monoclonal. This single clone appears to be stable and genetically unaffected by time and radio- and chemotherapy (Riehmer et al., 2014, in press) (Figure 29, page 102). In contrast, Sequential tumors might have started monoclonally. Over time the tumor acquired additional changes, perhaps as a consequence of therapy, and therefore, became polyclonal (Figure 29A). Alternatively, Sequential tumors could have started polyclonally consisting of a major clone having the initially detected genetic imbalances and additional minor clones harboring different genetic alterations. In this case, the alterations of the minor clones would not be detectable by array-CGH in the primary tumor due to small cell numbers, but could subsequently be detected in the recurrent tumor due to clonal expansion during or after therapy (Figure 29B). In the case of Discrepant tumors it can be speculated that they start polyclonally, some clones expand in the recurrent tumor in comparison to the primary tumor and therefore become detectable. On the other side, some clones disappear or the cell number of this clone is reduced, so that the genetic alterations harbored by these clones are no longer detectable. This would explain the phenomenon that primary tumors of Discrepant pairs display genetic alterations that are lost in the respective recurrent tumors (Figure 29C and D). Discrepant tumors might additionally acquire genomic alterations over time. The data presented in this study provides evidence that primary glioblastomas can consist of either one or several clones (Riehmer et al., 2014, in press). These

findings are in concordance with a recent report analyzing the genetic composition of cells within primary glioblastomas. Here, flow sorting and array-CGH were used and detected monogenomic tumors containing only one clone or polygenomic tumors containing multiple clones (Stieber et al., 2014).

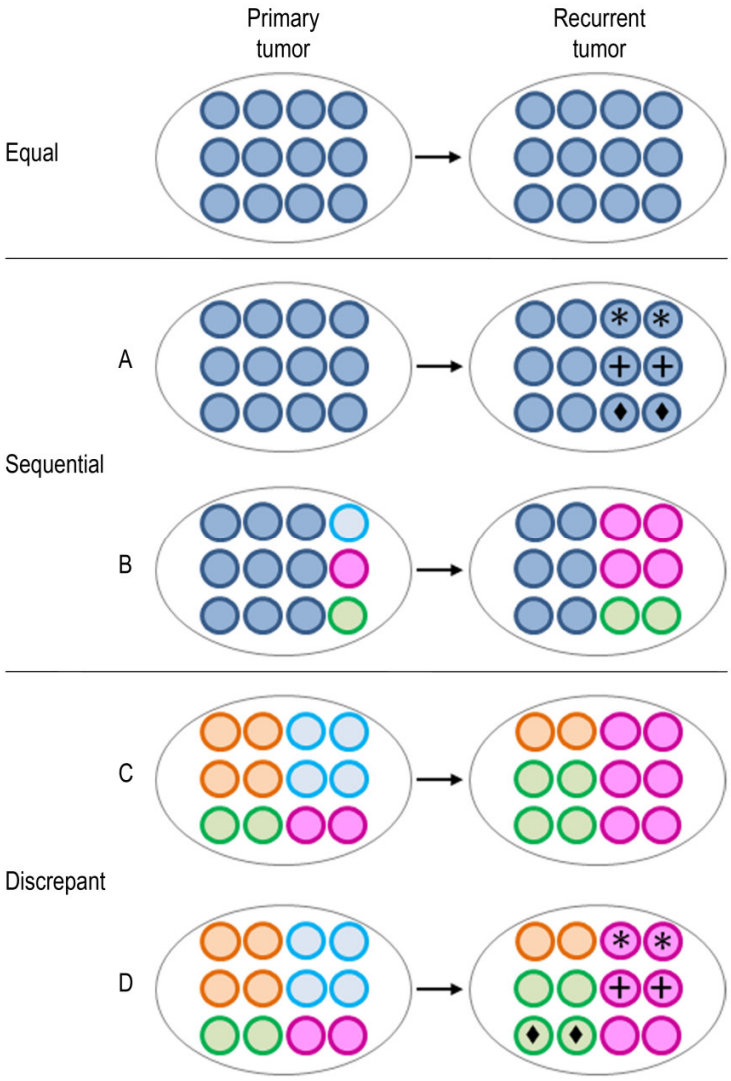

Figure 29: Scheme of possible genetic and clonal evolution in the defined molecular relapse groups.
Equal tumors are monoclonal (dark blue) in the primary and the recurrent tumor. Sequential tumors can start monoclonally (**A**) and have acquired additional changes in the recurrent tumor (black star, plus and diamond). Alternatively, the Sequential tumor starts polyclonally (**B**), but the minor subclones are not yet detectable due to small numbers of cells (light blue, pink and green circles). After recurrence, these clones either expand and become detectable (pink and green) or get eliminated (light blue) due to therapy. Discrepant tumors start polyclonally (**C** and **D**). **C:** In the recurrent tumor, some subclones have expanded (pink and green) or their size is reduced (orange) or they disappeared (blue). The chromosomal imbalances in the orange and light blue clones are no longer detectable in the recurrent tumor. **D:** Tumor starts polyclonally, some clones expand (green and pink) and even acquire additional changes (black star, plus and diamond), which are then detectable in the recurrent tumor. Other clones disappear (light blue) or are reduced in size (orange).

A comparison of the primary tumors from the three molecular relapse groups (Equal, Sequential and Discrepant) with respect to common DNA copy number changes showed that most genetic imbalances had the same frequencies in the three groups (Figure 18, page 78). However, losses on chromosomal arm 9p were larger and more pronounced in the primary tumors from Sequential and Discrepant tumor pairs. Especially, loss of chromosomal band 9p21.3 harboring genes like *ELAVL2*, *CDKN2A/CDKN2B*, *FOCAD* and the glioma susceptibility SNP rs4977756 (Shete et al., 2009) was significantly or remarkably more frequent in primary tumors from Sequential and Discrepant (non-Equal) pairs (Riehmer et al., 2014, in press). Since non-Equal tumors are genomically less stable than Equal tumors, the loss of chromosomal material from 9p21.3 may facilitate (or at least be a marker for) genetic instability, yielding recurrent tumors, that display a different composition on the cellular and genetic level from their corresponding primary tumors. Through its products p14, p15 and p16, the *CDKN2A/CDKN2B* gene cluster is involved in the apoptosis regulation via p53 signalling and G1/S progression via the RB pathway. Therefore, the *CDKN2A/CDKN2B* gene cluster plays an important role in glioma pathogenesis (Cancer Genome Atlas Research Network, 2008). Additive effects may come from the loss of the glioma susceptibility SNP rs4977756 which is located within the *CDKN2B-AS1* gene encoding the non-coding RNA ANRIL. This RNA is required for silencing *CDKN2B* (Kotake et al., 2011). Furthermore, the *FOCAD* gene also located in chromosomal band 9p21.3 was shown to have tumor suppressor function in gliomas (Brockschmidt et al., 2012).

In the chromosomal regions of genomic differences between primary and recurrent non-Equal tumor pairs 46 candidate genes were identified that were associated with therapy response or tumor recurrence according to the literature (Table 18, page 84). The identified candidate genes are involved in various processes playing a role in tumor progression, such as cell proliferation, migration, as well as cellular response to stress and hypoxia. In all non-Equal recurrent tumors carrying a genomic difference identified more than once, the copy number of genes encoding regulators of apoptosis, in particular the p53 family and pathway, and chromatin remodelers were changed (Riehmer et al., 2014, in press). This implies that during the expansion and reduction of tumor clones in non-Equal tumors, clones are selected for that escape apoptosis because the copy number of a positive regulator of apoptosis was decreased, or the copy number of a negative regulator of apoptosis was increased (Riehmer et al., 2014, in press).

Apart from *TP53* the identified genes encoding apoptosis regulators included *TP63*, *EP300*, *UBE4B*, *PARP1*, *PRDM2*, and *RELB* (Table 18 and Table 19, pages 84 and 85). While the p53 protein encoded by *TP53* is a well known positive regulator of apoptosis in glioblastoma, p63 encoded by *TP63* is a p53 homolog that modulates the p53 pathway (reviewed in England et al., 2013), p300 encoded by *EP300* facilitates p53 function (Tang et al., 2013), and *UBE4B* (ubiquitination factor E4B) promotes p53 polyubiquitination and degradation (Wu et al., 2011). In ten recurrent tumors from non-Equal pairs, a decrease in copy number of either *TP53*, *TP63* or *EP300* as well as an increase in copy number of *UBE4B* was detected, influencing the p53 pathway in a similar way. Notably, *UBE4B* has not been implicated in glioma pathogenesis previously. *PARP1* (poly(ADP-ribose) polymerase-1) and *PRDM2* (PR domain containing 2) have also been described to have the potential to induce cell death (He et

al., 1998; Koh et al., 2005). *RELB* (v-rel avian reticuloendotheliosis viral oncogene homolog B) appears to mediate survival signals that protect cells from apoptosis in most cells (reviewed in Sonenshein, 1997). The results presented here, namely a decrease in copy number of *PARP1* or *PRDM2*, or an increase in copy number of *RELB*, which has been found in six recurrent non-Equal tumors, may represent an alternative mechanism that reduces apoptosis.

Chromatin regulators have been increasingly found to play a role in the pathogenesis of cancer including neuroblastoma (Sausen et al., 2013; reviewed in Shain and Pollack, 2013). The copy number of *ARID1B* (AT-rich interaction domain-containing protein 1B) encoding a subunit of the SWI/SNF chromatin remodeling complex or of *PARP1*, the gene product of which is known to also act in the regulation of chromatin structure (reviewed in Wacker et al., 2007) was found to be decreased in four recurrent tumors. Previous studies reported on a role of *PARP1* in glioblastoma susceptibility (McKean-Cowdin et al., 2009). *ARID1B* was described as a candidate tumor suppressor gene in glioblastomas, due to the fact that it was identified to be the only gene located in a small overlapping region of deletion at 6q26 in six glioblastoma cases (Ichimura et al., 2006).

The comparison of primary and recurrent tumors implies that on the genetic level most recurrent tumors differ quite considerably from their primary tumors, even though the histopathologic appearance and the tumor grade were the same. As a consequence from these results, the recurrent glioblastomas are not necessarily the same tumors as their corresponding primary glioblastoma and may therefore benefit from different treatment approaches. Three copy number differences (involving regions harboring *TP63*, *EP300* and *RELB*) identified in a total of seven tumor pairs in this data set might provide a basis for novel targeted therapy options in recurrent glioblastoma (Riehmer et al., 2014, in press). This is supported by several recent findings. Firstly, it was shown that temozolomide induces *TP63* expression resulting in an inhibition of glioblastoma progression (Yamaki et al., 2013). In the data set presented here, a decreased *TP63* copy number was found in the recurrent tumors of three patients, whose primary tumors had been treated by surgical resection, radiotherapy and temozolomide (RT/TMZ). From this data it can be inferred that the basis of their recurrence following temozolomide treatment was identified, implying that these recurrent tumors might have benefited from a therapy with a different chemotherapeutic agent. The detected copy number change in these recurrent tumors additionally involved the *SST* gene encoding for somatostatin, which is located in close proximity to the *TP63* gene in the chromosomal band 3q27.3. Somatostatin and its analog are known to have an inhibitory effect on experimental and human gliomas (Merlo et al., 1999; Barbieri et al., 2009), so these recurrent tumors might have benefited from a therapy with somatostatin analog. Secondly, it has been found that the protein p300 acts as an activator of the *GFAP* (glial fibrillary acidic protein) gene and as a repressor of the *NES* (nestin) gene, thus inducing differentiation of glioblastoma cells (Panicker et al., 2010). Furthermore it has been shown that the inhibition of p300 expression by RNA interference enhanced the invasion potential of glioblastoma cells *in vitro* (Panicker et al., 2010). In this data set, two recurrent tumors displayed a decreased copy number of *EP300* suggesting that an alternative effective treatment in these cases may be an anti-invasive drug inducing differentiation such as valproic acid (Berendsen et

al., 2012). Thirdly, it was recently shown that the loss of *RELB* attenuated glioma cell survival, motility and invasion (Lee et al., 2013). In orthotopic mouse xenografts, RelB diminished tumor growth (Lee et al., 2013). These findings highlight the therapeutic potential of inhibiting the alternative NF-κB (RelB-mediated) pathway in order to treat glioblastoma (Lee et al., 2013). Recurrent tumors of this data set demonstrated an increased *RELB* copy number, suggesting that for these glioblastomas inhibiting kinases which are activated in alternative NF-κB signaling, i.e. NF-κB inducing kinase (NIK) and IKKα, by small molecules or chemical compounds might be an effective treatment (Gardam and Beyaert, 2011; Nogueira et al., 2011).

Taken together, this analysis of primary and recurrent glioblastoma pairs provides evidence that about 75% of *IDH1/2* wild-type recurrent glioblastoma have evolved genetically in comparison with their primary tumors. Moreover, the genetically evolution might be facilitated by the loss of genetic material from chromosomal band 9p21.3 in the primary glioblastomas. Characterization of genetic differences between primary and recurrent glioblastomas might allow identifying effective salvage therapies which target the new genetic properties of the recurrent tumor and will be beneficial for the patients.

In order to assess TMZ-resistance in more detail and to unravel the underlying mechanisms, a future approach could be to generate TMZ-resistant glioma cell lines followed by an analysis of the chromosomal differences between the wild-type versus the resistant cell line. Such an approach may be helpful to identify genes or genomic regions playing a role in TMZ-resistance.

4.4 Project 4: Genomic profiling to assess the clonal relationship between histologically distinct intracranial tumors

Array-CGH was used to assess the clonal relationship between two distinct intracranial tumors from the same patient (patient 1), the first tumor of which was initially classified as an unusual pituitary adenoma by three independent reference pathologists. Pituitary adenomas are non-metastasizing benign tumors (Ezzat et al., 2004, Garcia-Arnes et al., 2013), which can cause symptoms if hormonally active or fast growing (Ezzat et al., 2004; Asa and Ezzat, 2002). The first tumor was detected with a MRI scan as an intra-, para- and suprasellar mass suggestive of pituitary adenoma. After operative removal of the tumor, the patient recovered without any additional focal neurological deficits (Hofer et al., 2012). Diagnosis of intraoperative smear and frozen section revealed predominantly connective tissue with few clusters of epithelial cells. Similar findings were found by the histological analysis of the formalin-fixed paraffin-embedded material demonstrating loosely packed fibrous connective tissue of low to intermediate cellularity and interspersed islands of cells with epithelial aspect (Hofer et al., 2012). These islands were diagnosed as pituitary cells. But only three months after the first surgery, a secondary lesion was diagnosed with a CT and MRI scan in the pituitary region. This tumor was removed in two operations over a period of one week. Nevertheless, there was some residual tumor bilaterally within the cavernous sinus according to an early postoperative MRI scan (Hofer et al., 2012). Nine months later, the patient showed pronounced

tumor progression and despite a fourth operation in order to decompress the tumor, the patient died. The samples of the second, third and fourth surgeries were microscopically similar and contained tissue of high cellularity, with features which were not present in the tissue samples of the first operation. Due to the fact that the tumors of the first and the second operation showed different histologic features, array-CGH was used to determine if the first and the second tumor shared the same genomic imbalances and were, therefore, of the same origin (Hofer et al., 2012). Array-CGH analysis (3.4, page 85) revealed that approximately 80% of the genetic alterations detected in the second tumor were already present in the first tumor, indicating a clonal relationship of the first and second tumor. Therefore, it is likely that the second tumor is actually a recurrent tumor.

Histological and immunohistochemical analysis of the second tumor showed typical characteristics of MPNST WHO grade IV (Hofer et al., 2012). Therefore, array-CGH profiles of the primary and secondary tumor of patient 1 were compared with previously described array-CGH profiles of 122 malignant peripheral nerve sheath tumor (MPNST) cases listed in the Progenetix database. MPNST are associated with complex karyotypes containing numerical and structural chromosomal aberrations involving almost all chromosomes (Jhanwar et al., 1994; Mertens et al., 1995; Scheithauer et al., 2007). The most frequent copy number changes summarized for MPNST in the database are gains on 1q, 2, 5, 6, 7, 8, 12, 15q, 17q, 18, 20, and 21q and losses on 1p, 9, 10, 11 13q, and 17p. Interestingly, almost all of these chromosomal aberrations were also detected in the secondary tumor described here, with the exception of gains on chromosome 6 and chromosomal arm 21q and the loss of chromosomal arm 17p. These findings show a concordance of 83% between the imbalances of the second tumor of patient 1 and the previously reported MPNST cases listed in the database.

Considering the location of the tumor in patient 1 in the sellar region, it was unlikely that this tumor was an MPNST, because MPNSTs are rarely found in the sellar region due to the absence of larger peripheral nerves (Krayenbühl et al., 2007; Kim et al., 2007; Mohammed et al., 2010). Several reports have described a growth into the sella turcica from a suprasellar or perisellar location (Perone et al., 1984; Maartens et al., 2003). Alternatively, these tumors may originate from ectopic Schwann cells (Whee et al., 2002; Bhagat et al., 2002). The fact that in the analyzed specimen no peripheral nerve was detected supports the idea that the analyzed tumor originated from ectopic Schwann cells (Hofer et al., 2012). MPNST arise commonly from neurofibromas (Scheithauer et al., 2007), which was not the case in patient 1 because she did not present with neurofibromatosis.

Considering that patient 1 presented with an aggressive and rapid clinical course, it is likely that the first tumor diagnosed as an unusual pituitary adenoma was indeed an MPNST that infiltrated the pituitary gland. Due to its low cellular density it was apparently misinterpreted as a fibrotic pituitary adenoma. The array-CGH profiles support the idea that the first and the second tumor have the same cellular origin since they share 80% of genetic imbalances. Therefore array-CGH is a potent tool to identify the clonal relationship of tumors even in cases when they appear as two histologically distinct tumors.

This study demonstrates that genome-wide screening methods, such as array-CGH are important tools to unravel the molecular basis of certain pathologies, especially if they present with an unexpected clinical course.

4.5 Project 5: Dissecting the genotype in a patient with cancer predisposition using whole exome sequencing in addition to genome-wide copy number analysis

When patient 2 presented with a highly complex phenotype including cancer predisposition (a both-sided mixed malignant germ cell tumor of the ovaries and an acute pre-B-lymphoblastic leukemia), intellectual disability and anomalies of skin pigmentation, it was at first hypothesized that a single monogenic disease caused all of the symptoms. Syndromes including cognitive impairment, cancer predisposition and anomalies of skin pigmentation, e.g. neurofibromatosis type 1, tuberous sclerosis-1 or tuberous sclerosis-2 were suspected, but not confirmed.

Due to the complexity of the displayed symptoms, the original hypothesis was challenged. It was suspected that all symptoms might be explained by a microduplication or microdeletion syndrome. In the past few years, the number of microduplication or microdeletion syndromes that were described has been steadily increasing, due to advancement in technologies such as array-CGH. Using array-CGH, submicroscopic copy number changes, so called copy number variations (CNV), can be detected. The challenge is to differentiate between a benign and a pathogenic copy number variation. A CNV is usually considered pathogenic if it is not inherited but occurs *de novo* (e.g. Alesi et al., 2011), or if it is not detected in a high number of unrelated healthy control individuals (e.g. Willatt et al., 2005).

Intellectual disability is characterized by an impaired cognitive function, which might be caused by maternal drug abuse during pregnancy, perinatal oxygen distress or postnatal infections. More recently, genetic alterations such as microduplications or microdeletions have been identified to be causative (reviewed in Weise et al., 2012). These microduplication or microdeletion syndromes usually involve many genes in close proximity to each other. Also the gene dosage might play an essential role for causing specific clinical signs.

As primary approach, DNA from the peripheral blood of patient 2 was analyzed by array-CGH and, indeed, a 2.5 Mb microduplication in chromosomal band 22q11.21 was detected, reported to cause the 22q11.21 microduplication syndrome (Ensenauer et al., 2003, reviewed in Portnoi, 2009). In addition, a 0.26 Mb microduplication in 6q27 was detected, in part encompassing the *MLLT4* gene. However, both microduplications were inherited from the healthy mother.

The chromosomal region 22q11.2 harbors approximately 50 genes and has been shown to be susceptible to chromosomal rearrangements. Microdeletions in this region are associated with genomic diseases such as the DiGeorge/ velocardiofacial syndromes (Ensenauer et al., 2003). The genomic rearrangements in this region are facilitated by segmental duplications (regions of low copy repeats) allowing for mispairing and unequal crossing over between two homologous chromosomes (Portnoi, 2009). The 22q11.2 microduplication syndrome is associated with intellectual disability, and therefore gave a possible explanation for the intellectual disability in patient 2, but it is usually not as

severe (Portnoi, 2009). However, it has been described that the phenotype has a high variability, i.e. patients may have cognitive deficits that range from learning disabilities to mental retardation (Ensenauer et al., 2003; Yobb et al., 2005). This could explain why the mother, carrying the same microduplication, did not show any signs of intellectual disability and displayed a normal phenotype. The 22q11.21 microduplication explained the intellectual disability in patient 2, but is typically neither associated with skin hyper- and hypopigmentation nor related to malignant diseases early in life. However, one patient carrying a 22q11.21 microduplication had been described with a pre-B acute lymphoblastic leukemia (Chang et al., 2011).

In order to investigate whether the unexplained leukemia might be due to gene dosage effects of the respective copy number variants, both microduplications harboring a number of genes associated with leukemia, the gene expression levels of five genes (*DGCR2*, *CLTCL1*, *CDC45L*, *SEPT5* and *GP1BB*) residing in the 22q11.2 region and *MLLT4* residing in the 6q27 region were analyzed in cooperation with the Institute of Human Genetics, University of Bonn (Classen and Riehmer et al., 2013). *DGCR2*, *CLTCL1*, *CDC45L*, *SEPT5* and *GP1BB* have been proposed to be overexpressed in leukemia (Chang et al., 2011). *MLLT4* has been known to be a fusion partner of *MLL* in leukemic cells (Marschalek, 2011) and might be disrupted by the 6q27 microduplication. It has been found that the expression of *CDC45L* and *GP1BB* was increased and that the expression of *MLLT4* was decreased in comparison with age and sex matched controls (data not shown). The detected changes in gene expression levels might not only be the cause of the leukemia but a consequence of its therapy, as *CDC45L* plays a role in eukaryotic DNA replication (Pacek et al., 2006) presumably modulated by the used chemotherapeutic agents (Classen and Riehmer et al., 2013).

As the cancer predisposition in patient 2, was not explained by the 22q11.21 microduplication, the exomes of the patient as well as of her parents were analyzed by WES in order to find causative single nucleotide variants. The initial approach was to perform a trio-based *de novo* analysis, as suggested by recent studies (Vissers et al., 2010; de Ligt et al., 2012). The parents were also analyzed by WES in order to subtract the inherited variants from the detected variants in the patient the remaining variants are then *de novo*. This approach identified the *CHEK2* variant in patient 2. Next, other filtering strategies were applied based on quality measures, deleteriousness predictions, and the use of the mining tool Genome Trax^{TM}, utilizing available databases e.g. HGMD inherited disease mutations, COSMIC somatic disease mutations as well as PROTEOME and HGMD disease gene associations (Classen and Riehmer et al., 2013). This approach identified three variants related to cancer. Two mutations in the *BLM* gene were detected, which have been described as Bloom syndrome founder mutations (German et al., 2007). It was found that patient 2 was compound heterozygous for two stop mutations in the *BLM* gene, one of which was inherited from the mother and the other from the father (Figure 27, page 94). Bloom syndrome is a rare autosomal recessive hereditary disorder associated with most of the symptoms found in patient 2, including short stature, mild craniofacial dysmorphia, hypo- and hyper pigmented skin lesions and cancer predisposition (German et al., 2007). Bloom syndrome patients are diagnosed with cancer at an early age (German, 1997), which is in concordance with patient 2, who developed her first malignancy at the age of eight

years and the second at the age of 19 years. However, the severe mental retardation patient 2 displayed is usually not a symptom of Bloom syndrome. If patients with Bloom syndrome display intellectual disability, it is found to be mild. The data presented here suggests that the severe intellectual disability in patient 2 is caused by an additive effect of Bloom syndrome and the 22q11.2 microduplication syndrome, which can both be linked to developmental delay (Ensenauer et al., 2003, German et al., 2007). About 50% of Bloom syndrome patients develop cancer; up to 10% develop a secondary malignancy, including acute lymphoblastic leukemias and germ cell tumors (German, 1997, Bloom Syndrome Gene Reviews™). Presumably, the marked organ sensitivity to chemotherapy in patient 2 leading to enhanced toxicity of the treatment for both cancers is also linked to Bloom syndrome (Mao et al. 2010). Additionally to the two *BLM* stop mutations, the patient carried a heterozygous missense variant in the *CHEK2* gene which occurred *de novo*. This rare missense variant has been described as a "HGMD disease mutation" contributing to breast cancer susceptibility (Le Calvez-Kelm et al., 2011). This missense variant results in a mutant protein with essentially no kinase activity (Desrichard et al., 2011) and no response to DNA damage in an *in vivo* assay (Roeb et al., 2012). Heterozygous germline mutations in the *CHEK2* gene have been reported to cause Li-Fraumeni syndrome (Bell at al., 1999) and multi-organ cancer susceptibility (Cybulski et al., 2004). Taken together, it can be proposed that the cancer predisposition in patient 2 is caused by an additive effect of the two *BLM* founder mutations and the pathogenic *CHEK2* variant.

Had we only followed the initial approach to screen only for *de novo* variants by the so called trio-based analysis, the two *BLM* founder mutations would have been missed. The exome sequencing analysis of patient 2 was the first case in our research laboratory. The findings in patient 2 and the experiences made during the analysis made us overthink the filtering strategies and develop a workflow for analyzing WES data sets (4.5.1). Therefore a trio-based analysis is now only applied secondarily, when the other approaches have yielded no causative variants explaining the phenotype. These results show that a trio-based analysis is not always necessary with the advantage that the analysis is less expensive, because only the patient has to be sequenced.

Taken together, two genome-wide screening methods were used to unravel the genetic changes causing the highly complex phenotype of patient 2. Employing array-CGH and WES, two inherited microduplications as well as two inherited recessive founder mutations (*BLM*) and one *de novo* missense variant (*CHEK2*) were identified. Therefore, it can be concluded, that patient 2 is affected by Bloom syndrome in combination with the 22q11.2 microduplication syndrome, and the *CHEK2* associated cancer susceptibility syndrome explaining the severe intellectual disability and the cancer predisposition in the patient. WES is a useful tool to detect additional genomic causes of inherited syndromes even though a microduplication or microdeletion has been diagnosed. This is especially important in those complex phenotypes, in which not all clinical symptoms can be explained by the detected microduplication or microdeletion, or in cases in which the healthy unaffected parent displays the same microimbalance. This case also demonstrates that complex phenotypes may be caused by more than one genetic alteration, rather a combination of copy number variants and point mutations may be the cause.

4.5.1 Adjustment of WES filter strategy based on findings in patient 2 – future strategy

The big challenge of WES is the handling of the enormous amounts of generated data as well as the interpretation of detected variants (1.3.2, page 13). Various approaches and filtering strategies have been developed in order to identify the relevant and disease causing variants (Neveling and Hoischen, 2012; Bamshad et al., 2011). The findings in patient 2 showed that a trio-based *de novo* analysis is not always the best approach. Depending on the obtained results, filter strategies have to be adapted. Therefore, a workflow was developed which combines different filtering strategies (Figure 30, page 111).

Depending on the platform used, 20.000 to 40.000 variants are found in the exome from peripheral blood of one sample. In order to reduce the number of variants and to eliminate false positive calls, a first quality filter step was performed, which retains all variants having a coverage of at least 20. Coverage is the number of times one specific base position is sequenced. Secondly, all variants that do not have any influence on mRNA or protein structure e.g. synonymous variants are removed. Therefore, all remaining variants are so called "serious" variants, i.e. they are non-synonymous coding, causing a stop codon or a stop codon is lost, frameshift coding mutations, essential splice site or INDELs, these are small insertions or deletions. Thirdly, it is usually advisable to filter on the basis of deleteriousness prediction for non-synonymous variants. Prediction programs, e.g. SIFT, PolyPhen2, MutationTaster and Condel, can be employed, which predict, based on the detected base substitution, if a variant has a major effect on the gene product. Here, decisions on the stringency of filtering can be made. Frequently, a variant is retained if at least one prediction program calls the variant "probably damaging" or "disease causing". After removing all the synonymous and the "benign" variants, i.e. the variants predicted to have no damage, a combined analysis of two different strategies, which we call candidate and database strategy were used in order to further reduce the number of variants. The candidate strategy is based on a gene list, that has been prepared according to an own literature search and includes genes, which are known to be associated with the analyzed disease or phenotype. The database strategy employs mining tools such as Genome Trax™ to find disease related genes. The tool enables selecting variants in genes related to certain clinical features. The Genome Trax™ filtering tool is based on databases such as HGMD® (Human Gene Mutation Database) mutations. After application of the above mentioned filtering steps, the number of variants is reduced dramatically. Next, population based filtering is performed. During population based filtering, databases such as the ENSEMBL Genome Browser were employed to search for the minor allele and genotype frequencies of the given variant. According to the in-house internal standard we have defined, only variants displaying a minor allele frequency and genotype frequency smaller than 3% are retained. Minor allele frequencies are used from the population, e.g. Europeans or European Americans that the patients belong to. Further, the inheritance model was taken into consideration and variants from in-house exomes were subtracted. The latter is done to exclude variants caused by systematic errors and common variants. Usually a manageable number of variants remained, which were then verified by Sanger sequencing. If no appropriate variants resulted from

the filter strategy a trio-based sequencing strategy was employed in addition to detect *de novo* variants in the patients.

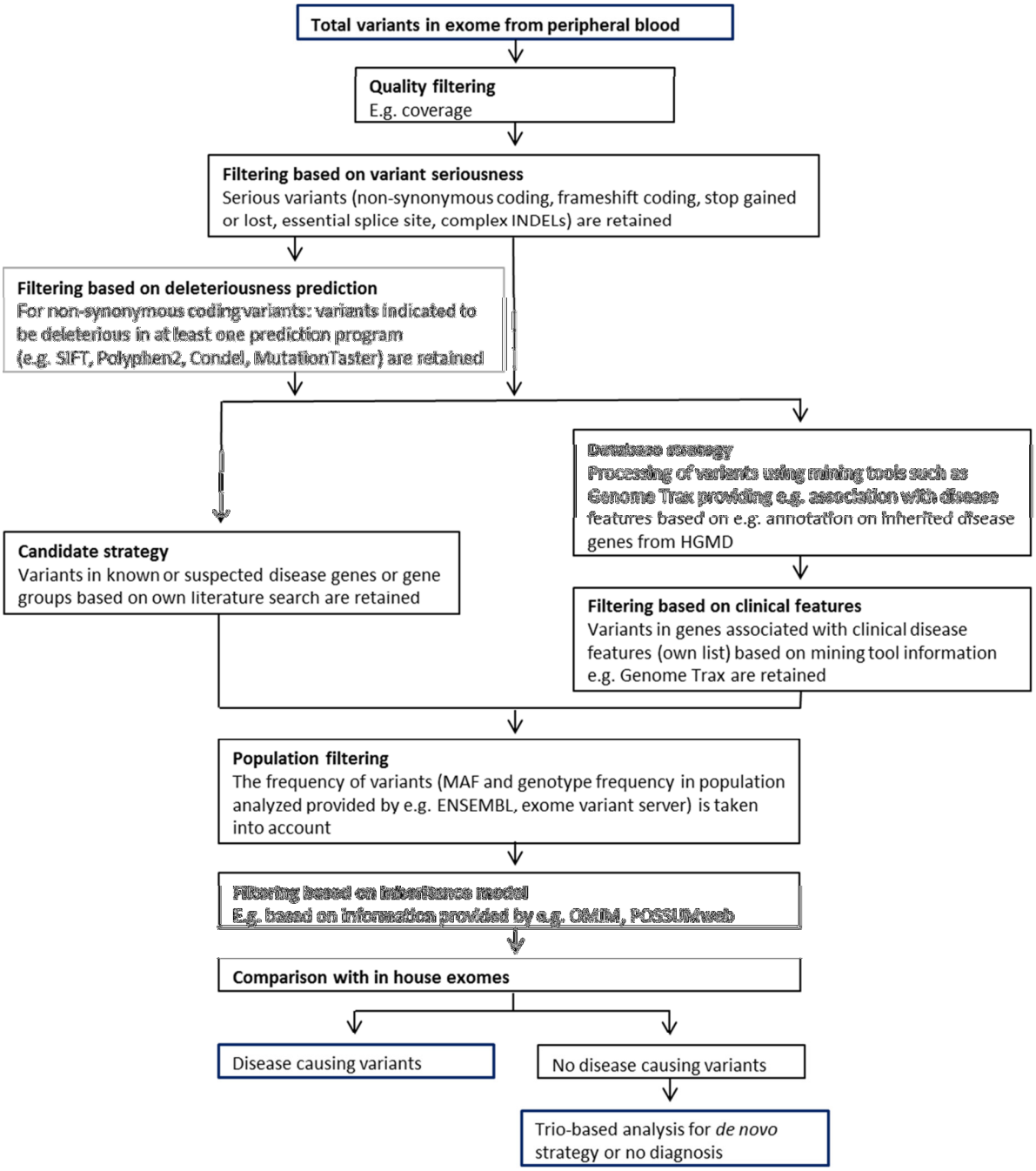

Figure 30: Scheme of filtering strategy used to reduce the number of variants identified by NGS and to identify the causative variants.

5 Summary

Since the development of screening methods that can be used on an exome- or genome-wide scale such as array-based comparative genomic hybridization (array-CGH) and next generation sequencing (NGS), these techniques have been employed to analyze large patient and tumor cohorts and are also frequently used for diagnostic purposes. In this study, array-CGH was used to analyze DNA from tumors of the central nervous system to identify somatic copy number changes. Approximately 300 tumor samples from the German Glioma Network and an intracranial malignant peripheral nerve sheath tumor were analyzed using array-CGH to identify specific patterns of copy number alterations in the different tumor entities. Furthermore, array-CGH and whole exome sequencing (WES) were performed on DNA from peripheral blood from a patient presenting with a complex phenotype including cancer predisposition to identify causative germline aberrations.

The first project addressed molecular aberrations in gliomas classified as grade II and grade III by the World Health Organization (WHO) including astrocytomas, oligoastrocytomas and oligodendrogliomas as well as anaplastic astrocytomas and anaplastic oligoastrocytomas. Tumor samples of the different glioma entities were analyzed using array-CGH, in order to detect common genetic imbalances in the gliomas of WHO grade II and III. Together with the German Glioma Network the mutation status in the *IDH1* (isocitrate-dehydrogenase 1) and *IDH2* genes was determined. Most of the WHO grade II and grade III gliomas harbored an *IDH1* or *IDH2* mutation. It could be shown that WHO grade II gliomas displayed DNA copy number changes less frequently than WHO grade III gliomas. Interestingly, a small group of *IDH1/2* wild-type WHO grade II astrocytomas were detected which displayed glioblastoma-like genomic imbalances. Patients with an *IDH1/2* wild-type astrocytoma of WHO grade II displaying a glioblastoma-like genomic profile, i.e. gains on chromosomes 7, 19 and 20 as well as losses of chromosomes 9 and 10, possibly would benefit from a more intensive therapy strategy. Therefore these analyses have future implications. Furthermore, frequent deletions of chromosomal arms 1p and 19q were found in oligodendroglial tumors or in mixed astrocytic tumors displaying also an oligodendroglial component. Both alterations were significantly less frequent in astrocytic tumors.

The molecular analysis of primary WHO grade IV glioblastomas was subdivided into two parts. As the prognosis of primary glioblastoma is still poor, long-term survival of more than three years after diagnosis is rare in these patients. Thus, the first part of the analysis (project 2 of this work) focused on tumors from patients who exhibited long-term survival. Genomic profiles of glioblastomas from long-term survivors were compared to those from short-term and intermediate-term survivors. The *IDH1/2* mutation and the *MGMT* promoter methylation status were also determined in these tumors. This analysis showed that patients with long-term survival were younger and corresponding tumors more often had an *IDH1/2* mutation and a *MGMT* promoter methylation. Genomic imbalances were prominently different between *IDH1/2* mutant and *IDH1/2* wild-type tumors, but not between survival groups of *IDH1/2* wild-type glioblastoma patients, suggesting that long-term survival is due to other, e.g. host-related factors.

The second part of the analysis (project 3 of this work) focused on tumor recurrence of primary WHO grade IV glioblastomas. Glioblastomas have a tendency to recur despite combined surgical resection, radiotherapy and temozolomide chemotherapy. When the tumor recurs the WHO grade remains the same, therefore, the recurrent tumor is treated similar to the primary tumor. Genomic profiles of 27 primary and recurrent *IDH1/2* wild-type glioblastoma from the same patient were compared to determine genetic patterns of glioblastoma progression. After comparing the array-CGH profiles of the primary and recurrent tumors, taking the tumor cell content into account, a difference profile for each tumor pair was generated. Subsequently, three molecular relapse groups were defined (Equal, Sequential and Discrepant). Seven of the 27 (26%) tumor pairs were identified to be Equal pairs, showing no DNA copy number differences between primary and recurrent tumor, suggesting a monoclonal cell composition of both tumors. In nine of 27 (33%) tumor pairs, the same and additional chromosomal imbalances were found in the recurrent tumor as compared to the primary tumor (Sequential pairs). These findings suggest a sequential acquisition or selection for aberrations during tumor progression. In eleven of 27 (41%) pairs, the difference profiles of primary and recurrent tumors were divergent, i.e. the recurrent tumors contained additional chromosomal aberrations but had also lost others (Discrepant pairs). These findings suggest a polyclonal composition of the primary tumors and considerable clonal evolution. Interestingly, losses on chromosomal band 9p21.3, harboring the *CDKN2A/B* locus, were significantly more common in primary tumors of the Sequential and Discrepant tumor pairs, also called non-Equal pairs. Analyzing regions of chromosomal differences between primary and recurrent tumors 46 candidate genes associated with tumor recurrence were identified. Frequently, the identified genes for apoptosis regulators, possibly explaining why these cells escape therapy induced apoptosis. Taken together about 75% of *IDH1/2* wild-type recurrent glioblastomas acquire additional genomic alterations during progression. This process is possibly facilitated by the loss of genetic material from chromosomal band 9p21.3 in the primary glioblastomas. These tumor recurrence-associated chromosomal changes may contribute to therapy resistance, e.g. by copy number alterations of apoptosis regulatory genes. The analysis of the genomic differences between primary and recurrent glioblastomas may identify newly acquired genetic properties targetable by salvage therapies for a more effective treatment of patients with recurrent glioblastoma.

In the fourth project of this work, two intracranial tumor samples from a 47-year old female patient were retrospectively analyzed using array-CGH in order to determine their clonal relationship. The histological diagnosis of the first tumor was an unusual pituitary adenoma, but the second tumor that had developed 3 months later was diagnosed as a rare malignant peripheral nerve sheath tumor. Though the two tumor samples were different in their histopathology, the question arose if the first and the second tumor contained the same copy number changes and thus most likely developed from the same origin. Array-CGH of the first tumor revealed a complex pattern of chromosomal imbalances affecting all chromosomes but one (chromosome 16). Array-CGH of the second tumor revealed a similarly complex profile. About 80% of the 29 copy number changes detected in the second tumor were already present in the first tumor. These findings provide strong evidence for a

clonal relationship between the two tumor samples and suggest that the second tumor was a recurrent tumor of the first lesion. It also could be shown that the genomic profiles of both tumors were highly similar to those of already published MPNST cases, indicating that the analyzed tumor indeed is a MPNST. Taken together, it could be shown that array-CGH can be successfully used to identify the clonal relationship between two histologically distinct tumors.

The fifth project of this work aimed at identifying the germline aberrations underlying a complex phenotype including cancer predisposition. Symptoms of the patient included cognitive impairment, two neoplastic diseases (a both-sided mixed malignant germ cell tumor of the ovaries and an acute pre-B-lymphoblastic leukemia) prior to the age of 20 years, anomalies of skin pigmentation and short stature. Using array-CGH on DNA from peripheral blood from the patient and her mother, two maternally inherited microduplications in the chromosomal bands 6q27 and 22q11.21 were detected. The microduplication with the size of 0.26 Mb in 6q27 encompassed parts of the *MLLT4* gene, a known fusion partner of *MLL* in leukemic cells. The microduplication in chromosomal band 22q11.21 had a size of 2.5 Mb, harboring approximately 50 genes. This region has been reported to be susceptible to chromosomal rearrangements and to cause the 22q11.21 microduplication syndrome when duplicated and is associated with a high variability, explaining in part the patient's intellectual disability but not its severity. Particularly the two malignancies of the patient were not explained by the detected microduplications. Therefore, DNA from peripheral blood from the patient as well as from her patents was screened by WES in order to find further causative germline aberrations. A trio-based *de novo* analysis, subtracting the parental variants from variants detected in the patient, revealed a *de novo CHEK2* variant (*CHEK2*,c.1427C>T;p.Thr476Met). This rare missense variant is a "HGMD disease mutation" contributing to breast cancer susceptibility. Using a different filter strategy for the WES data set of the patient, two known *BLM* founder mutations (*BLM*,c.1642C>T;p.Gln548X; *BLM*,c.2695C>T;p.Arg899X) were also detected. Sanger sequencing revealed that the patient was compound heterozygous for these two stop mutations in the *BLM* gene, i.e. that one of the mutations was inherited from the mother and the other from the father. Bloom syndrome, caused by mutations in the *BLM* gene is a rare autosomal recessive disorder associated with most of the symptoms found in the patient, including short stature, mild craniofacial dysmorphia, hypo- and hyper-pigmented skin lesions and cancer predisposition. Taken together, two genome-wide screening methods have been used to unravel the highly complex phenotype of the patient. Employing array-CGH and WES, two inherited microduplications as well as two inherited recessive founder mutations (*BLM*) and one *de novo* missense variant (*CHEK2*) were identified. The combination of Bloom syndrome with the 22q11.2 microduplication syndrome and the *CHEK2* associated multi-cancer susceptibility syndrome, are presumed to cause the severe intellectual disability, and explain the cancer predisposition in the patient. This case demonstrated that complex phenotypes may be caused by more than one genetic alteration, rather a combination of copy number variants and point mutations may be the cause.

In summary, array-CGH was used to detect somatic tumor aberrations in WHO grade II to WHO grade IV glioma entities as well as a case of a MPNST. Further, employing two genome-wide screening methods, array-CGH and WES, the complex genotype of a patient with syndromic cancer

predisposition was unraveled, indicating that complex phenotypes may be caused by a number of different genetic alterations.

6 Deutsche Zusammenfassung

Die Entwicklung von genomweiten Analyseverfahren, wie die Array-basierte komparative genomische Hybridisierung (Array-CGH) und die Sequenzierung humaner Exome oder Genome mittels *next generation sequencing,* hat in den letzten Jahren dazu geführt, dass große Patienten- und Tumorkollektive in immer kürzerer Zeit exom- oder genomweit analysiert werden konnten. Diese Methoden finden mittlerweile auch für diagnostische Zwecke ein großes Anwendungsspektrum. In dieser Arbeit wurden beide Methoden verwendet, um sowohl somatische Kopienzahlveränderungen in unterschiedlichen Tumoren des Zentralnervensystems, wie auch Veränderungen in der Keimbahn einer Patientin mit einer Krebsdisposition zu untersuchen. Dabei wurden annähernd 300 Tumorproben unterschiedlicher Gliomentitäten im Rahmen des Deutschen Gliomnetzwerkes mittels Array-CGH auf somatische DNA-Kopienzahlveränderungen hin untersucht. Zu den untersuchten Tumoren des Zentralnervensystems gehörten nach der World Health Organization (WHO) Klassifizierten Grad II bis Grad IV Gliome, sowie ein Fall eines malignen peripheren Nervenscheidentumors. Eine Kombination aus Array-CGH und Exomsequenzierung wurde in einem weiteren Projekt verwendet, um ursachliche Keimbahnveränderungen an DNA aus peripherem Blut bei einer Patientin mit einem komplexen Phänotyp einschließlich Krebsdisposition zu identifizieren.

Im ersten Projekt dieser Arbeit war es das Ziel, die DNA-Kopienzahlveränderungen von WHO Grad II Astrozytomen, Oligoastrozytomen und Oligodendrogliomen sowie die Kopienzahlveränderungen von WHO Grad III anaplastischen Astrozytomen und anaplastischen Oligoastrozytomen mittels Array-CGH zu identifizieren, und genomische Profile für die unterschiedlichen Tumorentitäten zu erstellen. Weiterhin wurden im Rahmen des Gliomnetzwerkes Mutationsanalysen im *IDH1* (Isocitrat-Dehydrogenase 1) und *IDH2* Gen durchgeführt. Die meisten WHO Grad II und III Gliome zeigten eine Mutation im *IDH1* oder *IDH2* Gen. Bei den WHO Grad II Gliomen waren weniger Kopienzahlveränderungen nachweisbar, als bei den WHO Grad III Gliomen. Dennoch gab es eine kleine Gruppe von *IDH1/2*-Wildtyp WHO Grad II Astrozytomen, die Glioblastom-typische Kopienzahlveränderungen aufwiesen. Die Patienten mit den *IDH1/2*-Wildtyp WHO Grad II Astrozytomen mit einem Glioblastom-typischen Array-CGH Profil, d.h. Gewinne auf den Chromosomen 7, 19 und 20 sowie Verlust auf den Chromosomen 9 und 10, würden möglicherweise von einer intensiveren Therapie profitieren. Insofern haben die Untersuchungen prospektiv eine translationale Bedeutung. Darüber hinaus wurde in oligodendroglialen Tumoren oder oligodendroglialen-astrozytären Mischtumoren häufig einen Verlust der Chromosomenarme 1p und 19q gefunden. Beide Veränderungen waren in astrozytären Tumoren deutlich seltener.

Die molekularen Analysen von primären WHO Grad IV Glioblastomen wurden in zwei weitere Projekte unterteilt. Der Schwerpunkt des ersten dieser Projekte (Projekt 2 dieser Arbeit) lag in der Analyse von WHO Grad IV Glioblastomen von Langzeit-Überlebern, da die Ursachen für das Langzeit-Überleben von der molekularen Seite noch schlecht charakterisiert sind. Unter Langzeit-Überlebern versteht man Patienten, die nach Diagnose länger als drei Jahre überlebt haben. Um spezifische genomweite Veränderungen zu identifizieren, die essentiell für das Langzeit-Überleben sind, wurden

genomweite Profile von primären Glioblastomen von Patienten mit kurzem, intermediärem oder langem Überleben erstellt und verglichen. Diese Analysen zeigten, dass Langzeit-Überleber meistens jünger als andere Patienten beim Zeitpunkt der Diagnose waren und dass die entsprechenden Tumoren oftmals eine *IDH1/2* Mutation, sowie eine Methylierung des *MGMT* Promotors aufwiesen. Zwischen Tumoren mit einer *IDH1/2* Mutation und Tumoren mit *IDH1/2*-Wildtypstatus konnte ein klarer Unterschied in den genomischen Profilen entdeckt werden, nicht aber in den Profilen zwischen den einzelnen Überlebensgruppen. Das lässt darauf schließen, dass das Langzeit-Überleben vermutlich auf andere, wie z.B. Patienten-spezifische Faktoren, zurückzuführen ist.

Im Zweiten Teil der molekularen Analysen von primären WHO Grad IV Glioblastomen (Projekt 3 dieser Arbeit) stand die Rezidivbildung und deren molekulare Charakterisierung im Vordergrund. Glioblastome haben die Tendenz lokal zu rezidivieren, auch nach intensiver und kombinierter Behandlung durch operative Maßnahmen, Strahlen- und Chemotherapien. In der Regel wird der Rezidivtumor ähnlich wie der Primärtumor behandelt. In dieser Studie wurden genomische Imbalancen von 27 primären Glioblastomen mit einem *IDH1/2*-Wildtypstatus und von den dazugehörigen Rezidivtumoren derselben Patienten untersucht. Beim Vergleich der genomischen Profile von Primär- und Rezidivtumor wurde der unterschiedliche Tumorzellanteil angeglichen und ein Differenzprofil für jedes Tumorpaar erstellt. Aufgrund der verschiedenen Differenzprofile wurden drei verschiedene Gruppen („Equal“, „Sequential“ und „Discrepant“) identifiziert. Sieben der 27 (26%) Tumorpaare wurden als „Equal“-Tumore bezeichnet, das heißt, dass keine DNA-Kopienzahlunterschiede zwischen Primär- und Rezidivtumor vorlagen. Das lässt vermuten, dass sowohl der Primär- als auch der Rezidivtumor eine monoklonale Zellkomposition aufwiesen. Bei neun der 27 (33%) Tumorpaare wiesen die Rezidivtumore gleiche Kopienzahlveränderungen sowie neu dazugewonnene chromosomale Veränderungen gegenüber dem Primärtumor auf („Sequential“). Dieses Ergebnis legt nahe, dass es eine sequentielle Akquisition oder eine Selektion für gewisse chromosomale Veränderungen während der Tumorprogression gibt. Elf der 27 (41%) Tumorpaare zeigten ein Differenzprofil mit vielen Unterschieden zwischen Primär- und Rezidivtumor („Discrepant“). Zum einen zeigte der Rezidivtumor zusätzliche DNA-Kopienzahlveränderungen, zum anderen konnten einige Veränderungen, die im Primärtumor vorhanden waren, im Rezidiv nicht mehr detektiert werden. Das lässt vermuten, dass der Primärtumor eine polyklonale Zellkomposition aufwies und dass eine ausgeprägte klonale Weiterentwicklung stattgefunden hat. Interessanterweise waren die Verluste in der chromosomalen Bande 9p21.3, die das *CDKN2A/B* Gen beinhaltet, in den Primärtumoren von „Sequential“- und „Discrepant“-Paaren stärker ausgeprägt. In den chromosomalen Regionen, die unterschiedliche Kopien Zahlen in Primär- und Rezidivtumor aufwiesen, waren 46 Kandidatengene lokalisiert, die aufgrund der Literaturlage mit der Rezidivbildung assoziiert sein könnten. Dabei zeigten sich häufig Kopienzahlunterschiede in Apoptoseregulatoren, was erklären könnte, warum diese Tumorzellen der therapieinduzierten Apoptose entgehen. Insgesamt konnte gezeigt werden, dass 75% der *IDH1/2*-Wildtyp Rezidivglioblastome während der Tumorprogression zusätzliche DNA-Kopienzahlveränderungen erwerben. Dieser Prozess könnte mit dem Verlust von genetischem Material aus 9p21.3

zusammenhängen. Die hier beschriebenen genomischen Unterschiede zwischen Primär- und Rezidivtumoren könnten neue Ansatzpunkte für alternative Therapiestrategien in Patienten mit einem rezidivierenden Glioblastom bieten.

Im vierten Projekt wurden zwei histologisch unterschiedliche Tumorproben einer 47-jährigen Patientin mittels Array-CGH hinsichtlich des klonalen Ursprungs untersucht. Ursprünglich wurde bei der Patientin ein benigner Hypophysentumor diagnostiziert, nach kürzester Zeit wurde jedoch ein Rezidiv entdeckt, das histologisch eher einem malignen peripheren Nervenscheidentumor glich. Es wurde eine Array-CGH an den DNAs aus beiden Tumorproben durchgeführt. Dabei zeigte sich im ersten Tumor ein genomisches Profil, in dem fast alle Chromosomen, außer Chromosom 16, DNA-Kopienzahlveränderungen aufwiesen. Das genomische Profil des zweiten Tumors zeigte ähnliche Kopienzahlveränderungen, ungefähr 80% der insgesamt 29 im ersten Tumor detektierten Veränderungen konnten auch im zweiten Tumor identifiziert werden. Dieses Ergebnis legt nahe, dass es einen klonalen Zusammenhang zwischen dem ersten und dem zweiten Tumor gibt, und lässt vermuten, dass der zweite Tumor ein Rezidiv des ersten ist. Außerdem konnte festgestellt werden, dass nicht nur das Rezidiv sondern auch der zuerst diagnostizierte Tumor chromosomale Veränderungen aufwies, die typisch für einen malignen peripheren Nervenscheidentumor sind. Daraus lässt sich schließen, dass Array-CGH eine geeignete Methode ist, um den Ursprung von Tumoren zu klären, besonders wenn diese histologisch enorme Unterschiede aufweisen.

In einem fünften Projekt wurde die Keimbahn einer Patientin mit einem komplexen Phänotyp einschließlich einer Krebsdisposition, auf genetische Ursachen hin untersucht. Zu den Hauptsymptomen gehörte eine mentale Retardierung, zwei Tumor-Erkrankungen (ein Ovarialkarzinom und eine akute B-Lymphoblastäre Leukämie) vor dem 20. Lebensjahr, Pigmentierungsstörungen der Haut und ein Kleinwuchs. Es wurde zunächst vermutet, dass dieser schwere Phänotyp auf ein Mikroduplikations- oder Mikrodeletionssyndrom zurückzuführen ist, da diese oft mehrere Gene betreffen und so die unterschiedlichen Merkmale des Phänotyps erklären könnten. Um den komplexen Phänotyp zu erklären, wurde an der aus peripherem Blut isolierten DNA der Patientin und ihrer Eltern zunächst eine Array-CGH-Analyse durchgeführt. Mittels Array-CGH wurden zwei Mikroduplikationen in den chromosomalen Banden 6q27 und 22q11.21 identifiziert, die beide von der Mutter ererbt waren. Die Mikroduplikation in der chromosomalen Bande 6q27 hatte eine Größe von 0,26 Mb und betraf einen Teil des *MLLT4* Gens, das bereits als Fusionspartner von *MLL* in Leukämiezellen beschrieben wurde. Die Mikroduplikation in der chromosomalen Bande 22q11.21 hatte eine Größe von 2.5 Mb und umfasste ungefähr 50 Gene. Diese chromosomale Region ist anfällig für chromosomale Umbauten und liegt dem 22q11.21 Mikroduplikationssyndrom zugrunde, das durch eine hohe Variabilität ausgezeichnet ist (z.B. Ausprägung der kognitiven Defizite). Diese Mikroduplikation erklärt zum Teil die mentale Retardierung der Patientin, aber nicht deren starke Ausprägung. Da die beiden Tumorerkrankungen der Patientin durch die beiden identifizierten Mikroduplikationen nicht wirklich erklärbar waren, wurde zusätzlich eine Exomsequenzierung durchgeführt. Mittels dieser wurde entdeckt, dass die Patientin Compoundheterozygot für zwei Stop-Mutationen im *BLM*-Gen war. Mutationen in diesem Gen verursachen das autosomal-rezessiv

erbliche Bloom Syndrom, welches u.a. zu Krebsdisposition, Hautanomalien und Kleinwuchs führt. Außerdem wurde eine *de novo CHEK2*-Variante entdeckt, die mit Krebsdisposition einhergeht. Zusammengefasst erklären die hier beschriebenen genomischen Veränderungen den komplexen Phänotyp der Patientin.

Zusammenfassend konnte in dieser Arbeit gezeigt werden, dass sich die beiden Methoden Array-CGH und Exomsequenzierung hervorragend dazu eignen, sowohl genomweite somatische Kopienzahlveränderungen in unterschiedlichen Tumoren des Zentralnervensystems zu identifizieren, als auch Keimbahnveränderungen bei Patienten mit Krebsdisposition durch exomweite Analysen aufzudecken.

7 References

Alberts, B. (2008) Molecular biology of the cell, 5th edn (New York: Garland Science).

Alkan, C., Coe, B.P., Eichler, E.E. (2011) Genome structural variation discovery and genotyping. Nat Rev Genet 12, 363-376.

Alesi, V., Barrano, G., Morara, S., Darelli, D., Petrilli, K., Capalbo, A., Pacella, M., Haass, C., Finocchi, M., Novelli, A., Bertoli, M. (2011) A previously undescribed de novo 4p15 deletion in a patient with apparently isolated metopic craniosynostosis. Am J Med Genet A 155A, 2543-2551.

Arai, M., Kondoh, N., Imazeki, N., Hada, A., Hatsuse, K., Matsubara, O., Yamamoto, M. (2009) The knockdown of endogenous replication factor C4 decreases the growth and enhances the chemosensitivity of hepatocellular carcinoma cells. Liver Int 29, 55-62.

Asa, S.L., Ezzat, S. (2002) The pathogenesis of pituitary tumors. Nat Rev Cancer 2, 836-849.

Balesaria, S., Brock, C., Bower, M., Clark, J., Nicholson, S.K., Lewis, P., de Sanctis, S., Evans, H., Peterson, D., Mendoza, N., Glaser, M.G., Newlands, E.S., Fisher, R.A. (1999) Loss of chromosome 10 is an independent prognostic factor in high-grade gliomas. Br J Cancer 81, 1371-1377.

Balss, J., Meyer, J., Mueller, W., Korshunov, A., Hartmann, C., von Deimling, A. (2008) Analysis of the *IDH1* codon 132 mutation in brain tumors. Acta Neuropathol 116, 597-602.

Bamshad, M.J., Ng, S.B., Bigham, A.W., Tabor, H.K., Emond, M.J., Nickerson, D.A., Shendure, J. (2011) Exome sequencing as a tool for Mendelian disease discovery. Nat Rev Genet 12, 745-755.

Barbieri, F., Pattarozzi, A., Gatti, M., Aiello, C., Quintero, A., Lunardi, G., Bajetto, A., Ferrari, A., Culler, M.D., Florio, T. (2009) Differential efficacy of *SSTR1*, -2, and -5 agonists in the inhibition of C6 glioma growth in nude mice. Am J Physiol Endocrinol Metab 297, E1078-1088.

Barbus, S., Tews, B., Karra, D., Hahn, M., Radlwimmer, B., Delhomme, N., Hartmann, C., Felsberg, J., Krex, D., Schackert, G., Martinez, R., Reifenberger, G., Lichter, P. (2011) Differential retinoic acid signaling in tumors of long- and short-term glioblastoma survivors. J Natl Cancer Inst 103, 598-606.

Bau, D.T., Tsai, C.W., Wu, C.N. (2011) Role of the *XRCC5/XRCC6* dimer in carcinogenesis and pharmacogenomics. Pharmacogenomics 12, 515-534.

Bell, D.W., Varley, J.M., Szydlo, T.E., Kang, D.H., Wahrer, D.C., Shannon, K.E., Lubratovich, M., Verselis, S.J., Isselbacher, K.J., Fraumeni, J.F., Birch, J.M., Li, F.P., Haber, D.A. (1999) Heterozygous germ line *hCHK2* mutations in Li- Fraumeni syndrome. Science 286, 2528-2531.

Berendsen, S., Broekman, M., Seute, T., Snijders, T., van Es, C., de Vos, F., Regli, L., Robe, P. (2012) Valproic acid for the treatment of malignant gliomas: review of the preclinical rationale and published clinical results. Expert Opin Investig Drugs 21, 1391-1415.

Beroukhim, R., Getz, G., Nghiemphu, L., Barretina, J., Hsueh, T., Linhart, D., Vivanco, I., Lee, J.C., Huang, J.H., Alexander, S., Du, J., Kau, T., Thomas, R.K., Shah, K., Soto, H., Perner, S., Prensner, J., Debiasi, R.M., Demichelis, F., Hatton, C., Rubin, M.A., Garraway, L.A., Nelson, S.F., Liau, L., Mischel,

P.S., Cloughesy, T.F., Meyerson, M., Golub, T.A., Lander, E.S., Mellinghoff, I.K., Sellers, W.R. (2007) Assessing the significance of chromosomal aberrations in cancer: methodology and application to glioma. Proc Natl Acad Sci U S A 104, 20007-20012.

Bertomeu, T., Zvereff, V., Ibrahim, A., Zehntner, S.P., Aliaga, A., Rosa-Neto, P., Bedell, B.J., Falardeau, P., Gourdeau, H. (2010) TLN-4601 peripheral benzodiazepine receptor (PBR/TSPO) binding properties do not mediate apoptosis but confer tumor-specific accumulation. Biochem Pharmacol 80, 1572-1579.

Bhagat, S., Smith, C., Teasdale, G.M., McFadzean, R.M. (2002) Nerve sheath tumors of the sellar region. J Neuroophthalmol 22, 275-278.

Birchmeier, C., Birchmeier, W., Gherardi, E., Vande Woude, G.F. (2003) Met, metastasis, motility and more. Nat Rev Mol Cell Biol 4, 915-925.

Bleeker, F.E., Lamba, S., Leenstra, S., Troost, D., Hulsebos, T., Vandertop, W.P., Frattini, M., Molinari, F., Knowles, M., Cerrato, A., Rodolfo, M., Scarpa, A., Felicioni, L., Buttitta, F., Malatesta, S., Marchetti, A., Bardelli, A. (2009) *IDH1* mutations at residue p.R132 (*IDH1*(R132)) occur frequently in high-grade gliomas but not in other solid tumors. Hum Mutat 30, 7-11.

Bloom, D. (1954) Congenital telangiectatic erythema resembling lupus erythematosus in dwarfs; probably a syndrome entity. A.M.A. Am J Dis Child 88, 754-758.

Brockschmidt, A., Trost, D., Peterziel, H., Zimmermann, K., Ehrler, M., Grassmann, H., Pfenning, P.N., Waha, A., Wohlleber, D., Brockschmidt, F.F., Jugold, M., Hoischen, A., Kalla, C., Waha, A., Seifert, G., Knolle, P.A., Latz, E., Hans, V.H., Wick, W., Pfeifer, A., Angel, P., Weber, R.G. (2012) *KIAA1797/FOCAD* encodes a novel focal adhesion protein with tumour suppressor function in gliomas. Brain 135, 1027-1041.

Cancer Genome Atlas Research Network (2008) Comprehensive genomic characterization defines human glioblastoma genes and core pathways. Nature 455, 1061-1068.

Capper, D., Weissert, S., Balss, J., Habel, A., Meyer, J., Jager, D., Ackermann, U., Tessmer, C., Korshunov, A., Zentgraf, H., Hartmann, C., von Deimling, A. (2010) Characterization of R132H mutation-specific *IDH1* antibody binding in brain tumors. Brain Pathol 20, 245-254.

Cash, T.P., Gruber, J.J., Hartman, T.R., Henske, E.P., Simon, M.C. (2011) Loss of the Birt-Hogg-Dube tumor suppressor results in apoptotic resistance due to aberrant *TGF*beta-mediated transcription. Oncogene 30, 2534-2546.

Chadalapaka, G., Jutooru, I., Safe, S. (2012) Celastrol decreases specificity proteins (Sp) and fibroblast growth factor receptor-3 (*FGFR3*) in bladder cancer cells. Carcinogenesis 33, 886-894.

Chang, V.Y., Quintero-Rivera, F., Baldwin, E.E., Woo, K., Martinez-Agosto, J.A., Fu, C., Gomperts, B.N. (2011) B-acute lymphoblastic leukemia and cystinuria in a patient with duplication 22q11.21 detected by chromosomal microarray analysis. Pediatr Blood Cancer 56, 470-473.

Chelli, B., Salvetti, A., Da Pozzo, E., Rechichi, M., Spinetti, F., Rossi, L., Costa, B., Lena, A., Rainaldi, G., Scatena, F., Vanacore, R., Gremigni, V., Martini, C. (2008) PK 11195 differentially affects cell survival in

human wild-type and 18 kDa translocator protein-silenced ADF astrocytoma cells. J Cell Biochem 105, 712-723.

Clark, M.J., Chen, R., Lam, H.Y., Karczewski, K.J., Euskirchen, G., Butte, A.J., Snyder, M. (2011) Comparison of exome DNA sequencing technologies. Nat Biotechnol 29, 908-914.

Classen, C.F., Riehmer, V., Landwehr, C., Kosfeld, A., Heilmann, S., Scholz, C., Kabisch, S., Engels, H., Tierling, S., Zivicnjak, M., Schacherer, F., Haffner, D., Weber, R.G. (2013) Dissecting the genotype in syndromic intellectual disability using whole exome sequencing in addition to genome-wide copy number analysis. Hum Genet 132, 825-841.

Cleator, S., Tsimelzon, A., Ashworth, A., Dowsett, M., Dexter, T., Powles, T., Hilsenbeck, S., Wong, H., Osborne, C.K., O'Connell, P., Chang, J.C. (2006) Gene expression patterns for doxorubicin (Adriamycin) and cyclophosphamide (cytoxan) (AC) response and resistance. Breast Cancer Res Treat 95, 229-233.

Colin, C., Voutsinos-Porche, B., Nanni, I., Fina, F., Metellus, P., Intagliata, D., Baeza, N., Bouvier, C., Delfino, C., Loundou, A., Chinot, O., Lah, T., Kos, J., Martin, P.M., Ouafik, L., Figarella-Branger, D. (2009) High expression of cathepsin B and plasminogen activator inhibitor type-1 are strong predictors of survival in glioblastomas. Acta Neuropathol 118, 745-754.

Coupienne, I., Fettweis, G., Rubio, N., Agostinis, P., Piette, J. (2011) *5-ALA-PDT* induces *RIP3*-dependent necrosis in glioblastoma. Photochem Photobiol 10, 1868-1878.

Csete, B., Lengyel, Z., Kadar, Z., Battyani, Z. (2009) Poly(adenosine diphosphate-ribose) polymerase-1 expression in cutaneous malignant melanomas as a new molecular marker of aggressive tumor. Pathol Oncol Res 15, 47-53.

Cybulski, C., Gorski, B., Huzarski, T., Masojc, B., Mierzejewski, M., Debniak, T., Teodorczyk, U., Byrski, T., Gronwald, J., Matyjasik, J., Zlowocka, E., Lenner, M., Grabowska, E., Nej, K., Castaneda, J., Medrek, K., Szymańska, A., Szymańska, J., Kurzawski, G., Suchy, J., Oszurek, O., Witek, A., Narod, S.A., Lubiński, J. (2004) *CHEK2* is a multiorgan cancer susceptibility gene. Am J Hum Genet 75, 1131-1135.

de Ligt, J., Willemsen, M.H., van Bon, B.W., Kleefstra, T., Yntema, H.G., Kroes, T., Vulto-van Silfhout, A.T., Koolen, D.A., de Vries, P., Gilissen, C., del Rosario, M., Hoischen, A., Scheffer, H., de Vries, B.B., Brunner, H.G., Veltman, J.A., Vissers, L.E. (2012) Diagnostic exome sequencing in persons with severe intellectual disability. N Engl J Med 367, 1921-1929.

Desrichard, A., Bidet, Y., Uhrhammer, N., Bignon, Y.J. (2011) *CHEK2* contribution to hereditary breast cancer in non-*BRCA* families. Breast Cancer Res 13, R119.

Donson, A.M., Birks, D.K., Schittone, S.A., Kleinschmidt-DeMasters, B.K., Sun, D.Y., Hemenway, M.F., Handler, M.H., Waziri, A.E., Wang, M., Foreman, N.K. (2012) Increased immune gene expression and immune cell infiltration in high-grade astrocytoma distinguish long-term from short-term survivors. J Immunol 189, 1920-1927.

Ducatman, B.S., Scheithauer, B.W., Piepgras, D.G., Reiman, H.M., Ilstrup, D.M. (1986) Malignant peripheral nerve sheath tumors. A clinicopathologic study of 120 cases. Cancer 57, 2006-2021.

England, B., Huang, T., Karsy, M. (2013) Current understanding of the role and targeting of tumor suppressor p53 in glioblastoma multiforme. Tumour Biol 34, 2063-2074.

Ensenauer, R.E., Adeyinka, A., Flynn, H.C., Michels, V.V., Lindor, N.M., Dawson, D.B., Thorland, E.C., Lorentz, C.P., Goldstein, J.L., McDonald, M.T., Smith, W.E., Simon-Fayard, E., Alexander, A.A., Kulharya, A.S., Ketterling, R.P., Clark, R.D., Jalal, S.M. (2003) Microduplication 22q11.2, an emerging syndrome: clinical, cytogenetic, and molecular analysis of thirteen patients. Am J Hum Genet 73, 1027-1040.

Ernst, A., Hofmann, S., Ahmadi, R., Becker, N., Korshunov, A., Engel, F., Hartmann, C., Felsberg, J., Sabel, M., Peterziel, H., Durchdewald, M., Hess, J., Barbus, S., Campos, B., Starzinski-Powitz, A., Unterberg, A., Reifenberger, G., Lichter, P., Herold-Mende, C., Radlwimmer, B. (2009) Genomic and expression profiling of glioblastoma stem cell-like spheroid cultures identifies novel tumor-relevant genes associated with survival. Clin Cancer Res 15, 6541-6550.

Esteller, M., Garcia-Foncillas, J., Andion, E., Goodman, S.N., Hidalgo, O.F., Vanaclocha, V., Baylin, S.B., Herman, J.G. (2000) Inactivation of the DNA-repair gene *MGMT* and the clinical response of gliomas to alkylating agents. N Engl J Med 343, 1350-1354.

Ezzat, S., Asa, S.L., Couldwell, W.T., Barr, C.E., Dodge, W.E., Vance, M.L., McCutcheon, I.E. (2004) The prevalence of pituitary adenomas: a systematic review. Cancer 101, 613-619.

Felsberg, J., Erkwoh, A., Sabel, M.C., Kirsch, L., Fimmers, R., Blaschke, B., Schlegel, U., Schramm, J., Wiestler, O.D., Reifenberger, G. (2004) Oligodendroglial tumors: refinement of candidate regions on chromosome arm 1p and correlation of 1p/19q status with survival. Brain Pathol 14, 121-130.

Felsberg, J., Thon, N., Eigenbrod, S., Hentschel, B., Sabel, M.C., Westphal, M., Schackert, G., Kreth, F.W., Pietsch, T., Loeffler, M., Weller, M., Reifenberger, G., Tonn, J.C.; German Glioma Network (2011) Promoter methylation and expression of *MGMT* and the DNA mismatch repair genes *MLH1*, *MSH2*, *MSH6* and *PMS2* in paired primary and recurrent glioblastomas. Int J Cancer 129, 659-670.

Fiegler, H., Carr, P., Fiegler, H., Carr, P., Douglas, E.J., Burford, D.C., Hunt, S., Scott, C.E., Smith, J., Vetrie, D., Gorman, P., Tomlinson, I.P., Carter, N.P. (2003) DNA microarrays for comparative genomic hybridization based on DOP-PCR amplification of BAC and PAC clones. Genes, Chromosomes Cancer 36, 361-374.

Fiegler, H., Redon, R., Carter, N.P. (2007) Construction and use of spotted large-insert clone DNA microarrays for the detection of genomic copy number changes. Nat Protoc 2, 577-587.

Folgueira, M.A., Carraro, D.M., Brentani, H., Patrao, D.F., Barbosa, E.M., Netto, M.M., Caldeira, J.R., Katayama, M.L., Soares, F.A., Oliveira, C.T., Reis, L.F., Kaiano, J.H., Camargo, L.P., Vêncio, R.Z., Snitcovsky, I.M., Makdissi, F.B., e Silva, P.J., Góes, J.C., Brentani, M.M. (2005) Gene expression profile associated with response to doxorubicin-based therapy in breast cancer. Clin Cancer Res 11, 7434-7443.

Gan, H.K., Kaye, A.H., Luwor, R.B. (2009) The *EGFRvIII* variant in glioblastoma multiforme. J Clin Neurosci 16, 748-754.

Garber, J.E., Offit, K. (2005) Hereditary cancer predisposition syndromes. J Clin Oncol 23, 276-292.

Garcia-Arnes, J.A., Gonzalez-Molero, I., Oriola, J., Mazuecos, N., Luque, R., Castano, J., Arraez, M.A. (2013) Familial isolated pituitary adenoma caused by a *Aip* gene mutation not described before in a family context. Endocr Pathol 24, 234-238.

Gardam, S., Beyaert, R. (2011) The kinase *NIK* as a therapeutic target in multiple myeloma. Expert Opin Ther Targets 15, 207-218.

German, J. (1993) Bloom syndrome: a mendelian prototype of somatic mutational disease. Medicine 72, 393-406.

German, J. (1997) Bloom's syndrome. XX. The first 100 cancers. Cancer Genet Cytogenet 93, 100-106.

German, J., Sanz, M.M., Ciocci, S., Ye, T.Z., Ellis, N.A. (2007) Syndrome-causing mutations of the BLM gene in persons in the Bloom's Syndrome Registry. Hum Mutat 28, 743-753.

Gerson, S.L. (2004) *MGMT*: its role in cancer aetiology and cancer therapeutics. Nat Rev Cancer 4, 296-307.

Gilkes, D.M., Bajpai, S., Wong, C.C., Chaturvedi, P., Hubbi, M.E., Wirtz, D., Semenza, G.L. (2013) Procollagen lysyl hydroxylase 2 is essential for hypoxia-induced breast cancer metastasis. Mol Cancer Res 11, 456-466.

Griffin, C.A., Burger, P., Morsberger, L., Yonescu, R., Swierczynski, S., Weingart, J.D., Murphy, K.M. (2006) Identification of der(1;19)(q10;p10) in five oligodendrogliomas suggests mechanism of concurrent 1p and 19q loss. J Neuropathol Exp Neurol 65, 988-994.

Guan, M., Fousek, K., Jiang, C., Guo, S., Synold, T., Xi, B., Shih, C.C., Chow, W.A. (2011) Nelfinavir induces liposarcoma apoptosis through inhibition of regulated intramembrane proteolysis of *SREBP-1* and *ATF6*. Clin Cancer Res 17, 1796-1806.

Guo, D., Prins, R.M., Dang, J., Kuga, D., Iwanami, A., Soto, H., Lin, K.Y., Huang, T.T., Akhavan, D., Hock, M.B., Zhu, S., Kofman, A.A., Bensinger, S.J., Yong, W.H., Vinters, H.V., Horvath, S., Watson, A.D., Kuhn, J.G., Robins, H.I., Mehta, M.P., Wen, P.Y., DeAngelis, L.M., Prados, M.D., Mellinghoff, I.K., Cloughesy, T.F., Mischel, P.S. (2009) *EGFR* signaling through an Akt-SREBP-1-dependent, rapamycin-resistant pathway sensitizes glioblastomas to antilipogenic therapy. Sci Signal 2, ra82.

Guo, Y.F., Wang, X.B., Tian, X.Y., Li, Y., Li, B., Huang, Q., Zhang, M., Li, Z. (2012) Tumor-derived hepatocyte growth factor is associated with poor prognosis of patients with glioma and influences the chemosensitivity of glioma cell line to cisplatin in vitro. World J Surg Oncol 10, 128.

Hampel, H., Peltomaki, P. (2000) Hereditary colorectal cancer: risk assessment and management. Clin Genet 58, 89-97.

Hanahan, D., Weinberg, R.A. (2000) The hallmarks of cancer. Cell 100, 57-70.

Hartmann, C., Nümann, A., Mueller, W., Holtkamp, N., Simon, M., von Deimling, A. (2004) Fine mapping of chromosome 22q tumor suppressor gene candidate regions in astrocytoma. Int J Cancer 108, 839-844.

Hartmann, C., Meyer, J., Balss, J., Capper, D., Mueller, W., Christians, A., Felsberg, J., Wolter, M., Mawrin, C., Wick, W., Weller, M., Herold-Mende, C., Unterberg, A., Jeuken, J.W., Wesseling, P., Reifenberger, G., von Deimling, A. (2009) Type and frequency of *IDH1* and *IDH2* mutations are related to astrocytic and oligodendroglial differentiation and age: a study of 1,010 diffuse gliomas. Acta Neuropathol 118, 469-474.

Hartmann, C., Hentschel, B., Simon, M., Westphal, M., Schackert, G., Tonn, J.C., Loeffler, M., Reifenberger, G., Pietsch, T., von Deimling, A., Weller, M.; German Glioma Network (2013) Long-term survival in primary glioblastoma with versus without isocitrate dehydrogenase mutations. Clin Cancer Res 19, 5146-5157.

He, L., Yu, J.X., Liu, L., Buyse, I.M., Wang, M.S., Yang, Q.C., Nakagawara, A., Brodeur, G.M., Shi, Y.E., Huang, S. (1998) *RIZ1*, but not the alternative *RIZ2* product of the same gene, is underexpressed in breast cancer, and forced *RIZ1* expression causes G2-M cell cycle arrest and/or apoptosis. Cancer Res 58, 4238-4244.

Hegi, M.E., Diserens, A.C., Gorlia, T., Hamou, M.F., de Tribolet, N., Weller, M., Kros, J.M., Hainfellner, J.A., Mason, W., Mariani, L., Bromberg, J.E., Hau, P., Mirimanoff, R.O., Cairncross, J.G., Janzer, R.C., Stupp, R. (2005) *MGMT* gene silencing and benefit from temozolomide in glioblastoma. N Engl J Med 352, 997-1003.

Hickson, I.D. (2003) RecQ helicases: caretakers of the genome. Nat Rev Cancer 3, 169-178.

Hinkle, D.A., Mullett, S.J., Gabris, B.E., Hamilton, R.L. (2011) DJ-1 expression in glioblastomas shows positive correlation with p53 expression and negative correlation with epidermal growth factor receptor amplification. Neuropathology 31, 29-37.

Hodgson, J.G., Yeh, R.F., Ray, A., Wang, N.J., Smirnov, I., Yu, M., Hariono, S., Silber, J., Feiler, H.S., Gray, J.W., Spellman, P.T., Vandenberg, S.R., Berger, M.S., James, C.D. (2009) Comparative analyses of gene copy number and mRNA expression in glioblastoma multiforme tumors and xenografts. Neuro Oncol 11, 477-487.

Hofer, M.J., Riehmer, V., Kuhnt, D., Braun, V., Nimsky, C., Weber, R.G., Sommer, C., Pagenstecher, A. (2012) Genomic profiling to assess the clonal relationship between histologically distinct intracranial tumours. Neuropathol Appl Neurobiol 38, 500-504.

Horbinski, C. (2013) What do we know about *IDH1/2* mutations so far, and how do we use it? Acta Neuropathol 125, 621-636.

Horn, H., Ziepert, M., Becher, C., Barth, T.F., Bernd, H.W., Feller, A.C., Klapper, W., Hummel, M., Stein, H., Hansmann, M.L., Schmelter, C., Möller, P., Cogliatti, S., Pfreundschuh, M., Schmitz, N., Trümper, L., Siebert, R., Loeffler, M., Rosenwald, A., Ott, G.; German High-Grade Non-Hodgkin Lymphoma Study Group (2013) *MYC* status in concert with *BCL2* and *BCL6* expression predicts outcome in diffuse large B-cell lymphoma. Blood 121, 2253-2263.

Hotta, T., Saito, Y., Fujita, H., Mikami, T., Kurisu, K., Kiya, K., Uozumi, T., Isowa, G., Ishizaki, K., Ikenaga, M. (1994) O6-alkylguanine-DNA alkyltransferase activity of human malignant glioma and its clinical implications. J Neurooncol 21, 135-140.

Hu, G., Chong, R.A., Yang, Q., Wei, Y., Blanco, M.A., Li, F., Reiss, M., Au, J.L., Haffty, B.G., Kang, Y. (2009) MTDH activation by 8q22 genomic gain promotes chemoresistance and metastasis of poor-prognosis breast cancer. Cancer Cell 15, 9-20.

Huang, G., Ho, B., Conroy, J., Liu, S., Qiang, H., Golubovskaya, V. (2014) The microarray gene profiling analysis of glioblastoma cancer cells reveals genes affected by Fak Inhibitor Y15 and combination of Y15 and temozolomide. Anticancer Agents Med Chem 14, 9-17.

Huang, Y., Li, L.Z., Zhang, C.Z., Yi, C., Liu, L.L., Zhou, X., Xie, G.B., Cai, M.Y., Li, Y., Yun, J.P. (2012) Decreased expression of zinc-alpha2-glycoprotein in hepatocellular carcinoma associates with poor prognosis. J Transl Med 10, 106.

Ichimura, K., Schmidt, E.E., Miyakawa, A., Goike, H.M., Collins, V.P. (1998) Distinct patterns of deletion on 10p and 10q suggest involvement of multiple tumor suppressor genes in the development of astrocytic gliomas of different malignancy grades. Genes Chromosomes Cancer 22, 9-15.

Ichimura, K., Bolin, M.B., Goike, H.M., Schmidt, E.E., Moshref, A., Collins, V.P. (2000) Deregulation of the p14ARF/MDM2/p53 pathway is a prerequisite for human astrocytic gliomas with G1-S transition control gene abnormalities. Cancer Res 60, 417-424.

Ichimura, K., Mungall, A.J., Fiegler, H., Pearson, D.M., Dunham, I., Carter, N.P., Collins, V.P. (2006) Small regions of overlapping deletions on 6q26 in human astrocytic tumours identified using chromosome 6 tile path array-CGH. Oncogene 25, 1261-1271.

Ito, M., Wakabayashi, T., Natsume, A., Hatano, H., Fujii, M., Yoshida, J. (2007) Genetically heterogeneous glioblastoma recurring with disappearance of 1p/19q losses: case report. Neurosurgery 61, E168-169; discussion E169.

Jenkins, R.B., Blair, H., Ballman, K.V., Giannini, C., Arusell, R.M., Law, M., Flynn, H., Passe, S., Felten, S., Brown, P.D., Shaw, E.G., Buckner, J.C. (2006) A t(1;19)(q10;p10) mediates the combined deletions of 1p and 19q and predicts a better prognosis of patients with oligodendroglioma. Cancer Res 66, 9852-9861.

Jeuken, J.W., von Deimling, A., Wesseling, P. (2004) Molecular pathogenesis of oligodendroglial tumors. J Neurooncol 70, 161-181.

Jhanwar, S.C., Chen, Q., Li, F.P., Brennan, M.F., Woodruff, J.M. (1994) Cytogenetic analysis of soft tissue sarcomas. Recurrent chromosome abnormalities in malignant peripheral nerve sheath tumors (MPNST). Cancer Genet Cytogenet 78, 138-144.

Josson, S., Xu, Y., Fang, F., Dhar, S.K., St Clair, D.K., St Clair, W.H. (2006) RelB regulates manganese superoxide dismutase gene and resistance to ionizing radiation of prostate cancer cells. Oncogene 25, 1554-1559.

Kärrlander, M., Lindberg, N., Olofsson, T., Kastemar, M., Olsson, A.K., Uhrbom, L. (2009) Histidine-rich glycoprotein can prevent development of mouse experimental glioblastoma. PloS One 4, e8536.

Kim, K.M., Park, C.K., Park, S.H., Paek, S.H., Kim, D.G., Jung, H.W. (2007) Malignant Triton tumour mistaken for pituitary adenoma. Acta Neurochir 149, 1265-1267.

Kinzler, K.W., Nilbert, M.C., Su, L.K., Vogelstein, B., Bryan, T.M., Levy, D.B., Smith, K.J., Preisinger, A.C., Hedge, P., McKechnie, D., Finniear, R., Matrkam, A., Groffen, J., Boguski, M.S., Altschul, S.F., Horit, A., Ando, H., Miyoshi, Y., Miki, Y., Nishisho, I., Nakamura, Y. (1991) Identification of *FAP* locus gene form chromosome 5q21. Science 253, 661-665.

Kiuru, A., Lindholm, C., Heinavaara, S., Ilus, T., Jokinen, P., Haapasalo, H., Salminen, T., Christensen, H.C., Feychting, M., Johansen, C., Lönn, S., Malmer, B., Schoemaker, M.J., Swerdlow, A.J., Auvinen, A. (2008) *XRCC1* and *XRCC3* variants and risk of glioma and meningioma. J Neurooncol 88, 135-142.

Kleihues, P., Schauble, B., zur Hausen, A., Esteve, J., Ohgaki, H. (1997) Tumors associated with p53 germline mutations: a synopsis of 91 families. Am J Pathol 150, 1-13.

Kleihues, P., Burger, P.C., Rosenblum, M.K., Paulus, W., Scheithauer, B.W. IN: Louis D.N., Ohgaki H., Wiestier O.D., Cavenee W.K. (Eds.): WHO Classification of Tumours of the Central Nervous System. IARC: Lyon 2007, p30-33.

Kleihues, P., Burger, P.C., Aldape, K.D., Brat, D.J., Biernat, W., Bigner, D.D., Nakazato, Y., Plate, K.H., Giangaspero, F., von Deimling, A., Ohgaki, H., Cavenee, W.K. IN: Louis D.N., Ohgaki H., Wiestier O.D., Cavenee W.K. (Eds.): WHO Classification of Tumours of the Central Nervous System. IARC: Lyon 2007, p33-47.

Knoch, J., Kamenisch, Y., Kubisch, C., Bernebrug, M. (2012) Rare hereditary diseases with defects in DNA-repair. Eur J Dermatol 22, 443-455.

Knudson, A.G., Jr. (1971) Mutation and cancer: statistical study of retinoblastoma. Proc Natl Acad Sci U S A 68, 820-823.

Koh, D.W., Dawson, T.M., Dawson, V.L. (2005) Mediation of cell death by poly(ADP-ribose) polymerase-1. Pharmacol Res 52, 5-14.

Kotake, Y., Nakagawa, T., Kitagawa, K., Suzuki, S., Liu, N., Kitagawa, M., Xiong, Y. (2011) Long non-coding RNA ANRIL is required for the *PRC2* recruitment to and silencing of p15(*INK4B*) tumor suppressor gene. Oncogene 30, 1956-1962.

Krayenbühl, N., Heppner, F., Yonekawa, Y., Bernays, R.L. (2007) Intrasellar malignant peripheral nerve sheath tumor (MPNST). Acta Nneurochir 149, 201-205; discussion 205-206.

Krex, D., Klink, B., Hartmann, C., von Deimling, A., Pietsch, T., Simon, M., Sabel, M., Steinbach, J.P., Heese, O., Reifenberger, G., Weller, M., Schackert, G.; German Glioma Network (2007) Long-term survival with glioblastoma multiforme. Brain 130, 2596-2606.

Kühne, A., Tzvetkov, M.V., Hagos, Y., Lage, H., Burckhardt, G., Brockmöller, J. (2009) Influx and efflux transport as determinants of melphalan cytotoxicity: Resistance to melphalan in *MDR1* overexpressing tumor cell lines. Biochem Pharmacol 78, 45-53.

Lass, U., Hartmann, C., Capper, D., Herold-Mende, C., von Deimling, A., Meiboom, M., Mueller, W. (2013) Chromogenic in situ hybridization is a reliable alternative to fluorescence in situ hybridization for diagnostic testing of 1p and 19q loss in paraffin-embedded gliomas. Brain Pathol 23, 311-318.

Lassmann, S., Weis, R., Makowiec, F., Roth, J., Danciu, M., Hopt, U., Werner, M. (2007) Array CGH identifies distinct DNA copy number profiles of oncogenes and tumor suppressor genes in chromosomal- and microsatellite-unstable sporadic colorectal carcinomas. J Mol Med 85, 293-304.

Le Calvez-Kelm, F., Lesueur, F., Damiola, F., Vallee, M., Voegele, C., Babikyan, D., Durand, G., Forey, N., McKay-Chopin, S., Robinot, N., Nguyen-Dumont, T., Thomas, A., Byrnes, G.B.; Breast Cancer Family Registry, Hopper, J.L., Southey, M.C., Andrulis, I.L., John, E.M., Tavtigian, S.V. (2011) Rare, evolutionarily unlikely missense substitutions in *CHEK2* contribute to breast cancer susceptibility: results from a breast cancer family registry case-control mutation-screening study. Breast Cancer Res 13, R6.

Lee, D.W., Ramakrishnan, D., Valenta, J., Parney, I.F., Bayless, K.J., Sitcheran, R. (2013) The NF-kappaB RelB protein is an oncogenic driver of mesenchymal glioma. PloS One 8, e57489.

Li, F.P., Fraumeni, J.F., Jr. (1969) Rhabdomyosarcoma in children: epidemiologic study and identification of a familial cancer syndrome. J Natl Cancer Inst 43, 1365-1373.

Li, F.P., Fraumeni, J.F., Jr., Mulvihill, J.J., Blattner, W.A., Dreyfus, M.G., Tucker, M.A., Miller, R.W. (1988) A cancer family syndrome in twenty-four kindreds. Cancer Res 48, 5358-5362.

Li, S.C., Vu, L.T., Ho, H.W., Yin, H.Z., Keschrumrus, V., Lu, Q., Wang, J., Zhang, H., Ma, Z., Stover, A., Weiss, J.H., Schwartz, P.H., Loudon, W.G. (2012) Cancer stem cells from a rare form of glioblastoma multiforme involving the neurogenic ventricular wall. Cancer Cell Int 12, 41.

Li, T., Wang, H., Sun, Y., Zhao, L., Gang, Y., Guo, X., Huang, R., Yang, Z., Pan, Y., Wu, K., Xu, L., Liu, Z., Fan, D. (2013) Transcription factor *CUTL1* is a negative regulator of drug resistance in gastric cancer. The J Biol Chem 288, 4135-4147.

Link, B.C., Reichelt, U., Schreiber, M., Kaifi, J.T., Wachowiak, R., Bogoevski, D., Bubenheim, M., Cataldegirmen, G., Gawad, K.A., Issa, R., Koops, S., Izbicki, J.R., Yekebas, E.F. (2007) Prognostic implications of netrin-1 expression and its receptors in patients with adenocarcinoma of the pancreas. Ann Surg Oncol 14, 2591-2599.

Louis, D.N., Ohgaki, H., WIestler, O.D., Cavenee, W.K., Burger, P.C., Jouvet, A., Scheithauer, B.W., Kleihues, P. (2007a) The 2007 WHO classification of tumours of the central nervous system. Acta Neuropathol 114, 97-109.

Louis D.N., Ohgaki H., Wiestier O.D., Cavenee W.K. (Eds.): WHO Classification of Tumours of the Central Nervous System. IARC: Lyon 2007b.

Lourenço, S.V., Coutinho-Camillo, C.M., Buim, M.E., de Carvalho, A.C., Lessa, R.C., Pereira, C.M., Vettore, A.L., Carvalho, A.L., Fregnani, J.H., Kowalski, L.P., Soares, F.A. (2010) Claudin-7 down-regulation is an important feature in oral squamous cell carcinoma. Histopathology 57, 689-698.

Lucito, R., Healy, J., Alexander, J., Reiner, A., Esposito, D., Chi, M., Rodgers, L., Brady, A., Sebat, J., Troge, J., West, J.A., Rostan, S., Nguyen, K.C., Powers, S., Ye, K.Q., Olshen, A., Venkatraman, E., Norton, L., Wigler, M. (2003) Representational oligonucleotide microarray analysis: a high-resolution method to detect genome copy number variation. Genome Res 13, 2291-2305.

Ma, J., Cui, W., He, S.M., Duan, Y.H., Heng, L.J., Wang, L., Gao, G.D. (2012) Human U87 astrocytoma cell invasion induced by interaction of betaig-h3 with integrin alpha5beta1 involves calpain-2. PloS One 7, e37297.

Maartens, N.F., Ellegala, D.B., Vance, M.L., Lopes, M.B., Laws, E.R., Jr. (2003) Intrasellar schwannomas: report of two cases. Neurosurgery 52, 1200-1205; discussion 1205-1206.

Maeda, A., Maeda, T., Ohguro, H., Palczewski, K., Sato, N. (2002) Vaccination with recoverin, a cancer-associated retinopathy antigen, induces autoimmune retinal dysfunction and tumor cell regression in mice. Eur J Immunol 32, 2300-2307.

Malkin, D., Li, F.P., Strong, L.C., Fraumeni, J.F., Jr., Nelson, C.E., Kim, D.H., Kassel, J., Gryka, M.A., Bischoff, F.Z., Tainsky, M.A., Friend, S.H. (1990) Germ line p53 mutations in a familial syndrome of breast cancer, sarcomas, and other neoplasms. Science 250, 1233-1238.

Mao, F.J., Sidorova, J.M., Lauper, J.M., Emond, M.J., Monnat, R.J. (2010) The human *WRN* and *BLM* RecQ helicases differentially regulate cell proliferation and survival after chemotherapeutic DNA damage. Cancer Res 70, 6548-6555.

Marie, Y., Carpentier, A.F., Omuro, A.M., Sanson, M., Thillet, J., Hoang-Xuan, K., Delattre, J.Y. (2005) *EGFR* tyrosine kinase domain mutations in human gliomas. Neurology 64, 1444-1445.

Marschalek, R. (2011) Mechanisms of leukemogenesis by MLL fusion proteins. Br J Haematol 152, 141-154.

Martinez, R., Rohde, V., Schackert, G. (2010) Different molecular patterns in glioblastoma multiforme subtypes upon recurrence. J Neurooncol 96, 321-329.

Massa, A., Barbieri, F., Aiello, C., Iuliano, R., Arena, S., Pattarozzi, A., Corsaro, A., Villa, V., Fusco, A., Zona, G., Spaziante, R., Schettini, G., Florio, T. (2004) The phosphotyrosine phosphatase eta mediates somatostatin inhibition of glioma proliferation via the dephosphorylation of ERK1/2. Ann N Y Acad Sci 1030, 264-274.

Merlo, A., Hausmann, O., Wasner, M., Steiner, P., Otte, A., Jermann, E., Freitag, P., Reubi, J.C., Müller-Brand, J., Gratzl, O., Mäcke, H.R. (1999) Locoregional regulatory peptide receptor targeting with the diffusible somatostatin analogue 90Y-labeled DOTA0-D-Phe1-Tyr3-octreotide (DOTATOC): a pilot study in human gliomas. Clin Cancer Res 5, 1025-1033.

McKean-Cowdin, R., Barnholtz-Sloan, J., Inskip, P.D., Ruder, A.M., Butler, M., Rajaraman, P., Razavi, P., Patoka, J., Wiencke, J.K., Bondy, M.L., Wrensch, M. (2009) Associations between polymorphisms in DNA repair genes and glioblastoma. Cancer Epidemiol Biomarkers Prev 18, 1118-1126.

Mertens, F., Rydholm, A., Bauer, H.F., Limon, J., Nedoszytko, B., Szadowska, A., Willen, H., Heim, S., Mitelman, F., Mandahl, N. (1995) Cytogenetic findings in malignant peripheral nerve sheath tumors. Int J Cancer 61, 793-798.

Metzker, M.L. (2010) Sequencing technologies – the next generation. Nat Rev Genet 11, 31-46.

Miller, C.R., Dunham, C.P., Scheithauer, B.W., Perry, A. (2006) Significance of necrosis in grading of oligodendroglial neoplasms: a clinicopathologic and genetic study of newly diagnosed high-grade gliomas. J Clin Oncol 24, 5419-5426.

Miller, D.T., Adam, M.P., Aradhya, S., Biesecker, L.G., Brothman, A.R., Carter, N.P., Church, D.M., Crolla, J.A., Eichler, E.E., Epstein, C.J., Faucett, W.A., Feuk, L., Friedman, J.M., Hamosh, A., Jackson, L., Kaminsky, E.B., Kok, K., Krantz, I.D., Kuhn, R.M., Lee, C., Ostell, J.M., Rosenberg, C., Scherer, S.W., Spinner, N.B., Stavropoulos, D.J., Tepperberg, J.H., Thorland, E.C., Vermeesch, J.R., Waggoner, D.J., Watson, M.S., Martin, C.L., Ledbetter, D.H. (2010) Consensus statement: chromosomal microarray is a first-tier clinical diagnostic test for individuals with developmental disabilities or congenital anomalies. Am J Hum Genet 86, 749-764.

Miller, D.T., Shen, Y., Wu, B.L. (2012) Oligonucleotide microarrays for clinical diagnosis of copy number variation and zygosity status. Curr Protoc Hum Genet Chapter 8, Unit8 12.

Mohammed, S., Kovacs, K., Munoz, D., Cusimano, M.D. (2010) A short illustrated review of sellar region schwannomas. Acta Neurochir 152, 885-891.

Mueller, W., Hartmann, C., Hoffmann, A., Lanksch, W., Kiwit, J., Tonn, J., Veelken, J., Schramm, J., Weller, M., Wiestler, O.D., Louis, D.N., von Deimling, A. (2002) Genetic signature of oligoastrocytomas correlates with tumor location and denotes distinct molecular subsets. Am J Pathol 161, 313-319.

Nataranjan, A.T., Vermeulen, S., Darroudi, F., Valentine, M.B., Brent, T.P., Mitra, S., Tano, K. (1992) Chromosomal localization of human O6-methylguanine-DNA methyltransferase (*MGMT*) gene by in situ hybridization. Mutagenesis 7, 83-85.

Neveling, K. and Hoischen, A. (2012) Exom-Sequenzierung zur Identifizierung von Krankheitsgenen. Medizinische Genetik 24:4-11.

Nicholson, R.I., Gee, J.M., Harper, M.E. (2001) *EGFR* and cancer prognosis. Eur J Cancer 37 Suppl 4, S9-15.

Nickel, G.C., Barnholtz-Sloan, J., Gould, M.P., McMahon, S., Cohen, A., Adams, M.D., Guda, K., Cohen, M., Sloan, A.E., LaFramboise, T. (2012) Characterizing mutational heterogeneity in a glioblastoma patient with double recurrence. PloS One 7, e35262.

Nobusawa, S., Watanabe, T., Kleihues, P., Ohgaki, H. (2009) *IDH1* mutations as molecular signature and predictive factor of secondary glioblastomas. Clin Cancer Res 15, 6002-6007.

Nogueira, L., Ruiz-Ontanon, P., Vazquez-Barquero, A., Moris, F., Fernandez-Luna, J.L. (2011) The NFkappaB pathway: a therapeutic target in glioblastoma. Oncotarget 2, 646-653.

Noushmehr, H., Weisenberger, D.J., Diefes, K., Phillips, H.S., Pujara, K., Berman, B.P., Pan, F., Pelloski, C.E., Sulman, E.P., Bhat, K.P., Verhaak, R.G., Hoadley, K.A., Hayes, D.N., Perou, C.M., Schmidt, H.K., Ding, L., Wilson, R.K., Van Den Berg, D., Shen, H., Bengtsson, H., Neuvial, P., Cope, L.M., Buckley, J., Herman, J.G., Baylin, S.B., Laird, P.W., Aldape, K.; Cancer Genome Atlas Research Network (2010) Identification of a CpG island methylator phenotype that defines a distinct subgroup of glioma. Cancer Cell 17, 510-522.

Nutt, C.L., Mani, D.R., Betensky, R.A., Tamayo, P., Cairncross, J.G., Ladd, C., Pohl, U., Hartmann, C., McLaughlin, M.E., Batchelor, T.T., Black, P.M., von Deimling, A., Pomeroy, S.L., Golub, T.R., Louis, D.N. (2003) Gene expression-based classification of malignant gliomas correlates better with survival than histological classification. Cancer Res 63, 1602-1607.

O'Roak, B.J., Deriziotis, P., Lee, C., Vives, L., Schwartz, J.J., Girirajan, S., Karakoc, E., Mackenzie, A.P., Ng, S.B., Baker, C., Rieder, M.J., Nickerson, D.A., Bernier, R., Fisher, S.E., Shendure, J., Eichler, E.E. (2011) Exome sequencing in sporadic autism spectrum disorders identifies severe *de novo* mutations. Nat Genet 43, 585-589.

Ohgaki, H., Kleihues, P. (2005a) Population-based studies on incidence, survival rates, and genetic alterations in astrocytic and oligodendroglial gliomas. J Neuropathol Exp Neurol 64, 479-489.

Ohgaki, H., Kleihues, P. (2005b) Epidemiology and etiology of gliomas. Acta Neuropathol 109, 93-108.

Ohhira, M., Fujimoto, Y., Matsumoto, A., Ohtake, T., Ono, M., Kohgo, Y. (1996) Hepatocellular carcinoma associated with alcoholic liver disease: a clinicopathological study and genetic polymorphism of aldehyde dehydrogenase 2. Alcohol Clin Exp Res 20, 378A-382A.

Ohtsuka, T., Zhou, T. (2002) Bisindolylmaleimide VIII enhances DR5-mediated apoptosis through the MKK4/JNK/p38 kinase and the mitochondrial pathways. J Biol Chem 277, 29294-29303.

Okamura, Y., Nomoto, S., Kanda, M., Hayashi, M., Nishikawa, Y., Fujii, T., Sugimoto, H., Takeda, S., Nakao, A. (2011) Reduced expression of reelin (*RELN*) gene is associated with high recurrence rate of hepatocellular carcinoma. Ann Surg Oncol 18, 572-579.

Osawa, T., Muramatsu, M., Watanabe, M., Shibuya, M. (2009) Hypoxia and low-nutrition double stress induces aggressiveness in a murine model of melanoma. Cancer Sci 100, 844-851.

Ou, Z., Kang, S.H., Shaw, C.A., Carmack, C.E., White, L.D., Patel, A., Beaudet, A.L., Cheung, S.W., Chinault, A.C. (2008) Bacterial artificial chromosome-emulation oligonucleotide arrays for targeted clinical array-comparative genomic hybridization analyses. Genet Med 10, 278-289.

Pacek, M., Tutter, A.V., Kubota, Y., Takisawa, H., Walter, J.C. (2006) Localization of *MCM2-7*, *Cdc45*, and *GINS* to the site of DNA unwinding during eukaryotic DNA replication. Mol Cell 21, 581-587.

Panicker, S.P., Raychaudhuri, B., Sharma, P., Tipps, R., Mazumdar, T., Mal, A.K., Palomo, J.M., Vogelbaum, M.A., Haque, S.J. (2010) p300- and Myc-mediated regulation of glioblastoma multiforme cell differentiation. Oncotarget 1, 289-303.

Parsons, D.W., Jones, S., Zhang, X., Lin, J.C., Leary, R.J., Angenendt, P., Mankoo, P., Carter, H., Siu, I.M., Gallia, G.L., Olivi, A., McLendon, R., Rasheed, B.A., Keir, S., Nikolskaya, T., Nikolsky, Y., Busam, D.A., Tekleab, H., Diaz, L.A., Jr., Hartigan, J., Smith, D.R., Strausberg, R.L., Marie, S.K., Shinjo, S.M., Yan, H., Riggins, G.J., Bigner, D.D., Karchin, R., Papadopoulos, N., Parmigiani, G., Vogelstein, B., Velculescu, V.E., Kinzler, K.W. (2008) An integrated genomic analysis of human glioblastoma multiforme. Science 321, 1807-1812.

Perone, T.P., Robinson, B., Holmes, S.M. (1984) Intrasellar schwannoma: case report. Neurosurgery 14, 71-73.

Peterziel, H., Müller, J., Danner, A., Barbus, S., Liu, H.K., Radlwimmer, B., Pietsch, T., Lichter, P., Schutz, G., Hess, J., Angel, P. (2012) Expression of podoplanin in human astrocytic brain tumors is controlled by the *PI3K-AKT-AP-1* signaling pathway and promoter methylation. Neuro Oncol 14, 426-439.

Petty, R.D., Samuel, L.M., Murray, G.I., MacDonald, G., O'Kelly, T., Loudon, M., Binnie, N., Aly, E., McKinlay, A., Wang, W., Gilbert, F., Semple, S., Collie-Duguid, E.S. (2009) *APRIL* is a novel clinical chemo-resistance biomarker in colorectal adenocarcinoma identified by gene expression profiling. BMC Cancer 9, 434.

Phillips, H.S., Kharbanda, S., Chen, R., Forrest, W.F., Soriano, R.H., Wu, T.D., Misra, A., Nigro, J.M., Colman, H., Soroceanu, L., Williams, P.M., Modrusan, Z., Feuerstein, B.G., Aldape, K. (2006) Molecular subclasses of high-grade glioma predict prognosis, delineate a pattern of disease progression, and resemble stages in neurogenesis. Cancer Cell 9, 157-173.

Pinkel, D., Segraves, R., Sudar, D., Clark, S., Poole, I., Kowbel, D., Collins, C., Kuo, W.L., Chen, C., Zhai, Y., Dairkee, S.H., Ljung, B.M., Gray, J.M., Alberton, D.G. (1998) High resolution analysis of DNA copy number variation using comparative genomic hybridization to microarrays. Nat Genet 20, 207-211.

Portnoi, M.F. (2009) Microduplication 22q11.2: a new chromosomal syndrome. Eur J Med Genet 52, 88-93.

Prudent, R., Vassal-Stermann, E., Nguyen, C.H., Pillet, C., Martinez, A., Prunier, C., Barette, C., Soleilhac, E., Filhol, O., Beghin, A., Valdameri, G., Honoré, S., Aci-Sèche, S., Grierson, D., Antonipillai, J., Li, R., Di Pietro, A., Dumontet, C., Braguer, D., Florent, J.C., Knapp, S., Bernard, O., Lafanechère, L. (2012) Pharmacological inhibition of LIM kinase stabilizes microtubules and inhibits neoplastic growth. Cancer Res 72, 4429-4439.

Pulvirenti, T., Van Der Heijden, M., Droms, L.A., Huse, J.T., Tabar, V., Hall, A. (2011) Dishevelled 2 signaling promotes self-renewal and tumorigenicity in human gliomas. Cancer Res 71, 7280-7290.

Raif, A., Marshall, G.M., Bell, J.L., Koach, J., Tan, O., D'Andreti, C., Thomas, W., Sekyere, E., Norris, M., Haber, M., Kavallaris, M., Cheung, B.B. (2009) The estrogen-responsive B box protein (*EBBP*) restores retinoid sensitivity in retinoid-resistant cancer cells via effects on histone acetylation. Cancer Lett 277, 82-90.

Raverot, G., Wierinckx, A., Dantony, E., Auger, C., Chapas, G., Villeneuve, L., Brue, T., Figarella-Branger, D., Roy, P., Jouanneau, E., Jan, M., Lachuer, J., Trouillas, J.; HYPOPRONOS (2010) Prognostic factors in prolactin pituitary tumors: clinical, histological, and molecular data from a series of 94 patients with a long postoperative follow-up. J Clin Endocrinol Metab 95, 1708-1716.

Reifenberger, J., Reifenberger, G., Liu, L., James, C.D., Wechsler, W., Collins, V.P. (1994) Molecular genetic analysis of oligodendroglial tumors shows preferential allelic deletions on 19q and 1p. Am J Pathol 145, 1175-1190.

Reifenberger, G., Collins, V.P. (2004) Pathology and molecular genetics of astrocytic gliomas. J Mol Med 82, 656-670.

Reifenberger, G., Kros, J.M., Louis, D.N., Collins, V.P. IN: Louis D.N., Ohgaki H., Wiestier O.D., Cavenee W.K. (Eds.): WHO Classification of Tumours of the Central Nervous System. IARC: Lyon 2007, p53-66.

Reifenberger, G., Weber, R.G., Riehmer, V., Kaulich, K., Willscher, E., Wirth, H., Gietzelt, J., Hentschel, B., Westphal, M., Simon, M., Schackert, G., Schramm, J., Matschke, J., Sabel, M.C., Gramatzki, D., Felsberg, J., Hartmann, C., Steinbach, J., Schlegel, U., Wick, W., Radlwimmer, B., Pietsch, T., Tonn, J.C., von Deimling, A., Binder, H., Weller, M., Loeffler, M.; German Glioma Network (2014) Molecular characterization of long-term survivors of glioblastoma using genome- and transcriptome-wide profiling. Int J Cancer [Epub ahead of print].

Riehmer, V., Gietzelt, J., Beyer, U., Hentschel, B., Westphal, M., Schackert, G., Sabel, M.C., Radlwimmer, B., Pietsch, T., Reifenberger, G., Weller, M., Weber, R.G., Loeffler, M.; German Glioma Network (2014) Genomic profiling reveals distinctive molecular relapse patterns in *IDH1/2* wild-type glioblastoma. Genes Chromosomes Cancer (in press).

Riemenschneider, M.J., Reifenberger, G. (2009) Astrocytic tumors. Recent Results Cancer Res 171, 3-24.

Riemenschneider, M.J., Jeuken, J.W., Wesseling, P., Reifenberger, G. (2010) Molecular diagnostics of gliomas: state of the art. Acta Neuropathol 120, 567-584.

Roeb, W., Higgins, J., King, M.C. (2012) Response to DNA damage of *CHEK2* missense mutations in familial breast cancer. Hum Mol Genet 21, 2738-2744.

Roth, W., Wagenknecht, B., Klumpp, A., Naumann, U., Hahne, M., Tschopp, J., Weller, M. (2001) *APRIL*, a new member of the tumor necrosis factor family, modulates death ligand-induced apoptosis. Cell Death Differ 8, 403-410.

Roversi, G., Pfundt, R., Moroni, R.F., Magnani, I., van Reijmersdal, S., Pollo, B., Straatman, H., Larizza, L., Schoenmakers, E.F. (2006) Identification of novel genomic markers related to progression to glioblastoma through genomic profiling of 25 primary glioma cell lines. Oncogene 25, 1571-1583.

Rowley, J.D. (1973) Letter: A new consistent chromosomal abnormality in chronic myelogenous leukaemia identified by quinacrine fluorescence and Giemsa staining. Nature 243, 290-293.

Rustgi, A.K. (2007) The genetics of hereditary colon cancer. Genes Dev 21, 2525-2538.

Sanson, M., Marie, Y., Paris, S., Idbaih, A., Laffaire, J., Ducray, F., El Hallani, S., Boisselier, B., Mokhtari, K., Hoang-Xuan, K., Delattre, J.Y. (2009) Isocitrate dehydrogenase 1 codon 132 mutation is an important prognostic biomarker in gliomas. J Clin Oncol 27, 4150-4154.

Sausen, M., Leary, R.J., Jones, S., Wu, J., Reynolds, C.P., Liu, X., Blackford, A., Parmigiani, G., Diaz, L.A., Jr., Papadopoulos, N., Vogelstein, B., Kinzler, K.W., Velculescu, V.E., Hogarty, M.D. (2013) Integrated genomic analyses identify *ARID1A* and *ARID1B* alterations in the childhood cancer neuroblastoma. Nat Genet 45, 12-17.

Scheithauer, B.W., Louis, D.N., Hunter, S., Woodruff, J.M., Antonescu, C.R. IN: Louis D.N., Ohgaki H., Wiestier O.D., Cavenee W.K. (Eds.): WHO Classification of Tumours of the Central Nervous System. IARC: Lyon 2007, p160-162.

Schraivogel, D., Weinmann, L., Beier, D., Tabatabai, G., Eichner, A., Zhu, J.Y., Anton, M., Sixt, M., Weller, M., Beier, C.P., Meister, G. (2011) *CAMTA1* is a novel tumour suppressor regulated by miR-9/9* in glioblastoma stem cells. EMBO J 30, 4309-4322.

Schröck, E., Blume, C., Meffert, M.C., du Manoir, S., Bersch, W., Kiessling, M., Lozanowa, T., Thiel, G., Witkowski, R., Ried, T., Cremer, T. (1996) Recurrent gain of chromosome arm 7q in low-grade astrocytic tumors studied by comparative genomic hybridization. Genes Chromosomes Cancer 15, 199-205.

Sen, G.S., Mohanty, S., Hossain, D.M., Bhattacharyya, S., Banerjee, S., Chakraborty, J., Saha, S., Ray, P., Bhattacharjee, P., Mandal, D., Bhattacharya, A., Chattopadhyay, S., Das, T., Sa, G. (2011) Curcumin enhances the efficacy of chemotherapy by tailoring p65NFkappaB-p300 cross-talk in favor of p53-p300 in breast cancer. J Biol Chem 286, 42232-42247.

Shain, A.H., Pollack, J.R. (2013) The spectrum of *SWI/SNF* mutations, ubiquitous in human cancers. PloS One 8, e55119.

Shen, Y., Irons, M., Miller, D.T., Cheung, S.W., Lip, V., Sheng, X., Tomaszewicz, K., Shao, H., Fang, H., Tang, H.S., Irons, M., Walsh, C.A., Platt, O., Gusella. J.F., Wu, B.L. (2007) Development of a focused oligonucleotide-array comparative genomic hybridization chip for clinical diagnosis of genomic imbalance. Clin Chem 53, 2051-2059.

Shen, Y., Wu, B.L. (2009) Microarray-based genomic DNA profiling technologies in clinical molecular diagnostics. Clin Chem 55, 659-669.

Shete, S., Hosking, F.J., Robertson, L.B., Dobbins, S.E., Sanson, M., Malmer, B., Simon, M., Marie, Y., Boisselier, B., Delattre, J.Y., Hoang-Xuan, K., El Hallani, S., Idbaih, A., Zelenika, D., Andersson, U., Henriksson, R., Bergenheim, A.T., Feychting, M., Lönn, S., Ahlbom, A., Schramm, J., Linnebank, M., Hemminki, K., Kumar, R., Hepworth, S.J., Price, A., Armstrong, G., Liu, Y., Gu, X., Yu, R., Lau, C., Schoemaker, M., Muir, K., Swerdlow, A., Lathrop, M., Bondy, M., Houlston, R.S. (2009) Genome-wide association study identifies five susceptibility loci for glioma. Nat Genet 41, 899-904.

Shinawi, T., Hill, V.K., Krex, D., Schackert, G., Gentle, D., Morris, M.R., Wei, W., Cruickshank, G., Maher, E.R., Latif, F. (2013) DNA methylation profiles of long- and short-term glioblastoma survivors. Epigenetics 8, 149-156.

Silber, J.R., Blank, A., Bobola, M.S., Ghatan, S., Kolstoe, D.D., Berger, M.S. (1999) O6-methylguanine-DNA methyltransferase-deficient phenotype in human gliomas: frequency and time to tumor progression after alkylating agent-based chemotherapy. Clin Cancer Res 5, 807-814.

Simpson, N.E., Lambert, W.M., Watkins, R., Giashuddin, S., Huang, S.J., Oxelmark, E., Arju, R., Hochman, T., Goldberg, J.D., Schneider, R.J., Reiz, L.F., Soares, F.A., Logan, S.K., Garabedian, M.J. (2010) High levels of Hsp90 cochaperone p23 promote tumor progression and poor prognosis in breast cancer by increasing lymph node metastases and drug resistance. Cancer Res 70, 8446-8456.

Smith, J.S., Jenkins, R.B. (2000) Genetic alterations in adult diffuse glioma: occurrence, significance, and prognostic implications. Front Biosci 5, D213-231.

Solinas-Toldo, S., Lampel, S., Stilgenbauer, S., Nickolenko, J., Benner, A., Dohner, H., Cremer, T., Lichter, P. (1997) Matrix-based comparative genomic hybridization: biochips to screen for genomic imbalances. Genes Chromosomes Cancer 20, 399-407.

Sonenshein, G.E. (1997) Rel/NF-kappa B transcription factors and the control of apoptosis. Semin Cancer Biol 8, 113-119.

Spiegl-Kreinecker, S., Pirker, C., Marosi, C., Buchroithner, J., Pichler, J., Silye, R., Fischer, J., Micksche, M., Berger, W. (2007) Dynamics of chemosensitivity and chromosomal instability in recurrent glioblastoma. Br J Cancer 96, 960-969.

Stieber, D., Golebiewska, A., Evers, L., Lenkiewicz, E., Brons, N.H., Nicot, N., Oudin, A., Bougnaud, S., Hertel, F., Bjerkvig, R., Vallar, L., Barrett, M.T., Niclou, S.P. (2014) Glioblastomas are composed of genetically divergent clones with distinct tumourigenic potential and variable stem cell-associated phenotypes. Acta Neuropathol 127, 203-219.

Strachan, T., Read, A.P. (2011) Human molecular genetics, 4th edn (New York: Garland Science).

Stupp, R., Mason, W.P., van den Bent, M.J., Weller, M., Fisher, B., Taphoorn, M.J., Belanger, K., Brandes, A.A., Marosi, C., Bogdahn, U., Curschmann, J., Janzer, R.C., Ludwin, S.K., Gorlia, T., Allgeier, A., Lacombe, D., Cairncross, J.G., Eisenhauer, E., Mirimanoff, R.O.; European Organisation for Research and Treatment of Cancer Brain Tumor and Radiotherapy Groups; National Cancer Institute of Canada Clinical Trials Group (2005) Radiotherapy plus concomitant and adjuvant temozolomide for glioblastoma. N Engl J Med 352, 987-996.

Sturm, D., Witt, H., Hovestadt, V., Khuong-Quang, D.A., Jones, D.T., Konermann, C., Pfaff, E., Tönjes, M., Sill, M., Bender, S., Kool, M., Zapatka, M., Becker, N., Zucknick, M., Hielscher, T., Liu, X.Y., Fontebasso, A.M., Ryzhova, M., Albrecht, S., Jacob, K., Wolter, M., Ebinger, M., Schuhmann, M.U., van Meter, T., Frühwald, M.C., Hauch, H., Pekrun, A., Radlwimmer, B., Niehues, T., von Komorowski, G., Dürken, M., Kulozik, A.E., Madden, J., Donson, A., Foreman, N.K., Drissi, R., Fouladi, M., Scheurlen, W., von Deimling, A., Monoranu, C., Roggendorf, W., Herold-Mende, C., Unterberg, A., Kramm, C.M., Felsberg, J., Hartmann, C., Wiestler, B., Wick, W., Milde, T., Witt, O., Lindroth, A.M., Schwartzentruber, J., Faury, D., Fleming, A., Zakrzewska, M., Liberski, P.P., Zakrzewski, K., Hauser, P., Garami, M., Klekner, A., Bognar, L., Morrissy, S., Cavalli, F., Taylor, M.D., van Sluis, P., Koster, J., Versteeg, R., Volckmann, R., Mikkelsen, T., Aldape, K., Reifenberger, G., Collins, V.P., Majewski, J., Korshunov, A., Lichter, P., Plass, C., Jabado, N., Pfister, S.M. (2012) Hotspot mutations in *H3F3A* and *IDH1* define distinct epigenetic and biological subgroups of glioblastoma. Cancer Cell 22, 425-437.

Su, X., Chakravarti, D., Flores, E.R. (2013) p63 steps into the limelight: crucial roles in the suppression of tumorigenesis and metastasis. Nat Rev Cancer 13, 136-143.

Svojgr, K., Kalina, T., Kanderova, V., Skopcova, T., Brdicka, T., Zuna, J. (2012) The adaptor protein NTAL enhances proximal signaling and potentiates corticosteroid-induced apoptosis in T-ALL. Exp Hematol 40, 379-385.

Tang, Z., Chen, W.Y., Shimada, M., Nguyen, U.T., Kim, J., Sun, X.J., Sengoku, T., McGinty, R.K., Fernandez, J.P., Muir, T.W., Roeder, R.G. (2013) *SET1* and p300 act synergistically, through coupled histone modifications, in transcriptional activation by p53. Cell 154, 297-310.

Tavtigian, S.V., Simard, J., Teng, D.H., Abtin, V., Baumgard, M., Beck, A., Camp, N.J., Carillo, A.R., Chen, Y., Dayananth, P., Desrochers, M., Dumont, M., Farnham, J.M., Frank, D., Frye, C., Ghaffari, S., Gupte, J.S., Hu, R., Iliev, D., Janecki, T., Kort, E.N., Laity, K.E., Leavitt, A., Leblanc, G., McArthur-Morrison, J., Pederson, A., Penn, B., Peterson, K.T., Reid, J.E., Richards, S., Schroeder, M., Smith, R., Snyder, S.C., Swedlund, B., Swensen, J., Thomas, A., Tranchant, M., Woodland, A.M., Labrie, F., Skolnick, M.H., Neuhausen, S., Rommens, J., Cannon-Albright, L.A. (2001) A candidate prostate cancer susceptibility gene at chromosome 17p. Nat Genet 27, 172-180.

Terret, C., Albrand, G., Moncenix, G., Droz, J.P. (2011) Karnofsky Performance Scale (KPS) or Physical Performance Test (PPT)? That is the question. Crit Rev Oncol Hematol 77, 142-147.

Tesser-Gamba, F., Petrilli, A.S., de Seixas Alves, M.T., Filho, R.J., Juliano, Y., Toledo, S.R. (2012) *MAPK7* and *MAP2K4* as prognostic markers in osteosarcoma. Hum Pathol 43, 994-1002.

Toedt, G., Barbus, S., Wolter, M., Felsberg, J., Tews, B., Blond, F., Sabel, M.C., Hofmann, S., Becker, N., Hartmann, C., Ohgaki, H., von Deimling, A., Wiestler, O.D., Hahn, M., Lichter, P., Reifenberger, G., Radlwimmer, B. (2011) Molecular signatures classify astrocytic gliomas by *IDH1* mutation status. Int J Cancer 128, 1095-1103.

van den Boom, J., Wolter, M., Kuick, R., Misek, D.E., Youkilis, A.S., Wechsler, D.S., Sommer, C., Reifenberger, G., Hanash, S.M. (2003) Characterization of gene expression profiles associated with glioma progression using oligonucleotide-based microarray analysis and real-time reverse transcription-polymerase chain reaction. Am J Pathol 163, 1033-1043.

van Vuurden, D.G., Hulleman, E., Meijer, O.L., Wedekind, L.E., Kool, M., Witt, H., Vandertop, P.W., Wurdinger, T., Noske, D.P., Kaspers, G.J., Cloos, J. (2011) *PARP* inhibition sensitizes childhood high grade glioma, medulloblastoma and ependymoma to radiation. Oncotarget 2, 984-996.

Varley, J.M. (2003a) Germline *TP53* mutations and Li-Fraumeni syndrome. Hum Mutat 21, 313-320.

Varley, J.M. (2003b) *TP53*, *hChk2*, and the Li-Fraumeni syndrome. Methods Mol Biol 222, 117-129.

Vasseur, S., Afzal, S., Tardivel-Lacombe, J., Park, D.S., Iovanna, J.L., Mak, T.W. (2009) *DJ-1/PARK7* is an important mediator of hypoxia-induced cellular responses. Proc Natl Acad Sci U S A 106, 1111-1116.

Verhaak, R.G., Hoadley, K.A., Purdom, E., Wang, V., Qi, Y., Wilkerson, M.D., Miller, C.R., Ding, L., Golub, T., Mesirov, J.P., Alexe, G., Lawrence, M., O'Kelly, M., Tamayo, P., Weir, B.A., Gabriel, S., Winckler, W., Gupta, S., Jakkula, L., Feiler, H.S., Hodgson, J.G., James, C.D., Sarkaria, J.N., Brennan, C., Kahn, A., Spellman, P.T., Wilson, R.K., Speed, T.P., Gray, J.W., Meyerson, M., Getz, G., Perou, C.M., Hayes, D.N.; Cancer Genome Atlas Research Network (2010) Integrated genomic analysis identifies clinically relevant subtypes of glioblastoma characterized by abnormalities in *PDGFRA*, *IDH1*, *EGFR*, and *NF1*. Cancer Cell 17, 98-110.

Vierimaa, O., Georgitsi, M., Lehtonen, R., Vahteristo, P., Kokko, A., Raitila, A., Tuppurainen, K., Ebeling, T.M., Salmela, P.I., Paschke, R., Gündogdu S., De Menis, E., Mäkinen, M.J., Launonen, V., Karhu, A., Aaltonen, L.A. (2006) Pituitary adenoma predisposition caused by germline mutations in the *AIP* gene. Science 312, 1228-1230.

Vissers, L.E., de Ligt, J., Gilissen, C., Janssen, I., Steehouwer, M., de Vries, P., van Lier, B., Arts, P., Wieskamp, N., del Rosario, M., van Bon, B.W., Hoischen, A., de Vries, B.B., Brunner, H.G., Veltman, J.A. (2010) *De novo* paradigm for mental retardation. Nat Genet 42, 1109-1112.

Vogelstein, B., Kinzler, K.W. (2004) Cancer genes and the pathways they control. Nat Med 10, 789-799.

Vogelstein, B., Papadopoulos, N., Velculescu, V.E., Zhou, S., Diaz, L.A., Jr., Kinzler, K.W. (2013) Cancer genome landscapes. Science 339, 1546-1558.

von Deimling, A., Burger, P.C., Nakazato, Y., Ohgaki, H., Kleihues, P. IN: Louis D.N., Ohgaki H., Wiestier O.D., Cavenee W.K. (Eds.): WHO Classification of Tumours of the Central Nervous System. IARC: Lyon 2007, p25-30.

Wacker, D.A., Frizzell, K.M., Zhang, T., Kraus, W.L. (2007) Regulation of chromatin structure and chromatin-dependent transcription by poly(ADP-ribose) polymerase-1: possible targets for drug-based therapies. Subcellular Biochem 41, 45-69.

Watanabe, T., Katayama, Y., Yoshino, A., Yachi, K., Ohta, T., Ogino, A., Komine, C., Fukushima, T. (2007) Aberrant hypermethylation of p14ARF and O6-methylguanine-DNA methyltransferase genes in astrocytoma progression. Brain Pathol 17, 5-10.

Weber, R.G., Sommer, C., Albert, F.K., Kiessling, M., Cremer, T. (1996) Clinically distinct subgroups of glioblastoma multiforme studied by comparative genomic hybridization. Lab Invest 74, 108-119.

Weise, A., Mrasek, K., Klein, E., Mulatinho, M., Llerena, J.C., Jr., Hardekopf, D., Pekova, S., Bhatt, S., Kosyakova, N., Liehr, T. (2012) Microdeletion and microduplication syndromes. J Histochem Cytochem 60, 346-358.

Weller, M., Felsberg, J., Hartmann, C., Berger, H., Steinbach, J.P., Schramm, J., Westphal, M., Schackert, G., Simon, M., Tonn, J.C., Heese, O., Krex, D., Nikkhah, G., Pietsch, T., Wiestler, O., Reifenberger, G., von Deimling, A., Loeffler, M. (2009) Molecular predictors of progression-free and overall survival in patients with newly diagnosed glioblastoma: a prospective translational study of the German Glioma Network. J Clin Oncol 27, 5743-5750.

Weller, M., Stupp, R., Hegi, M., Wick, W. (2012) Individualized targeted therapy for glioblastoma: fact or fiction? Cancer J 18, 40-44.

Wessels, P.H., Twijnstra, A., Kessels, A.G., Krijne-Kubat, B., Theunissen, P.H., Ummelen, M.I., Ramaekers, F.C., Hopman, A.H. (2002) Gain of chromosome 7, as detected by in situ hybridization, strongly correlates with shorter survival in astrocytoma grade 2. Genes Chromosomes Cancer 33, 279-284.

Whee, S.M., Lee, J.I., Kim, J.H. (2002) Intrasellar schwannoma mimicking pituitary adenoma: a case report. J Korean Med Sci 17, 147-150.

Wheeler, D.A., Srinivasan, M., Egholm, M., Shen, Y., Chen, L., McGuire, A., He, W., Chen, Y.J., Makhijani, V., Roth, G.T., Gomes, X., Tartaro, K., Niazi, F., Turcotte, C.L., Irzyk, G.P., Lupski, J.R., Chinaut, C., Song, X.Z., Liu, Y., Yuan, Y., Nazareth, L., Qin, X., Muzny, D.M., Margulies, M., Weinstock,

G.M., Gibbs, R.A., Rothberg, J.M. (2008) The complete genome of an individual by massively parallel DNA sequencing. Nature 452, 872-876.

Willatt, L., Cox, J., Barber, J., Cabanas, E.D., Collins, A., Donnai, D., FitzPatrick, D.R., Maher, E., Martin, H., Parnau, J., Pindar, L., Ramsay, J., Shaw-Smith, C., Sistermans, E.A., Tettenborn, M., Trump, D., de Vries, B.B., Walker, K., Raymond, F.L. (2005) 3q29 microdeletion syndrome: clinical and molecular characterization of a new syndrome. Am J Hum Genet 77, 154-160.

Wu, H., Pomeroy, S.L., Ferreira, M., Teider, N., Mariani, J., Nakayama, K.I., Hatakeyama, S., Tron, V.A., Saltibus, L.F., Spyracopoulos, L., and Leng, R.P. (2011) *UBE4B* promotes Hdm2-mediated degradation of the tumor suppressor p53. Nat Med 17, 347-355.

Yamaguchi, U., Hasegawa, T., Hirose, T., Chuman, H., Kawai, A., Ito, Y., Beppu, Y. (2003) Low grade malignant peripheral nerve sheath tumour: varied cytological and histological patterns. J Clin Pathol 56, 826-830.

Yamaki, T., Suenaga, Y., Iuchi, T., Alagu, J., Takatori, A., Itami, M., Araki, A., Ohira, M., Inoue, M., Kageyama, H., Yokoi, S., Saeki, N., Nakagawara, A. (2013) Temozolomide suppresses *MYC* via activation of TAp63 to inhibit progression of human glioblastoma. Sci Rep 3, 1160.

Yan, H., Parsons, D.W., Jin, G., McLendon, R., Rasheed, B.A., Yuan, W., Kos, I., Batinic-Haberle, I., Jones, S., Riggins, G.J., Friedman, H., Friedman, A., Reardon, D., Herndon, J., Kinzler, K.W., Velculescu, V.E., Vogelstein, B., Bigner, D.D. (2009) *IDH1* and *IDH2* mutations in gliomas. N Engl J Med 360, 765-773.

Yip, P.Y., Kench, J.G., Rasiah, K.K., Benito, R.P., Lee, C.S., Stricker, P.D., Henshall, S.M., Sutherland, R.L., Horvath, L.G. (2011) Low *AZGP1* expression predicts for recurrence in margin-positive, localized prostate cancer. Prostate 71, 1638-1645.

Ylstra, B., van den Ijssel, P., Carvalho, B., Brakenhoff, R.H., Meijer, G.A. (2006) BAC to the future! or oligonucleotides: a perspective for micro array comparative genomic hybridization (array CGH). Nucleic Acids Res 34, 445-450.

Yobb, T.M., Somerville, M.J., Willatt, L., Firth, H.V., Harrison, K., MacKenzie, J., Gallo, N., Morrow, B.E., Shaffer, L.G., Babcock, M., Chernos, J., Bernier, F., Sprysak, K., Christiansen, J., Haase, S., Elyas, B., Lilley, M., Bamforth, S., McDermid, H.E. (2005) Microduplication and triplication of 22q11.2: a highly variable syndrome. Am J Hum Genet 76, 865-876.

Zage, P.E., Sirisaengtaksin, N., Liu, Y., Gireud, M., Brown, B.S., Palla, S., Richards, K.N., Hughes, D.P., Bean, A.J. (2013) *UBE4B* levels are correlated with clinical outcomes in neuroblastoma patients and with altered neuroblastoma cell proliferation and sensitivity to epidermal growth factor receptor inhibitors. Cancer 119, 915-923.

Zhao, Z., Liu, Y., He, H., Chen, X., Chen, J., Lu, Y.C. (2011) Candidate genes influencing sensitivity and resistance of human glioblastoma to Semustine. Brain Res Bull 86, 189-194.

Zheng, S., Chheda, M.G., Verhaak, R.G. (2012) Studying a complex tumor: potential and pitfalls. Cancer J 18, 107-114.

8 Publications

Hofer, M.J., Riehmer, V., Kuhnt, D., Braun, V., Nimsky, C., Weber, R.G., Sommer, C., Pagenstecher, A. (2012) Genomic profiling to assess the clonal relationship between histologically distinct intracranial tumours. Neuropathol Appl Neurobiol 38:500-504.

Classen, C.F.*, Riehmer, V.* (*Co-Firstautor), Landwehr, C., Kosfeld, A., Heilmann, S., Scholz, C., Kabisch, S., Engels, H., Tierling, S., Zivicnjak, M., Schacherer, F., Haffner, D., Weber, R.G. (2013) Dissecting the genotype in syndromic intellectual disability using whole exome sequencing in addition to genome-wide copy number analysis. Hum Genet 132:825-841.

Reifenberger, G., Weber, R.G., Riehmer, V., Kaulich, K., Willscher, E., Wirth, H., Gietzelt, J., Hentschel, B., Westphal, M., Simon, M., Schackert, G., Schramm, J., Matschke, J., Sabel, M.C., Gramatzki, D., Felsberg, J., Hartmann, C., Steinbach, J., Schlegel, U., Wick, W., Radlwimmer, B., Pietsch, T., Tonn, J.C., von Deimling, A., Binder, H., Weller, M., Loeffler, M.; German Glioma Network (2014) Molecular characterization of long-term survivors of glioblastoma using genome- and transcriptome-wide profiling. Int J Cancer, 2014, [Epub ahead of print].

Riehmer, V., Gietzelt, J., Beyer, U., Hentschel, B., Westphal, M., Schackert, G., Sabel, M.C., Radlwimmer, B., Pietsch, T., Reifenberger, G., Weller, M., Weber, R.G., Loeffler, M., German Glioma Network (2014) Genomic profiling reveals three molecular relapse patterns in *IDH1/2* wild-type glioblastoma. Genes Chromosomes and Cancer (in press).

Abstracts

Riehmer, V., Wagener, R., Heimbach, A., Littmann, E., Hans, V.H., Brockschmidt, A., Weber, R.G. ALC1 as a candidate oncogene in human malignant glioma. European Human Genetics Conference, Nürnberg, 23.-26.06.2012.

Riehmer, V., Classen, C.F., Landwehr, C., Kosfeld, A., Heilmann, S., Scholz, C., Kabisch, S., Engels, H., Tierling, S., Zivicnjak, M., Schacherer, F., Haffner, D., Weber, R.G. Dissecting the genotype in syndromic intellectual disability using whole exome sequencing in addition to genome-wide copy number analysis. European Human Genetics Conference, Paris, Frankreich, 08.-11.06.2013.

Weber, R.G., Kosfeld, A., Kreuzer, M., Riehmer, V., Pape, L., Haffner, D. Whole exome sequencing in patients with sporadic severe bilateral renal hypodysplasia reveals genetic heterogeneity and identifies causative genes in most cases. 16th Congress of the International Pediatric Nephrology Association, Shanghai, China, 30.08.-03.09.2013.

Kosfeld, A., Kreuzer, M., Scholz, C., Riehmer, V., Horstmann, D., Pape, L., Haffner, D., Weber, R.G. Whole exome sequencing reveals rare homozygous *ARID1B* and heterozygous *MTOR* missense variants in a patient with bilateral cystic-dysplastic kidneys and features of Coffin-Siris syndrome and tuberous sclerosis. European Human Genetics Conference, Mailand, Italien, 31.05.-03.06.2014.

9 Acknowledgements

First of all I would like to thank Prof. Dr. Ruthild G. Weber for offering me such interesting and challenging projects and for excellent supervision. Thank you for waking my interest in the field of Human Genetics.

I would like to thank Prof. Dr. W. Witke for taking over co-supervision and for co-reviewing my thesis.

Further, I would like to thank all former colleagues from the Department of Human Genetics, Rheinische Friedrich-Wilhelms-University, Bonn. Especially, Dr. Antje Brockschmidt, Dr. Christina Landwehr, Dr. Boi-Dinh Chung-Ueck and Dr. André Heimbach.

I am very grateful to Dr. Frank Brand, Dr. Ulrike Beyer and Dr. Anne Kosfeld, from the Department of Human Genetics, Medical School Hannover, for their guidance, discussions and a great time during the last two years. Thank you very much!

A special thanks goes to my friends and family, supporting me during the last years in every possible way.